

BIOTRANSFORMATION OF BIOACTIVE COMPOUNDS FROM *Sonchus arvensis* L. AND
Pterocarpus macrocarpus Kurz. BY *Aspergillus niger*



A Dissertation Submitted in Partial Fulfillment of the Requirements
for the Degree of Doctor of Philosophy in Botany

Department of Botany

FACULTY OF SCIENCE

Chulalongkorn University

Academic Year 2021

Copyright of Chulalongkorn University

การเปลี่ยนแปลงโครงสร้างสารออกฤทธิ์ทางชีวภาพจาก *Sonchus arvensis* L. และ *Pterocarpus macrocarpus* Kurz. โดย *Aspergillus niger*



วิทยานิพนธ์นี้เป็นส่วนหนึ่งของการศึกษาตามหลักสูตรปริญญาวิทยาศาสตรดุษฎีบัณฑิต
สาขาวิชาพฤกษศาสตร์ ภาควิชาพฤกษศาสตร์
คณะวิทยาศาสตร์ จุฬาลงกรณ์มหาวิทยาลัย
ปีการศึกษา 2564
ลิขสิทธิ์ของจุฬาลงกรณ์มหาวิทยาลัย

ตี กุสุมา วาห์ยูนิ : การเปลี่ยนแปลงโครงสร้างสารออกฤทธิ์ทางชีวภาพจาก *Sonchus arvensis* L. และ *Pterocarpus macrocarpus* Kurz. โดย *Aspergillus niger*. (BIOTRANSFORMATION OF BIOACTIVE COMPOUNDS FROM *Sonchus arvensis* L. AND *Pterocarpus macrocarpus* Kurz. BY *Aspergillus niger*) อ.ที่ปรึกษาหลัก : สีหนาท ประสงค์สุข, อ.ที่ปรึกษาร่วม : สัมฤทธิ์ วัชรสินธุ์, วชิราณี แบนศิริ

การดัดแปรโครงสร้างของสารสำคัญด้วยจุลินทรีย์เป็นกระบวนการที่มีความสำคัญในเชิงบวกต่อสิ่งแวดล้อมจึงมีการพัฒนาขึ้นสำหรับเตรียมสารประกอบที่มีฤทธิ์ทางเภสัชกรรมในช่วงระยะเวลาหลายปีที่ผ่านมา ซึ่งจากการนำกระบวนการนี้มาประยุกต์ใช้พบว่าสามารถดัดแปรโครงสร้างของสารสำคัญได้หลายชนิด รวมทั้งมีผลในการเพิ่มฤทธิ์ทางยาของสารที่เป็นผลผลิตจากกระบวนการได้ ดังนั้นวัตถุประสงค์ของวิทยานิพนธ์นี้เพื่อ (1) คัดแยกและระบุชนิดของสารสกัดที่มีฤทธิ์ทางชีวภาพจาก *Sonchus arvensis* L. และ *Pterocarpus macrocarpus* Kurz. (2) ดัดแปรโครงสร้างของสารสกัดที่มีฤทธิ์ทางชีวภาพที่คัดเลือกด้วยรา *Aspergillus niger* และ (3) ตรวจสอบฤทธิ์ทางชีวภาพของสารสกัดทั้งก่อนและหลังการดัดแปรโครงสร้างของสารด้วยวิธีทางชีวภาพ สารสกัดของ *S. arvensis* L. leaf และ *P. macrocarpus* Kurz. เตรียมได้จากการหมักตัวอย่างร่วมกับเฮกเซน เอทิลอะซิเตท หรือเอทานอล จากนั้นวิเคราะห์ปริมาณของสารสกัดโดยใช้วิธีมาตรฐาน คัดแยกสารประกอบและตรวจสอบโครงสร้างของสารด้วยโครมาโตกราฟีแบบชั้นบาง (TLC) แก๊สโครมาโตกราฟี-แมสสเปกโตรโฟโตเมตรี (GC-MS) ฟลูออโรเมตริกสเปกโตรโฟโตเมตรี (FTR) สเปกโทรสโกปี และนิวเคลียร์แมกเนติกเรโซแนนซ์ (NMR) ทำการดัดแปรโครงสร้างของสาร Taraxasterol ที่สกัดจากใบของ *S. arvensis* L. และสาร homopterocarpin จากแก่นของ *P. macrocarpus* Kurz. โดยผสมในอาหารเลี้ยงเชื้อชนิด soy bean meal (SBM) ที่เพาะเลี้ยง *A. niger* จากนั้นนำสารสกัดจากเอทิลอะซิเตทของ *S. arvensis* L. ที่ผ่านการดัดแปรโครงสร้างมาทดสอบฤทธิ์ต้านพลาสโมเดียม ฤทธิ์ป้องกันตับ ฤทธิ์ป้องกันไต และฤทธิ์กระตุ้นภูมิคุ้มกันกับหนูที่ติดเชื้อ *P. berghei* ซึ่งออกแบบการทดลองตาม Peter's 4-day suppressive test สำหรับสารสกัดที่ไม่ดัดแปรโครงสร้างจะตรวจสอบฤทธิ์ทางชีวภาพในหลอดทดลอง ได้แก่ ฤทธิ์ต้านมาลาเรียกับเชื้อ *Plasmodium falciparum* สายพันธุ์ 3D7 ทดสอบฤทธิ์ต้าน SARS-CoV-2 โดยสร้างแบบจำลอง (*in silico*) ฤทธิ์ต้านอนุมูลอิสระร่วมกับสาร 1,1-diphenyl-2-picrylhydrazyl (DPPH) และ 2,2-azino-bis(3-ethylbenzothiazoline-6-sulfonic acid (ABTS) และตรวจสอบฤทธิ์ต้านจุลชีพกับ *Candida albicans*, *Bacillus subtilis*, *Escherichia coli* และ *Staphylococcus aureus* สำหรับการศึกษาความเป็นพิษต่อเซลล์และฤทธิ์ยับยั้งการเจริญของเซลล์มะเร็งจะตรวจสอบร่วมกับเซลล์ที่ได้มาจากตับ (Huh7it-1cells) ร่วมกับ 3(4,5-dimethylthiazol-2-yl)-2,5-diphenyltetrazolium bromide โดยเทคนิค MTT Assay สารสกัดเฮกเซน เอทิลอะซิเตท และเอทานอลจากใบของ *S. arvensis* L. แสดงฤทธิ์ต้านพลาสโมเดียมที่ดี โดยมีค่า IC_{50} เท่ากับ 5.119 ± 3.27 , 2.916 ± 2.34 และ 8.026 ± 1.23 ไมโครกรัมต่อมิลลิกรัมตามลำดับ สารสกัดแต่ละชนิดมีฤทธิ์ต้านอนุมูลอิสระสูงโดยมีผลเป็นพิษต่อเซลล์ต่ำ นอกจากนี้สารสกัดเอทิลอะซิเตทยังแสดงให้เห็นฤทธิ์ต้านพลาสโมเดียมในร่างกายที่ค่า ED_{50} เท่ากับ 46.31 ± 9.36 มิลลิกรัมต่อกิโลกรัมน้ำหนักตัว ตลอดจนมีฤทธิ์ป้องกันตับ และกระตุ้นภูมิคุ้มกันในหนูที่ติดเชื้อ *P. berghei* สารสกัดเอทิลอะซิเตท เอทานอล และเฮกเซนของ *P. macrocarpus* Kurz. และสาร homopterocarpin บริสุทธิ์มีฤทธิ์ต้านพลาสโมเดียม *P. falciparum* 3D7 ที่ 1.78, 2.21, 7.11 และ 0.52 ไมโครกรัมต่อมิลลิกรัมตามลำดับและมีความเป็นพิษต่ำ จากการศึกษาแบบจำลองโครงสร้างของสารพบว่าสารประกอบที่ระบุโดย GC-MS สามารถจับ stigmasterol และ helicase ได้ โดยมีค่าสัมพรรคภาพในการจับที่ -8.2 กิโลแคลอรีต่อโมลจึงมีผลในการต้าน SARS-CoV-2 นอกจากนี้สารสกัดทั้งหมดมีฤทธิ์ต้านอนุมูลอิสระต่อ DPPH และ ABTS รวมทั้งมีฤทธิ์ต้านการเจริญของ *B. subtilis* ในขณะที่สารสกัดเอทานอลและเอทิลอะซิเตทสามารถต้านการเจริญของ *E. coli* และ *C. albicans* และสารสกัดเอทานอลสามารถต้านการเจริญของ *S. aureus* จากการวิเคราะห์ชนิดและโครงสร้างของสารสกัดเฮกเซนจาก *S. arvensis* L. ด้วยวิธี GC-MS พบว่าสารที่สกัดได้ประกอบด้วย β -amyrin, lupeol, α -amyrin, betulin และ taraxasterol เมื่อนำสารเหล่านี้มาทดสอบฤทธิ์ต้าน SARS-CoV-2 ด้วยแบบจำลองพบว่าสารทั้งหมดมีความสามารถในการจับและยับยั้งกิจกรรมของโปรตีนจาก SARS-CoV-2 จึงคาดการณ์ว่าจะเป็นสารต้านไวรัสที่มีประสิทธิภาพจากการดัดแปรโครงสร้างของ homopterocarpin ด้วย *Aspergillus niger* พบว่ามีสารประกอบ 2 ชนิดที่คัดแยกได้แก่ 6-isopropenyl-4,8a-dimethyl-1,2,3,5,6,7,8,8a-octahydro-naphthalene-2-ol ซึ่งเป็นสารประกอบหลัก และ medicarpin ที่เกิดจากการกำจัดหมู่เมทิลของ homopterocarpin ซึ่งสารนี้มีฤทธิ์ต้านการออกซิเดชันของ DPPH และ ABTS ที่ค่า IC_{50} เท่ากับ 7.49 ± 1.7 และ 0.61 ± 0.4 ไมโครกรัมต่อมิลลิกรัมตามลำดับ รวมทั้งสามารถต้านพลาสโมเดียมในหลอดทดลองได้ด้วยความเข้มข้น 0.414 ไมโครกรัมต่อมิลลิกรัม และยับยั้งการเจริญของเซลล์มะเร็งที่มีค่า IC_{50} เท่ากับ 34.96 ไมโครกรัมต่อมิลลิกรัม จากการศึกษานี้มีผลในการค้นพบข้อมูลของสารที่มีฤทธิ์ทางยาจากผลิตภัณฑ์ธรรมชาติ ร่วมกับการเพื่อประสิทธิภาพทางยาจากการดัดแปรโครงสร้างของสารสกัดจากพืชที่มีสรรพคุณทางยาจากไทยและอินโดนีเซีย รวมทั้งพื้นที่อื่น ๆ ในโลก

สาขาวิชา	พฤกษศาสตร์	ลายมือชื่อนิสิต
ปีการศึกษา	2564	ลายมือชื่อ อ.ที่ปรึกษาหลัก
		ลายมือชื่อ อ.ที่ปรึกษาร่วม
		ลายมือชื่อ อ.ที่ปรึกษาร่วม

6172815823 : MAJOR BOTANY

KEYWORD: biotransformation, *Sonchus arvensis* L., *Pterocarpus macrocarpus* Kurz., *Aspergillus niger*, MalariaDwi Kusuma Wahyuni : BIOTRANSFORMATION OF BIOACTIVE COMPOUNDS FROM *Sonchus arvensis* L. AND *Pterocarpus macrocarpus* Kurz. BY *Aspergillus niger*. Advisor: Assoc. Prof. SEHANAT PRASONGSUK, Ph.D. Co-advisor: Prof. SUMRIT WACHARASINDHU, Ph.D., WICHANEE BANKEEREE, Ph.D.

In recent years, microbial transformation is progressing significantly from a limited interest in the highly active area in green chemistry, including the preparation of pharmaceutical compounds. Many biotransformation studies have been found in a variety of analogous compounds and exhibited more potent pharmacological activities. The objectives of this study are (i) to isolate and identify bioactive compounds from *Sonchus arvensis* L. and *Pterocarpus macrocarpus* Kurz., (ii) to transform selected bioactive compounds from *S. arvensis* L. and *P. macrocarpus* Kurz. by *Aspergillus niger*, (iii) to determine bioactivities of selected bioactive compounds from *Sonchus arvensis* L. and *Pterocarpus macrocarpus* Kurz. before and after biotransformation. The extracts from *S. arvensis* L. leaf and *P. macrocarpus* Kurz. heartwood prepared by successive maceration with *n*-hexane, ethyl acetate, and ethanol and then subjected to quantitative phytochemical analysis using standard methods. Isolated compound was evaluated by thin-layer chromatography (TLC), gas chromatography-mass spectrophotometry (GC-MS), Fourier transform infrared (FTIR) spectroscopy, and nuclear magnetic resonance (NMR). Taraxasterol (*S. arvensis* L. leaf) and homopterocarpin (*P. macrocarpus* Kurz. heartwood) were transformed in soy bean meal (SBM) medium by *Aspergillus niger*. The Peter's 4-day suppressive test model with *P. berghei*-infected mice was used to evaluate the *in vivo* antiplasmodial activities, hepatoprotective, nephroprotective, and immunomodulatory (ethyl acetate extract of *S. arvensis* L.). For all natural products were conducted the *in vitro* antimalarial activity assay against *Plasmodium falciparum* 3D7 strain, *in silico* anti-SARS-CoV-2, *in vitro* antioxidant against 1,1-diphenyl-2-picrylhydrazyl (DPPH) and 2,2-azino-bis (3-ethylbenzothiazoline-6-sulfonic acid (ABTS), and antimicrobial disc diffusion method against *Candida albicans*, *Bacillus subtilis*, *Escherichia coli*, and *Staphylococcus aureus*) activities were established. Hepatocyte-derived cellular carcinoma cell line (Huh7it-1cells) was used for an *in vitro* cytotoxicity and anticancer assay [3(4,5-dimethylthiazol-2-yl)-2,5-diphenyltetrazolium bromide; MTT]. The *n*-hexane, ethyl acetate, and ethanolic extract exhibited a good activity on *in vitro* antiplasmodial activity of *S. arvensis* L. leaf, with IC_{50} values were 5.119 ± 3.27 , 2.916 ± 2.34 , and 8.026 ± 1.23 $\mu\text{g/mL}$, respectively. Each extract also exhibited high antioxidants with low cytotoxic effects. Furthermore, the ethyl acetate extract showed *in vivo* antiplasmodial activity with $ED_{50} = 46.31 \pm 9.36$ mg/kg, body weight, as well as hepatoprotective, nephroprotective, and immunomodulatory activities in mice infected with *P. berghei*. The ethyl acetate, ethanol, and *n*-hexane extracts of *P. macrocarpus* Kurz., as well as homopterocarpin, exhibited antiplasmodial activity at 1.78, 2.21, 7.11, and 0.52 $\mu\text{g/mL}$, respectively, against *P. falciparum* 3D7 with low toxicity. A compound identified by GC-MS showed *in silico* anti-SARS-CoV-2 binding affinity with stigmasterol and SARS-CoV-2 helicase of -8.2 kcal/mol. All extracts exhibited antioxidant activity against DPPH and ABTS. They also demonstrated antimicrobial activity against *B. subtilis*, the ethanol and ethyl acetate extracts against *E. coli* and *C. albicans*, and the ethanol extract against *S. aureus*. GC-MS analysis of fraction of *S. arvensis* L. *n*-hexane extract revealed β -amyrin, lupeol, α -amyrin, betulin, and taraxasterol. The *in silico* anti-SARS-CoV-2 assay showed that they were predicted as effective antiviral candidates by having the ability to act as inhibitors of SARS-CoV-2 protein activity. Therefore, the molecular dynamic analysis data strengthen the notion that the interactions resulting from the five compounds of *n*-hexane fractions of *S. arvensis* L. leaves were stable and predicted to be effective antiviral candidates by having the ability to act as inhibitors of SARS-CoV-2 protein activity. Biotransformation of homopterocarpin was succeed by *Aspergillus niger*. Two compounds have been isolated from biotransformation culture extract. They are 6-isopropenyl-4,8a-dimethyl-1,2,3,5,6,7,8,8a-octahydro-naphthalene-2-ol (major compound) and medicarpin. Medicarpin could be predicted transformed from homopterocarpin by demethylation. It showed *in vitro* antioxidant activity against DPPH ($IC_{50} = 7.49 \pm 1.7$ $\mu\text{g/mL}$) and 2,2-azino-bis ABTS ($IC_{50} = 0.61 \pm 0.4$ $\mu\text{g/mL}$), *in vitro* antiplasmodial (0.414 $\mu\text{g/mL}$), and *in vitro* anticancer ($IC_{50} = 34.96$ $\mu\text{g/mL}$). Overall, this study collectively advances our knowledge of important drug discovery from natural products with a major impact in improving of natural product isolation and biotransformation from Thai and Indonesian medicinal plant and elsewhere around the world.

จุฬาลงกรณ์มหาวิทยาลัย
CHULALONGKORN UNIVERSITY

Field of Study: Botany
Academic Year: 2021Student's Signature
Advisor's Signature
Co-advisor's Signature
Co-advisor's Signature

ACKNOWLEDGEMENTS

I would like to express my profound gratitude to my advisor, Associate Professor Sehatat Prasongsuk, Ph.D. whose expertise was helpful in establishing the study objectives and methodology. Your informative criticism encouraged me to improve my thoughts and raise the quality of my work. Your input in perusing my reports and manuscripts is highly appreciated. Professor Sumrit Wacharasindhu, Ph.D. and Wichanee Bankeeree, Ph.D., my co-advisors, your patience and sacrifices in educating me, particularly in the subject of Biotransformation, are really appreciated. Even when my spirit was down, you believed in me. I would not be where I am now if it weren't for your criticism.

I would like to appreciate my doctoral dissertation committee members; Professor Dr. Hunsu Punapayak (Chairman/the external examiner), Assistant Professor Dr. Kanogwan Seraypheap, Assistant Professor Dr. Jitra Piapukiew, and Associate Professor Dr. Rachaneekorn Tammachote, for their suggestions and contributions.

I would also like to appreciate the Universitas Airlangga Scholarship and the Human Resources Division of the Universitas Airlangga, Surabaya, Indonesia for supporting me for my Ph.D program and research funding.

To my wonderful husband, Mr. Rosyid Anwar, and my four amazing daughters, Raissa, Alisha, Alana, and Adelia, thank you for being supportive, encouraging, and sacrificing your happiness for my cause. Thank you very much. Your prayers and counsel, my parents, kept me going even when I felt like giving up. You will be richly rewarded by Allah SWT. Special thanks to brother and sister. I appreciate your prayers and support.

I will never forget my wonderful friends and colleagues at the Department of Botany's Center of Plant Biomass Utilization Research Unit (PBURU). Thank you for your support. You all worked diligently to guarantee my success, and I appreciate the outpouring of love. To my friends, Max, Taufik, Indah, Budi, Alvi, Evi, Rahmi, Namtan, Pla, Sai, Hang, Bet, Ploi, Tedtee, Susinya, Pipob, Wikrom, Gam, Oat, Triono, Widya, Putu, and Noinha,

Dwi Kusuma Wahyuni

TABLE OF CONTENTS

	Page
.....	iii
ABSTRACT (THAI).....	iii
.....	iv
ABSTRACT (ENGLISH).....	iv
ACKNOWLEDGEMENTS.....	v
TABLE OF CONTENTS.....	vi
LIST OF TABLES.....	xii
LIST OF FIGURES.....	xv
CHAPTER ONE.....	1
1.1 General Introduction.....	1
1.2 The objectives.....	3
1.3 The expected benefits.....	3
CHAPTER TWO.....	1
<i>In vitro</i> and <i>in vivo</i> antiplasmodial activities of leaf extracts from <i>Sonchus arvensis</i> L.	1
Abstract.....	1
2.1 Background.....	2
2.2 Materials and Methods.....	3
2.2.1 Plant collection and identification.....	3
2.2.2 Plant extraction.....	4
2.2.3 Phytochemical screening.....	4
2.2.4 Thin Layer Chromatography (TLC) Analysis.....	4

2.2.5 Antioxidant assay	4
2.2.6 <i>In vitro</i> antiplasmodial activity assay.....	5
2.2.7 Cytotoxicity test	6
2.2.8 <i>In vivo</i> antiplasmodial activity assay.....	7
2.2.9 Biochemical analysis	8
2.2.10 Data analysis.....	9
2.2.12 Ethics approval.....	9
2.3 Results	9
2.3.1 The extract yields and phytochemical screening.....	9
2.3.2 Terpenoid screening of the extracts of <i>Sonchus arvensis</i> L. by thin-layer chromatography (TLC).....	10
2.3.3 Antioxidant activities.....	11
2.3.4 <i>In vitro</i> antiplasmodial activity.....	12
2.3.5 Toxicity and selectivity index (SI)	12
2.3.6 <i>In vivo</i> antiplasmodial activity.....	13
2.3.7 Whole blood analysis of <i>P. berghei</i> infected mice.....	14
SGOT and SGPT levels.....	14
BUN and creatinine levels	15
Cytokine production	15
2.4 Discussion.....	16
2.5 Conclusion	21
CHAPTER THREE	29
Anti-SARS-CoV-2, antiplasmodial, antioxidant, and antimicrobial activities of crude extracts and homopterocarpin from heartwood of <i>Pterocarpus macrocarpus</i> Kurz. .	29

3.3.4 Antioxidant activity	47
3.3.5 <i>In vitro</i> antimalarial activity	48
3.3.6 <i>In vitro</i> toxicity and selectivity index.....	49
3.3.7 Antimicrobial activity.....	50
3.4 Conclusion.....	51
CHAPTER FOUR.....	59
<i>In silico</i> anti-SARS-CoV-2 and <i>in vitro</i> antiplasmodial activities of compounds from <i>n</i> -hexane fractions of <i>Sonchus arvensis</i> L. leaves.....	59
Abstract.....	60
4.1 Introduction.....	61
4.2 Methods	62
4.2.1 Plant Material Collection and Identification	62
4.2.2 Extraction.....	62
4.2.3 Thin Layer Chromatography (TLC).....	62
4.2.4 Purification and Isolation.....	62
4.2.5 Gas Chromatography-Mass Spectrophotometry (GC-MS).....	63
4.2.6 Sample Preparation of <i>in silico</i> anti-SARS-CoV-2 activity	64
4.2.7 Drug-likeness Identification	64
4.2.8 Bioactivity Prediction.....	64
4.2.9 Molecular Docking Simulation.....	65
4.2.10 Ligand-Protein Interactions and 3D Visualization.....	65
4.2.11 Molecular Dynamic Analysis.....	65
4.2.12 <i>In Vitro</i> antiplasmodial Assay	66
4.2.13 Cytotoxicity Assay and Selectivity index (SI).....	66

5.1.8 <i>In vitro</i> antimalarial assay.....	94
5.1.9 <i>In vitro</i> anticancer assay.....	95
5.1.10 Selectivity index (SI).....	95
5.1.11 Data analysis.....	95
5.2 Result.....	96
5.2.1 The number of <i>Aspergillus niger</i> spores during transformation culture of homopterocarpin from <i>Pterocarpus macrocarpus</i> Kurz. heartwood.....	96
5.2.2 Metabolite profiles by GC-MS during biotransformation.....	96
5.2.3 Biotransformation Compound.....	99
Demethylhomopterocarpin/ 3-Hydroxy-9-methoxycarpan/Medicarpin....	99
6-isopropenyl-4,8a-dimethyl-1,2,3,5,6,7,8,8a-octahydro-naphthalene-2-ol	
.....	102
5.2.4 Antioxidant activities.....	103
5.2.5 <i>In vitro</i> antimalarial activity.....	103
5.2.6 Selectivity index (SI).....	103
5.2.7 <i>In vitro</i> anticancer.....	103
CHAPTER SIX.....	105
Conclusion.....	105
APPENDIXES.....	107
.....	107
REFERENCES.....	165
VITA.....	170

LIST OF TABLES

	Page
Table 1. Experimental design of in vivo study for antiplasmodial activity and biochemical analysis.....	8
Table 2. Extraction yield of <i>Sonchus arvensis</i> L. leaf.....	10
Table 3. Phytochemical screening of <i>Sonchus arvensis</i> L. leaf extract.....	10
Table 4. In vitro antioxidant activity of <i>Sonchus arvensis</i> L. leaf extract.....	12
Table 5. In vitro antiplasmodial activity of <i>Sonchus arvensis</i> L. leaf extracts against <i>P. falciparum</i> strain 3D7.....	12
Table 6. In vitro toxicity and selectivity index (SI) of <i>Sonchus arvensis</i> L. leaf extract.....	13
Table 7. Parasitemia, growth, and inhibition percentage of <i>Sonchus arvensis</i> L. ethyl acetate extract against <i>Plasmodium berghei</i>	14
Table 8. Serum IL-10, TNF- α , SGOT, SGPT, BUN, and creatinine levels of mice infected with <i>P. berghei</i> strain ANKA after treatment with <i>S. arvensis</i> L. leaf ethyl acetate extract.....	16
Table 9. Phytochemical screening of <i>Pterocarpus macrocarpus</i> Kurz. heartwood extracts.....	38
Table 10. The yield of crystals at each step of crystallization of the n-hexane extract of <i>Pterocarpus macrocarpus</i> Kurz. heartwood.....	39
Table 11. Phytochemical components identified from GC/MS analysis of <i>Pterocarpus macrocarpus</i> Kurz. heartwood n-hexane extract at each crystallization cycle.....	41
Table 12. The observed ^1H and ^{13}C -NMR homopterocarpin (3,9-dimethoxy-pterocarpan) compound in CDCl_3	43
Table 13. Prediction results of target compound activity.....	44

Table 14. Simulation results of molecular docking with SARS-CoV-2 proteins.....	46
Table 15. In vitro antioxidant activity of <i>Pterocarpus macrocarpus</i> Kurz. heartwood extract.....	48
Table 16. In vitro antimalarial activity, in vitro toxicity, and selectivity index (SI) of <i>Pterocarpus macrocarpus</i> Kurz. heartwood extracts against <i>P. falciparum</i> strain 3D7 .	50
Table 17. Diameter of inhibition zone and percentage of inhibition of heartwood extract of <i>Pterocarpus macrocarpus</i> Kurz.	51
Table 18. Column chromatographic separation of <i>Sonchus arvensis</i> L. n-hexane extract.....	68
Table 19. Phytochemical components from GC-MS analysis of fractions 2-12 of <i>Sonchus arvensis</i> L. n-hexane extract.....	69
Table 20. Phytochemical components from GC-MS analysis of fractions 15–28 of <i>Sonchus arvensis</i> L. n-hexane extract.....	70
Table 21. Drug-likeness analysis of compounds from n-hexane fractions of <i>Sonchus arvensis</i> L. leaves.....	71
Table 22. Prediction of inhibitory activities of n-hexane fractions of <i>Sonchus arvensis</i> L. compounds	72
Table 23. Docking results of compounds contained by <i>Sonchus arvensis</i> L. n-hexane fraction with SARS-CoV-2 proteins	74
Table 24. Results of identification of molecular interactions of n-hexane fractions of <i>Sonchus arvensis</i> L. leaves	75
Table 25. The percent parasitemia, growth percentage, and inhibition percentage of fractions 5–12 of <i>Sonchus arvensis</i> L of n-hexane extract against <i>P. falciparum</i> strain 3D7.....	78
Table 26. The percent parasitemia, growth percentage, and inhibition percentage of fractions 15–28 of <i>Sonchus arvensis</i> L of n-hexane extract against <i>P. falciparum</i> strain 3D7.....	79

Table 27. In vitro toxicity and selectivity index (SI) of <i>Sonchus arvensis</i> L. extract	80
Table 28. Phytochemical components from GC/MS analysis of <i>Pterocarpus macrocarpus</i> Kurz. heartwood n-hexane extract in every crystallization.....	97
Table 29. ¹ H-(400MHz, CDCl ₃) chemical shift assignments of homopteroicarpin and (500MHz, CDCl ₃) medicarpin.....	100
Table 30. ¹³ C-(400MHz, CDCl ₃) chemical shift assignments of homopteroicarpin and (125MHz, CDCl ₃) medicarpin.....	101
Table 31. In vitro antioxidant activity of <i>Pterocarpus macrocarpus</i> Kurz. heartwood extract.....	103
Table 32. In vitro antimalarial activity of bioactive compound from homopteroicarpin transformation by <i>Aspergillus niger</i> against <i>P. falciparum</i> strain 3D7	104
Table 33. In vitro anticancer activity of bioactive compound from homopteroicarpin transformation by <i>Aspergillus niger</i> against hepatocyte-derived cellular carcinoma cell line (Huh7it-1cells).....	104

LIST OF FIGURES

	Page
Figure 1. Chromatogram of <i>Sonchus arvensis</i> L. extracts TLC. A. Day light, B. UV 254nm, C. UV366nm, D. After sprayed by p-anisaldehyde sulfuric acid (the purple spot is terpenoid), I. n-Hexane extract, II. Ethyl acetate extract, III. Ethanol extract....	11
Figure 2. Chromatogram of n-hexane extracts of <i>Pterocarpus macrocarpus</i> Kurz. heartwood at each crystallization cycle. A. n-hexane extract, B. first crystallization, C. second crystallization, D. third crystallization, E. fourth crystallization. black arrow: 2-naphthalenemethanol; green arrow: homopterocarpin; blue arrow: pterocarpin; yellow arrow: stigmasterol; red arrow: γ -sitosterol.....	40
Figure 3. The structure of homopterocarpin	43
Figure 4. The 3D visualization of the molecular docking results. Ligands are indicated by black circles (A) Stigmasterol_Helicase (B) Stigmasterol_RdRp (C) Stigmasterol_Mpro (D) Stigmasterol_RBD-Spike.	45
Figure 5. The 2D visualization of the molecular interactions. (A) Stigmasterol_Helicase, (B) Stigmasterol_RdRp, (C) Stigmasterol_Mpro, (D) Stigmasterol_RBD-Spike.....	47
Figure 6. Chromatogram of <i>Sonchus arvensis</i> L. extract. (A) Solvent only (n-hexane : ethyl acetate at 4:1). (B) UV light at 254 nm. (C) UV light at 366 nm. (D) Anisaldehyde sulfuric acid (the purple spot at 0.35 is a terpenoid).....	67
Figure 7. Representative chromatogram of fractions 5–12 of <i>Sonchus arvensis</i> L. n-hexane extract. Red arrow, octadecyl ester exadecenoic acid; green arrow, hexadecyl ester tetradecanoic acid.....	69
Figure 8. Representative chromatogram of fractions 15–28 of <i>Sonchus arvensis</i> L. n-hexane extract. Red arrow, hexacosanol; blue arrow, β -amyirin; green arrow, lupeol; yellow arrow, α -amyirin; brown arrow, botulin; black arrow, taraxasterol.....	70

- Figure 9. The 3D visualizations of molecular docking results. (A) α -Amyrin-Helicase, (B) α -Amyrin-Spike-RBD, (C) β -Amyrin-RdRp, and (D) β -Amyrin-M^{PRO} 75
- Figure 10. RMSF values of protein-ligand complexes. (A) α -Amyrin_Helicase, (B) α -Amyrin_Spike-RBD, (C) β -Amyrin_RdRp, and (D) β -Amyrin_M^{PRO}..... 76
- Figure 11. Protein 3D structures determined by molecular dynamic simulation. (A) α -Amyrin-Helicase, (B) α -Amyrin-Spike-RBD, (C) β -Amyrin-RdRp, and (D) β -Amyrin-M^{PRO}. 76
- Figure 12. Spores number of *Aspergillus niger* during biotransformation culture of homopterocarpin from *Pterocarpus macrocarpus* Kurz. heartwood..... 96
- Figure 13. Chromatogram profile of biotransformation culture of homopterocarpin from *Pterocarpus macrocarpus* Kurz. heartwood by *Aspergillus niger*. A. First day of culture, B. Third day of culture, C. Fifth day of culture, D. Seventh day of culture. 1. Glycerine, 2. 4H-Pyran-4-one,2,3-dihydro-3,5-dihydroxy-6-methyl-, 3. 6-Isopropenyl-4,8a-dimethyl-1,2,3,5,6,7,8,8a-octahydro-naphthalen-2-ol, 4. 9-Octadecenamamide, (Z)-, 5. medicarpin..... 98
- Figure 14. The structure of homopterocarpin (1) and medicarpin (2)..... 99
- Figure 15. Chromatogram profile of 6-isopropenyl-4,8a-dimethyl-1,2,3,5,6,7,8,8a-octahydro-naphthalene-2-ol by GC-MS. A. GC-MS spectra with retention time, B. 6-isopropenyl-4,8a-dimethyl-1,2,3,5,6,7,8,8a-octahydro-naphthalene-2-ol of spectra.. 102

CHAPTER ONE

1.1 General Introduction

WHO estimates that around 80% of the world population use natural compounds from medicinal plant (Kumar et al.). Because the phenomena, it is needed a specific effort to explore the natural material well, not only for inhibiting but also for providing effective cures without causing excessive side effect (A. Younis et al., 2016). Natural products are structurally and biologically interesting metabolites, but they may be isolated in a small amount (Hegazy et al., 2015). Some bioactive compounds have very bioavailability but low solubility and structural instability (An et al., 2017). A lot of efforts are being made to improve the quality of natural compound, such as biotransformation (Kang et al., 2019; Parshikov & Sutherland, 2014).

Biotransformation is a biocatalytic process for the conversion or modification of organic chemicals to potential products using an enzyme or whole cells (Anwar et al., 2019) or structural modification in chemical compound by organism / enzyme that lead to the formation of molecules with greater polarity (Singh, 2017). In recent years, microbial transformation is progressing significantly from limited interest into the highly active area in green chemistry including preparation of pharmaceutical products (A. M. Younis et al., 2016), chemical and food industries because of numerous advantages compared to chemical synthesis (Parshikov & Sutherland, 2014).

Microbial-transformation have been extensively employed in drug discovery and development, mainly due to their ability to produce regio- and stereo-selective products. In many cases, the use of toxic and expensive chemical catalyst has been substituted by biotransformation, which is eco-friendly and cost-effective, and based on readily available biological catalysts. Diverse classes of organic compound have been successfully transformed into their structurally novel and biologically active metabolites by applying biotransformation methods (Hussain et al., 2016). In the field of pharmaceutical research and development, biotransformation investigated found many analogous compounds. They exhibited more potent pharmacological activities

(Asakawa et al., 2018; Wu et al., 2015). The resulting products of biotransformation may have more useful pharmacological or other biochemical activity. It may be less toxic than the starting material (Singh, 2017).

Aspergillus niger, described as a species by van Tieghem in 1867, is a widespread aerobic fungus that grows on a large variety of substrates (Chen et al., 2017). *A. niger* strains produce enzymes such as hydrolases, amylases, pectinases, and chitinases (Parshikov & Sutherland, 2014; Yang et al., 2017). Some previous studies have shown that *A. niger* transform a lot of substrates, but never been any report about biotransformation natural products from *Sonchus arvensis* L. and *Pterocarpus macrocarpus* Kurz., therefore *A. niger* will be applied to transform bioactive compound from *S. arvensis* L. and *P. macrocarpus* Kurz. in this study.

S. arvensis L. belongs to Asteraceae. It is spreading throughout the world and highly invasive. Morpho-anatomical characters of *S. arvensis* L. in Indonesia has herbaceous habitus and erect, annual herb, but there is perennial one in Pakistan, reaches 64 cm tall (Suharyanto et al., 2019). *S. arvensis* L. has chemical compounds such as flavonoids (Khan & Omoloso, 2003; Rohaeti et al., 2011; Seal, 2016), coumarin, taraxasterol, phenolic acids, ascorbic acid (Seal, 2016) and terpenoids (Rumondang, 2013). Many studies show that *S. arvensis* L. possess antioxidant activity (Khan & Omoloso, 2003), anti-uric acid (Hendriani et al., 2016), anti-inflammatory activity and inhibitory effect in locomotion and gastro intestinal motility (Hendriani et al., 2016; Poudel et al., 2015), immunomodulatory activity and antibacterial activity (Rumondang, 2013). Evaluation of teratogenic effect of *S. arvensis* L. extract did not show teratogenic effect (Sukandar & Safitri, 2016). Several compounds have been successfully isolated from *S. arvensis* L., including sesquiterpene lactones which have antimicrobial activity (Xia et al., 2009), sesquiterpenes and quinic acid esters which have antioxidant activity, kumoric acid, and a flavonoid class of chalcone (Putra et al., 2013).

P. macrocarpus Kurz., is valued globally for its beauty, wood quality, medicinal properties and valuable bioactive compound content (Jiao, 2018). *P. macrocarpus* Kurz. belongs to Fabaceae. It mainly grows in Laos, Thailand, Myanmar, and Vietnam. The application value of *P. macrocarpus* Kurz. lies in heartwood that

can give people visual enjoyment and psychological pleasure regarding to a unique woody flavour, promoting human blood circulation and enhancing the body's immune function (K.C.A et al., 2017), antimicrobial activity (Chen et al., 2017), treating cough and phlegm, detoxification and diuretic (Gao et al., 2017), anti-Alzheimer's disease and antispasmodic properties, anticancer (Chen et al., 2017), immunomodulator activity (Mohd Ataa et al., 2017), and insect antifeedants (Morimoto et al.). Macrocarposide, (-)-homopterocarpin, (-)-hydroxy-homopterocarpin, (+)-pterocarpol have been isolated from *P. macrocarpus* Kurz. (Abdelhamid & Maa, 2019).

In this research, natural product from *S. arvensis* L. and *P. macrocarpus* Kurz. was used for antioxidant, atiplasmodial, antimicrobial and anti-SAR-CoV-2 assay (Chapter 2-4). Bioactive compound from *P. macrocarpus* Kurz., homopterocarpin has been transformed by *A. niger* to medicarpin with anticancer activity (Chapter 5). This report provides remarkable information about anti-SAR-CoV-2, antimalarial, antimicrobial, antioxidant and anticancer activities with low toxicity of natural products from *S. arvensis* L. and *P. macrocarpus* Kurz.. Moreover, it could be expected to provide data for the further use of these natural products as drug candidates for infectious diseases therapy with positive complementary effects and safety.

1.2 The objectives

The specific objectives of this study include: (i) to isolate and identify bioactive compound from *S. arvensis* L. and *P. macrocarpus* Kurz. (Chapter 2-4), (ii) to transform selected bioactive compounds by *Aspergillus niger* (Chapter 5), (iii) to determine bioactivities of selected bioactive compounds before and after biotransformation (Chapter 2-5).

1.3 The expected benefits

The result of the study will contribute to the basic and applied knowledge of bioactive compounds from *S. arvensis* L., and *P. macrocarpus* Kurz., including their pharmaceutical potential to be used as a drug in the future.

CHAPTER TWO

***In vitro* and *in vivo* antiplasmodial activities of leaf extracts from *Sonchus arvensis* L.**

Dwi Kusuma Wahyuni^{1,2**}, Sumrit Wacharasindhu³, Wichanee Bankeeree¹, Sri Puji Astuti Wahyuningsih², Wiwied Ekasari⁴, Hery Purnobasuki², Hunsu Punnapayak¹, and Sehanat Prasongsuk^{1,2*}

¹Plant Biomass Utilization Research Unit, Department of Botany, Faculty of Science, Chulalongkorn University, Bangkok, 10330 Thailand.

²Department of Biology, Faculty of Science and Technology, Universitas Airlangga Surabaya, East Java, 60115, Indonesia.

³Department of Chemistry, Faculty of Science, Chulalongkorn University, Bangkok, 10330 Thailand.

⁴Department of Pharmaceutical Sciences, Faculty of Pharmacy, Universitas Airlangga, Surabaya, East Java, 60115, Indonesia.

^{#a}Address: Department of Botany, Faculty of Science, Chulalongkorn University, Bangkok, 10330 Thailand. Tel: +662185485; Fax: +6622528979

^{#b}Address: Department of Biology, Faculty of Science and Technology, Airlangga University Surabaya, East Java, 60115, Indonesia. Tel: +6231 5936501. Fax: +62315936502.

*Corresponding author:

Email: Sehanat.p@chula.ac.th.

**Co-corresponding author:

Email: dwi-k-w@fst.ac.id

Abstract

Background: Malaria continues to be a global problem due to the limited efficacy of current drugs and the natural product is a potential source for discovering the new antimalarial agents. Therefore, the aims of this study were to investigate phytochemical properties, cytotoxic effect, antioxidant, and antiplasmodial activities of *Sonchus arvensis* L. leaf extracts both *in vitro* and *in vivo*.

Methods: The extracts from *S. arvensis* L. leaf were prepared by successive maceration with *n*-hexane, ethyl acetate, and ethanol, and then subjected to quantitative phytochemical analysis using standard methods. The antimalarial activities of crude extracts were tested *in vitro* against *Plasmodium falciparum* 3D7 strain while the Peter's 4-day suppressive test model with *P. berghei*-infected mice was used to evaluate the *in vivo* antiplasmodial activities, hepatoprotective, nephroprotective, and immunomodulatory. The cytotoxic tests were also carried out using human hepatic cell lines in [3(4,5-dimethylthiazol-2-yl)-2,5-diphenyltetrazolium bromide] (MTT) assay.

Result: The *n*-hexane, ethyl acetate, and ethanolic extract *in vitro* antiplasmodial activity of *S. arvensis* L. leaf exhibited a good activity, with IC₅₀ values were 5.119±3.27, 2.916±2.34, and 8.026±1.23 µg/mL, respectively. Each of the extracts also exhibited high antioxidants with low cytotoxic effects. Furthermore, the ethyl acetate extract showed *in vivo* antiplasmodial activity with ED₅₀ = 46.31±9.36 mg/kg, body weight, as well as hepatoprotective, nephroprotective, and immunomodulatory activities in mice infected with *P. berghei*.

Conclusion: This study highlighted the antiplasmodial activities of *S. arvensis* L. leaf ethyl acetate extract against *P. falciparum* and *P. berghei* as well as the antioxidant, nephroprotective, hepatoprotective, and immunomodulatory activities with low toxicity. These results have the potential to be developed into a new antimalarial drug candidate. However, the compounds and transmission-blocking strategies for malaria control of *S. arvensis* L. extracts are essential for further study.

Keywords: Antioxidant, Antiplasmodial, Hepatoprotective, Immunomodulator, Nephroprotective, Malaria, *Plasmodium berghei*, *Plasmodium falciparum*, *Sonchus arvensis* L.

2.1 Background

Malaria is an endemic disease in tropical areas of Asia, Africa, and Central and South America, and is known to spread even in vaccinated populations [1]. In 2020, malaria accounted for 241 million new infections and 627 thousand deaths worldwide in 87 endemic countries. There were 14 million more malaria cases and

47,000 more deaths compared to 2019 [2]. Therefore, one of the United Nations Millennium Development Goals (MDGs) is to reduce the incidence and subsequent morbidity and mortality associated with malaria [2]. The malaria elimination target in Indonesia is 75% of the country, with no high-endemic district by the end of 2024 [3]. However, the significant obstacles to the treatment and prognosis of malaria are its resistance to chloroquine [4,5] and artemisinin-based combination therapy [2]. There is an urgent need to develop new antimalarial drugs and many researchers are currently exploring the efficacy of synthetic and natural products [6].

An estimated 80% of the global population uses natural products to treat various illnesses and diseases [7,8]. In the case of malaria, 75% of patients have been reported to treat with traditional medicines derived from various plant sources, including *Cinchona succirubra* L., as well as relatively newer medicines, such as artemisinin, which is produced from *Artemisia annua* L. [9]. In Indonesia, *Sonchus arvensis* L., a highly invasive species of the family Asteraceae, is used as a traditional medicinal plant for malaria treatment [10]. This plant contains various active compounds including flavonoids, saponins, and polyphenols [11], which have been reported for moderate to high antioxidant [12], hepatoprotective [13], nephroprotective [14], anti-inflammatory [15], and antibacterial activities [16-18]. Although *S. arvensis* L. has pharmaceutical benefits, it has never been evaluated for *in vivo* treatment of malaria.

The aim of the present study was to determine the *in vitro* and *in vivo* antiplasmodial activities of crude extracts from *S. arvensis* L. leaf, as well as the *in vitro* toxicity, *in vitro* antioxidant activities, and whole blood analysis of mice infected with *Plasmodium berghei*. The study results provide useful information regarding the antiplasmodial activity of a *S. arvensis* L. crude extract.

2.2 Materials and Methods

2.2.1 Plant collection and identification

S. arvensis L. was from Taman Husada Graha Famili (Medicinal Plant Graden of Graha Famili) Surabaya, East Java, Indonesia. The plant was cultivated in private field and harvested at 2–3 months before the generative stage. The leaves were green and

healthy, with no indications of damage due to insects or microbes. The plant material used was confirmed by botanist researcher at Purwodadi Botanical Garden, Indonesian Institute of Sciences, Purwodadi, East Java, Indonesia (number of determination 1020/IPH.3.04/HM/X/2019). The voucher specimen was deposited in the Plant Systematics Laboratory, Department of Biology, Faculty of Science and Technology, Universitas Airlangga (No. SA.0110292021).

2.2.2 Plant extraction

The leaf of *S. arvensis* L. was air-dried and then ground into a powder (60-mesh size sieves). Each 1 kg of powder was separately macerated with different solvents including *n*-hexane, ethyl acetate, and ethanol for 24 h at room temperature ($28\pm 2^\circ\text{C}$) three times, filtered with filter paper (pore diameter 110 mm; Merck KGaA, Darmstadt, Germany), and then evaporated in a rotary evaporator at 60°C to acquire crude extracts. The yields of the extracts (w/w) were measured prior to storage at 4°C .

2.2.3 Phytochemical screening

The crude extracts of *S. arvensis* L. leaf was screened for phytochemical content by standard methods including the Wilstatter "cyanidin" test for flavonoids, Mayer's test for alkaloids, the ferric chloride test for polyphenols, the Liebermann–Burchard test for terpenoids, and the foam test for saponins [19].

2.2.4 Thin Layer Chromatography (TLC) Analysis

Five mg of each crude extract of *S. arvensis* L leaf were dissolved in 100 μL of *n*-hexane, ethyl acetate, and ethanol, respectively. Aliquots of samples (5 μL) were spotted and allowed to dry on a TLC plate (Silica gel GF254). The plate was developed with *n*-hexane: ethyl acetate (4:1) as the mobile phase. Detection of compounds was achieved by spraying with *p*-anisaldehyde sulfuric acid reagent [18], then heating at 105°C for 10 min or until the colored bands appeared.

2.2.5 Antioxidant assay

Antioxidant activity was evaluated by a method of 2,2-diphenyl-1-picryl-hydrazyl-hydrate (DPPH) assay [20]. In brief, 100 μL of methanolic DPPH reagent (0.2 mM) was mixed with 100 μL of each sample in methanol at different concentrations (1.75, 3.15, 6.25, 10, 12.5, 15, 25, 35, 50, 75, 100, 150, and 200 $\mu\text{g}/\text{mL}$) and methanol as the

control. The mixtures were incubated for 30 min in the dark at room temperature and the absorbance was measured at 517 nm. The assay was conducted in twofold wells for each sample and control for calculating the IC₅₀ value and replicated three times.

The inhibition of DPPH was calculated using the following equation:

$$\text{DPPH inhibition (\%)} = (A_{\text{control}} - A_{\text{sample}}) / A_{\text{control}} \times 100\%. \quad (1)$$

where A_{sample} is the absorbance of the sample and A_{control} is the absorbance of the DPPH reagent at the wavelength of 517 nm. The percentage of inhibition results at different concentrations were then plotted and regressed linearly to obtain the IC₅₀ values of DPPH. The IC₅₀ value was calculated as the mean and standard deviation from three replication.

2.2.6 *In vitro* antiplasmodial activity assay

In this study, the antiplasmodial activity of leaf extracts was investigated against the chloroquine-sensitive strain of *P. falciparum* (3D7). The parasite was cultured in human O^{Rh+} red blood cells according to the method of Trager and Jensen [21] using Roswell Park Memorial Institute 1640 (RPMI-1640) medium supplemented with 50 µg/mL hypoxanthine, 2 mg/mL sodium bicarbonate (NaHCO₃), 5.94 g/L of N-2-hydroxyethyl piperazine-N-2-ethane sulfonic acid (HEPES) and 10% serum blood group O^{Rh+}. The parasitized culture suspension containing 1% parasitemia was prepared in complete RPMI-1640 and 150-µL volume of this was dispensed in a 24-well microplate (5% hematocrit). The extracts were dissolved in dimethyl sulfoxide (DMSO), diluted with medium to obtain the required concentrations (0.01, 0.1, 1, 10, and 100 µg/mL), and aliquoted (50 µL) into each well of parasitized culture suspension. The parasitized cultures without plant extract (DMSO) served as negative controls whereas cultures with chloroquine diphosphate served as positive controls. The plates containing parasite cultures were incubated in an incubator (at 37°C, 5% CO₂, 95% humidity) for 48 h. The treatments were carried out in three times (n=3). Afterward, the suspensions were collected, thinly smeared on glass slides, fixed with methanol, and stained with 10% Giemsa. The number of parasites was counted under a microscope and compared with the negative control to determine the extent of parasite growth inhibition. The equation

for calculating parasitemia, inhibition, and growth percentage used the equation method as described in a previous study [18].

The percentage of parasitemia was calculated using the formula:

$$\% \text{ Parasitemia} = \frac{\sum \text{infected eritrocyte}}{5000 \text{ of total eritrocyte}} \times 100\% \quad (2)$$

The percentage of inhibition was counted using the equation:

$$\% \text{ Inhibition} = 100\% - \left[\frac{X_p}{X_k} \times 100\% \right] \quad (3)$$

The percentage of growth was calculated using the formula:

$$\% \text{ Growth} = \% \text{ parasitemia Un} - \% \text{ parasitemia Do} \quad (4)$$

Where:

Xp = Treatment parasitemia

Xk = Negative control parasitemia

Un = % parasitemia in each concentration

Do = % parasitemia at the start

The probit analysis was conducted to calculate the IC₅₀ values.

2.2.7 Cytotoxicity test

Cytotoxicity of extracts was assessed by the method of 3-[4, 5-dimethylthiazol-2-yl] 2,5-diphenyl tetrazolium bromide (MTT) assay as described by Fosenca et al. [22]. Dimethyl sulfoxide (DMSO) was used to dissolve the extracts, then they were diluted with medium to obtain the required concentrations (6.25, 12.5, 25, 50, 100, 200, 400, 600, 800, and 1000 µg/mL). hepatocyte-derived cellular carcinoma cells (Huh7it-1 cells) line were cultured in complete Dulbecco's modified Eagle's medium (DMEM) supplemented with 1% (v/v) glutamine (200 mM) at 37°C under an atmosphere of 5% of carbon dioxide atmosphere and 95% humidity. The culture was conducted three times. The cell numbers were determined by measuring the absorbance at 560 nm and 750 nm using multiplate reader and the viability were assessed.

The viability of cells was calculated using the equation:

$$\% \text{ of viability} = (A_{\text{sample}}/A_{\text{control}}) \times 100\% \quad (5)$$

where A_{sample} was the absorbance sample at 560 nm-Absorbance sample at 750 nm and A_{control} was the absorbance DMEM medium. The percentage of cell viability was

then plotted and regressed linearly to obtain the CC_{50} values. The selectivity index (SI) values were calculated based on the ratio between the CC_{50} value of cytotoxicity and antiplasmodial activity *P. falciparum* 3D7 from each extract (IC_{50}).

2.2.8 *In vivo* antiplasmodial activity assay

The extract with the highest antiplasmodial activity against *P. falciparum* 3D7 was selected to subsequently analyze the antiplasmodial activity against *P. berghei* (the mice-infected Plasmodium) with Peter's method [23]. The strain of *P. berghei* ANKA was obtained from the Eijkman Institute of Molecular Biology (Jakarta, Indonesia). Blood infected with *P. berghei* ANKA was taken from mice with 20% parasitemia and diluted with phosphate-buffered saline. Swiss mice *Mus musculus* of BALB/c strain (male; body weight 25 ± 3 g; 6–8 weeks old) were intraperitoneally injected with 0.2 mL blood (1×10^6 ANKA parasitized erythrocytes) and randomly divided ($n = 7$ per group) into four experimental groups and three control groups (normal, negative, and positive control). The experimental groups were orally treated with 0.25 mL single dose of 1, 10, 100, or 200 mg/kg BW of leaf extract (in 0.5% sodium carboxymethyl cellulose (Na-CMC)) two times per day for four days for antiplasmodial assay and continued seven days for biochemical analysis. The negative and positive control groups were treated with 0.5% Na-CMC suspension and 10 mg/kg BW of chloroquine diphosphate, respectively. The normal control group was the uninfected and untreated mice group (Table 1). On each day, blood was collected from the tail vein of each mouse, thinly smeared on a glass slide, fixed with methanol, and then stained with Giemsa. The slides were then observed under a microscope to calculate the percentage of parasitemia, inhibition, and growth. The formula of them used as described in *in vitro* antiplasmodial activity against *P. falciparum* 3D7. The median effective dose or effective dose for 50% of the population (ED_{50}) was calculated with Probit analysis. The ED_{50} was calculated from each replication, and then averaged getting the mean and deviation standard.

Table 1. Experimental design of *in vivo* study for antiplasmodial activity and biochemical analysis

Experiment Group	<i>Plasmodium berghei</i> -infected mice	Treatment	Days	Replication
Normal Control	-	Na-CMC	7	7
Positive Control	+	Chloroquine-phosphate	7	7
Negative Control	+	Na-CMC	7	7
P1	+	1 mg/kg BW	7	7
P2	+	10 mg/kg BW	7	7
P3	+	100 mg/kg BW	7	7
P4	+	200 mg/kg BW	7	7

Note: Mice blood sample was analyzed for the percentage of parasitemia for 4 days except for the normal control and biochemical analysis on the seventh day for all treatment and control.

2.2.9 Biochemical analysis

After seven-day treatments, blood samples (0.5-0.75 mL) were collected from the left ventricle of each mouse into 1.5-mL microtubes and left standing at room temperature for 2 h. Then, serum was isolated by centrifugation at 3000 rpm for 20 min. The levels of serum glutamic-oxaloacetic transaminase (SGOT) and serum glutamic-pyruvic transaminase (SGPT) in obtained serum were measured using commercial enzyme-linked immunosorbent assay (ELISA) kits (DiaSys Diagnostic System, Holzheim, Germany) to assess the hepatoprotective effects of the selected extract on infected mice. For analyzing nephroprotective effects, blood urea nitrogen (BUN) and creatinine levels were measured using commercial ELISA kits (DiaSys Diagnostic System, Holzheim, Germany). The level of tumor necrosis factor-alpha (TNF- α) and interleukin 10 (IL-10) in serum was also analyzed to investigate the

immune response of treated/control mice using commercial ELISA kits (BioLegend, San Diego, CA, USA). The replication of samples was four to seven times (Table 1).

2.2.10 Data analysis

Data are expressed as the mean \pm standard deviation (SD). The IC_{50} of antioxidant and CC_{50} of cytotoxicity were counted using regression linearly (Microsoft Excel). The Probit analysis was conducted to calculate the IC_{50} and ED_{50} values. Statistical significance was determined with the one-way analysis of variance (ANOVA) continued with Duncan Multiple Range Test (DMRT) for IL-10 and TNF- α , with a nonparametric independent *t*-test for SGOT and SGPT, and Kruskal–Wallis continued with Mann Whitney test for BUN and creatinine data. The level of significance was set at 0.05. All statistical analyses were conducted using IBM SPSS Statistics for Windows, version 20.0. (IBM Corporation, Armonk, NY, USA).

2.2.12 Ethics approval

This study was carried out in strict accordance with the recommendations in the Guide for the Care and Use of Laboratory Animals of the National Institutes of Health. The study protocol was approved by the Institutional Animal Care and Use Committee of the Faculty of Veterinary Medicine of Universitas Airlangga (Surabaya, East Java, Indonesia) (approval no. 499/HRECC.FODM/XI/2020). All surgery was performed under sodium pentobarbital anesthesia, and all efforts were made to minimize suffering.



2.3 Results

2.3.1 The extract yields and phytochemical screening

The dried leaf was successively macerated and each kilogram of dried leaf yielded 59.26 ± 2.04 g of ethanol extract, 10 ± 1.1 g of ethyl acetate extract, and 25.9 ± 5.5 g of *n*-hexane extract (Table 2).

Table 2. Extraction yield of *Sonchus arvensis* L. leaf

No.	Extract	Yield (g/kg)
1	<i>n</i> -Hexane	25.9±5.5
2	Ethyl acetate	10±1.1
3	Ethanol	59.26±2.04

Note: The data were represented as mean ± standard deviation (SD), n=3.

Secondary metabolites including terpenoids, flavonoids, and alkaloids were present in all extracts. However, saponins were only present in the ethanol extract, and polyphenols were present in ethanol and ethyl acetate extracts (Table 3).

Table 3. Phytochemical screening of *Sonchus arvensis* L. leaf extract

No	Phytochemical	Marker	<i>n</i> -Hexane	Ethyl acetate	Ethanol
1	Terpenoids	Deep green color	++	+++	+
2	Flavonoids	Pink orange or violet	+	++	++
3	Alkaloids	White precipitated	+	+	+
4	Saponin	Foam	-	-	++
5	Polyphenol	Blackish green	-	+	++

Note: ++, Strongly positive; +, Weakly positive; -, Not determined

2.3.2 Terpenoid screening of the extracts of *Sonchus arvensis* L. by thin-layer chromatography (TLC)

The *n*-hexane, ethyl acetate, and ethanol extracts of *Sonchus arvensis* L. were observed by TLC and there were two visible spots in daylight and under 254-nm UV light (R_f value = 0.12 and 0.18). Under 366-nm UV light, there were five separate stains with R_f values of 0.14, 0.24, 0.19, 0.35, and 0.53. After staining using *p*-anisaldehyde sulfuric acid, three separate purple stains were seen, with R_f values of 0.31, 0.59, and 0.71 (Fig. 1).

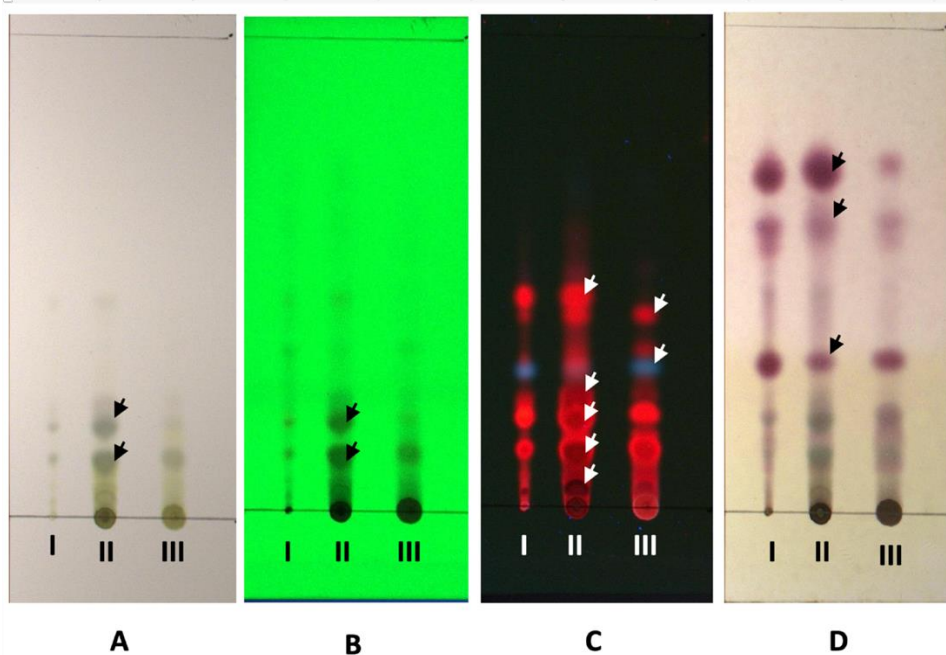


Figure 1. Chromatogram of *Sonchus arvensis* L. extracts TLC. A. Day light, B. UV 254nm, C. UV366nm, D. After sprayed by p-anisaldehyde sulfuric acid (the purple spot is terpenoid), I. n-Hexane extract, II. Ethyl acetate extract, III. Ethanol extract

2.3.3 Antioxidant activities

The DPPH assay was conducted to assess antioxidant activities. The IC_{50} value of all extracts was shown in Table 4. All extracts possessed antioxidant activities. From lowest to highest, the IC_{50} values were 8.27 ± 4.93 , 12.36 ± 10.40 , 31.35 ± 3.27 , and 108.59 ± 11.24 $\mu\text{g/mL}$ for the ethyl acetate, ethanol, methanol, and *n*-hexane extracts, respectively. Furthermore, the IC_{50} of ascorbic acid as standard was 22.63 ± 1.40 $\mu\text{g/mL}$ (Appendix 1: Supplementary Data I).

Table 4. *In vitro* antioxidant activity of *Sonchus arvensis* L. leaf extract

No.	Extract	Antioxidant activity (IC ₅₀ , µg/mL)
1.	<i>n</i> -Hexane	108.59±11.24
2.	Ethyl acetate	8.27±4.93
3.	Ethanol	12.36±10.40
4.	Methanol	31.35±3.27
5.	Ascorbic acid	22.63±1.40

Note: The data were represented as mean ± standard deviation (SD), n=3.

2.3.4 *In vitro* antiplasmodial activity

The IC₅₀ values of all extracts of *Sonchus arvensis* L. leaf at various doses were shown in Table 4. As determined by the IC₅₀ values, the ethyl acetate extract had the highest *in vitro* antimalarial activity, followed by the *n*-hexane and ethanol extracts (2.916±2.34, 5.119±3.27, and 8.026±1.23 µg/mL, respectively) (Table 5) (Appendix 1: Supplementary data II).

Table 5. *In vitro* antiplasmodial activity of *Sonchus arvensis* L. leaf extracts against *P. falciparum* strain 3D7

No.	Extract	% Inhibition at each concentration (µg/mL)						IC ₅₀ (µg/mL)
		100	10	1	0.1	0.01	0.001	
1	<i>n</i> -Hexane	100±0	53.81±0.65	45.21±1.94	35.79±3.9	31.73±3.73	-	5.119±2.34
2	Ethyl acetate	100±0	75.82±1.93	65.68±3.09	44.89±9.73	34.84±1.49	-	2.916±3.27
3	Ethanol	93.6±0.53	27.54±2.51	23.50±1.11	13.09±1.49	6.94±0.36	-	8.026±1.23
4	Chloroquine diphosphate	100±0	100±0	100±0	79.76±4.51	40.49±5.29	17.17±2.31	0.014±0.0021

Note: The data were represented as mean ± standard deviation (SD), n=3.

2.3.5 Toxicity and selectivity index (SI)

The toxicity of all *Sonchus arvensis* L. extracts to hepatocytes was determined. From highest to lowest, the IC₅₀ values of the extracts were 1420.88±20.88, 437.39±7.46, and 778.77±10.53 µg/mL for *n*-hexane, ethanol, and ethyl acetate extract,

respectively (Table 6). Then, the SI was calculated by comparing the toxicity and in vitro antimalarial activity. From highest to lowest, the SI values were 277.57 ± 5.77 , 150 ± 3.62 , and 97.03 ± 13.13 for *n*-hexane, ethanol, and ethyl acetate extract, respectively (Table 6) (Appendix 1: Supplementary Data III).

Table 6. In vitro toxicity and selectivity index (SI) of *Sonchus arvensis* L. leaf extract

No.	Extract	<i>In Vitro</i> Toxicity, IC ₅₀ (µg/mL)	Selectivity Index (SI)
1	<i>n</i> -Hexane	1420.88±20.88	277.57±5.77
2	Ethyl Acetate	437.39±7.46	150±3.62
3	Ethanol	778.77±10.53	97.03±13.13

Note: The data were represented as mean ± standard deviation (SD), n=3.

2.3.6 *In vivo* antiplasmodial activity

The *in vivo* antimalarial activity of the ethyl acetate extract was also determined. As shown in Table 7, the parasitemia rates decreased with increasing doses. The inhibition rates of doses at 1, 10, 100, and 200 mg/kg BW were 0%, $32.86 \pm 7.5\%$, $56.32 \pm 2.64\%$ and $77.48 \pm 2.93\%$, respectively. Probit analysis determined that the ED₅₀ value of the ethyl acetate extract was 46.31 ± 9.36 mg/kg BW. This result was significant as compared to the negative control (Na-CMC) (Appendix 1: Supplementary data IV).

Table 7. Parasitemia, growth, and inhibition percentage of *Sonchus arvensis* L. ethyl acetate extract against *Plasmodium berghei*

Sample	Dose (mg/kg)	Mean % Parasitemia		Mean % growth	Mean % inhibition	ED ₅₀ (mg/kg)
		Day 0	Day 4			
Ethyl acetate extract of <i>S. arvensis</i> L.	1	1.51± 0.07	7.44± 0.21	5.93± 0.17	-	46.31±9.36
	10	1.42± 0.07	5.39± 0.43	3.97± 0.44	32.86± 7.50	
	100	1.51± 0.07	5.09± 0.56	2.57± 0.12	56.32± 2.64	
	200	1.46± 0.09	3.96± 0.68	1.36± 0.12	77.48± 2.93	
Na-CMC	-	1.44± 0.12	7.36± 0.24	5.91± 0.31	-	
Chloroquine diphosphate	10	1.48± 0.09	0.02± 0.01	-	-	

Noted: The data were represented as mean ± standard deviation (SD), n=7. The Na-CMC: sodium carboxymethyl cellulose.

2.3.7 Whole blood analysis of *P. berghei* infected mice

Mice infected with *P. berghei* were orally administered ethyl acetate extract of *S. arvensis* L. two times per day for 7 days. Afterward, blood samples were collected to determine the hepatoprotective (SGOT and SGPT), nephroprotective (BUN and creatinine), and immunomodulatory (IL-10 and TNF- α) effects (Table 8).

SGOT and SGPT levels

SGOT and SGPT are produced in response to liver injury. Higher serum levels of SGOT and SGPT indicate more significant liver injury. As compared to the negative control (201.87 U/L), serum SGOT levels of mice infected with *P. berghei* were significantly decreased by treatment with ethyl acetate extract at 1, 10, 100, and 200 mg/kg BW (100.68, 73.85, 69.82, and 33.11 U/L, respectively, $p<0.05$). However, there was no different significant between normal control (40.76 U/L), positif (32.92 U/L), and treatment groups (200 mg/kg BW),

Furthermore, as compared to negative control (24.13 U/L) and treatment with ethyl acetate extract at 1 mg/kg BW (32.36 U/L) and 10 mg/kg BW (22.74 U/L), serum SGPT levels were significantly decreased in the groups treated with 100 and 200 mg/kg BW (13.45 and 2.75 U/L, respectively) as well as the positive and normal control groups (5.4 and 12.4 U/L, respectively). Overall, the SGOT and SGPT levels

significantly decreased in the treatment groups compared with the negative control group ($p < 0.05$).

BUN and creatinine levels

Relatively higher serum levels of BUN and creatinine are indicative of severe renal injury. As compared to the negative control group (7.00 mg/dL), the serum BUN levels of the infected mice were significantly decreased by treatment with the ethyl acetate extract at 1, 10, 100, and 200 mg/kg BW (2.61, 2.95, 4.75, and 2.01 mg/dL, respectively), $p < 0.05$. In addition, as compared to the negative control group (1.99 mg/dL), serum creatinine levels were significantly decreased by treatment with the ethyl acetate extract at 1, 10, 100, and 200 mg/kg BW (0.14, 0.37, 0.27, and 0.23 mg/dL, respectively), $p < 0.05$.

Cytokine production

Serum IL-10 and TNF- α levels were significantly increased in the treatment groups as compared to the normal and negative control groups. As compared to the negative control group (88.00 pg/mL), serum IL-10 levels were significantly increased in the positive control group (131.09 pg/mL) and slightly increased in the groups treated with the ethyl acetate extract at 1, 10, 100, and 200 mg/kg BW (113.27, 106.36, 116.55, and 119.64 pg/mL, respectively, $p < 0.05$), while there was no significant difference as compared to the normal control group.

Moreover, as compared to treatment with the ethyl acetate extract at 1 mg/kg BW (287.93 ng/mL), serum levels of TNF- α were significantly increased by treatment with 10, 100, and 200 mg/kg BW (794.93, 848.07, and 729.64 ng/mL, respectively, $p < 0.05$). There were also significant differences among the negative, normal control, and positive control groups (237.64, 249.64, and 257.93 ng/mL, respectively, $p < 0.05$). Collectively, these results suggested that ethyl acetate extract of *S. arvensis* L. enhances the immune response of mice against *P. berghei* infection.

Table 8. Serum IL-10, TNF- α , SGOT, SGPT, BUN, and creatinine levels of mice infected with *P. berghei* strain ANKA after treatment with *S. arvesis* L. leaf ethyl acetate extract

Treatment	IL-10 (pg/mL)	TNF- α (ng/mL)	SGOT (U/mL)	SGPT (U/mL)	BUN (mg/mL)	Creatinine (mg/mL)
Normal Control	105.27 \pm 10.25 ^b	249.64 \pm 99.97 ^a	40.76 \pm 9.59 ^a	12.4 \pm 0.84 ^b	3.42 \pm 0.08 ^c	0.23 \pm 0.06 ^b
Positive control (chloroquine diphosphate)	131.09 \pm 8.13 ^c	257.93 \pm 160.33 ^a	32.92 \pm 6.07 ^a	5.4 \pm 2.73 ^a	0.75 \pm 0.36 ^a	0.39 \pm 0.01 ^c
Negative control (Na-CMC)	88.06 \pm 22.96 ^a	237.64 \pm 113.82 ^a	201.87 \pm 91.73 ^d	24.13 \pm 2.45 ^c	7.00 \pm 0.255 ^d	1.99 \pm 0.29 ^d
Ethyl acetate extract (mg/kg BW)						
1	113.27 \pm 13.21 ^b	387.93 \pm 123.59 ^a	100.68 \pm 2.98 ^c	32.37 \pm 13.61 ^c	2.61 \pm 1.62 ^b	0.14 \pm 0.02 ^a
10	106.36 \pm 11.32 ^b	794.93 \pm 427.89 ^b	73.85 \pm 10.41 ^b	22.74 \pm 2.08 ^c	2.95 \pm 1.19 ^b	0.37 \pm 0.04 ^c
100	116.55 \pm 6.95 ^{bc}	848.07 \pm 216.86 ^b	69.82 \pm 7.1 ^b	13.45 \pm 3.4 ^b	4.75 \pm 0.97 ^c	0.27 \pm 0.04 ^b
200	119.64 \pm 2.84 ^{bc}	729.64 \pm 126.89 ^b	33.11 \pm 13.16 ^a	2.75 \pm 0.59 ^a	2.01 \pm 1.33 ^b	0.23 \pm 0.09 ^b

Note: The experiment was conducted in 4-7 replications. Normal control is uninfected and untreated mice group. The values followed by the same letter show no significant difference in the one-way analysis of variance (ANOVA) continued with Duncan Multiple Range Test (DMRT) for IL-10 and TNF- α , with a nonparametric independent *t*-test for SGOT and SGPT, and Kruskal-Wallis continued with Mann Whitney test for BUN and creatinine data. The significant level was set 0.05 (Appendix 1: Supplementary data V).

2.4 Discussion

Management and accessibility of healthcare are important problems in Eastern Indonesia. Hence, home treatment with traditional medicines is the most common method for the treatment of malaria. The use of traditional medicine is safe, cost-effective, and efficient to ensure access to healthcare services. According to the World Health Organization (WHO), the use of traditional medicines continues to increase worldwide. Traditional medicines are rooted in Indonesian culture and history, although many traditional treatments have not been scientifically validated. Among the strategic objectives proposed by the WHO, the safety and effectiveness of

traditional medicines are primary goals before integrating traditional drugs in modern healthcare [2].

S. arvensis L. is the seventh most popular medicinal plant for treating various diseases in Indonesia, especially in Java and Bali [12]. Although the extract of *S. arvensis* L. callus is reported to possess antiplasmodial activities [17,18], the efficiency and safety for malaria treatment have not been registered. Hence, the aim of this study was to evaluate the antiplasmodial, toxicity, and antioxidant activity of crude extracts of *S. arvensis* L. leaf.

One kilogram of dried *S. arvensis* L. leaf was extracted by successive maceration with *n*-hexane, ethyl acetate, and ethanol. From each solvent, different extract weights were obtained. Each of the *S. arvensis* L. extracts was screened for the presence of phytochemicals. The ethanol extract contained flavonoids, alkaloids, terpenoids, saponins, and polyphenols, while the ethyl acetate extract included flavonoids, alkaloids, terpenoids, and polyphenols, and the *n*-hexane extract contained flavonoids, alkaloids, and terpenoids.

The Wilstatter "cyanidin" test confirmed the presence of flavonoids, while testing of the extract showed the presence of alkaloids, as indicated by the formation of a white precipitate after the addition of Mayer reagent. The Liebermann–Burchard test results confirmed the presence of terpenoids, as indicated by the yellow color of the solution. After adding a few drops of 10% FeCl₃, the color of the solution changed to dark green, indicating the presence of tannins. Meanwhile, the presence of saponins was confirmed if the foam extract did not disappear after the addition of distilled water and shaking [11].

Polyphenols were present in the ethanol extract, whereas relatively large amounts of terpenoids were confirmed in the ethyl acetate and *n*-hexane extracts. These findings are consistent with similar studies conducted by Khan [24] and Seal [25]. Many triterpenoids have been isolated from the *n*-hexane extract of *S. arvensis* L. [16]. Additionally, some phytochemicals may be responsible for the various activities of *S. arvensis* L. For example, flavonoid and phenolic compounds possess antioxidant activities [24], saponins have anti-inflammatory activities [26], and terpenoids exhibit antimicrobial activities [16].

Furthermore, *S. arvensis* L extract showed antioxidant activities. The ethyl acetate and ethanol extracts exhibited potent antioxidant activities ($IC_{50} < 50 \mu\text{g/mL}$), with IC_{50} value $8.27 \pm 4.93 \mu\text{g/mL}$ and $12.36 \pm 10.40 \mu\text{g/mL}$ respectively. While *n*-hexane extract had moderate antioxidant activity ($101 > IC_{50} < 250 \mu\text{g/mL}$) [27]. The IC_{50} value (the antioxidant activity) of ethyl acetate extract was lower than ascorbic acid as standard ($22.63 \pm 1.40 \mu\text{g/mL}$) (Table 3). Moreover, compared to the other studies, the leaf extract from *S. arvensis* L was lower than those of plants and callus *Trifolium pratense* L. [28], *Callisia fragrance* leaf juice [29], and *Centella asiatica* L. leaf [30] that have been previously reported as high antioxidant compound. The potent antioxidant activity of the *S. arvensis* L. extract was probably due to the presence of active ingredients with antioxidant activities, such as polyphenols and flavonoids. These findings are similar to those of previous studies of different plant sources [15,24,25,31].

The antioxidant activity of the ethyl acetate extract was as good as the *in vitro* antimalarial effect. In general, an IC_{50} value less than $10 \mu\text{g/mL}$ is considered to indicate the high activity, while $10 < IC_{50} \leq 25 \mu\text{g/mL}$ can be regarded as moderately active and values $>25 \mu\text{g/mL}$ are deemed inactive [32,33]. All plant extracts in this study presented the IC_{50} values less than $10 \mu\text{g/mL}$; therefore, they were primarily considered as the new candidates for antimalarial-drug development. The IC_{50} values of the ethyl acetate extract, *n*-hexane, and ethanol extracts were 2.916, 5.119, and $8.026 \mu\text{g/mL}$, respectively. The IC_{50} value criteria for antiplasmodial activity is currently still being debated. Therefore, the industry standardizes the IC_{50} value, a pure compound is said to be active as antiplasmodial activity if the IC_{50} value is below $10 \mu\text{g/mL}$ [6].

The toxicity of *S. arvensis* L. extracts were evaluated by calculating the ratio of cytotoxicity with human hepatic cell lines to *in vitro* antiplasmodial activity (SI=selectivity index). A higher SI, theoretically, indicates greater drug effectiveness and safety for the treatment of plasmodial infections. An ideal drug would be cytotoxic only at very high concentrations and have antiplasmodial activities at low concentrations, thus yielding a high SI value and eliminating the plasmodial target at concentrations well below the cytotoxic concentration [34]. The IC_{50} values of

extracts toxicity were 1420.88 ± 20.88 , 778.77 ± 10.53 , and 437.39 ± 7.46 , $\mu\text{g/mL}$, and then the SI value were 277.57 ± 5.77 , 97.03 ± 13.13 , and 150 ± 3.62 for *n*-hexane, ethanol, and ethyl acetate extract respectively. de Souza et al. [35] mentioned that “the natural product has been suggested that the $SI > 10$ indicate a favorable safety window between the effective concentration against the parasite and the toxic concentration to human cell”. Aryanti et al. [36] reported that the extract or fraction has high selectivity if the value of $SI \geq 3$, and less selectivity if the value of $SI \leq 313$. So, all *S. arvensis* L. leaf extracts exhibited low toxicity. Nurianti et al. [37] found that an ethyl acetate extract of *S. arvensis* L had no toxic effects, and Harun et al. [38] revealed that an ethanol extract of *S. arvensis* L. was not toxic to healthy male albino rats. The antioxidant activities suggest that these extracts are relatively non-toxic because oxidative stress represents an imbalance between the production of free radicals and the ability of a biological system to readily detoxify reactive intermediates or repair the resulting damage [39].

Moreover, the ethyl acetate extract of *S. arvensis* L. was chosen for the assessment of *in vivo* antiplasmodial activity because it exhibited the highest antioxidant and *in vitro* antiplasmodial activities, with $IC_{50} = 8.27$ and $2.916 \mu\text{g/mL}$ respectively. *In vivo* antiplasmodial activity can normally be classified as moderate, good, and very good if an extract displayed percentage inhibition equal to or greater than 50% at a dose of 500, 250, and 100 mg/kg BW per day, respectively [40]. Method and criteria are varied among the treatment groups examining antimalarial potency of plants by using the rodent animal model. *P. berghei*-infected mice given orally 50–250 mg/kg/day of extract exhibiting inhibition percentage $> 60\%$ are considered to be active or very active, and those exhibiting inhibition percentage $> 30\%$ are considered to be moderately active [32,33]. Based on this classification, the ethyl acetate extract of *S. arvensis* L. showed excellent *in vivo* antiplasmodial activity below 100 mg/kg/day with an ED_{50} of 46.31 ± 9.36 mg/kg. The ED_{50} of ethyl acetate extract of *S. arvensis* L. was higher than the ethanolic extract of *H. annuus* root has an ED_{50} value of 10.6 ± 0.2 mg/kg [41] but lower than the *Tagetes erecta* L. and *Synedrella nodiflora* (L.) Gaertn. extract can significantly suppress parasitemia in

malaria-infected mice by 50.82% and 57.67% respectively at 400 mg/kg BW dose [40]. Compared to another Asteraceae member, the ethyl acetate extract of *S. arvensis* L. could be developed as an antiplasmodial agent.

Furthermore, blood was collected from the experimental mice to determine the nephroprotective, hepatoprotective, and immunomodulatory activities after 7 days of treatment with ethyl acetate extract of *S. arvensis* L. Many studies have reported that *S. arvensis* L. extracts exhibited antioxidant [24], hepatoprotective [13], nephroprotective [42], and immunomodulatory [43] activities. The present study was conducted to assess the effect of an ethyl acetate extract of *S. arvensis* L. against *P. berghei* infection in mice.

An increase in SGPT and SGOT serum levels indicates liver damage [15], and a rise in BUN and creatinine levels suggests a failure of the kidneys or their possible malfunction [39]. The results showed that the ethyl acetate extract protected the liver and kidneys by reducing SGOT, SGPT, creatinine, and BUN levels.

Overall, the serum levels suggested that the ethyl acetate extract of *S. arvensis* L. showed nephroprotective, hepatoprotective, and immunomodulatory activities in mice infected with *P. berghei*. The result is very interesting because the pathogenesis caused by *P. berghei* is multifactorial and has not been well characterized. There were several hypotheses suggesting that erythrocyte cytoadherence, proinflammatory response, nephrotoxicity, and oxidative stress are involved in the pathogenesis of *P. berghei* [44,45]. Free heme-mediated oxidative stress, in which free heme is produced by parasites that consume hemoglobin during the intra-erythrocytic phase, has been implicated in lipoprotein oxidation [46] and serious kidney damage [46]. In addition, malaria infection is caused by parasites and host factors, where there will be microvascular disturbances in the host's body. *P. berghei* parasites will infect erythrocytes and activate cytokines of phagocytic cells and endothelial cells to produce TNF- α , IL-10, IFN- γ , and free radicals (ROI, ROS, and NO). Free radicals are molecules with one unpaired electron in their outer orbit which makes the molecule unstable [42]. Free radicals can cause oxidative stress. It has implications for various pathological conditions [48]. The involvement of oxidative stress can cause the amount of antioxidant status to decrease [42].

Oxidative stress condition is defined as in-balance condition between antioxidants and free radicals, where the state of free radicals is higher than antioxidants [14]. The number of antioxidants decreases because the body used to balance the high free radicals due to the presence of parasites. The more severe the infection from *P. berghei*, the use of antioxidants in the body will increase, causing the number of antioxidants in the body to decrease [42]. The biochemical data of serum of mice infected *P. berghei* supported that the *S. arvensis* L. ethyl acetate extract is active as antiplasmodial. Particularly, the *S. arvensis* L. leaf ethyl acetate extract increases the mice immune response to *P. berghei* infections. It is very valuable for the further investigation of efficacious the *S. arvensis* L. leaf as antiplasmodial drug candidate,

The comprehensive tests and discussions in this study confirmed that ethyl acetate extract possessed antimalarial both *in vitro* and *in vivo* with nephroprotective, hepatoprotective, and immunomodulatory activities in mice infected with *P. berghei*. This study highlighted that *S. arvensis* L. crude extract had antimalarial activity. Completely, these results suggested that ethyl acetate extract of *S. arvensis* L. could be used to develop new antimalarial drugs in the future from a natural resource.

2.5 Conclusion

The results of this study confirmed the antiplasmodial activity of ethyl acetate extract of *S. arvensis* L. both *in vitro* and *in vivo* as well as the antioxidant, nephroprotective, hepatoprotective, and immunomodulatory activities with low toxicity. It was strongly suggesting the potential as an antimalarial drug. These findings lay a foundation for further investigations of new antimalarial compounds for future pharmaceutical applications. Further research, including bioassay-guided fractionation, was also recommended to identify new antimalarial drug candidates.

Abbreviations

BUN	blood urea nitrogen
SGOT	serum glutamic oxaloacetic transaminase
SGPT	serum glutamic pyruvic transaminase
TNF- α	tumor necrosis factor alpha

IL-10	interleukin 10
IC ₅₀	half maximal inhibitory concentration
ED ₅₀	median effective dose
DPPH	2,2-diphenyl-1-picryl-hydrazyl-hydrate

Ethical approval and consent to participate

Applicable. Experimental research and field studies on plants was complied with relevant institutional, national, and international guidelines and legislation. The permission was obtained from Taman Husada Graha Famili (Medicinal Plant Garden of Graha Famili) Surabaya, East Java, Indonesia, managed by Universitas Airlangga and PT. Intiland Development Tbk., Surabaya, East Java, Indonesia, with the Memorandum of Understanding number 3001/UN3.1.8/2014 and the Memorandum of Activity number 142/GFV-PM HSG/SRT/HH/VIII/2021. The study was reported in accordance with ARRIVE guidelines (<https://arriveguidelines.org>).

Consent for publication

Not applicable

Data Availability and material

The datasets generated and analyzed during the current study are not online available due to **funding policy** however they are available from the corresponding author or first authors on reasonable request.

Competing interests

The authors declare that they have no competing interests

Funding

This work was supported by the Universitas Airlangga, Contract No. 405/UN3.14/PT/2020

Authors' contributions

DKW: conceived and conducted the experiments, analysed the data, and wrote the manuscript, SW: assisted the plant extractions and screened the phytochemicals, WB: assisted the experiments and interpreted the results, SPAW: analysed the biochemical blood and interpreted the results reviewed. WE: helped with in vitro and in vivo antimalarial assay design. HP: assisted the collection, identification, and classification of plant material, HP: assisted with conception and material preparation,

and SP was the primary author of the manuscript. All authors read and approved the final manuscript.

Acknowledgments

The authors would like to acknowledge Universitas Airlangga Rector Scholarship. The authors also would like to thank Nindy Tresiana Putri, Rizal Adistya Putra Pradana, and Manikya Pramudya for their support in the *in vivo* antimalarial assays, Shilfiana Rahayu, Hikma, and Talita for coordinating the preparation of the raw plant extracts studied and whole blood analysis of mice.

2.6 References

1. World Health Organization. Guidelines for the Treatment of Malaria. 3rd ed. Italy: WHO Press, World Health Organization; 2015.
2. World Health Organization. World Malaria Report 2021. Geneva, Switzerland: WHO Press, World Health Organization; 2021.
3. APMEN. The Asia pacific malaria elimination network (APMEN). 2020. <https://www.apmen.org/>. Accessed January 25, 2021.
4. Aguiar ACC, Santos RdM, Figueiredo FJB, Cortopassi WA, Pimentel AS, França TCC. Antimalarial Activity and Mechanisms of Action of Two Novel 4-Aminoquinolines against Chloroquine-Resistant Parasites. PLoS ONE. 2012; 7(5): e37259. doi: 10.1371/journal.pone.0037259
5. Davanco MG, Aguiar ACC, Dos Santos LA, Padilha EC, Campos ML. Evaluation of antimalarial activity and toxicity of a new primaquine prodrug. PLoS ONE. 2014; 9(8): e105217. doi: 10.1371/journal.pone.0105217
6. Tajuddeen N, Van Heerden FR. Antiplasmodial natural products: an update. Malar J. 2019; 18(404):1-62. doi:10.1186/s12936-019-3026-1
7. Katiyar D, Singh K, Ali M. Phytochemical and pharmacological profile of Pterocarpus marsupium: a review. J Pharm Innov. 2016; 5:31-9.
8. Waiganjo B, Moriasi G, Onyancha J, Elias N, Muregi F. Antiplasmodial and cytotoxic activities of extract of selected medicinal plants used to treat malaria in Embu County, Kenya. J Parasitol Res. 2020; 2020:1-12.

9. Haidara M, Haddad M, Denou A, Marti G, Bourgeade-Delmas S, Sanogo R. In vivo validation of antimalarial activity of crude extracts of *Terminalia macroptera*, a Malian medicinal plant. *Malar J.* 2018; 17:68. doi: 10.1186/s12936-018-2223-7.
10. Wahyuni DK, Shilfiana Rahayu, Putut Rakhmad Purnama, Triono Bagus Saputro, Suharyanto, Nastiti Wijayanti et al. Morpho-anatomical structure and DNA barcode of *Sonchus arvensis* L. *Biodiversitas.* 2019; 20:2417-26. doi: 10.13057/biodiv/d200841.
11. Delyan E. Analysis of composition of volatile compounds of field sow thistle (*Sonchus arvensis* L.) leaf using the method of gas chromatography with mass-detection. *J Pharm Innov.* 2016; 5:118-21.
12. Yuliarti W, Kusriani D, Isolasi FE. Identification and antioxidant activity of phenolic acid from tempuyung (*Sonchus arvensis* L.) leaf with 1,1-difenil-2-pikrilhidrasil (DPPH) method. *Chem Inform.* 2013; 1:294-304.
13. Hendriani R, Sukandara EY, Anggadiredja K. Sukrasno. In vitro evaluation of xanthine oxidase inhibitory activity of *Sonchus arvensis* leaf. *Int J Pharm Pharm.* 2014; 6:501-3.
14. Imelda I, Azaria C, Lucretia T. Protective effect of ethanol extract tempuyung leaf (*Sonchus arvensis* L.) against gentamicin induced renal injury viewed from blood ureum level. *Med Health.* 2017; 1:575-82. doi: 10.28932/jmh.v1i6.555.
15. Hendriani R, Sukandar EY, Anggadiredja K. Sukrasno. In vitro evaluation of xanthine oxidase inhibitory activity of selected medicinal plants. *Int J Pharm Clin.* 2015; 8:235-8.
16. Rumondang M, Kusriani D, Fachriyah E. Isolation, identification and antibacterial test of triterpenoid compounds from n-hexane extract of tempuyung leaf (*Sonchus arvensis* L.). *Pharm Sci.* 2013; 05:506-7.
17. Wahyuni DK, Purnobasuki H, Kuncoro EP, Ekasari W. Callus induction of *Sonchus arvensis* L. and its antiplasmodial activity. *Afr J Infect Dis.* 2020; 14:1-7. doi: 10.21010/ajid.v14i1.1.
18. Wahyuni DK, Rahayu S, Zaidan AH, Ekasari W, Prasongsuk S, Purnobasuki H. Growth, secondary metabolite production, and in vitro antiplasmodial activity of

- Sonchus arvensis L. callus under dolomite [CaMg(CO₃)₂] treatment. PLoS ONE. 2021; 16(8): e0254804. doi: 10.1371/journal.pone.0254804.
19. Hanoon LK, Joshi SDS, Yasir AK, Prasad AM, Alapati KS. Phytochemical screening and antioxidant activity of *Pseuderanthemum malabaricum*. J Pharmacogn Phytochem. 2019; 8:972-7.
 20. Lin J, Li X, Chen L, Lu W, Chen X, Han L et al. Protective effect against hydroxyl radical-induced DNA damage and antioxidant mechanism of [6]-gingerol: A Chemical Study. Bull Korean Chem Soc. 2014; 35:1633-8. doi: 10.5012/bkcs.2014.35.6.1633.
 21. Trager W, Jensen JB. Human malarial parasites in continuous culture. Science. 1976; 193:673-5.
 22. Fonseca AG, Dantas LLSFR, Fernandes JM, Zucolotto SM, Lima AAN, Soares LAL et al. In vivo and in vitro toxicity evaluation of hydroethanolic extract of *Kalanchoe brasiliensis* (Crassulaceae) leaf. J Toxicol. 2018; 6849765:1-8. doi: 10.1155/2018/6849765
 23. Peters W, Portus JH, Robinson BL. The chemotherapy of rodent malaria. XXII. The value of drug-resistant strains of *P. berghei* in screening for blood schizontocidal activity. Ann Trop Med Parasitol. 1975; 69(2): 155–171.
 24. Khan RA. Evaluation of flavonoids and diverse antioxidant activities of *Sonchus arvensis* L. Chem Cent J. 2012; 6:1-7.
 25. Seal T. Quantitative HPLC analysis of phenolic acids, flavonoids, and ascorbic acid in four different solvent extracts of two wild edible leaf, *Sonchus arvensis* and *Oenanthe linearis* of North-Eastern region in India. J App Pharm Sci. 2016; 6:157-66. doi: 10.7324/JAPS.2016.60225.
 26. Poudel BK, Sah JP, Subedi SR, Amatya MP, Amatya S, Shrestha TM. Pharmacological studies of methanolic extracts of *Sonchus arvensis* from Kathmandu. J Pharmacognosy Phytother. 2015; 7:263-7. doi: 10.5897/JPP2015.0359.
 27. Prieto JM. Procedure: Preparation of DPPH radical, and antioxidant scavenging assay. Prieto's DPPH Microplate Protocol. 2012. Available: <https://www.researchgate.net/file.PostFileLoader.html?id=503cd1c9e39d5ead110>

- 00043&assetKey=AS%3A271744332435456%401441800305338. Accessed 30 March, 2021.
28. Esmaili AK, Taha RM, Mohajer S, Banisalam B. Antioxidant activity and total phenolic and flavonoid content of various solvent extracts from in vivo and in vitro grown *Trifolium pratense* L. (Red Clover). *BioMed Res Int*. 2015; 643285:1-11. doi: 10.1155/2015/643285.
 29. Olennikov DN, Zilfikarov IN, Toropova AA, Ibragimov TA. Chemical composition of *Callisia fragrans* wood juice and its antioxidative activity (in vitro). *Chem Plant Raw Mater*. 2008; 4:95–100.
 30. Yahya MA, Nurrosyidah IH. Antioxidant activity ethanol extract of gotu kola (*Centella asiatica* L.) with DPPH method (2,2-diphenyl-1-pikrilhidrazil). *Journal Halal Product and Reseacrch*. 2020; 3:106-112. doi: 10.20473/jhpr.vol.3-issue.2.106-112.
 31. Putra BRS, Kusri D, Fachriyah E. Antioxidant compound isolation from tempuyung (*Sonchus arvensis* L) leaf ethyl acetate fraction. *J Kim Sains Apl*. 2013; 16:69-72.
 32. Upadhyaya HC, Sisodia BS, Cheema HS, Agrawal J, Pal A, Darokar MP. Novel antiplasmodial agents from *Christia vespertilionis*. *Nat Prod Commun*. 2013; 8:1591-4. doi: 10.1016/j.jep.2012.11.034.
 33. Lima RB, Rocha e Silva LF, Melo MR, Costa JS, Picanço NS, Lima ES. In vitro and in vivo antimalarial activity of plants from the Brazilian Amazon. *Malar J*. 2015; 14:508. doi: 10.1186/s12936-015-0999-2.
 34. Mellado-García P, Maisanaba S, Puerto M, Prieto AI, Marcos R, Pichardov S, Cameán AM. In vitro toxicological assessment of an organosulfur compound from *Allium* extract: cytotoxicity, mutagenicity and genotoxicity studies. *Food Chem Toxicol*. 2017; 99:231-240. doi: 10.1016/j.fct.2016.12.007.
 35. De Souza GE, Bueno RV, de Souza JO, Zanini CL, Cruz FC, Oliva G, Guido RC, Caroline ACA. Antiplasmodial profile of selected compounds from Malaria Box: In vitro evaluation, speed of action and drug combination studies. *Malar J*. 2019; 18(404):447–459.

36. Aryanti TME, Kartika IP, Rita MD. Antimalarial activity assay of *Artemisia* spp. against *Plasmodium falciparum*. *Majalah Farmasi Indonesia*. 2006; 17:81-4.
37. Nurianti Y, Hendriani R, Sukandar EY, Anggadiredja K. Acute and subchronic oral toxicity studies of ethyl acetate extract of *Sonchus arvensis* L. leaf. *Int J Pharm Pharm*. 2014; 6:343-7.
38. Harun N, Fitria V, Karningsih D. Effect of ethanol extract *Sonchus arvensis* Linn. Leaf on acute toxicity in healthy male albino rat (*Rattus norvegicus*). *J Phys Conf S. IOP Conference Series*. 2019; 1179:012163 IOP Publishing. doi: 10.1088/1742-6596/1179/1/012163.
39. Flora G, Gupta D, Tiwari A. Toxicity of lead: a review with recent updates. *Interdiscip Toxicol*. 2012; 5:47-58. doi: 10.2478/v10102-012-0009-2
40. Chaniad P, Techarang T, Phuwajaroanpong A, Na-ek P, Viriyavejakul P, Punsawad C. In vivo antimalarial activity and toxicity study of extracts of *Tagetes erecta* L. and *Synedrella nodiflora* (L.) Gaertn. from the Asteraceae family. *Evid Based Complement Alternat Med*. 2021; 1270902:1-9. doi : 10.1155/2021/1270902.
41. Ekasari W, Pratiwi DW, Amanda Z, Suciati WA, Arwati H. Various parts of *Helianthus annuus* plants as new source of antimalarial drugs. *Evid Based Complement Alternat Med*. 2019; 2019:7390385. doi: 10.1155/2019/7390385.
42. Imelda A, Sekarwana N. Protective Effect of ethanolic extract of *Sonchus arvensis* L. in gentamicin-Induced acute tubular necrosis on wistar rats. *Indonesian J Pharm*. 2018; 29:86-93. doi: 10.14499/indonesianjpharm29iss2pp86.
43. Sukmayadi AE, Sumuwi SA, Aryanti AD. Immunomodulatory activity of tempuyung (*Sonchus arvensis* Linn.) leaf ethanolic extract. *Int J Biosci Technol*. 2014; 1:1-8.
44. Somsak V, Chachiyo S, Jaihan U, Nakinchat S. Protective effect of aqueous crude extract of neem (*Azadirachta indica*) leaf on *Plasmodium berghei*-induced renal damage in mice. *J Trop Med*. 2015; 961205. doi: 10.1155/2015/961205
45. Elias RM, Costa MC, Barreto CR, Silva RC, Hayashida C, Castoldi A, Camara NS. Oxidative stress and modification of renal vascular permeability are associated with acute kidney injury during *P. berghei* ANKA infection. In F. Costa (Ed.). 2012; 7(8):1-11.

46. Kumar S, Bandyopadhyay U. Free heme toxicity and its detoxification systems in human. *Toxicol Lett.* 2005; 157:175–188.
47. Jeney V, Balla J, Yachie A, Varga Z, Vercellotti GM. Pro-oxidant and cytotoxic effects of circulating heme. *Blood.* 2002; 100:879–887.
48. Valko M, Leibritz D, Moncol J, Cronin MTD, Mazur, Telser J. Free radicals and antioxidants in normal physiological functions and human disease. *Inter J Biochem Cell Biol.* 2007; 39:44-84.



CHAPTER THREE

Anti-SARS-CoV-2, antiplasmodial, antioxidant, and antimicrobial activities of crude extracts and homopterocarpin from heartwood of *Pterocarpus macrocarpus* Kurz.

Dwi Kusuma Wahyuni^{1,2}, Sumrit Wacharasindhu³, Wichanee Bankeeree¹, Hunsu Punapayak¹, and Sehanat Prasongsuk^{1,2*}

¹Plant Biomass Utilization Research Unit, Department of Botany, Faculty of Science, Chulalongkorn University, Bangkok, 10330 Thailand

²Department of Biology, Faculty of Science and Technology, Universitas Airlangga Surabaya, East Java, 60115, Indonesia

³Department of Chemistry, Faculty of Science, Chulalongkorn University, Bangkok, 10330, Thailand

*Corresponding author: Sehanat Prasongsuk

Plant Biomass Utilization Research Unit, Department of Botany, Faculty of Science, Chulalongkorn University, Bangkok, 10330 Thailand

Department of Biology, Faculty of Science and Technology, Universitas Airlangga Surabaya, East Java, 60115, Indonesia

e-mail: sehanat.p@chula.ac.th.

Abstract

Background: Natural products play an essential role in the process of new drug discovery. In the present study, we determined the *in silico* anti-SARS-CoV-2, *in vitro* antioxidant, *in vitro* antiplasmodial, and antimicrobial activities of *Pterocarpus macrocarpus* Kurz. heartwood and structurally characterized the bioactive compounds.

Methods: *P. macrocarpus* Kurz. heartwood was macerated with *n*-hexane, ethyl acetate, and ethanol, respectively, for 7 days. This was repeated three times. The compounds were isolated by recrystallization with *n*-hexane and evaluated by thin-layer chromatography (TLC), gas chromatography-mass spectrophotometry (GC-MS), Fourier transform infrared (FITR) spectroscopy, and nuclear magnetic resonance

(NMR). The *in silico* anti-SARS-CoV-2, *in vitro* antioxidant against 1,1-diphenyl-2-picrylhydrazyl (DPPH) and 2,2-azino-bis (3-ethylbenzothiazoline-6-sulfonic acid (ABTS), *in vitro* antiplasmodial against *Plasmodium falciparum* strain 3D7, and antimicrobial (disk diffusion method) against *Candida albicans*, *Bacillus subtilis*, *Escherichia coli*, and *Staphylococcus aureus*) activities were established. Hepatocyte-derived cellular carcinoma cell line (Huh7it-1cells) were used for an *in vitro* cytotoxicity assay [3(4,5-dimethylthiazol-2-yl)-2,5-diphenyltetrazolium bromide; MTT].

Results:

The ethyl acetate, ethanol, and *n*-hexane extracts, as well as homopterocarpin, exhibited antiplasmodial activity at 1.78, 2.21, 7.11, and 0.52 µg/ml, respectively, against *P. falciparum* 3D7 with low toxicity. A compound identified by GC-MS showed *in silico* anti-SARS-CoV-2 binding affinity with stigmasterol and SARS-CoV-2 helicase of -8.2 kcal/mol. All extracts exhibited antioxidant activity against DPPH and ABTS. They also demonstrated antimicrobial activity against *B. subtilis*, the ethanol and ethyl acetate extracts against *E. coli* and *C. albicans*, and the ethanol extract against *S. aureus*.

Conclusion: The results highlighted antiplasmodial activity of a crude extract and homopterocarpin from *P. macrocarpus* Kurz. heartwood and its potent binding *in silico* to anti-SARS-CoV-2 proteins with low toxicity. This study also confirmed that all extracts exhibited antioxidant and antimicrobial activity. Further studies are needed to assess the safety and bioactivity of *P. macrocarpus* Kurz. for development as a new drug candidate.

Keywords: anti-SARS-CoV-2, antimicrobe, antioxidant, antiplasmodial, homopterocarpin, malaria, *Pterocarpus macrocarpus* Kurz.

3.1 Introduction

Severe acute respiratory syndrome-related coronavirus-2 (SARS-CoV-2) is currently a serious worldwide health problem, with more than 205 million people afflicted with this virus and the occurrence of more than 4 million deaths. To reduce the harmful sequelae of this infection, efforts are underway to identify agents for preventive, supportive, and therapeutic care against SARS-CoV-2^[1]. Moreover, the

emergence and spread of drug- or antimicrobial-resistant pathogens is another major threat that has increased the morbidity and mortality of infectious diseases, especially for chloroquine- or artemisinin-resistant *Plasmodium falciparum* malaria^[2]. These strains are resistant to nearly all available antimalarial drugs, which reinforces the need to identify new antimalarial and antimicrobial agents. Researchers are currently exploring the efficacy of phytochemicals from medicinal plants as a source of active compounds to reduce the time and cost of developing new synthetic drugs^[3].

Herbal medicine and therapy were the best options according to traditional folklore. WHO estimates that around 80% of the world's population uses herbal medicines to treat health problems because they have many benefits, such as low costs, positive complementary effects, and negligible side effects^[4]. Many plants that have been used in traditional medicine exhibit antiviral properties. The anti-SARS-CoV-2 activity of plant extracts and their components has been evaluated, such as bioactive compounds from *Centella asiatica*^[5], *Vitis amurensis*^[6], and *Boesenbergia rotunda*^[7]. They have been explored in many bioactivities studies, including antioxidant and antimicrobial activity^[8-12].

Pterocarpus macrocarpus Kurz. belongs to Fabaceae, which primarily grows in Laos, Thailand, Myanmar, and Vietnam. The benefits of *P. macrocarpus* Kurz. is associated with its heartwood, which provides visual enjoyment and psychological pleasure because of its unique woody flavor^[13]. In addition, medicinal properties are associated with the extracts from this plant including human blood circulatory, antimicrobial^[14], detoxification^[15], Alzheimer's disease, antispasmodic, anticancer^[16], immunomodulatory^[17], and insecticide activities^[18].

In this report, we evaluated the effects of *P. macrocarpus* extracts including the antioxidant, antimicrobial, and antimalarial activities, and used computational analysis to determine the potency of these extracts against SARS-CoV-2 proteins; then we compared them with bioactive commercial compounds. MTT assay was also conducted to evaluate the cytotoxicity level. This report provides remarkable information about anti-SAR-CoV-2, antimalarial, antimicrobial, and antioxidant activities with low toxicity of natural products from *P. macrocarpus* Kurz.. Moreover, it could be

expected to provide data for the further use of these extracts as drug candidates for infectious diseases therapy with positive complementary effects and safety.

3.2 Materials and methods

3.2.1 Plant material collection and identification

Pterocarpus macrocarpus Kurz. was obtained from a traditional market in Bangkok, Thailand, and authenticated in the Plant Systematic Laboratory, Department of Biology, Faculty of Science and Technology, Universitas Airlangga. A voucher specimen was deposited in the Plant Systematic Laboratory, Department of Biology, Faculty of Science and Technology Universitas Airlangga (No. PM.0210292021).

3.2.2. Extraction and phytochemical screening

The heartwood (1 kg) was air-dried, ground into powder (80 mesh size) and macerated sequentially in polar organic solvents including *n*-hexane, ethyl acetate, and ethanol. Each maceration was done for 7 days, 3 times at room temperature ($28 \pm 2^\circ\text{C}$). The resulting extracts were filtered through filter paper, evaporated with a rotary evaporator at 60°C to acquire a dry residue, weighed to calculate the yield of each extract, and stored at 4°C . The crude extracts were screened for phytochemical content by standard methods including the Wilstatter "cyanidin" test for flavonoids, Mayer's test for alkaloids, the ferric chloride test for tannins, the Liebermann–Burchard test for terpenoids, and the foam test for saponins^[19].

3.2.3 Isolation and structural analysis of bioactive compounds

The *n*-hexane extract was crystallized by dissolving 1 g of sample into 20 ml of *n*-hexane, shaking for 10 min, and incubating at 4°C for 24 hours. The crystals were separated by filtration through filter paper, weighed to calculate yield, and recrystallized. The process was repeated until the color of the crystals had become white. The thin-layer chromatography (TLC) with a mixture of *n*-hexane: ethyl acetate (4:1 v/v) as a mobile phase was used to separate the chemical constituents of the *n*-hexane extract before and after crystallization. The samples were dissolved in *n*-hexane and spotted (5 μL , equivalent to crude extract weight of 250 μg of sample) on a silica gel precoated plate. The plate was developed in vanillin sulfuric acid and heated until purple-blue nodes were revealed on the plate as terpenoids^[20]. Gas

chromatography-mass spectrophotometry (GC-MS) was used to establish compound profiles from the *n*-hexane extract during the recrystallization steps. GC-MS analysis was performed using an Agilent GC-MSD (Agilent 19091S-433UI) equipped with a capillary column (30 m × 250 μm × 0.25 μm) and a mass detector was operated in electron impact (EI) mode with full scan (50550 amu). Helium was used as the carrier gas at a flow rate of 3 ml/min with a total flow rate of 14 ml/min. The injector was operated at 280°C and the oven temperature was programmed at an initial temperature of 60°C and increased 3°C per minute to obtain a final temperature at 250°C. The peaks in the chromatogram were identified based on their mass spectra. The ¹H, ¹³C, HMBC, and HMQC NMR spectra of the compounds were analyzed using a JEOL JNM-ECS instrument at 400 MHz in chloroform solvent. The melting point was analyzed using a melting point tester (Stuart SMP30) and confirmed by Fourier transform infrared spectroscopy (FITR, Shimadzu IRTracer 100).

3.2.4 In silico anti-SARS-Cov-2

3.2.4.1 Protein and ligand sample preparation

The proteins involved in, entry, replication, and assembly of the SARS-CoV-2 virus in humans, such as helicase (PDB ID 6ZSL), receptor binding domain of spike glycoprotein (RBD-spike; PDB ID 6LZG), RNA dependant RNA polymerase (RdRp; PDB ID 6M71), and main protease (Mpro; PDB ID 7ALH) were identified as potential drug targets in this study. The crystal structures of these proteins were obtained from the PDB (<https://www.rcsb.org>). Molnupiravir (control 1; CID 145996610) and PF-07321332 (control 2; CID 155903259) were used as control COVID-19 drugs. To evaluate anti-SARS-CoV-2 activity, the three-dimensional structures of the identified compounds from the *n*-hexane extracts of *P. macrocarpus*, including butylated hydroxytoluene (CID 31404), 2-naphthalene methanol (CID 74128), homopterocarpin (CID 101795), pterocarpan (CID 1715306), campesterol (CID 173183), γ -sitosterol (CID 133082557), and stigmasterol (CID 5280794), were downloaded from PubChem database (<https://pubchem.ncbi.nlm.nih.gov>). The compounds (or ligands) were subjected to energy minimization using the PyRx 0.9.9 tool to increase the flexibility and to optimize binding. The native ligands were then removed through sterilization by PyMol version 2.5^[21]. The drug-likeness of these compounds was analyzed using Lipinski's rule of five on the

SCFBIO web server (<http://www.scfbio-iitd.res.in/software/drugdesign/lipinski.jsp>). The compounds that were identified as drug candidates with drug-like molecule properties were selected for further analysis^[22].

3.2.4.2 Molecular docking simulation

The docking of selected compounds to target proteins was performed using PyRx version 0.9.9 software. The docking type was screened with a control molecule to ignore the functional side of the target protein, while the analysis focused on the binding energy. The binding energy was expressed as binding affinity (kcal/mol), which is the energy formed when a molecule interacts with another molecule. This energy indicates the level of bonding activity and the interaction pattern with a ligand^[23].

3.2.4.3 Molecular interaction analysis

BIOVIA Discovery Studio 2017 software was used to analyze the interactions and positions of chemical bonds in the docked molecular complex. Weak bonds consisting of hydrophobic, Van der Waals, hydrogen, electrostatic, and -alkyl are shown by the software. Weak bonds are formed when ligands and proteins interact to initiate specific biological responses, such as activation and inhibition. Pocket binding domains on target proteins have a key role in this regard, because they consist of specific amino acids^[24]. The results of the molecular docking simulation in this study were displayed by PyMol software (<https://pymol.org/2/>), the structure of the ligand-protein molecules consisted of cartoons, surfaces, and sticks that underwent staining selection^[25].

3.2.5 In Vitro antioxidant activity

3.2.5.1 The 2,2-diphenyl-1-picryl-hydrazyl-hydrate (DPPH) inhibition assay.

The DPPH inhibition assay was done according to Prieto^[26] with modifications. Sample (100 μ l) at different concentrations from 1.075 to 200 μ g/ml in methanol were mixed with 100 μ l DPPH reagent (0.2 mM) and incubated for 30 min in the at room temperature. Ascorbic acid and Trolox were used as positive controls. The inhibition of DPPH was measured at 517 nm.

The percentage of DPPH inhibition was calculated by the equation:

$$(A_{\text{control}} - A_{\text{sample}}) / A_{\text{control}} \times 100\% \quad (1)$$

Where A_{sample} is the absorbance from the mixture of DPPH reagent and the sample, whereas A_{control} is the absorbance from the DPPH reagent. The percentage of inhibition at each concentration was plotted and regressed linearly to obtain the half-maximal inhibitory concentration (IC_{50}) value.

3.2.5.2 The 2,2'-azino-bis (3-ethylbenzthiazoline-6-sulphonic acid) (ABTS) inhibition assay

The ABTS inhibition assay was conducted according to the method of Fu et al.^[27]. The ABTS reagent was prepared by mixing 7 mM ABTS solution with 2.4 mM potassium persulphate solution and storing at room temperature for 12–16 hours in the dark. Then, the absorbance of the solution at 734 nm was measured (0.7–0.72). The sample (100 μl) at different concentrations from 1.075 to 200 $\mu\text{g}/\text{ml}$ in methanol was mixed with 100 μl ABTS reagent and the absorbance was measured at 734 nm after incubating for 5 mins in the dark at room temperature. The percent inhibition and IC_{50} value were calculated as described for the DPPH inhibition assay.

3.2.6 *In vitro* antimalarial Assay

An *in vitro* antimalarial assay using cultures of *Plasmodium falciparum* strain 3D7 (Trager and Jensen 1972) was carried out, which was adapted from Wahyuni et al.^[28]. The composition of the medium included human O red blood cells, 5% hematocrit in Roswell Park Memorial Institute 1640 (RPMI 1640) (Gibco BRL, USA), 22.3 mM N-2-hydroxyethylpiperazine-N-2-ethanesulfonic acid (HEPES) (Sigma), hypoxanthine, sodium bicarbonate (NaHCO_3), and 10% human O⁺ plasma. Chloroquine diphosphate was used as a positive control. Sample (1 mg) was dissolved in 100 μl of DMSO (10,000 mg/ml) and used as a stock solution from which serial dilutions were prepared. The parasites used in this test were synchronous (ring stage) with $\pm 1\%$ parasitemia (5% hematocrit). Test solution (2 μl) at various concentrations were placed into each well (96 wells) and 198 μl of the parasite was added (the final concentration of the test material was 100 $\mu\text{g}/\text{ml}$, 10 $\mu\text{g}/\text{ml}$, 1 $\mu\text{g}/\text{ml}$, 0.1 $\mu\text{g}/\text{ml}$, and 0.01 $\mu\text{g}/\text{ml}$). The test well was placed into the chamber and exposed to a gas mixture (O_2 5%, CO_2 5%, and N_2 90%). The chamber containing the test wells was incubated for 48 h at 37°C. The cultures were then harvested, and a thin blood film was prepared by 20%

Giemsa staining. The number of infected erythrocytes per 1000 normal erythrocytes was counted under a microscope (1000X).

The data was used to calculate the percent growth and percent inhibition using the following formulas:

$$\% \text{ Growth} = \% \text{ Parasitemia} - D0 \quad (2)$$

$$\text{Percent inhibition} = 100\% - [(X_u/X_k) \times 100\%] \quad (3)$$

Where D0 is the percentage of growth at the 0-hour, whereas X_u and X_k are the percentage of growth in the test solution and negative control, respectively. Based on the percent inhibition data, statistical analysis was carried out using probit of the SPSS version 20 program to determine the IC_{50} value or the concentration of the test material that inhibits parasitic growth by 50%.

3.2.7 *In vitro* cytotoxicity assay

An MTT cytotoxicity assay was carried out *in vitro* on hepatocyte-derived cellular carcinoma cell line (Huh7it-1 cells) using 3-(4,5-dimethylthiazol-2-yl)-2,5-diphenyltetrazolium bromide as described by Fonseca et al.^[29]. Passage (P) 18 human hepatocyte cells were cultured in Dulbecco's modified Eagle's medium (DMEM) medium supplemented with 3.7 g of sodium bicarbonate ($NaHCO_3$), and adjusted to a pH of 7-7.2. A complete medium was made from 500 ml of DMEM media containing 50 ml of fetal bovine serum (FBS), 5 ml of nonessential amino acid (NEAA), and 6 ml of penstrep (penicillin-streptomycin). The samples were dissolved in DMSO and then diluted to various concentrations (0.1, 0.5, 1, 5, 10, 50, 100, 500, and 1000 $\mu\text{g/ml}$). The cells were incubated at 37°C under an atmosphere of 5% of carbon dioxide and 95% humidity for 48 h. The assay was done in duplicate wells. The viability of the cells was determined by measuring the absorbance at 560 nm and 750 nm with a multiplate reader. The percentage of cell viability was calculated using the formula:

$$\% \text{ viability: } (A_{\text{sample}}/A_{\text{control}}) \times 100\% \quad (4)$$

where A_{sample} was absorbance at 560 nm–750 nm and A_{control} is the absorbance of DMEM medium. The half cytotoxic concentration (CC_{50}) was determined by plotting the percent cell viability and regressing linearly using Microsoft Excel version 20.0 (IBM Corporation, Armonk, NY, USA).

3.2.8 Selectivity index (SI)

The SI was determined to describe the selective activity of an extract against *Plasmodium falciparum* strain 3D7 compared with the results of its cytotoxicity against human hepatocyte cells. The SI value was calculated by comparing the IC_{50} value of the extract with that of *P. falciparum* strain 3D7. The SI was used to describe the selective activity of the extract against *P. falciparum* strain 3D7 compared with the results of its cytotoxicity on human hepatocyte cells^[30].

3.2.9 Antimicrobial assay

The disc diffusion method was performed to analyze antimicrobial activity against *Bacillus subtilis*, *Escherichia coli*, *Staphylococcus aureus*, and *Candida albicans*^[31]. Nutrient agar media was used to culture the bacteria, whereas potato dextrose agar was used for cultivating yeast. The sterilized medium was poured into sterile petri plates and the inoculate from each strain was spread onto the agar plates after solidification. A stock solution of extract was prepared and serially diluted. The sterile disks, 6 mm in diameter, were impregnated into the extract solution at each concentration. Distilled water and chloramphenicol were used as negative and positive controls, respectively. All disks were fully dried before applying to the bacterial or yeast plates. Antibacterial activity was evaluated by measuring the diameter of the inhibition zone around the disks. The percentage of inhibition (PI) was calculated as follows:

$$PI = \frac{\text{the inhibition zone of the sample (cm)}}{\text{the zone of positive control (cm)}} \times 100\% \quad (5)$$

3.2.10 Data analysis

Data are expressed as the mean \pm standard deviation. Probit analysis was used to calculate the IC_{50} values for *in vitro* antimalarial activity using IBM SPSS Statistics for Windows, version 20.0. (IBM Corporation, Armonk, NY, USA). The IC_{50} values for *in vitro*

antioxidant and cytotoxicity were calculated by linear regression using Microsoft Excel version 20.0 (IBM Corporation, Armonk, NY, USA).

3.3 Results and discussion

3.3.1 The yield of extracts and phytochemical screening

Dried heartwood from *P. macrocarpus* Kurz. was sequentially extracted with different polar organic solvents. One kilogram of sample yielded 2.5 ± 0.3 , 10.2 ± 0.2 , and 42.9 ± 0.3 g of extract from the *n*-hexane, ethyl acetate, and ethanol fractions, respectively. According to phytochemical analysis, each fraction contained flavonoid, alkaloid, terpenoid, saponin, and polyphenol as secondary metabolites at different amounts, whereas saponins were only found in the ethanolic fraction (Table 9). Different phytochemicals have generally been considered to exhibit different activities. The *n*-hexane extract revealed an abundance of terpenoids. Therefore, crude extracts from the *n*-hexane fraction were selected for the isolation of bioactive compounds.

Table 9. Phytochemical screening of *Pterocarpus macrocarpus* Kurz. heartwood extracts

No	Phytochemicals	<i>n</i> -Hexane	Ethyl acetate	Ethanol
1	Terpenoids	+++	++	+
2	Flavonoids	+	++	+++
3	Alkaloids	+	++	++
4	Saponin	-	-	+
5	Polyphenol	+	+	+++

Note: ++, Strongly positive; +, Weakly positive; -, Not detected

3.3.2 Isolation and structural analysis of bioactive compounds

Recrystallization was performed to isolate the bioactive compounds. The yield, color, and number of spots on TLC plates from each cycle of recrystallization are listed in Table 10. The effectiveness of this isolation technique may be observed by the reduction of spots on the TLC from 6 (1st cycle) to 3 spots (2nd cycle). The different R_f values for every stain indicate the diversity of the compounds^[32]. The white crystals that yielded 596 mg/g of crude extract were obtained at the fifth cycle and the single

spot with an Rf value of 0.69 was also identified by TLC (Appendix 2: Supplementary Data I).

Table 10. The yield of crystals at each step of crystallization of the n-hexane extract of *Pterocarpus macrocarpus* Kurz. heartwood

Cycle	Number of spots	Rf value for major spot	Yield (mg/g)	Color
1	6	0.125, 0.375, 0.563, 0.625, 0.688, 0.938	290 ± 5	orange
2	3	0.125, 0.688, 0.938	80 ± 2	orange
3	3	0.125, 0.688, 0.938	12 ± 10	orange
4	3	0.125, 0.688, 0.938	10 ± 10	orange
5	1	0.688	592 ± 30	white

Note: The data were represented as mean±SD, n=3.

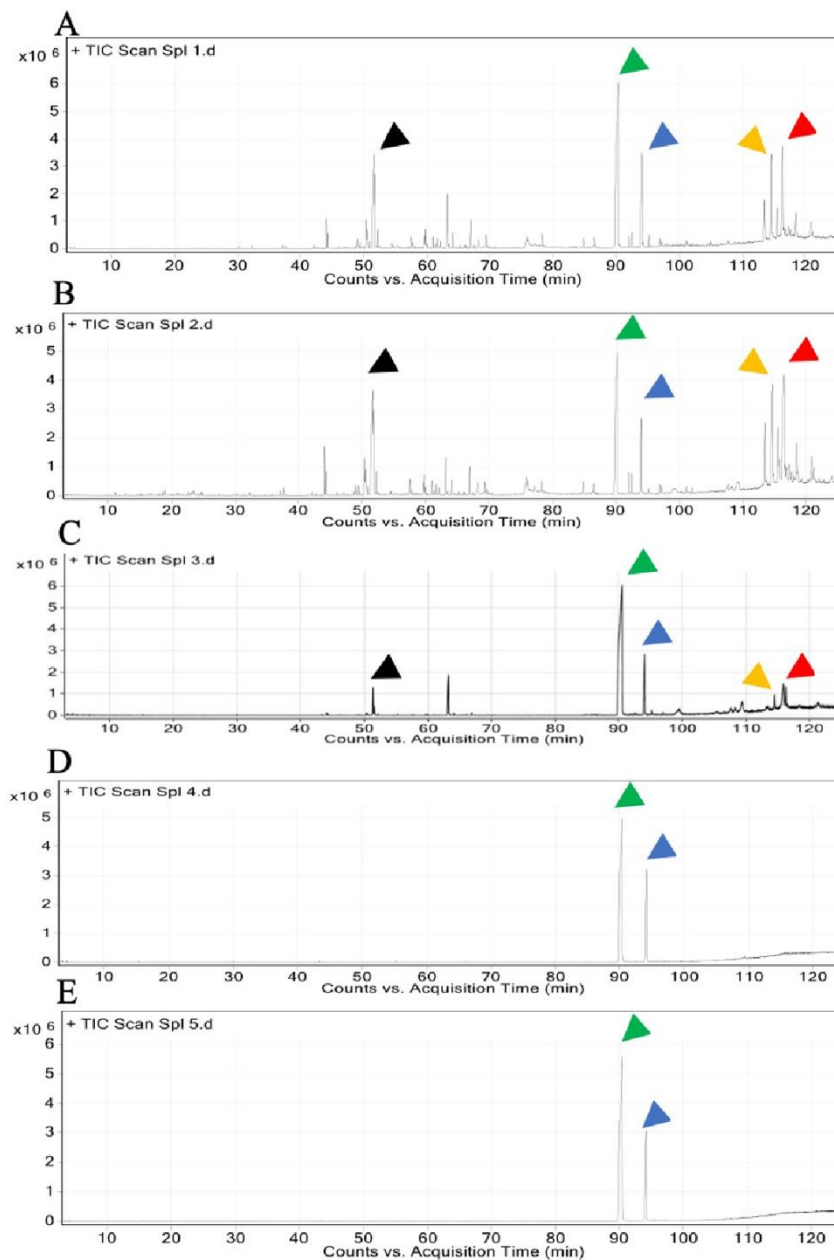


Figure 2. Chromatogram of n-hexane extracts of *Pterocarpus macrocarpus* Kurz. heartwood at each crystallization cycle. A. n-hexane extract, B. first crystallization, C. second crystallization, D. third crystallization, E. fourth crystallization. black arrow: 2-naphthalenemethanol; green arrow: homopterotharpin; blue arrow: pterotharpin; yellow arrow: stigmasterol; red arrow: γ -sitosterol

A GC-MS chemical analysis was used to identify the diverse compounds in the *n*-hexane extract from the four cycles of recrystallization. A total of 7 compounds were identified from the first crystallization, 3 from the second, and only 2 compounds were identified from the third cycle. Of these, homopterocarpin and pterocarpin were found at each cycle as major components (Table 11, Fig. 2, Appendix 2: Supplementary data II). These compounds have been reported as bioactive molecules in previous studies^[33-36].

Table 11. Phytochemical components identified from GC/MS analysis of *Pterocarpus macrocarpus* Kurz. heartwood *n*-hexane extract at each crystallization cycle

No.	Identified compound	Retention Time (min)	Relative area percentage (peak area relative to the total peak area) (%)				
			<i>n</i> -hexane extract	Crystallization			
				1 st	2 nd	3 rd	4 th
1	Butylated hydroxytoluene	44.04	3.81	9.04			
2	2-Naphthalenemethanol	51.53	32.17	57.85	4.03		
3	Homopterocarpin	90.40	100.00	100.00	100.00	100.00	100.00
4	Pterocarpin	94.14	23.34	20.64	13.34	31.17	23.42
5	Campesterol	113.64	7.93	19.7			
6	Stigmasterol	114.64	21.24	43.03			
7	γ -sitosterol	116.50	27.87	55.97			

The FTIR spectrum of the isolated products from the fifth recrystallization revealed absorption bands (cm^{-1}) for C-H alkane at 2949.16, 2908.65, and 2841.15; the C-H bending aromatic compound at 1876.74; C=C conjugated alkene at 1618.28; C=C cyclic alkene at 1587.42, O-H phenol at 1381.03 and 1344.38; C-O stretching alkyl aryl ether/aromatic ester/at tertiary alcohol 1197.79 and 1271.09; C=C stretching aliphatic ether at 1149.57 and 1130.29; and the C=C alkene at 973.40, 794.67, 723.31, and 682.80 (Appendix 2: Supplementary data III). The integration of the ^1H NMR spectrum (Table 12) showed the presence of two aromatic ring in the benzene skeleton at δ_{H} 7.43 (1H, *d*, 8.6Hz), 6.64 (2H, *dd*, 8.6Hz; 2.5Hz), 6.47 (1H, *d*, 2.5Hz) and 7.13 (1H, *d*, 8.5Hz), 6.46 (2H, *dd*, 8.5Hz; 2.3Hz), 6.44 (1H, *d*, 2.3). The two ether cyclic

groups were at δ_H 3.64 (3H, *t*, 11.0Hz), 4.25 (2H, *dd*, 11.0Hz; 5.3Hz), 3.53 (*m*). The appearance of singlets at δ_H 3.77 (s) and 3.79 (s) confirmed the presence of two OCH₃ groups on the aromatic ring (Appendix 2: Supplementary data IV). There were 17 carbon signals in the ¹³C NMR spectrum (125 MHz, CDCl₃, based on HMQC and HMBC experiments; Table 12). Signals at δ_C 156.7 and 60.8 resulted from benzene carbons bonded to the ether group. The signals at δ_C 131.9, 109.3, 101.7, 39.6, 124.8, 106.4, 97.1, and 78.7 indicated an aromatic CH, whereas signals at δ_C 112.4 and 119.2 were assigned to aromatic carbons. The other two signals at δ_C 161.2 and 161.1 belong to a benzene carbon with methoxy groups. Two signals at δ_C 55.6 and C₉ 55.5 were confirmed as methoxy carbons. The signal at δ_C 66,7 was a carbon ether cyclic with two hydrogen atoms (Appendix 2: Supplementary V). The data from the characterization of the compounds were compared with that reported in the literature^[37]. Homopterocarpin exhibited white crystals and yielded 0.592 ± 0.003 g (0.059%w/w). The melting point of this compound was at 83.6°C. Furthermore, a mass spectra analysis showed that the compound had an m/z of 284.1 and the molecular formula was C₁₇H₁₆O₄ (Fig. 3).

3.3.3 *In silico* anti-SARS-CoV-2 activity

The identified compounds include butylated homopterocarpin, pterocarpin, hydroxytoluene, 2-naphthalenemethanol, campesterol, γ -sitosterol, and stigmasterol from *P. macrocarpus* *n*-hexane extract were used as the ligands to analyze their potential activity as drug-like molecules according to the Lipinski Rule of Five. The rule requires a molecular mass > 500 Da, high lipophilicity < 5 Da, hydrogen bond donor < 5 Da, and a hydrogen bond acceptor < 10 Da^[38]. All compounds that act as drug candidates may trigger the activity of the target protein if they satisfy more than two of the Lipinski rules (Table 13).

Table 12. The observed ^1H and ^{13}C -NMR homopterothecarpin (3,9-dimethoxy-pterocarpan) compound in CDCl_3

No. C	Homopterothecarpin of <i>Pterocarpus macrocarpus</i> Kurz.		
	Type	δ_{H} (mult, J Hz)	δ_{C}
1	CH	7.43 (d, 8,6)	131.9
2	CH	6.64 (dd, 8,6; 2,5)	109.3
3	C	-	161.2
4	CH	6.47 (d, 2,5)	101.7
4a	C	-	156.7
6	CH ₂	3.64 (t, 11,0) 4.25 (dd, 11,0; 5,3)	66.7
6a	CH	3.53 (m)	39.6
6b	C	-	119.2
7	CH	7.13 (d, 8,5)	124.8
8	CH	6.46 (dd,8,5; 2,3)	106.4
9	C	-	161.1
10	C	6.44 (d, 2,3)	97.1
10a	C	-	160.8
11a	CH	5.51 (d, 6,8)	78.7
11b	C	-	112.4
3-OCH ₃	C-OCH ₃	3.77 (s)	55.6
9-OCH ₃	C-OCH ₃	3.79 (s)	55.5

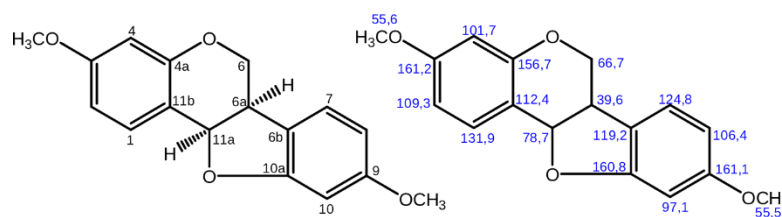


Figure 3. The structure of homopterothecarpin

Table 13. Prediction results of target compound activity

Compound	MW (Dalton)	LOGP	HBD	HBA	MR	Probability
Butylated hydroxytoluene	220.000	4.295	1	1	70.243	Drug-like molecule
2-Naphthalenemethanol	158.000	2.332	1	1	49.870	Drug-like molecule
Homopterocarpin	284.000	3.313	0	4	77.592	Drug-like molecule
Pterocarpin	298.000	3.033	0	5	77.163	Drug-like molecule
Campesterol	400.000	7.634	1	1	123.599	Drug-like molecule
γ -sitosterol	414.000	8.024	1	1	128.216	Drug-like molecule
Stigmasterol	412.000	7.800	1	1	128.122	Drug-like molecule

MW: Molecular Weight; LOGP: High Lipophilicity; HBD: Hydrogen Bond Donor; HBA: Hydrogen Bond Acceptor; MR: Molar Refractivity

The results of a molecular docking simulation indicated that all of the selected compounds had a higher negative binding affinity for each SARS-CoV-2 protein compared with that of molnupiravir (Control 1) and PF-07321332 (Control 2) (Table 14). Stigmasterol was the most effective compound predicted to bind with all SARS-CoV-2 proteins including helicase, RBD-spike, RdRp, and Mpro with negative binding affinities of -8.2 , -7.8 , -7.8 and -7.3 kcal/mol, respectively. Campesterol is another active compound that exhibited a more negative binding affinity with all target SARS-CoV-2 proteins compared with the two control drugs. The molecular docking simulation results were displayed in 3D with transparent surfaces, cartoon structures with the target proteins, and a ligand with stick views (Fig. 4). The weak bonds in the molecular complex from the docking simulation consisted of hydrogen, alkyl, Van der Waals, hydrophobic, and electrostatic interactions. The presence of weak binding interactions can activate specific biological responses in proteins, such as inhibition through specific domains^[39]. The seven bioactive compounds in this study could theoretically bind to specific protein domains through weak binding, such as alkyl, hydrogen, pi sigma, and Van der Waals interactions (Fig. 5). The results suggest that each bioactive compound may inhibit SARS-CoV-2 protein activity.

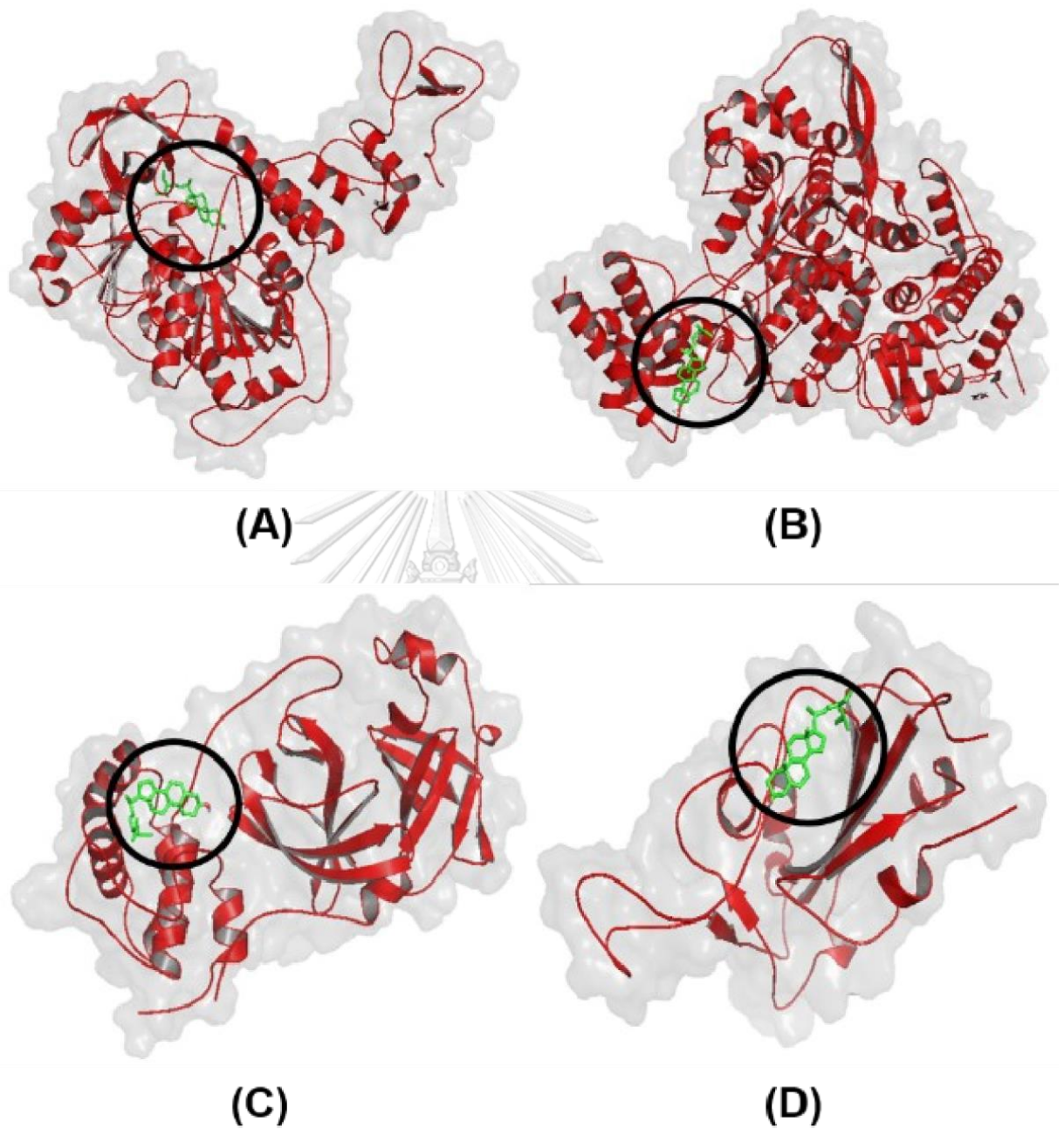


Figure 4. The 3D visualization of the molecular docking results. Ligands are indicated by black circles (A) Stigmasterol_Helicase (B) Stigmasterol_RdRp (C) Stigmasterol_Mpro (D) Stigmasterol_RBD-Spike.

Table 14. Simulation results of molecular docking with SARS-CoV-2 proteins

Target	Ligand	Binding Affinity (kcal/mol)	AutoGrid (Å)
Helicase	Butylated hydroxytoluene	-6.3	Center
	2-Naphthalenemethanol	-6.2	
	Homopterocarpin	-7.2	
	Pterocarpin	-7.7	X:-14.723 Y:30.321 Z:-66.631
	Campesterol	-7.7	Dimensions
	γ-sitosterol	-7.4	
	Stigmasterol	-8.2	
	Molnupiravir (Control 1)	-7.1	
	PF-07321332 (Control 2)	-7.1	X:91.761 Y:98.670 Z:106.327
RdRp	Butylated hydroxytoluene	-5.9	Center
	2-Naphthalenemethanol	-5.8	
	Homopterocarpin	-6.5	
	Pterocarpin	-7.2	X:119.72 Y:117.282 Z:117.111
	Campesterol	-7.6	Dimension
	γ-sitosterol	-7.1	
	Stigmasterol	-7.8	
	Molnupiravir (Control 1)	-6.8	
	PF-07321332 (Control 2)	-7.5	X:102.037 Y:108.952 Z:117.175
M ^{pro}	Butylated hydroxytoluene	-5.8	Center
	2-Naphthalenemethanol	-5.9	
	Homopterocarpin	-6.3	
	Pterocarpin	-7.1	X:-26.283 Y:12.599 Z:63.866
	Campesterol	-7.7	Dimension
	γ-sitosterol	-7.6	
	Stigmasterol	-7.8	
	Molnupiravir (Control 1)	-6.7	
	PF-07321332 (Control 2)	-6.5	X:66.125 Y:72.942 Z:61.258
RBD-Spike	Butylated hydroxytoluene	-5.6	Center
	2-Naphthalenemethanol	-5.6	
	Homopterocarpin	-6.4	
	Pterocarpin	-7.1	X:-32.325 Y:27.893 Z:21.076
	Campesterol	-6.9	Dimension
	γ-sitosterol	-6.7	
	Stigmasterol	-7.3	
	Molnupiravir (Control 1)	-6.7	

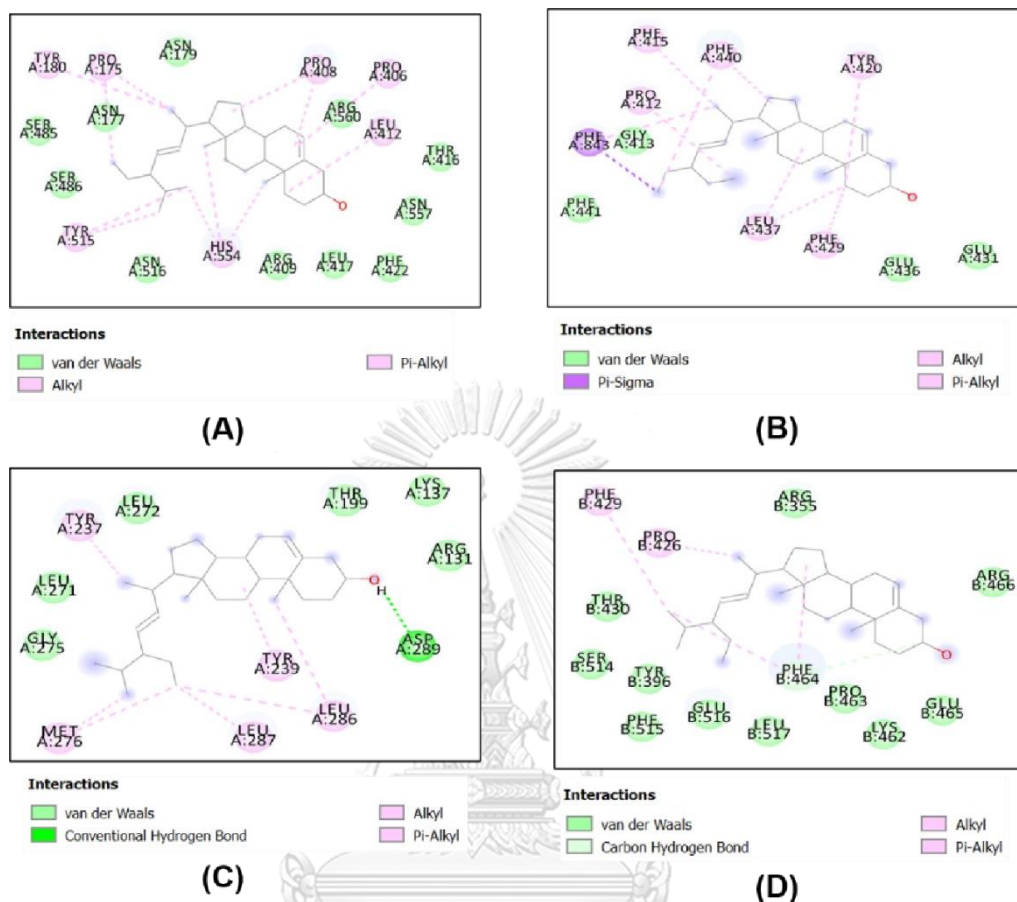


Figure 5. The 2D visualization of the molecular interactions. (A) Stigmasterol_Helicase, (B) Stigmasterol_RdRp, (C) Stigmasterol_Mpro, (D) Stigmasterol_RBD-Spike.

3.3.4 Antioxidant activity

DPPH and ABTS assays were done to assess the antioxidant activities of the extracts. The IC_{50} values of the crude extracts prepared with each solvent are shown in Table 15 (Appendix 2: Supplementary data VI). From lowest to highest, the IC_{50} values for ABTS were 0.61 ± 0.46 , 0.75 ± 0.42 , and 68.93 ± 4.34 $\mu\text{g/ml}$ for the ethanol, ethyl acetate extract, and *n*-hexane extract, respectively, whereas the IC_{50} values for DPPH were 0.76 ± 0.92 , 2.12 ± 0.97 , and 27.70 ± 4.29 $\mu\text{g/ml}$ for the ethanol, ethyl acetate extract, and *n*-hexane extracts, respectively. In addition, the IC_{50} of homopterocarpin was 194.90 ± 34.96 $\mu\text{g/ml}$ for DDPH assay and 30.94 ± 8.00

µg/ml for the ABTS assay. Compared with the control, the IC₅₀ for ethyl acetate and ethanol extracts were lower compared with that of Trolox and ascorbic acid for both assays. The potent antioxidant activity of the crude extract of *P. macrocarpus* Kurz. was likely due to the presence of active ingredients with antioxidant activities, such as polyphenols and flavonoids, especially in the ethanolic and ethyl acetate crude extracts (Table 9)^[40]. In previous study showed homopterocarpin from *Pterocarpus erinaceus* as antioxidant^[36]. Compared to the other studies that have been previously reported as high antioxidant compounds, the leaf extract from *P. macrocarpus* Kurz. was lower than *Centella asiatica* L. leaf^[41], plants and callus of *Trifolium pratense* L.^[42], and *Callisia fragrance* leaf juice^[43].

Table 15. *In vitro* antioxidant activity of *Pterocarpus macrocarpus* Kurz. heartwood extract

No.	Extract	Antioxidant activity, IC ₅₀ (µg/ml)	
		DPPH	ABTS
1	<i>n</i> -Hexane	27.70 ± 4.29	68.93 ± 4.34
2	Ethyl acetate	2.12 ± 0.97	0.75 ± 0.42
3	Ethanol	0.76 ± 0.92	0.61 ± 0.46
4	Homopterocarpin	194.90 ± 34.96	30.94 ± 8.00
5	Ascorbic acid	5.12 ± 2.43	2.77 ± 1.30
6	Trolox	0.97 ± 0.30	0.86 ± 0.97

Note: The data were represented as mean±SD, n=3.

3.3.5 *In vitro* antimalarial activity

The IC₅₀ values of the crude extracts and homopterocarpin from *P. macrocarpus* Kurz. at different doses are shown in Table 16 (Appendix 2: Supplementary data VII). All natural products are considered to have antimalarial activity at IC₅₀ values less than 10 µg/ml. The compounds with IC₅₀ values less than 5 µg/ml are classified as exhibiting very active antimalarial activity, whereas IC₅₀ values between 5 and 10 µg/ml are identified as active antimalarial agents^[44]. The results indicated that the ethyl acetate extract exhibited the highest *in vitro* antimalarial

activity with an IC₅₀ value of 1.78 µg/ml, followed by the ethanol (2.21 µg/ml) and *n*-hexane extracts (7.11 µg/ml), whereas the IC₅₀ of homopterocarpin was 0.52 µg/ml. Compared with other studies, the IC₅₀ values for the *S. arvensis* L. ethyl acetate extract was lower compared with that of the DCM extracts from *Commiphora africana* (A. Rich.) Engl. stem bark and *Dychrostachys cinerea* (L.) Wight & Arn. whole stem, which showed promising antiplasmodial activity with IC₅₀ values of 4.54 ± 1.80 and 11.47 ± 2.17 µg/ml, respectively^[3]. These results were lower compared with that of the ethanolic extracts from *Mussaenda erythrophylla*, including stem (29.6 ± 0.7 µg/ml) and leaves (3.7 ± 2.6 µg/ml), and *Mussaenda philippica* Dona Luz x *Mussaenda flava* leaves ethanolic extract (5.9 ± 0.4 µg/ml)^[45]. In addition, they were lower than *Pterocarpus erinaceus* Poir. leaf methanolic extract (IC₅₀ = 14.63 µg/ml)^[46]. Tajuddeen and Heerden^[47] concluded that a bioactive compound is considered interesting and worthy of further investigation as an antimalarial agent if the IC₅₀ is 3.0 µg/ml.

3.3.6 *In vitro* toxicity and selectivity index

In vitro toxicity was evaluated by the MTT assay using Huh7it-1 cells and the SI was calculated by comparing the cytotoxicity concentration at 50% (CC₅₀) and the IC₅₀ of the antiplasmodial activity of the natural product. The CC₅₀ of the crude *n*-hexane, ethyl acetate, and ethanol extracts, and homopterocarpin were 202.38, 67.237, 512.48, and 49.93 µg/ml, respectively. Moreover, the selectivity indices for the *n*-hexane, ethyl acetate, ethanol extracts of *P. macrocarpus* Kurz. heartwood and homopterocarpin were 28.46, 37.77, 231.89, and 96.02 µg/ml respectively (Table 16) (Appendix 2: Supplementary data VIII).

Table 16. *In vitro* antimalarial activity, in vitro toxicity, and selectivity index (SI) of *Pterocarpus macrocapus* Kurz. heartwood extracts against *P. falciparum* strain 3D7

No	Extract	Percentage of inhibition at each concentration (µg/ml)						IC ₅₀ (µg/ml)	<i>In Vitro</i> Toxicity, CC ₅₀ (µg/ml)	Selectivity Index (SI)
		100	10	1	0.1	0.01	0.001			
1	<i>n</i> -Hexane	84.21	55.20	23.21	9.11	1.75	ND*	7.11	202.38	28.46
2	Ethyl acetate	88.26	65.99	38.12	23.28	11.54	ND	1.78	67.237	37.77
3	Ethanol	81.78	67.00	43.05	23.55	5.33	ND	2.21	512.48	231.89
4	Homopterocarpin	-	97.98	78.68	52.16	30.30	15.39	0.52	49.93	96.02
5.	Chloroquine diphosphate	100	100	100	79.76	40.49	17.17	0.014		

*ND = not detectable

The drug's effectiveness and safety for treating the diseases were indicated by the SI value. The extract or fraction with SI values ranging from 10 to 313 was considered safe, regarding the effective concentration against a parasite and the toxic concentration toward human cells^[30,48]. Therefore, all natural products in this study were considered non-toxic.

3.3.7 Antimicrobial activity

Antimicrobial tests were carried out with all crude extracts against bacteria and yeast (Table 17). All extracts showed active antibacterial activity against *Bacillus subtilis* with a percentage of inhibition (PI) of $39.5 \pm 2.08\%$, $37.9 \pm 0.29\%$, and $38.7 \pm 3.27\%$ for the *n*-hexane, ethyl acetate, and ethanol extracts, respectively. The ethyl acetate and ethanol extracts showed active antimicrobial activity against *C. albicans* ($29.75 \pm 1.53\%$ and $27.40 \pm 6.13\%$ of inhibition, respectively) and *E. coli* ($48.82 \pm 7.48\%$ and $57.76 \pm 7.48\%$, respectively). Furthermore, only the ethanol extract exhibited active antimicrobial activity against *S. aureus* with a percentage inhibition of $44.78 \pm 0.42\%$. Compared to other study, diameter of inhibition zone of *P. macrocarpus* extract was wider than *P. indicus* bark ethanolic extract against to

Candida albicans, *E. coli*, and *S. aureus*^[49]. The antimicrobial activity of the *P. macrocarpus* extracts were seem related to the presence of active ingredients with antimicrobial activities (Table 9 and Table 3). Jiménez-González et al.^[50] study reported that pterocarpan have antifungal activity. However, in the present study, the antimicrobial activity of homopterocarpan was not determined because it did not show a significant inhibition zone against the tested microbes. These results are consistent with that of Cuellar et al.^[51] in which homopterocarpan exhibited weak antimicrobial activity against *E. coli*, *S. aureus*, *B. cereus*, and *E. faecalis*.

Table 17. Diameter of inhibition zone and percentage of inhibition of heartwood extract of *Pterocarpus macrocarpus* Kurz.

No.	Natural Products	<i>Bacillus subtilis</i>		<i>Candida albicans</i>		<i>Escherichia coli</i>		<i>Staphylococcus aureus</i>	
		DIZ (cm)	PI (%)	DIZ (cm)	PI (%)	DIZ (cm)	PI (%)	DIZ (cm)	PI (%)
1	N-hexane extract	1.1 ± 0.1	39.5 ± 2.08	ND	ND	ND	ND	ND	ND
2	Ethyl Acetate extract	1.31 ± 0.29	37.9 ± 0.29	1.20 ± 0.08	29.75 ± 1.53	1.03 ± 0.17	48.82 ± 7.48	ND	ND
3	Ethanol extract	1.17 ± 0.17	38.7 ± 3.27	1.03 ± 0.12	27.40 ± 6.13	1.06 ± 0.17	57.76 ± 7.48	1.2 ± 0.11	44.78 ± 0.42
4	Chloramphenicol	3.07 ± 0.39	ND	3.65 ± 0.71	ND	1.59 ± 0.27	ND	2.39 ± 0.81	ND

Note: The data are represented as mean±SD, n=3. DIZ: diameter inhibition zone (cm); DIZ: Diameter of Inhibition Zone (cm); PI: percentage of inhibition (%); positive control: Chloramphenicol.

3.4 Conclusion

This study highlighted homopterocarpan isolation from a *P. macrocarpus* Kurz. *n*-hexane extract by crystallization. Based on the result we conclude that several crude extracts and homopterocarpan isolated from *P. macrocarpus* Kurz. heartwood indicated a strong potential for antiplasmodial agents and with low toxicity. Seven bioactive compounds from the *n*-hexane fraction of this plant showed their potent binding *in silico* to anti-SARS-Cov-2 proteins. All of the extracts also exhibited antioxidant and antimicrobial activity. These findings provide a foundation for further investigations of natural product for infectious diseases treatment and various pharmaceutical applications. In future studies, bioassay-guided fractionation is recommended to identify new compound drug candidates from *P. macrocarpus* Kurz.

Declaration

Author contributions

DKW: conception, design, implementation, conducting experiments, analysis, interpretation of results, and writing the manuscript, SW: phytochemical screening and spectral analysis, WB: conducting experiments, analysis, and interpretation of results, HP: collection, identification, and classification of plant material. SP was the primary author of the manuscript. All authors read and approved the final manuscript.

Acknowledgments

The authors would like to thank Viol Dhea Kharisma and Arif Muhammad Nur Ansori for their support of the *in silico* anti-SARS-CoV-2 assays. The authors also would like to thanks to Natural Product Medicine Research and Development (NPMRD) laboratory, Institute of Tropical Disease (ITD), Universitas Airlangga for antiplasmodial and cytotoxicity assay.

Competing interests

The authors declare that they have no competing interests

Data availability statement

Additional data that support the findings of this study are available from the corresponding author upon reasonable request.

Consent for publication

Not applicable

Funding

This work was supported by the Universitas Airlangga, Contract No. 405 /UN3.14/PT/2020

3.5 References

- [1] WHO. *Coronavirus (Covid-19) outbreak*. <https://www.who.int>. July, 10th 2021, 03.40. Western Indonesian Time, 2020. October, 11th 2021, 03.40. Western Indonesian Time, (2021).
- [2] WHO. *World Malaria Report 2020*, Geneva, Switzerland: WHO Press, World Health Organization, (2020).

- [3] Kweyamba, P. A., Zofou, D., Efange, N., Assob, J. N. & Kitau, J. *In vitro* and *in vivo* studies on antimalarial activity of *Commiphora 53exadece* and *Dichrostahys cinerea* used by the Maasai in Arusha region, Tanzania. *Malar. J.* **18**, 119-125 (2019).
- [4] Katiyar, D., Singh, K., & Ali, M. Phytochemical and pharmacological profile of *Pterocarpus marsupium*: A review. *Pharm Innov J.* **5(4)**, 31-39.
- [5] Latha, D., Hrishikesh, D., Shibani, G., Chandrashekar, C., & Bharath, B. R. In silico, in vitro screening of plant extracts for anti-SARS-CoV-2 activity and evaluation of their acute and sub-acute toxicity. *Phytomedicine Plus*, **2**, 100233. (2022).
- [6] Gurung, B. A., Ajmal Ali, M., Al-Hemaid, F., El-Zaidy, M., & Lee, J. In silico analyses of major active constituents of fingerroot (*Boesenbergia rotunda*) unveils inhibitory activities against SARS-CoV-2 main protease enzyme. *Saudi J. Biol. Sci.* **29**, 65-74. (2022).
- [7] Souid, I., Korchef, A., & Souid, S. In silico evaluation of *Vitis amurensis* Rupr. Polyphenol compounds for their inhibition potency against COVID-19 main enzymes Mpro and RdRp. *Saudi Pharm. J.* In Press. (2022).
- [8] Idris, FN., & Nadzir, MM. Comparative studies on different extraction methods of *Centella asiatica* and extracts bioactive compounds effects on antimicrobial activities. *Antibiotics.* **10**, 457. (2021).
- [9] Kumari, S., Deori, M., Elancheran, R., Kotoky, J., & Devi, R. *In vitro* and *in vivo* antioxidant, anti-hyperlipidemic properties and chemical characterization of *Centella asiatica* (L.) extract. *Front. Pharmacol.* **7**, 400. (2016).
- [10] Kabir, F., Sultana, MS., & Kurnianta, H. Antimicrobial activities of grape (*Vitis vinifera* L.) pomace polyphenols as a source of naturally occurring bioactive components. *Afr. J. Biotechnol.* **4(26)**, 2157-2161. (2015).
- [11] Lee, HR., Bak, MJ., Jeong, WS., Kim, YC., & Chung, SK. Antioxidant properties of proanthocyanidin fraction isolated from wild Grape (*Vitis amurensis*) seed. *J. Korean Soc. Appl. Biol. Chem.* **52(5)**, 539-544. (2009).
- [12] Jitvaropasa, R., Saenthaweesuka, S., Somparna, N., Thuppiiaa, A., Sireeratawonga, S. & Phoolcharoen, W. Antioxidant, antimicrobial and wound healing activities of *Boesenbergia rotunda*. *Nat. Prod. Commun.* **7(7)**, 909 – 912. (2012).

- [13] Wisittipanich, S., Khadee, C., & Jintana, P. Shoot production of plus tree branch log and it's cutting test of *Tectona grandis* Linn and *Pterocarpus macrocarpus* Kurz. *Kasetsart University Conference*, 2580, (2012).
- [14] Hongxia, C., Xiutang, K., Longjie, Y., Chengzhang, W., & Jianzhong, Y. Chemical component and antibacterial activity of essential oil from Myanmar *Pterocarpus macrocarpus*, *Chem. Ind. For. Prod.* **37**, 65-72. (2017).
- [15] Gao, W., Wang, Y., Basavanagoud, B., & Jamil, M.K. Characteristics studies of molecular structures in drugs. *Saudi Pharm. J.* **25**, 580–586. (2017).
- [16] Chen, J., Ge, S., Liu, Z., & Peng, W. GC-MS explores health care components in the extract of *Pterocarpus macrocarpus* Kurz.,” *Saudi J. Biol. Sci.* **25**, 1196-1201. (2018).
- [17] Ataa, S., Hazmi, I. R., & Samsudin, S. F. Insect's visitation on *Melastoma malabathricum* in UKM Bangi forest reserve. *EES.* **1**, 20–22. (2017).
- [18] Morimoto, M., Fukumoto, H., Hiratani, M., Chavasiri, W., & Komai, K. Insect aantifeedants, pterocarpan, and pterocarpol, in heartwood of *Pterocarpus macrocarpus* Kurz.. *Biosci. Biotechnol. Biochem.* **70**, 1864-1868. (2014).
- [19] Hanoon, L. K., Joshi, S. D. S. D., Yasir, A. K., Prasad, A. M., & Alapati, K. S. Phytochemical screening and antioxidant activity of *Pseuderanthemum malabaricum*. *J. Pharmacogn. Phytochem.* **8**, 972-977 (2019).
- [20] Wahyuni, D. K., Rahayu, S., Zaidan, A. H., Ekasari, W., Prasongsuk, S., & Purnobasuki, H. Growth, secondary metabolite production, and *in vitro* antiplasmodial activity of *Sonchus arvensis* L. callus under dolomite [CaMg(CO₃)₂] treatment. *PloS ONE.* **16**, e0254804. (2021).
- [21] Kharisma, V. D., Ansori, A. N. M., & Nugraha, A. P. Computational study of ginger (*Zingiber officinale*) as E6 inhibitor in human papillomavirus type 16 (HPV-16) infection. *Biochem. Cell. Arch.* **20**. 3155-3159. (2020).
- [22] Putra, W.E., Kharisma, V. D., & Susanto, H. Potential of *Zingiber officinale* bioactive compounds as inhibitory agent against the IKK-B. *AIP Conference Proceedings.* **2231**. 040048. (2020).
- [23] Prahasanti, C., Nugraha, A. P., Kharisma, V. D., Ansori, A. N. M., Devijanti, R., Ridwan, T. P. S. P., Ramadhani, N. F., Narmada, I. B., Ardani, I. G. A. W., & Noor, T.

- N. E. B. A. A bioinformatic approach of hydroxyapatite and polymethylmethacrylate composite exploration as dental implant biomaterial. *J. Pharm. Pharmacogn. Res.* **9**, 746-754. (2021).
- [24] Wijaya, R. M., Hafidzhah, M. A., Kharisma, V. D., Ansori, A. N. M., & Parikesit, A. A. COVID-19 in silico drug with *Zingiber officinale* natural product compound library targeting the Mpro protein. *Makara J. Sci.* **25**, 162-171. (2021).
- [25] Vania, L., Widyananda, M. H., Kharisma, V. D., Ansori, A. N. M., Naw, S. W., Maksimiuk, N., Derkho, M., Denisenko, A., Sumantri, N. I., & Nugraha A. P. Anti-cancer activity prediction of *Garcinia mangostana* L. 55exadec her2-positive breast cancer through Inhibiting EGFR, HER2 and IGF1R protein: a bioinformatics study. *Biochem. Cell. Arch.* **21**, 3313-3321. (2021).
- [26] Prieto, J. M. Procedure: Preparation of DPPH Radical, and antioxidant scavenging assay. Prieto's DPPH Microplate Protocol. <https://www.researchgate.net/file.PostFileloader.html?id=503cd1c9e39d5ead11000043&assetKey=AS%3A271744332435456%401441800305338>, March, 30th, 17.30 Western Indonesian Time, 2021. (2012).
- [27] Fu, R., Zhang, Y., Guo, Y., Liu, F., & Chen, F. Determination of phenolic contents and antioxidant activities of extracts of *Jatropha curcas* L. seed shell, a by-product, a new source of natural antioxidant. *Ind. Crops. Prod.* **58**, 265-270. (2014).
- [28] Wahyuni, D. K., Purnobasuki, H., Kuncoro, E. P., & Ekasari, W. Callus induction of *Sonchus arvensis* L. and its antiplasmodial activity. *Afr. J. Infect.* **14**, 1-7. (2020).
- [29] Fonseca, A. G., Dantas, L. L. S. F. R., Fernandes, J. M., Zucolotto, S. M., Lima, A. A. N., Soares, L. A. L., Rocha, H. A. O., & Lemos, T. M. A. M. *In vivo* and *in vitro* toxicity evaluation of hydroethanolic extract of *Kalanchoe brasiliensis* (Crassulaceae) Leaves. *J. Toxicol.* 6849765. 1-8. (2018).
- [30] de Souza, G. E. D., Bueno, R. V., de Souza, J. O., Zanini, C. L., Cruz, F. C., Oliva, G., Guido, R. C., & Caroline, A. C. A. Antiplasmodial profile of selected compounds from Malaria Box: *In vitro* evaluation, speed of action and drug combination studies. *Malar. J.* **18**, 447-459. (2019).

- [31] Yadav, A., Yadav, M., Kumar, S., & Yadav J. P. Bactericidal effect of *Acacia nilotica*: in vitro antibacterial and time-kill kinetic studies. *Int. J. Curr. Res.* **7**, 22289-22294. (2015).
- [32] Ahamed, T., Rahman, S. K. M., & Shohae, A. M. Thin-layer chromatographic profiling and phytochemical screening of six medicinal plants in Bangladesh. *Int. J. Biosci.* **11**, 131-140. (2017).
- [33] Yehye, W. A., Rahman, N. A., Alhadi, A. A., Khaledi, H., Ng, S. W., & Ariffin, A. Butylated hydroxytoluene analogs: synthesis and evaluation of their multipotent antioxidant activities. *Molecules.* **17**, 7645-7665. (2012).
- [34] Zeb, M. A., Khan, S. U., Rahman, T. U., Sajid, M., & Seloni, S. Isolation and biological activity of β -sitosterol and stigmasterol from the roots of *Indigofera heterantha*. *PPIJ.* **5**, 204–207. (2017).
- [35] Sirikhansaeng, P., Tanee, T., Sudmoon, R., & Chaveerach, A. Major phytochemical as γ -sitosterol disclosing and toxicity testing in Lagerstroemia species. *Evid. -based Complement. Altern.* 7209851. (2017).
- [36] Akinmoladun, A. C., Olaleye, T. M., Komolafe, K., & Adetuyi, A. O. Effect of homopterocarpin, an isoflavonoid from *Pterocarpus erinaceus*, on indices of liver injury and oxidative stress in acetaminophen-provoked hepatotoxicity. *JBCPP.* **26**, 555-562. (2015).
- [37] National Institutes of Health. National Library of Medicine. National Center for Biotechnology Information., *Homopterocarpin*, <https://pubchem.ncbi.nlm.nih.gov/compound/-Homopterocarpin>. 12.28 Western Indonesain Time. August, 9th, (2021).
- [38] Choy, Y. B., & Prausnitz, M. R. The rule of five for non-oral routes of drug delivery: ophthalmic, inhalation and transdermal. *Pharm. Res.* **28**, 943–948. (2011).
- [39] Abdelli, I., Hassani, F., Brikci, S. B., & Ghalem, S. In silico study the inhibition of angiotensin converting enzyme 2 receptor of COVID-19 by *Ammoides 56exadecenoic* components harvested from Western Algeria. *J Biomol Struct Dyn.* 1–14. (2020).

- [40] Hassan, A., Akmal, Z., & Khan, N. The phytochemical screening and antioxidants potential of *Schoenoplectus triqueter* L. Palla. *Journal of Chemistry*. 3865139. (2020).
- [41] Yahya, M. A., & Nurrosyidah, I. H. Antioxidant activity ethanol extract of gotu kola (*Centella asiatica* L.) with DPPH method (2,2-diphenyl-1-pikrilhidrazil). *Journal Halal Product and Research*. **3**,106-112. (2020).
- [42] Esmaili, A. K., Taha, R. M., Mohajer, S., & Banisalam, B. Antioxidant activity and total phenolic and flavonoid content of various solvent extracts from *in vivo* and *in vitro* grown *Trifolium pratense* L. (Red Clover). *BioMed Res Int*. 643285:1-11. (2015).
- [43] Olennikov, D. N., Zilfikarov, I. N., Toropova, A. A., & Ibragimov, T. A. Chemical composition of *Callisia fragrans* wood juice and its antioxidative activity (*in vitro*). *Chem. Plant Raw Mater*. **4**, 95–100. (2008)
- [44] Upadhyaya, H. C., Sisodia, B. S., Cheema, H. S., Agrawal, J., Pal, A., Darokar, M. P., & Srivastava, S. K. Novel antiplasmodial agents from *Christia vespertilionis*. *Nat. Prod. Commun*. **8**, 1591–1594. (2013).
- [45] Chaniad, P., Phuwajaroanpong, A., Techarang, T., Viriyavejakul, P., Chukaew, A. & Punsawad, C. Antiplasmodial activity and cytotoxicity of plant extracts from the Asteraceae and Rubiaceae families. *Heliyon*. **8(1)**, e08848. (2022).
- [46] Noufou, O., André, T., Richard, S. W., Yerbanga, S., Maminata, T., Ouédraogo, S., Anne, E. H., Irène, G. & Pierre, G. I. Anti-inflammatory and anti-plasmodial activities of methanol extract of *Pterocarpus erinaceus* Poir. (Fabaceae) leaves. *Int. J. Pharmacol*. **89**, 291-294. (2016).
- [47] Tajuddeen, N., & van Heerden, N. Antiplasmodial natural products: An update. *Malar J*. **18**. 1-62. (2019).
- [48] Safitri, R. A., Saptarini, O., & Sunarni, T. Cytotoxic activity, expression of p53, and Bcl-2 extract fraction of Kelakai Herbs (*Stenochleana palustris* (Burm.F.) Bedd.) to breast cancer T47D cells. *Jurnal Biotek Medisiana Indonesia*. **9**. 113-127. (2020).
- [49] Saivaraj, S., & Chandramohan, G. Antimicrobial activity of natural dyes obtained from *Pterocarpus indicus* Willd. Bark. *Asian J. Pharm. Res. Dev*. **6**, 6-8. (2018).

- [50] Jiménez-González, L., lvarez-Corral, M. A., Muñoz-Dorado, M., & Rodríguez-García, I. Pterocarpan: interesting natural products with antifungal activity and other biological properties. *Phytochem. Rev.* **7**. 125–154. (2008).
- [51] Cuellar, J. E., Martínez, J., Rojano, B, Gil, J. H., & Durango, D. Chemical composition and antioxidant and antibacterial activity of *Platymiscium gracile* Benth.: A species threatened by extinction. *J. King Saud Univ. Sci.* **32**. 702–708. (2020).



CHAPTER FOUR

***In silico* anti-SARS-CoV-2 and *in vitro* antiplasmodial activities of compounds from *n*-hexane fractions of *Sonchus arvensis* L. leaves**

Dwi Kusuma Wahyuni^{1,2}, Sumrit Wacharasindu³, Wichanee Bankeeree², Hunsu Punapayak², Hery Purnobasuki¹, Junairiah¹, Arif Nur Muhammad Ansori⁴, Viol Dhea Kharisma⁵, Arli Aditya Parikesit⁶, Listyani Suhargo¹, and Sehanat Prasongsuk^{1,2*}

¹Department of Biology, Faculty of Science and Technology, Universitas Airlangga Surabaya, East Java, 60115, Indonesia

²Plant Biomass Utilization Research Unit, Department of Botany, Faculty of Science, Chulalongkorn University, Bangkok, 10330, Thailand

³Department of Chemistry, Faculty of Science, Chulalongkorn University, Bangkok, 10330, Thailand

⁴Professor Nidom Foundation, Surabaya, East Java, 60115, Indonesia

⁵Department of Biology, Faculty of Mathematics and Natural Sciences, Universitas Brawijaya, Malang, East Java, 65145, Indonesia

⁶Department of Bioinformatics, School of Life Science, Indonesia International Institute for Life Sciences, Jakarta, 13210, Indonesia

*Corresponding author: Sehanat Prasongsuk

sehanat.p@chula.ac.th.

Plant Biomass Utilization Research Unit, Department of Botany, Faculty of Science, Chulalongkorn University, Bangkok, 10330, Thailand

Abstract

Infectious diseases, especially SARS-CoV-2 and malaria, are global health concerns. This is the first report of *in silico* anti-SARS-CoV-2 and *in vitro* antiplasmodial activities of *n*-hexane fractions of *Sonchus arvensis* L. leaves. The leaves were harvested before the generative phase, then dried and extracted with *n*-hexane. The *n*-hexane extract was fractionated by column chromatography. The secondary metabolites of the selected fractions were identified by gas chromatography-mass spectrometry (GC-MS) and thin layer chromatography. The *in silico* anti-SARS-CoV-2 and *in vitro* antiplasmodial activities of the selected fractions (5–12 and 15–28) were determined. *In silico* anti-SARS-CoV-2 analysis was conducted for compounds identified by GC-MS with the target proteins, consisting of the helicase (PDB ID 6ZSL), RdRp (PDB ID 6M71), Mpro (PDB ID), and RBD-Spike (PDB ID 6LZG) proteins of SARS-CoV-2. The *in silico* assay was performed using software. PyRx software ver. 0.9.9 was used for docking simulation, Lipinski's Rule of Five (<http://www.scfbioiitd.res.in/software/drugdesign/lipinski.jsp>) was used to predict drug-like molecules, the Molinspiration v2018.03 server (<https://www.molinspiration.com/cgi-bin/properties>) was used to predict inhibitor activity, PyMol software ver. 2.5 (<https://pymol.org/2/>) was used to display the three-dimensional structures of the molecular complexes predicted by molecular docking simulation, and CABS-flex ver. 2.0 (<http://biocomp.chem.uw.edu.pl/-CABSflex2/index>) was used to generate molecular dynamic simulations. Antiplasmodial testing was performed on blood cultures infected with *Plasmodium falciparum* strain D317 using the Rieckmann method. GC-MS analysis identified hexacosanol, β -amyrin, lupeol, α -amyrin, 60exadec, and taraxasterol as the major bioactive molecules of fractions 15–28. The *in silico* anti-SARS-CoV-2 assay showed that β -amyrin, lupeol, α -amyrin, 60exadec, and taraxasterol were predicted as effective antiviral candidates by having the ability to act as inhibitors of SARS-CoV-2 protein activity. Moreover, fractions 5–12 and 15–28 had *in vitro* antiplasmodial activities with IC₅₀ values of 2.38 and 5.03 μ g/mL, respectively. Therefore, the molecular dynamic analysis data strengthen the notion that the interactions resulting from the five compounds of *n*-hexane fractions of *S. arvensis* L. leaves were stable and predicted to be effective antiviral candidates by

having the ability to act as inhibitors of SARS-CoV-2 protein activity. The *in vitro* results showed that the *n*-hexane fractions of *S. arvensis* L. leaves had antiplasmodial activities.

Keywords: *Sonchus arvensis* L., antiplasmodial, *Plasmodium falciparum*, SARS-CoV-2, *n*-hexane fractions

4.1 Introduction

Severe acute respiratory syndrome-related coronavirus-2 (SARS-CoV-2) remains a serious health concern that impacts all aspects of human life worldwide and efforts to develop new drugs are ongoing. All scientific activities have been mobilized to discover alternative drugs against SARS-CoV-2^[1]. Moreover, the emergence of drug-resistant parasites is a major threat to the control of infectious diseases, including malaria, thereby increasing the risks of morbidity and mortality. Resistance to artemisinin-based combination therapy has been a significant obstacle to the treatment and prognosis of malaria^[2], thus the development of new antimalarial drugs is particularly urgent.

Recent studies have explored the efficacy of synthetic and natural products as antimalarial drugs^[3]. According to estimates by the World Health Organization, about 80% of the world population use natural compounds derived from medicinal plants as herbal drug preparations^[4]. However, the requirement for new and useful compounds has been growing each year^[5,6].

Sonchus arvensis L., a highly invasive species of the family Asteraceae, is used as a traditional medicinal plant for the treatment of malaria in Indonesia^[7]. This plant contains various active compounds, including flavonoids, saponins, and polyphenols^[8], which reportedly have moderate to high antioxidant^[9], hepatoprotective^[10], nephroprotective^[11], anti-inflammatory^[12], and antibacterial^[13] activities. In spite of these pharmaceutical benefits, the active compounds of *S. arvensis* L. have not been evaluated *in vivo* for treatment of malaria. A previous study reported that methanol extracts of *S. arvensis* L. calluses had antiplasmodial activities a half-maximal inhibitory concentration (IC₅₀) of 0.343 µg/mL at 1 mg/L of 2,4-dichlorophenoxyacetic acid and 0.5 mg/L of benzyl amino purine incubated without light^[14].

The aim of the present study was to determine the *in silico* anti-SARS-CoV-2 and *in vitro* antiplasmodial activities of compound *n*-hexane fractions of *S. arvensis* L. leaves. The results showed that compound *n*-hexane fractions of *Sonchus arvensis* L. had *in silico* anti-SARS-CoV-2 and *in vitro* antiplasmodial activities.

4.2 Methods

4.2.1 Plant Material Collection and Identification

S. arvensis L. was collected from Mount Merapi, Daerah Istimewa Yogyakarta, Indonesia, by local people. The plants were 2–3 months old (pre-generative stage) and the leaves were green and apparently healthy with no signs of destruction by insects or microbes. The plant material was confirmed as *S. arvensis* L. by the staff of the Purwodadi Botanical Garden (Pasuruan, East Java, Indonesia) operated by the Indonesian Institute of Sciences (Jakarta, Indonesia). A voucher specimen was deposited in the Plant Systematics Laboratory, Department of Biology, Faculty of Science and Technology, Universitas Airlangga, Surabaya City, East Java, Indonesia (no. SA.0110292021).

4.2.2 Extraction

The leaves of *S. arvensis* L. were air-dried, ground into powder at room temperature, and macerated three times with *n*-hexane for 24 h each at room temperature. The liquid extract was filtered through Whatman no. 1 filter paper (pore diameter, 11 μm ; Cytiva, Marlborough, MA, USA), then evaporated in a rotary evaporator at 60°C to acquire crude extracts, which were stored at 4°C for later use.

4.2.3 Thin Layer Chromatography (TLC)

n-Hexane-extracted *S. arvensis* L. leaves (5 mg) were dissolved in *n*-hexane (100 μL) and 5- μL aliquots were spotted on a TLC plate (silica gel GF254; Sigma-Aldrich Corporation, St. Louis, MO, USA). Once dried, the TLC plate was developed with *n*-hexane and ethyl acetate (4:1), dried, sprayed with *p*-anisaldehyde sulfuric acid, and heated. Terpenoids on the TLC plate appeared as a purplish / blue nodes^[15].

4.2.4 Purification and Isolation

n-Hexane-extracted *S. arvensis* L. leaves were subjected to chromatography using a column (length, 80 cm length; cross-section, 2.5 cm) containing silica gel 60

(particle size, 0.063–0.200 mm; Merck KgaA, Darmstadt, Germany). The silica gel was weighed using a ratio of the adsorbent to extract of 80:10. A slurry of silica gel (80 g) was prepared with 100% *n*-hexane and poured into the column. The crude extract (10 g) was dissolved in dichloromethane (10 mL) in a beaker and adsorbed in the silica gel (10 g). The mixture was stirred at room temperature until all the dichloromethane had evaporated and placed on top of a previously packed column. Initially, elution was conducted with 80% *n*-hexane and 20% ethyl acetate (Table 1). Fractions were collected in 10-mL Falcon™ bottles (Corning Inc., Corning, NY, USA) until the compounds were eluted entirely from the column. TLC fractions with the same R_f values were combined (Table 1).

4.2.5 Gas Chromatography-Mass Spectrophotometry (GC-MS)

GC-MS analysis was used to determine the phytochemical profiles of *S. arvensis* L. *n*-hexane fractions 5–12 and 15–28. Each fraction (15 mL) was dissolved in chloroform (1 mL), then passed through a 45- μ m filter. Triple quadrupole GC-MS/MS was performed with an Agilent 7890B GC system and Agilent 7633 ALS detector (Agilent Technologies, Inc., Santa Clara, CA, USA) with an Agilent J&W HP-5ms column (5% phenyl-methylpolysiloxane; inner diameter, 0.25 mm; length, 30 m; film thickness, 0.25 μ m). The following settings were used for GC-MS analysis: flow rate of the mobile phase, 1 mL/min; average velocity, 36.445 cm/min; oven temperature, 40–320°C at 15°C/min and held for 3–20 min; post-run temperature, 320°C (2 mL/min) for 5 min; carrier gas, helium; flow rate of carrier gas, 29.75 mL/min; carrier flow rate, 1 mL/min (constant mode); sample volume, 10 μ L; total running time, 24 min; injector temperature, 50°C; injection volume, 0.3 μ L (fractions 15–28) or 1.8 μ L (fractions, 5–12); split ratio, 20:1 (fractions 15–28) or 10:1 (fractions, 2–12); and inlet temperature, 280°C. The interface and mass spectra ion source were maintained at 320°C and 250°C, respectively. The mass spectra were collected at 70 eV with a mass scan range of 30–5550 amu, solvent delay of 3 min, and transfer line temperature of 320°C. The identification of compounds was based on comparing the mass spectra with those of the Standard Reference Database (version 02.L; National Institute of Standards and Technology, Gaithersburg, MD, USA). The relative percentage of each

component was calculated as the relative percentage of the total peak area of the chromatograph.

4.2.6 Sample Preparation of *in silico* anti-SARS-CoV-2 activity

GC-MS analysis of *n*-hexane fractions 15–28 revealed the presence of α -amyrin (compound identification [CID] 73170), β -amyrin (CID 73145), 64exadec (CID 72326), lupeol (CID 259846), and taraxasterol (CID 441686). The covid-19 drugs EIDD-2801 or molnupiravir (CID 145996610 or Control 1) and PF-07321332 or paxlovid (CID 155903259 or Control 2) were used as positive controls (ligands) in this study. Samples of the selected chemical compounds were prepared by reference to the PubChem database (<https://pubchem.ncbi.nlm.nih.gov/>). The information obtained from the PubChem database consisted of the CID, three-dimensional (3D) structure, and canonical simplified molecular-input line-entry. The target proteins in this study consisted of helicase (Protein Data Bank identification [PDB ID] 6ZSL), RNA-dependent RNA polymerase (RdRp) (PDB ID 6M71), main protease (Mpro) (PDB ID 7ALH), and receptor-binding domain (RBD)-spike (PDB ID 6LZG) of SARS-CoV-2. The 3D structures of the proteins were obtained from the US Research Collaboratory for Structural Bioinformatics Protein Data Bank (<https://www.rcsb.org/>). The 3D structures of sterilized native ligands and water were obtained using PyMol software ver. 2.5^[16].

4.2.7 Drug-likeness Identification

Prediction of drug-like molecules of the *n*-hexane fractions of *S. arvensis* L. leaves was conducted in accordance with Lipinski's Rule of Five (<http://www.scfbioiitd.res.in/software/drug-design/lipinski.jsp>). The parameters of the chemical compounds as drug candidates included molecular weight, high lipophilicity ($\log P > 5$), hydrogen donor bonds, acceptors, and molar refractivity. Natural drug-based candidates with drug-like molecular properties were predicted to show a high success rate in triggering target protein activity^[17].

4.2.8 Bioactivity Prediction

Potential inhibitor activity of the *n*-hexane fractions compounds of *S. arvensis* L. leaves was investigated using the Molinspiration property engine v.2018.03 (<https://www.molinspiration.com/cgi-bin/properties>). Predictions were made by referencing the bioactivity score as an indicator for targeting of drug-binding sites via

GPCR ligands, ion channel modulators, inhibitors, modulators, and nuclear receptors. Positive predictive scores indicated specific activities, such as inhibitory effects, of the tested compounds^[18].

4.2.9 Molecular Docking Simulation

A molecular docking simulation method was used to predict the inhibitory ability of a ligand to a target protein^[19]. With a blind docking method, the functional side of the target protein is ignored, as the binding energy formed is a better indicator to screen ligand activity against a target protein^[20]. In this study, the mechanisms of action of the *S. arvensis* L. compounds are predicted to involve binding to and inhibiting the activities of the helicase, RdRp, M^{pro}, RBD-Spike proteins of SARS-CoV-2. The docking simulation was conducted using PyRx software ver. 0.9.9 (<https://pyrx.sourceforge.io/>) with academic license.

4.2.10 Ligand-Protein Interactions and 3D Visualization

The molecular complex resulting from the molecular docking simulation was analyzed for the positions and types of formed chemical bonds with BIOVIA Discovery Studio 2017 software (<https://discover.3ds.com/discovery-studio-visualizer-download>). The software was used to predict the types of weak bond interactions (i.e., hydrophobic, Van der Waals, hydrogen, electrostatic, and -alkyl) and display the results in two-dimensional images. The 3D structures of the molecular complexes predicted by molecular docking simulation were displayed using PyMol software. The protein-ligand molecular complexes are presented as cartoons, surface models, stick models, and selective staining^[21].

4.2.11 Molecular Dynamic Analysis

The stability of the binding interactions formed between ligands and specific proteins domains was identified by molecular dynamic simulation with the CABS-flex web server ver. 2.0 (<http://biocomp.chem.uw.edu.pl/CABSflex2/index>). The parameters used in this simulation consisted of protein rigidity (1.0), protein restraints (ss2 3 3.8 8.0), global c-alpha restraints weight (1.0), global side-chain restraints weight (1.0), number of cycles (50), cycles between trajectory (50), temperature range (1.40), and RNG seed (227). The final result of the simulation is shown as a fluctuating graph or root mean square fluctuation (RMSF) with a maximum distance of 1–3^[22].

4.2.12 *In Vitro* antiplasmodial Assay

Cultures of *Plasmodium falciparum* strain 3D7 were cultivated using the Trager and Jensen method^[23], as adapted by Ekasari *et al.* ^[24], in Roswell Park Memorial Institute 1640 medium (Gibco, Carlsbad, CA, USA) supplemented with human O-type red blood cells, 5% hematocrit, 22.3 mM HEPES buffer (4-(2-hydroxyethyl)-1-piperazineethanesulfonic acid; Sigma-Aldrich Corporation, St. Louis, MO, USA), 50µg/mL hypoxanthine, 2 mg/mL sodium bicarbonate, and 10% human O⁺ plasma. Chloroquine diphosphate was used as a positive control. An antiplasmodial assay was conducted using a 24-well microplate and incubation at 37°C for 48 h. The incubated materials were then collected, thinly smeared on a glass slide, fixed with methanol, and stained with Giemsa to assess the number of parasites under a microscope as compared with the negative control to determine the IC₅₀ value to achieve inhibition of parasitic growth. All IC₅₀ values were calculated using Probit analysis.

4.2.13 Cytotoxicity Assay and Selectivity index (SI)

Cytotoxicity assay was conducted using the micro tetra zolium MTT assay against human hepatic cells (Passage/P 18). The Dulbecco's modified Eagle's medium (DMEM) medium was used by adding 3.7 g of sodium bicarbonate (NaHCO₃), and pH adjustment of 7-7.2. The 500 ml of DMEM media, 50 ml of fetal bovine serum (FBS), 5 ml of nonessential amino acid (NEAA), and 6 ml of phenstrep (penicillin-streptomycin) were used as a complete medium. The complete medium was used culturing the cells during assay^[25].

The selectivity index (SI) was calculated to describe the selective activity of the extract against *Plasmodium falciparum* strain 3D7 compared with the results of its toxicity test on human hepatocyte cells. Here, the SI value was calculated by comparing the IC₅₀ value of the extract cytotoxicity and the IC₅₀ value of *P. falciparum* strain 3D7. The selectivity index (SI) was calculated to describe the selective activity of the extract against *P. Falciparum* strain 3D7 compared with the results of its toxicity test on human hepatocyte cells^[26].

4.3 Result and Discussion

4.3.1 Terpenoid Screening of the *n*-hexane extract of *Sonchus arvensis* L. by TLC

The *n*-hexane extract of *S. Arvensis* L. Was analyzed by TLC using silica gel GF 254 as the stationary phase and *n*-hexane:ethyl acetate (4:1) as the mobile phase. There were two visible spots in daylight and under ultraviolet (UV) light at 254 nm (Rf value = 0.12 and 0.18). Under UV light at 366 nm, there were seven separate spots with Rf values of 0.14, 0.24, 0.29, 0.35, and 0.53. After staining with *p*-anisaldehyde sulfuric acid, three separate purple spots appeared, with Rf values of 0.31, 0.59, and 0.71 (Figure 6). TLC is an established method for separation of extracts of secondary metabolites of plant materials^[27]. The Rf value is an indicator of the diversity of terpenoid compounds separated from various extracts^[28].

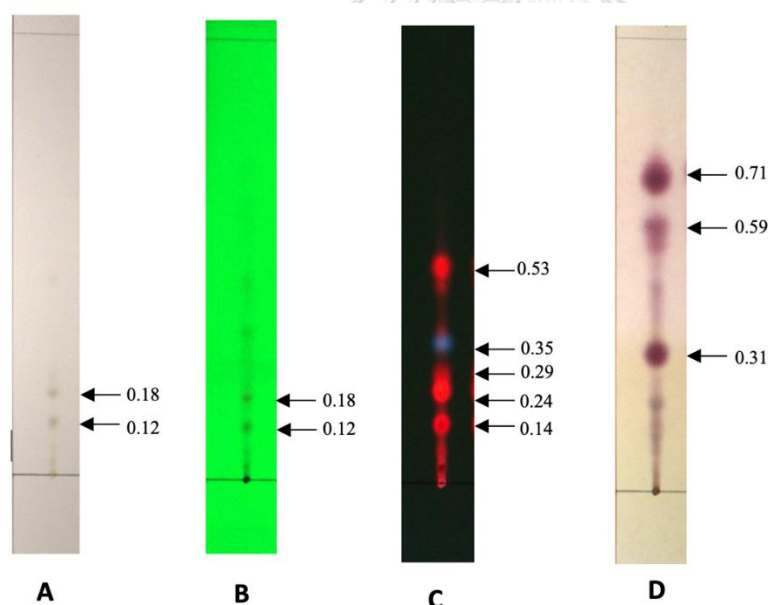


Figure 6. Chromatogram of *Sonchus arvensis* L. extract. (A) Solvent only (*n*-hexane : ethyl acetate at 4:1). (B) UV light at 254 nm. (C) UV light at 366 nm. (D) Anisaldehyde sulfuric acid (the purple spot at 0.35 is a terpenoid).

4.3.2 Isolation and Purification

Sixteen fractions were collected (Table 18). The TLC results of fractions 5–12 were notable and yellow crystals formed at the bottom of the falcon tubes of these

samples. Further crystallization was induced using *n*-hexane at 4°C for 24 h. White crystals of the mother liquor had also formed at the bottom of the flasks. The light-yellow crystals were further purified by crystallization with *n*-hexane (white crystal, 198 mg). The yield of the final product was 1.98% (w/w).

Furthermore, the TLC results of fractions 15–28 were also significant. Brown crystals had formed at the bottom of the falcon tubes of these samples. Further crystallization was induced using *n*-hexane at 4°C for 24 h. Finally, 379 mg of white crystal was produced at a yield of 3.79%. The purity of each isolated compound was determined by TLC before spectral analysis.

Table 18. Column chromatographic separation of *Sonchus arvensis* L. *n*-hexane extract

Fractions	Solvent	Volume collected (mL)	Combined fractions	Rf values of major spots	Number of spots	TLC solvent (<i>n</i> -hexane: ethyl acetate)
1–4	<i>n</i> -Hexane	40	1–4	0	0	4:1
5–12	<i>n</i> -Hexane	80	5–12	0.71	1	4:1
13–14	<i>n</i> -Hexane	20	13–14	0.71, 0.59, 0.31	3	4:1
15–28	<i>n</i> -Hexane	140	15–28	0.59, 0.31	2	4:1
29–35	<i>n</i> -Hexane	70	29–35	0.31, 0.24	2	4:1
36–60	<i>n</i> -Hexane	250	36–60	0.24, 1.8	1	4:1

Note: Conditions for GC-MS are indicated in italics

4.3.3 GC-MS Analysis

GC-MS was used to determine the metabolite profile of two groups of *n*-hexane fractions of *S. arvensis* L. leaves: 5–12 and 15–28. Fractions 5–12 contained two compounds (stearyl palmitate and cetyl myristate) (Table 19, Figure 7) (Appendix 3: Supplementary data I), while fractions 15–28 contained six (hexacosanol, β -amyrin, Lupeol, α -amyrin, 68hexadec, and taraxasterol) (Table 20, Figure 8) (Appendix 3: Supplementary data II). Octadecyl ester stearyl palmitate (fractions 5–12) and taraxasterol (fractions 15–28) were the major compounds among the eight detected.

Many phytochemicals have bioactivities. Stearyl palmitate and cetyl myristate have antimicrobial activities^[29,30]. Hexacosanol has a beneficial effect against detrusor overactivity in diabetic patients by ameliorating overexpression of muscarinic M₂ and M₃ receptor mRNAs^[31], neurotrophic activity^[32], and acetylcholinesterase inhibition activity in insects^[33]. β -Amyrin has antimicrobial^[34], antioxidant^[35], and anti-inflammatory^[36] activities. Lupeol has antimicrobial^[36], anti-inflammatory, and anti-arthritic^[37] activities. α -Amyrin has antimicrobial activities^[38] and stimulates human keratinocytes^[39]. Betulin has anticancer activities^[40] and has been used as a drug delivery system^[41] and as antiviral and antitumor agents^[42]. Taraxasterol has anticancer^[43] and anti-edematous activities and is reported to lower serum cholesterol levels^[44].

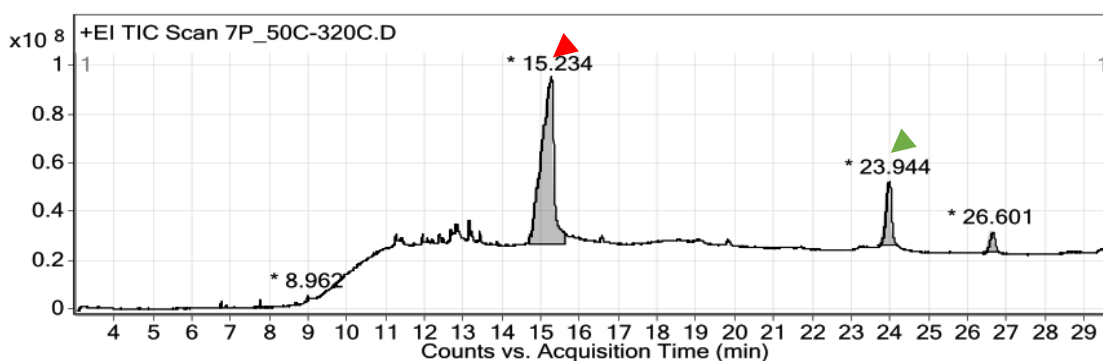


Figure 7. Representative chromatogram of fractions 5–12 of *Sonchus arvensis* L. *n*-hexane extract. Red arrow, octadecyl ester 69exadecenoic acid; green arrow, hexadecyl ester tetradecanoic acid.

Table 19. Phytochemical components from GC-MS analysis of fractions 2-12 of *Sonchus arvensis* L. *n*-hexane extract

No	Compound	Retention Time (minutes)	Percentage of Area (%)	Bioactivity
1	Stearyl palmitate	15.234	100	Antimicrobial activities ^[29,30]
2	Cetyl myristate	23.944	17	Antimicrobial and antifeedant activities ^[31]

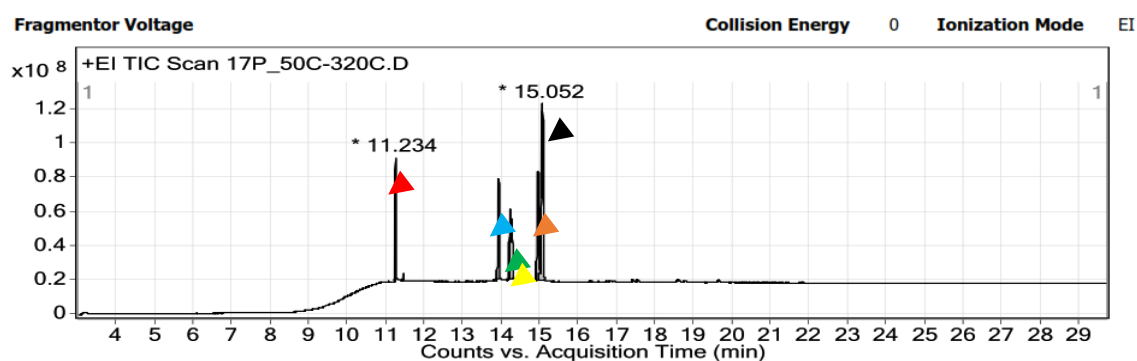


Figure 8. Representative chromatogram of fractions 15–28 of *Sonchus arvensis* L. n-hexane extract. Red arrow, hexacosanol; blue arrow, β -amyrin; green arrow, lupeol; yellow arrow, α -amyrin; brown arrow, betulin; black arrow, taraxasterol.

Table 20. Phytochemical components from GC-MS analysis of fractions 15–28 of *Sonchus arvensis* L. n-hexane extract

No	Compound	Retention Time (minutes)	Percentage of Area (%)	Bioactivities
1	Hexacosanol	11.234	27.37	Neurotrophic activities ^[32]
2	β -Amyrin	13.911	43.41	Antimicrobial ^[34] , antioxidant ^[35] , and anti-inflammatory ^[36] activities
3	Lupeol	14.207	31.26	Antimicrobial ^[34] , anti-inflammatory, and anti-arthritis ^[35] activities
4	α -Amyrin	14.255	25.91	Antimicrobial activities ^[38] , stimulation of human keratinocytes ^[41]
5	Betulin	14.965	59.51	Anticancer activities ^[42] , drug delivery system ^[41] , antiviral and antitumor agents ^[42]
6	Taraxasterol	15.052	100	Anticancer ^[43] and anti-edematous activities, lowers serum cholesterol levels ^[44] ,

4.3.4 Anti-SARS-CoV-2 activity

The main compounds identified by GC-MS analysis of the *n*-hexane fractions of *S. arvensis* L. leaves were α -amyrin, β -amyrin, lupeol, taraxasterol, and betulin (fractions 15–28) (Table 20). All five compounds were identified as drug-like in accordance with the Lipinski Rule of Five parameters. According to Benet *et al.*^[16], the Lipinski Rule of Five consists of molecular mass >500 D, high lipophilicity <5, hydrogen bond donor <5, and hydrogen bond acceptor <10. The Lipinski Rule of Five is also predictive of the ability to penetrate cell membranes and an early indicator of the effectiveness of query compounds^[45]. Molecular weight in Lipinski's rule can be used to predict the mechanism of action of a compound, as compounds with smaller weights move more quickly and are easily absorbed by target cells. All five compounds are potential drug-like molecules or candidate drug molecules because all met more than two of the Lipinski Rules of Five (Table 21). Hence, these five compounds were categorized as drug-like molecules and probable to trigger specific activity when forming complexes with target proteins.

Table 21. Drug-likeness analysis of compounds from *n*-hexane fractions of *Sonchus arvensis* L. leaves.

Compound	MW (Dalton)	LogP	HBD	HBA	MR	Probability
α -Amyrin	426.000	8.024	1	1	130.649	Drug-like molecule
β -Amyrin	426.000	8.168	1	1	130.719	Drug-like molecule
Lupeol	426.000	8.025	1	1	130.670	Drug-like molecule
Taraxasterol	426.000	8.024	1	1	130.649	Drug-like molecule
Betulin	442.000	6.997	2	2	132.061	Drug-like molecule

Abbreviations: HBA, hydrogen bond acceptor; HBD, hydrogen bond donor; LogP, high lipophilicity; MR: molar refractivity; MW, molecular weight

The potential inhibitor activity of the five compounds derived from *n*-hexane fractions of *S. arvensis* L. leaves classified as drug-like molecules in *Homo sapiens*^[46] was investigated. The focus of this study was inhibition activities against kinases, proteases, and other enzymes. The potential inhibitory activity of a query compound

is indicated by a more positive value^[47]. The results showed that all five compounds extracted from *S. arvensis* L. were probable inhibitors of enzyme activities (Table 22).

Table 22. Prediction of inhibitory activities of *n*-hexane fractions of *Sonchus arvensis* L. compounds

Compound	GPCR ligand	Inhibitory activity			Probability
		Kinase	Protease	Enzyme	
α -Amyrin	0.22	0.19	-0.41	0.60	Probable Inhibitor
β -Amyrin	0.22	0.11	-0.31	0.56	Probable Inhibitor
Lupeol	0.27	0.15	-0.42	0.52	Probable Inhibitor
Taraxasterol	0.17	0.08	-0.23	0.50	Probable Inhibitor
Betulin	0.21	0.09	-0.41	0.51	Probable Inhibitor

The molecular docking simulation with PyRx software ver. 0.9.9 showed that the bioactive compounds from *n*-hexane fractions of *S. arvensis* L. leaves had the most negative binding affinity for each SARS-CoV-2 protein as compared to the drug controls. α -Amyrin had the lowest binding affinity for the helicase and RBD-spike proteins (-9.8 and -8.3 kcal/mol, respectively), while β -amyrin had the lowest binding affinity for the RdRp and M^{pro} proteins (-9.0 and -8.3 kcal/mol, respectively) (Table 23). The activity level of a candidate compound against a target protein is influenced by the binding affinity to the molecular complex, where a more negative value indicates greater potential for target activity. Two of the test compounds were predicted to produce inhibitory effects against four of the test target proteins because each produced a more negative binding affinity than other compounds and the drug control. The two compounds were also potential dual inhibitors because each had the potential to inhibit two of the four target proteins of SARS-CoV-2 (Table 23). PyMol software ver. 2.5 was used to visualize the docking simulation results and produce transparent surfaces, cartoons, stick structures, and colorations of the protein-ligand molecular complex structure (Figure 9).

The weak bond interactions formed in the docking complex consisted of alkyl, hydrogen, hydrophobic, Van der Waals, and electrostatic interactions. The existence of weak binding interactions supports the existence of biological activities

of proteins by binding of ligands to specific domains. All of the tested bioactive compounds bound to the target protein domains with weak binding interactions, consisting of alkyl, hydrogen, pi, sigma, and Van der Waals interactions (Table 23), which support the prediction that each bioactive compound inhibited the activity of the target protein. The stability of binding to the molecular complex could be analyzed with molecular dynamic simulation by calculating the RMSF value of each complex, as an indicator of the movement of interacting atoms on the residues that made up peptides and proteins within a certain distance. A distance of 4 Å indicates complex stability^[46]. The results showed that a stable complex was formed at the most negative lowest energy value with the highest RMSF value of 4 Å. The results of this study indicated that the RMSF values of α -amyrin, β -amyrin, lupeol, taraxasterol, and betulin at the pocket-binding domain of each target protein were 4 Å, indicating stability (Figures 12 and 13). So, the molecular dynamic analysis data strengthen the notion that the interactions of the five tested compounds were stable and predicted as effective antiviral candidates by having the ability to act as inhibitors of SARS-CoV-2 protein activity.

Table 23. Docking results of compounds contained by *Sonchus arvensis* L. n-hexane fraction with SARS-CoV-2 proteins

Target	Ligand	Grid Positions (Å)		Binding Affinity (kcal/mol)
		Center	Dimensions	
Helicase	α -Amyrin			-9.8
	β -Amyrin			-9.4
	Lupeol	X: -17,182	X:76,703	-8.9
	Taraxasterol	Y:30,909	Y:96,531	-9.3
	Betulin	Z: -74,684	Z:76,610	-8.8
	EIDD-2801 (Control 1)			-6.8
	PF-07321332 (Control 2)			-7.7
RdRp	α -Amyrin			-8.6
	β -Amyrin			-9.0
	Lupeol	X:119,717	X:79,274	-7.9
	Taraxasterol	Y:123,605	Y:84,541	-8.6
	Betulin	Z:115,595	Z:95,129	-7.7
	EIDD-2801 (Control 1)			-6.8
	PF-07321332 (Control 2)			-7.0
M ^{pro}	α -Amyrin			-8.0
	β -Amyrin			-8.3
	Lupeol	X: -26,256	X:57,450	-7.3
	Taraxasterol	Y:11,525	Y:69,117	-8.0
	Betulin	Z:58,967	Z:59,607	-7.3
	EIDD-2801 (Control 1)			-6.7
	PF-07321332 (Control 2)			-6.9
RBD-Spike	α -Amyrin			-8.3
	β -Amyrin			-8.2
	Lupeol	X:212,130	X:102,969	-8.0
	Taraxasterol	Y:184,834	Y:99,563	-8.1
	Betulin	Z:203,765	Z:190,569	-7.0
	EIDD-2801 (Control 1)			-6.2
	PF-07321332 (Control 2)			-6.6

Table 24. Results of identification of molecular interactions of *n*-hexane fractions of *Sonchus arvensis* L. leaves

Molecular Complex	Molecular Interaction
α -Amyrin_Helicase	Alkyl: Pro175, Tyr180, His554, Pro408, Pro406, Leu412 Hydrogen: Leu117, Asn557
α -Amyrin_RBD-Spike	Alkyl: Tyr789, Pro792 Van der Waals: Ile794, Asp796, Lys790, Gln895, Thr883, Phe797
β -Amyrin_RdRp	Alkyl: Met380, His381, Leu371, Ala375, His381 Pi Sigma: Trp509 Van der Waals: Phe340, Tyr374, Leu514, Tyr515
β -Amyrin_M ^{pro}	Van der Waals: Leu271, Gly275, Met276, Asn238, Thr199, Asp197, Arg131, Thr198 Alkyl: Tyr239, Tyr237, Leu272, Leu287 Hydrogen: Lys137

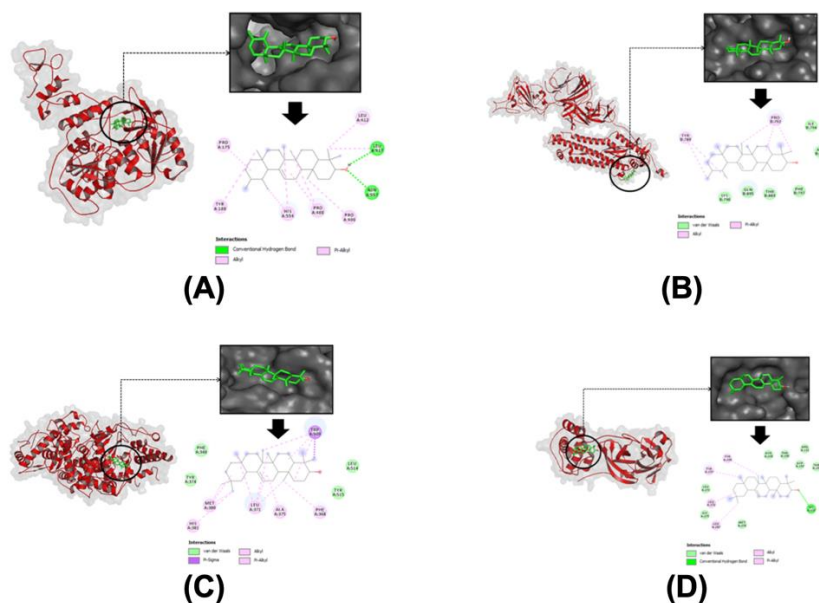


Figure 9. The 3D visualizations of molecular docking results. (A) α -Amyrin-Helicase, (B) α -Amyrin-Spike-RBD, (C) β -Amyrin-RdRp, and (D) β -Amyrin-M^{pro}

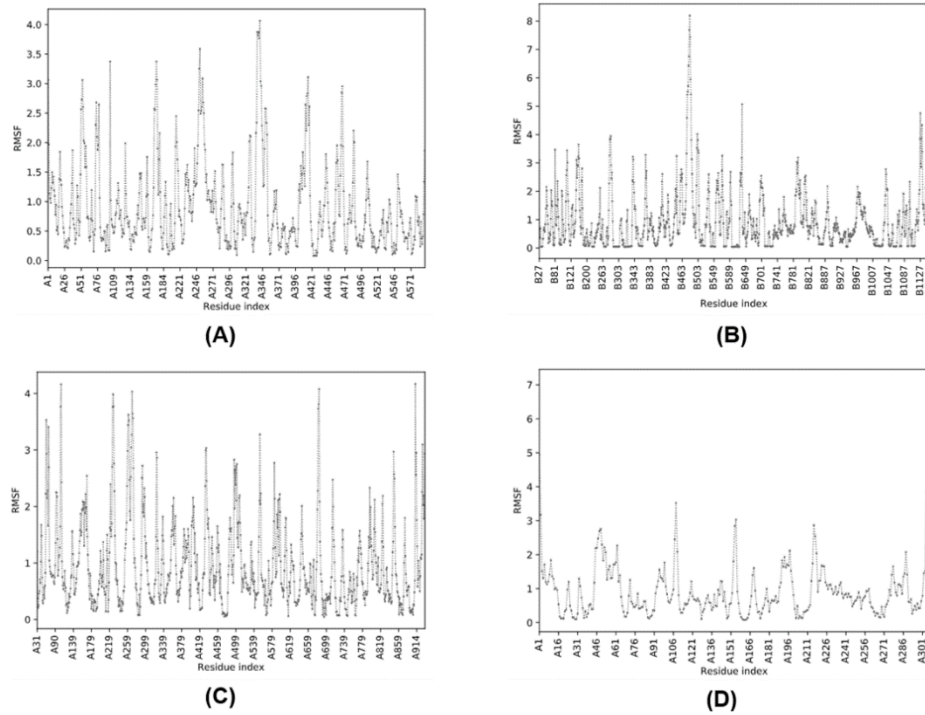


Figure 10. RMSF values of protein-ligand complexes. (A) α -Amyrin_Helicase, (B) α -Amyrin_Spike-RBD, (C) β -Amyrin_RdRp, and (D) β -Amyrin_M^{pro}.

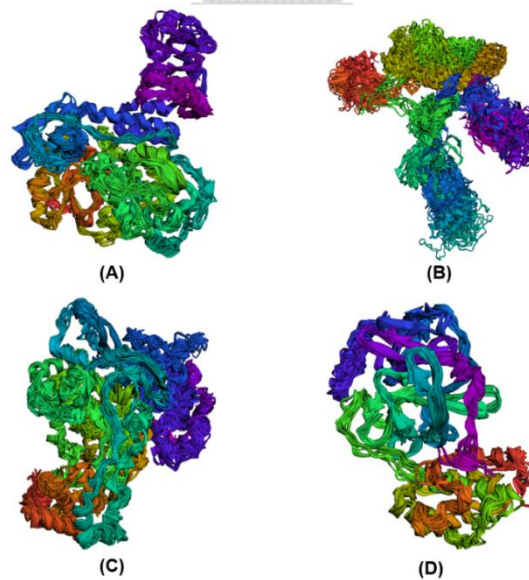


Figure 11. Protein 3D structures determined by molecular dynamic simulation. (A) α -Amyrin-Helicase, (B) α -Amyrin-Spike-RBD, (C) β -Amyrin-RdRp, and (D) β -Amyrin-M^{pro}.

4.3.5 Antimalaria activity of fraction of *n*-hexane extract of *Sonchus arvensis* L. against *P. falciparum* strain 3D7

The IC_{50} values of *n*-hexane fractions of *S. arvensis* L. at various doses are shown in Tables 25 and 26. As determined by the IC_{50} values, fractions 12–28 had the highest *in vitro* antiplasmodial activities, followed by fractions 2–5 extracted with ethanol and *n*-hexane (2.38 and 5.03 $\mu\text{g/mL}$, respectively). Many studies concluded that extracts with IC_{50} values of 1–10 $\mu\text{g/mL}$ are potential antiplasmodial agents^[48,49]. A study conducted in China reported an extract with an IC_{50} of 0.008–15.38 $\mu\text{g/mL}$ as a potential antimalarial drug^[50]. According to the criteria proposed by Kayano *et al.*^[51], an extract is very active as an antimalarial at $IC_{50} < 5 \mu\text{g/mL}$, active at $10 \mu\text{g/mL} > IC_{50} > 5 \mu\text{g/mL}$, and inactive at $IC_{50} > 10 \mu\text{g/mL}$. Also, according to the criteria proposed by Lima *et al.*^[52] a plant extract with an IC_{50} value of 10 $\mu\text{g/mL}$ can be considered active, $10 \mu\text{g/mL} < IC_{50} < 25 \mu\text{g/mL}$ as quite active, and $IC_{50} > 25 \mu\text{g/mL}$ as inactive as an antimalarial agent. Kigundu *et al.*^[53] classified the antiplasmodial potential of the crude extracts and fractions of plants as (a) highly active ($IC_{50} = 1\text{--}5 \mu\text{g/mL}$), (b) promisingly active ($IC_{50} = 5.1\text{--}10 \text{ mg/mL}$), (c) good activity ($IC_{50} = 10.1\text{--}20 \mu\text{g/mL}$), (d) moderate activity ($IC_{50} = 20.1\text{--}40 \mu\text{g/mL}$), (e) marginal potency ($IC_{50} = 40.1\text{--}70 \mu\text{g/mL}$), and (f) poor or inactive ($IC_{50} = 70.1\text{--}4100 \mu\text{g/mL}$).

As compared to previous research, the IC_{50} values of the *S. arvensis* L. fractions were lower than those of dichloromethane extracts of *Commiphora africana* (A. Rich.) Engl. stem bark and *Dychrostachys cinerea* (L.) Wight & Arn. whole stem, which showed promising antiplasmodial activities ($IC_{50} = 4.54 \pm 1.80$ and $11.47 \pm 2.17 \mu\text{g/mL}$, respectively)^[3], and lower than those of *Phyllanthus emblica* L. leaf with IC_{50} against *P. falciparum* strain 3D7 of 7.25 $\mu\text{g/mL}$ (ethyl acetate extract) and 3.125 $\mu\text{g/mL}$ (methanol extract), and *Syzygium aromaticum* L. flower bud with IC_{50} of 13 $\mu\text{g/mL}$ (ethyl acetate extract) and 6.25 $\mu\text{g/mL}$ (methanol extract)^[54], and that of *Pterocarpus erinaceus* Benth. ex Walp. ($IC_{50} = 16\text{--}30 \mu\text{g/mL}$)^[55].

Table 25. The percent parasitemia, growth percentage, and inhibition percentage of fractions 5–12 of *Sonchus arvensis* L of *n*-hexane extract against *P. falciparum* strain 3D7

Concentration (µg/ml)	Replication	% Parasitemia		Growth Percentage (%)	Inhibition Percentage (%)	IC ₅₀ (µg/ml)
		0 h	48 h			
Negative control	1	0.93	6.61	5.43	-	5.029
	2	1.10	6.30			
	Average	1.02	6.45			
10	1	0.93	3.34	2.38	56.17	
	2	1.10	3.45			
	Average	1.02	3.40			
1	1	0.93	4.27	3.43	36.83	
	2	1.10	4.62			
	Average	1.02	4.45			
0.1	1	0.93	5.26	4.11	24.31	
	2	1.10	5.00			
	Average	1.02	5.13			
0,01	1	0.93	5.60	4.66	14.18	
	2	1.10	5.75			
	Average	1.02	5.68			
0,001	1	0.93	7.01	5.68	0.00	
	2	1.10	6.39			
	Average	1.02	6.70			

Table 26. The percent parasitemia, growth percentage, and inhibition percentage of fractions 15–28 of *Sonchus arvensis* L of *n*-hexane extract against *P. falciparum* strain 3D7

Concentration (µg/ml)	Replication	% Parasitemia		Growth Percentage (%)	Inhibition Percentage (%)	IC ₅₀ (µg/ml)
		0 h	48 h			
Negative control	1	0.93	6.05	5.18	-	2.38
	2	1.10	6.34			
	Average	1.02	6.20			
10	1	0.93	3.21	2.13	58.88	
	2	1.10	3.10			
	Average	1.02	3.15			
1	1	0.93	3.48	2.54	50.96	
	2	1.10	3.64			
	Average	1.02	3.56			
0.1	1	0.93	4.83	4.24	18.15	
	2	1.10	5.70			
	Average	1.02	5.26			
0.01	1	0.93	6.56	5.36	0.00	
	2	1.10	6.20			
	Average	1.02	6.38			
0.001	1	0.93	6.63	5.72	0.00	
	2	1.10	6.85			
	Average	1.02	6.74			

4.3.6 *In vitro* toxicity and selectivity index (SI)

In vitro toxicity was carried out by the MTT assay method against human hepatic cells. Then, calculating the selectivity index (SI), by comparing the CC₅₀ of toxicity and the IC₅₀ of antiplasmodial activity of the natural product. The 50% toxicity concentration (CC₅₀) of fraction no. 5-12 and 15-28 of *Sonchus arvensis* L. *n*-hexane extract were 253.83 and 121.45 µg/ml respectively (Appendix 3: Supplementary data III). Moreover, the selectivity index was 50.47 and 51.03 respectively (Table 27).

The extract or fraction was said to have high selectivity if the value of SI ≥ 3, and to be less selective if the value of SI ≤ 3 (Safitri et al., 2020). de Souza et al.

(2019) categorized that natural product has been suggested that the SI > 10 indicated a favorable safety window between the effective concentration against the parasite and the toxic concentration to the human cell. All of the natural products in this study were found to be non-toxic.

Table 27. *In vitro* toxicity and selectivity index (SI) of *Sonchus arvensis* L. extract

No.	Extract	<i>In vitro</i> toxicity, CC ₅₀ (µg/ml)	Selectivity index (SI)
1	Fractions no. 5-12	253.83	50.47
2	Fractions no 15-28	121.45	51.03

4.4 Conclusion

The results of this study highlight the *in silico* anti-SARS-CoV-2 and *in vitro* antiplasmodial activities of *n*-hexane fractions of *Sonchus arvensis* L leaves. These findings lay a foundation for further investigations of anti-SARS-CoV-2 and antiplasmodial compounds for future pharmaceutical applications. Additionally, the development of anti-SARS-CoV-2 and antiplasmodial assays is recommended to assess the bioactivities of compounds for treatment of SARS-CoV-2 and malaria.

List of Abbreviations

GC-MS, gas chromatography-mass spectrophotometry; IC₅₀, half maximal inhibitory concentration; RMSF, root mean square fluctuation; SARS-CoV-2, severe acute respiratory syndrome coronavirus 2; TLC, thin layer chromatography

Authors' contributions

DKW: conception, design, implementation, conducting experiments, analysis, interpretation of results, and writing of the manuscript; SW: preparation of extraction, GC-MS analysis, and manuscript review; WB: conducting experiments, analysis, interpretation of results, and manuscript review; HP: collection, identification, and classification of plant material; HP: assisted with conception and material preparation; J: sample collection and preparation; VDK, ANMA, and AAP: *in silico* anti-SARS-CoV-2

analysis, and SP: primary author. All authors read and approved the final version of the manuscript.

Author details

¹Department of Biology, Faculty of Science and Technology, Universitas Airlangga, Surabaya, East Java, Indonesia, 60115; ²Plant Biomass Utilization Research Unit, Department of Botany, Faculty of Science, Chulalongkorn University, Bangkok, Thailand, 10330; ³Department of Chemistry, Faculty of Science, Chulalongkorn University, Bangkok, Thailand, 10330; ⁴Professor Nidom Foundation, Surabaya, East Java, Indonesia, 60115; ⁵Department of Biology, Faculty of Mathematics and Natural Sciences, Brawijaya University, Malang, East Java, Indonesia, 65145; ⁶Department of Bioinformatics, School of Life Science, Indonesia International Institute for Life Sciences, Jakarta, 13210.

*Corresponding author: Sehanat Prasongsuk, sehanat.p@chula.ac.th., Plant Biomass Utilization Research Unit, Department of Botany, Faculty of Science, Chulalongkorn University, Bangkok, 10330, Thailand.

Acknowledgments

The authors would like to thank Taman Husada Graha Famili Surabaya Indonesia for supplying the plant material.

Competing interests

The authors have no competing interests to declare.

Availability of data and materials.

The data and results obtained in the present study are available from the corresponding author upon request.

Consent for publication

Not applicable.

Funding.

This work was funded by Universitas Airlangga Surabaya, Indonesia (grant no. RC.1056/UN3.15/PT/2021).

4.5 References

- [1] WHO, *Coronavirus (Covid-19) outbreak*. <https://www.who.int>. July, 10th 2021, 03.40. Western Indonesian Time, 2020. October, 11th 2021, 03.40. Western Indonesian Time, 2021.
- [2] WHO, *World Malaria Report 2020*, Geneva, Switzerland: WHO Press, World Health Organization, 2020.
- [3] Kweyamba PA, Zofou D, Efange N, Assob JN, Kitau J. In vitro and in vivo studies on antimalarial activity of *Commiphora africana* and *Dichrostahys cinerea* used by the Maasai in Arusha region, Tanzania. *Malaria J.* 2019;18(1):119-125.
- [4] Katiyar D, Singh K, Ali M. Phytochemical and pharmacological profile of *Pterocarpus marsupium*: A review. *The Pharma Innovation Journal.* 2016;5(4):31-39.
- [5] Hegazy MF, Mohamed TA, Elshamy AI, Mohamed AH, Mahale UA, Reda EH, Shaheen AM, Tawfik WA, Shahat AA, Shams KA, Abdel-Azim NS, Hammouda FM. Microbial transformation as a tool for drug development based on natural products from mevalonic acid pathway: A review. *Journal of Advanced Research.* 2015;6:17-33.
- [6] Kang X, Csetenyl L, Gadd GM. Biotransformation of lanthanum by *Aspergillus niger*. *Applied Microbiology and Biotechnology.* 2019;103:981-993.
- [7] Wahyuni DK, Rahayu S, Purnama PR, Saputro TB, Suharyanto, Wijayanti N. Morpho-anatomical structure and DNA barcode of *Sonchus arvensis* L.. *Biodiversitas*, 2019;20(24):17-26.
- [8] Delyan E. Analysis of composition of volatile compounds of field sow thistle (*Sonchus arvensis* L.) leaves using the method of gas chromatography with mass-detection. *Journal of Pharmaceutical Innovation.* 2016;5:118-21.
- [9] Yuliarti W, Kusriani D, Isolasi FE. identifikasi dan uji antioksidan asam fenolat dalam daun tempuyung (*Sonchus arvensis* L.) dengan metode 1,1-difenil-2-pikrilhidrasil (DPPH). *Chemical Informatics.* 2013;1:294-304.

- [10] Hendriani R, Sukandara EY, Anggadiredja K. Sukrasno. In vitro evaluation of xanthine oxidase inhibitory activity of *Sonchus arvensis* leaves. *International Journal of Pharmaceutical and Clinical Research*. 2014;6:501-3.
- [11] Imelda I, Azaria C, Lucretia T. Protective Effect of ethanol Extract Tempuyung Leaf (*Sonchus arvensis* L.) against gentamicin induced renal injury viewed from blood ureum level. *Journal of Medicine and Health*. 2017;1:575-82.
- [12] Hendriani R, Sukandar EY, Anggadiredja K. Sukrasno. In vitro evaluation of xanthine oxidase inhibitory activity of selected medicinal plants. *International Journal of Pharmaceutical and Clinical Research*. 2015;8:235-238.
- [13] Rumondang M, Kusriani D, Fachriyah E. Isolation, identification and antibacterial test of triterpenoid compounds from n-hexane extract of tempuyung leaves (*Sonchus arvensis* L.). *PharmSci*. 2013;05:506-507.
- [14] Wahyuni DK, Purnobasuki H, Kuncoro EP, Ekasari W. Callus induction of *Sonchus arvensis* L. and its antiplasmodial activity. *African Journal of Infectious Diseases*. 2020;14:1-7.
- [15] Wahyuni DK, Rahayu S, Zaidan AH, Ekasari W, Prasongsuk S, Purnobasuki H. Growth, secondary metabolite production, and in vitro antiplasmodial activity of *Sonchus arvensis* L. callus under dolomite $[CaMg(CO_3)_2]$ treatment. *PLOS ONE*, 2021;6(8): e0254804.
- [16] Putra WE, Kharisma VD, Susanto H. Potential of *Zingiber officinale* bioactive compounds as inhibitory agent against the IKK-B. *AIP Conference Proceedings*, 2020;2231(1):040048.
- [17] Kharisma VD, Agatha A, Ansori ANM, Widyananda MH, Rizky WC, Dings TGA, Derkho M, Lykasova I, Antonius Y, Rosadi I, Zainul R (2022) Herbal combination from *Moringa oleifera* Lam. and *Curcuma longa* L. as SARS-CoV-2 antiviral via dual inhibitor pathway: A viroinformatics approach. *Journal of Pharmacy and Pharmacognosy Research*. 2022;10(1):138–146.
- [18] Shaheen U, Akka J, Hinore JS, Girdhar A, Bandaru S, Sumithnath TG, Nayarisseri A, Munshi A. Computer aided identification of sodium channel blockers in the clinical treatment of epilepsy using molecular docking tools. *Bioinformation*. 2015;11(3):131-137.

- [19] Hassan NM, Alhossary AA, Mu Y, Kwoh CK. Protein-ligand blind docking using quickvina-w with inter-process spatio-temporal integration. *Scientific Reports*. 2017;7(1):15451.
- [20] Kharisma VD, Ansori ANM, Nugraha AP. Computational study of ginger (*Zingiber officinale*) as E6 inhibitor in human papillomavirus type 16 (HPV-16) infection. *Biochemical and Cellular Archives* 2020;20 (Suppl 1):3155-3159.
- [21] Prahasanti C, Nugraha AP, Kharisma VD, Ansori ANM, Devijanti R, Ridwan TPSP, Ramadhani NF, Narmada IB, Ardani IGAW, Noor TNEBA. A bioinformatic approach of hydroxyapatite and polymethylmethacrylate composite exploration as dental implant biomaterial. *Journal of Pharmacy and Pharmacognosy Research*, 2021;9(5):746-754.
- [22] Wijaya RM, Hafidzhah MA, Kharisma VD, Ansori ANM, Parikesit AA. COVID-19 in silico drug with *Zingiber officinale* natural product compound library targeting the Mpro protein. *Makara Journal of Science*, 2021;25(3):162-171.
- [23] Trager W, Jensen JB, Human malarial parasites in continuous culture. *Science* 1976;193:673-676,
- [24] Ekasari W, Widyawaruyanti A, Zaini NC, Syafruddin A, Honda T, Morita H. Antimalarial activity of cassiarin a from the leaves of *Cassia siamea*. *Heterocycles*. 2009;78:1831-6.
- [25] de Souza GED, Bueno RV, de Souza JO, Zanini CL, Cruz FC, Oliva G, Guido RC, Caroline ACA. Antiplasmodial profile of selected compounds from Malaria Box: In vitro evaluation, speed of action and drug combination studies. *Malaria Journal*. 2019;18:404, pp. 447–459, 2019.
- [26] Fonseca AG, Dantas LLSFR, Fernandes JM, Zucolotto SM, Lima AAN, Soares LAL, Rocha HAO, Lemos TMAM. In vivo and in vitro toxicity evaluation of hydroethanolic extract of *Kalanchoe brasiliensis* (Crassulaceae) Leaves. *Journal Toxicology*, 2018;6849765:1-8.
- [26] Ali KS, Mohammed ASA, Munayem RT. Phytochemical Screening and thin layer chromatography of *Acacia etbaica* ssp. *Ucinata* leaves. *World Journal of Pharmaceutical Research*. 2017;6(12):1278-1283.

- [27] Ahamed T, Rahman SKM, Shohae AM. Thin layer chromatographic profiling and phytochemical Screening of six medicinal plants in Bangladesh. *International Journal of Biosciences*. 2017; 11(1):131-140.
- [28] Aldakheel RK, Rehman S, Almessiere MA, Khan FA, Gondal MA, Mostafa A, and Abdulhadi Baykal A. Bactericidal and in vitro cytotoxicity of *Moringa oleifera* seed extract and its elemental analysis using laser-induced breakdown spectroscopy, *Pharmaceuticals*. 2020;13(8):193.
- [29] Duke JA, *Handbook of Phytochemical Constituents of GRAS Herbs and Other Economic Plants*, CRC Press, Boca Raton, FL, USA 1992.
- [30] Saito M, Kinoshita Y, Satoh I, Bex A, Bertaccini A. Ability of cyclohexenonic long-chain fatty alcohol to reverse diabetes-induced cystopathy in the rat. *European Urology*. 2006;51(2): pp 479-488.
- [31] Borg J, Toazara J, Hietter H, Henry M, Schmitt G, and Luu B. Neurotrophic effect of naturally occurring long-chain fatty alcohols on cultured CNS. *Neurons*. 1987;213(2): 406-410.
- [32] Gade S, Rajamanikyam M, Vadlapudi V, Nukala MK, Aluvala R, Giddigari C, Karanam NJ, Barua NC, Pandey R, Upadhyayula VSV, Srpadi P, Amanchy R, Upadhyayula SM. Acetylcholinesterase inhibitory activity of stigmasterol & hexacosanol is responsible for larvicidal and repellent properties of *Chromolaena odorata*, *Biochimica et Biophysica Acta*. 2017;1861(3):541-550.
- [33] Ogwuche CE, Amupitan JO, Ayo RG. Isolation and biological activity of the triterpene β -amyirin from the aerial plant parts of *Maesobotrya barteri* (Baill). *Medicinal Chemistry*. 2014;4:729–733.
- [34] Sunil C, Irudayaraj SS, Duraipandiyar V, AlDhabi NA, Agastian P, Ignacimuthu S. Antioxidant and free radical scavenging effects of β -amyirin isolated from *S. cochinchinensis* Moore. leaves. *Industrial Crops and Products*. 2014;61:510–516.
- [35] Okoye NN, Ajaghaku DL, Okeke HN, Ilodigwe EE, Nworu CS, Okoye FBC. Beta-amyirin and alpha-amyirin acetate isolated from the stem bark of *Alstonia*

- boonei display profound anti-inflammatory activity. *Pharmaceutical Biology*. 2014;52:1478–1486.
- [36] Wal A, Rai A, Wal P, Sharma G. Biological activities of lupeol, in *Systematic Reviews in Pharmacy*, 2011.
- [37] Ekalu A, Ayo RGO, Habila JD, Hamisu. Bioactivities of Phaeophytin a, α -Amyrin, and lupeol from *Brachystelma togoense* Schltr, *JOTCSA*. 2019; 6(3):411-418.
- [38] Biskup E, Golebiowski R, Stepnowski P, and Lojkowska E. Triterpenoid α -amyrin stimulates proliferation of human keratinocytes but does not protect them against UVB damage, *Acta Biochimica Polonica*, 2012;59(2):255–260.
- [39] So HM, Eom HJ, Lee D, Kim S, Kang KS, Lee IK, Baek KH, Park JY, Kim KH. Bioactivity evaluations of betulin identified from the bark of *Betula platyphylla* var. *japonica* for cancer therapy, *Archives of Pharmacal Research*. 2018;41(8):815-822.
- [40] Niewolik D, Bednarczyk-Cwynar B, Ruszkowski P, Sosnowski TR, Jaszcz K. Bioactive botulin and PEG based polyanhydrides for use in drug delivery systems. *International Journal of Molecular Sciences*. 2021;22:1090.
- [41] Tolstikov GA, Flekhter OB, Shultz EE, Baltina LA, Tolstikov AG. Betulin and its derivatives. *Chemistry and biological activity. Chemistry for Sustainable Development*. 2005;2005(13):129-135.
- [42] Sharma K, Zafar R. Occurrence of taraxerol and taraxasterol in medicinal plants. *Pharmacognosy Reviews*. 2015;9(17):19-23.
- [43] Elnakady YA, Rushdi AI, Franke R, Abutaha N, Ebaid H, Baabbad M, Omar MOM, Al Ghamdi, AA. Characteristics, chemical compositions and biological activities of propolis from honey bee. *Scientific Reports*. 7:41453.
- [44] Widyananda MH, Pratama SK, Samoedra RS, Sari FN, Kharisma VD, Ansori ANM, Antonius Y (2021) Molecular docking study of sea urchin (*Arbacia lixula*) peptides as multi-target inhibitor for non-small cell lung cancer (NSCLC) associated proteins. *Journal of Pharmacy and Pharmacognosy Research*. 9(4): 484-496.

- [45] Susanto H, Kharisma VD, Listyorini D. Effectivity of black tea polyphenol in adipogenesis related IGF-1 and its receptor pathway through in silico based study. *Journal of Physics: Conference Series*. 2018; 1093: 012037.
- [46] Mousavi SS, Karami A, Haghighi TM, Tumilaar SG, Fatimawali, Idroes R, Mahmud S, Celik I, Ağagündüz D, Tallei TE, Emran TB, Capasso R. In silico evaluation of iranian medicinal plant phytoconstituents as inhibitors against main protease and the receptor-binding domain of SARS-CoV-2. *Molecules*. 2021; 26(18): 5724.
- [47] Weenen H, Nkunya MH, Bray DH, Mwasumbi LB, Kinabo LS, Kilimali VA. Antimalarial activity of Tanzanian medicinal plants. *Planta Medica*. 1990;56(4):368-370.
- [48] Upadhyaya HC, Sisodia BS, Cheema HS, Agrawal J, Pal A, Darokar MP, Srivastava SK. Novel antiplasmodial agents from *Christia vespertilionis*. *Natural Product Communication*. 2013; 8: 1591–1594.
- [49] Aryanti TM, Ermayanti IP, Kartika MD. Uji daya antimalarial *Artemisia* spp. terhadap *Plasmodium falciparum* Indonesia. *Majalah Farmasi Indonesia*. 2006;17(2): 81-84.
- [50] Kayano CAV, Lopes SCP, Bueno FG, Cabral EC, Souza-Neiras WC, Yamauchi LM, Foglio MA, M.N., Eberlin CJP, Mello FTM Costa, In vitro and in vivo assesment of the anti-malarial activity of *Caesalpinia pluviosa*. *Malaria Journal*, 2011;10(112):1-12.
- [51] Lima RB, Rocha e Silva LF, Melo MR, Costa JS, Picanço NS, Lima ES, Vasconcellos MC, Boleti AP, Santos JM, Amorim RC, Chaves FC, Coutinho JP, Tadei WP, Krettli AU, Pohlit AM. In vitro and in vivo anti-malarial activity of plants from the Brazilian Amazon. *Malaria Journal*. 2015;14(508):508.
- [52] Kigundu EVM, Rukunga GM, Gathirwa JW, Irungu BN, Mwikwabe NM, Amalemba GM, Omar SA, Kirira PG. Antiplasmodial and cytotoxicity activities of some selected plants used by the Maasai community. *South African Journal of Botany*. 2011;77(3):725–729.

- [53] Bagavan, A. A. Rahuman, N. K. Kaushik, D. Sahal, In vitro antimalarial activity of medicinal plant extracts against Plasmodium falciparum. Parasitology Research. 2011;108(1):15-22.
- [54] Karou D, Dicko MH, Sanon S, Simpore J, Traore AS. Antimalarial activity of Sida acuta Burm.f (Malvaceae) and Pterocarpus erinaceus Poir (Fabaceae). Journal of Ethnopharmacology. 2003;89(2-3):291-294.



CHAPTER FIVE

Biotransformation of homopterocarpin from *Pterocarpus macrocarpus* Kurz. heartwood by *Aspergillus niger*

Dwi Kusuma Wahyuni^{1,2}, Sumrit Wacharasindhu³, Wichanee Bankeeree¹, Hunsu Punapayak¹, and Sehanat Prasongsuk^{1,2*}

¹Plant Biomass Utilization Research Unit, Department of Botany, Faculty of Science, Chulalongkorn University, Bangkok, 10330 Thailand

²Department of Biology, Faculty of Science and Technology, Universitas Airlangga Surabaya, East Java, 60115, Indonesia

³Department of Chemistry, Faculty of Science, Chulalongkorn University, Bangkok, 10330, Thailand

*Corresponding author: Sehanat Prasongsuk

sehanat.p@chula.ac.th.

Plant Biomass Utilization Research Unit, Department of Botany, Faculty of Science, Chulalongkorn University, Bangkok, Thailand

Abstract

The requirement for new and useful compounds are growing. Some bioactive compounds have very bioavailability but low solubility and structural instability. Because of the phenomena, it is needed a specific effort to explore the natural material well, such as biotransformation. Therefore, the aims of this study were to transform homopterocarpin from *Pterocarpus macrocarpus* Kurz. heartwood and evaluate the bioactivity (antioxidant, antiplasmodial and anticancer) of biotransformation derived compound. Biotransformation of homopterocarpin isolated from *P. macrocarpus* Kurz. heartwood was performed by *Aspergillus niger* (UI X-172) in soy bean meal medium (SBM) for a week. Biotransformation derived compound was identified as medicarpin. Medicarpin exhibited in vitro antioxidant activity against 1,1-diphenyl-2-picrylhydrazyl (DPPH) ($IC_{50} = 7.49 \pm 1.7 \mu\text{g/mL}$) and 2,2-azino-bis (3-ethylbenzothiazoline-6-sulfonic acid (ABTS) ($IC_{50} = 0.61 \pm 0.4 \mu\text{g/mL}$), *in vitro* antiplasmodial against *Plasmodium falciparum* strain 3D7 with $IC_{50} = 0.414 \mu\text{g/mL}$,

and anticancer against hepatocyte-derived cellular carcinoma cell line (Huh7it-1 cells) with $IC_{50} = 34.96 \mu\text{g/mL}$. This study highlighted the biotransformation of homopterocarpin to medicarpin. It showed the good antioxidant, antiplasmodial and anticancer activities. These results have the potential to be developed into a new drug candidate. However, the compounds and transmission-blocking strategies for diseases control of medicarpin is essential for further study.

5.1 Methods

5.1.2 Chemicals and *Aspergillus niger* strain

Homopterocarpin was isolated from *n*-hexane extract of *Pterocarpus macrocarpus* Kurz. heartwood. The heartwood was air-dried until the dry weight obtained. One kg dried wood was then grounded into powder at room temperature and macerated three times with *n*-hexane for seven days at room temperature. The *n*-hexane extract was crystallized by *n*-hexane solvent five times or until the crystals were white.

Aspergillus niger (UI X-172) was used from Plant Utilization Research Unit Laboratory, Department of Botany, Chulalongkorn University. The spore bank was maintained at -20°C in cryovials in plate count broth medium (1 mL) mixed with glycerol (0.5 mL) as a cryoprotectant agent. The working spore bank was conserved at 4°C in plate count agar (PCA) slants for 6 months and used for seed cultures.

5.1.2 Microbial transformation

The culture medium for biotransformation was prepared by dissolving glucose (20 g), yeast extract (5g), NaCl (5g), KH_2PO_4 (5g), and soy bean meal (5g) in distilled water (1L), namely soy bean meal medium (SBM medium) (Hoffmann and Punnapayak, 1988). The medium solution was adjusted to pH 7 and sterilized by autoclaving at 121°C for 15 min, 1.2 atm pressure. One ml of *Aspergillus niger* spores (1×10^6 in 1% tween 80) from agar slant will be added into 50 mL of SBM medium and incubated at $27 \pm 2^\circ\text{C}$ on a rotary shaker (150 rpm). After incubated 2 days, 5 mL of culture added to 50 mL new SBM brought medium and incubated at $27 \pm 2^\circ\text{C}$ on a rotary shaker (150 rpm). The 40 mg of homopterocarpin will be added into the 50 mL of culture medium after 24 h of incubation. After seven days of incubation, the

culture will be pooled, filtered and extracted with an equal volume of dichloromethane (DCM) in 24-h intervals, three times. The extracts will be collected together and then evaporated in rotary evaporator under reduced pressure, and the residue will be dissolved in DCM for TLC analysis. The extracts will be fractionated and purified to isolate the compound.

5.1.3 Separation of bio-transformed compound

The combined DCM extract of bio-transformed compound of homopterocarpin were chromatographed on silica gel column using *n*-hexane/ethyl acetate gradient system. Compound were isolated from the fraction 25-29 and 49-69. Further separation and purification were done using preparative TLC plate for compound 1 and 3. The system used was *n*-hexane/ethyl acetate 7:3 for compound 1 and 2:8 for compound 2. Moreover, purification of compound 2 used crystallization. One hundred milligram of fraction 49-69 were dissolved in DCM and boiled at 100°C, added a little *n*-hexane and stored at refrigerator (9±4°C) with open cap condition for 24h. Colorless crystal was formed in the bottom of tube.

5.1.4 Metabolite extraction

For metabolite characterization, 50 mL of microbial culture were collected from 0,3,5, and 7 days culture. They were simultaneously extracted from three different culture from each day culture. Each culture was dried in freeze drier and macerated with 10 mL of a 9:1 methanol:water solution followed by incubation at room temperature for 24 h three times. A total of crude extract was collected and stored at refrigerator. The solution (1 µL) was then injected into a GC-MS.

5.1.5 Metabolomic analysis using GC-MS/MS of *Aspergillus niger*-transformation culture

GC-MS analysis was used to determine the phytochemical profiles of homopterocarpin transformation culture for a week. Culture extract was dissolved in methanol (40 mg/mL), then passed through a 45-µm filter. Triple quadrupole GC-MS/MS was performed with an Agilent 7890B GC system and Agilent 7633 ALS detector (Agilent Technologies, Inc., Santa Clara, CA, USA) with an Agilent J&W HP-5ms column (5% phenyl-methylpolysiloxane; inner diameter, 0.25 mm; length, 30 m; film thickness, 0.25 µm, part no. 19091S-433UI). The following settings were used for

GC-MS analysis: flow rate of the mobile phase, 1 mL/min; average velocity, 36.966 cm/min; oven temperature, 80–320°C at 7°C/min and held for 2-5 min; post-run temperature, 310°C (2 mL/min) for 5 min; carrier gas, helium; flow rate of carrier gas, 29.75 mL/min; carrier flow rate, 1 mL/min (constant mode); sample volume, 10 μ L; total running time, 24 min; injector temperature, 50°C; injection volume, 1 μ L. The interface and mass spectra ion source were maintained at 250°C. The mass spectra were collected at 70 eV with a mass scan range of 30–500 amu, solvent delay of 3 min, and transfer line temperature of 300°C. The identification of compounds was based on comparing the mass spectra with those of the Standard Reference Database (version 02.L; National Institute of Standards and Technology, Gaithersburg, MD, USA). The relative percentage of each component was calculated as the relative percentage of the total peak area of the chromatograph.

5.1.6 Spectrophotometric analysis of biotransformation derivative compound

Gas chromatography-mass spectrometry (GC-MS) was conducted to identify biotransformation derivative compound. The compound was dissolved in Chloroform (CHCl₃). The GC-MS analysis was carried out using an Agilent GC-MSD (Agilent 19091S-433UI) equipped with a capillary column (30 m x 250 μ m x 0.25 μ m), and a mass detector was operated in electron impact (EI) mode with full scan (50550 amu). Helium was the carrier gas at a flow rate of 3 mL/min with a total flow of 14 mL/min, the injector was operated at 280°C, and the oven temperature was programmed as follows: 60°C, at 3°C/min to 250°C. The peaks in the chromatogram were identified based on their mass spectra. Interpretation of the mass spectrum of GC-MS was made using the National Institute Standard and Technology (NIST). The mass spectrum of phytochemicals was compared with the spectrum of known compounds stored in the NIST library. The quality of compounds above 85% was shown in this study. Each component's relative percentage was calculated by the relative percentage of the chromatogram's total peak area. The ¹H, and ¹³C, NMR spectra of the compound were analyzed using the JEOL JNM-ECS instrument at 400MHz in chloroform solvent.

5.1.7 *In Vitro* Antioxidant Activity

5.1.7.1 *The 2,2-diphenyl-1-picryl-hydrazyl-hydrate (DPPH) inhibition assay.*

The DPPH inhibition assay was modified from Prieto (2012). One hundred microliters of sample were mixed with 100 μ l DPPH reagent in methanol (0.2mM), then incubated for 30 mins in dark conditions at room temperature. The concentration of samples and positive control (ascorbic acid and trolox) were made from 1.075, 3.15, 6.25, 10, 15, 25, 35, 50, 75, 100, 150, and 200 μ g/ml in methanol. The inhibition of DPPH was measured at 517 nm using a SpectraMax M3 reader. The percentage of DPPH inhibition was calculated by an equation adapted from Prieto (2012):

$$(A_{\text{control}} - A_{\text{sample}}) / A_{\text{control}} \times 100\%$$

Where A_{sample} was the absorbance from the reaction of DPPH reagent and the sample, while A_{control} was the absorbance from DPPH reagent. The percent inhibition results from the varying concentration were then plotted and regressed linearly to get the half-maximal inhibitory concentration (IC_{50}) value. IC_{50} means the concentration of the samples when inhibiting 50% of DPPH.

5.1.7.2 *The 2,2-azino-bis (3 ethylbenzothiazoline-6-sulfonic acid) diammonium salt (ABTS) inhibition assay*

The ABTS inhibition assay was from Fu et al. (2014). The 86.02mg of 2,2-azino-bis (3 ethylbenzothiazoline-6-sulfonic acid) diammonium salt (ABTS) was solved in 25ml acetic buffer (solution A). The 66.24mg of potassium persulphate was solved in 100 acetic buffer (solution B). Then, 5ml of solution A and B were combined and stored at room temperature for 12-16 hours in dark condition (solution C). The 2.8 ml of solution C was solved in 65 ml of acetic buffer, and then incubated for 30 min in room temperature ($26 \pm 2^\circ\text{C}$). The absorbance of solution C was measured immediately (0.7-0.72, at 734nm). One hundred microliters of sample were mixed with 100 μ l ABTS reagent (solution C), then incubated for 6 mins in dark conditions at room temperature. The concentration of samples and positive control (ascorbic acid and trolox) were made from 1.075, 3.15, 6.25, 10, 15, 25, 35, 50, 75, 100, 150, and

200 µg/ml in methanol. The inhibition of DPPH was measured at 734 nm using a SpectraMax M3 reader. The calculation of percent inhibition and IC₅₀ value was similar to DPPH inhibition assay.

5.1.8 *In vitro* antimalarial assay

In this research, *in vitro* antimalarial assay used cultures of *Plasmodium falciparum* strain 3D7 (Trager and Jensen 1972). The composition of the medium was human O red blood cells, 5% hematocrit in Roswell Park Memorial Institute 1640 (RPMI 1640) (Gibco BRL, USA), 22.3 mM N-2-hydroxyethylpiperazine-N-2-ethanesulfonic acid (HEPES) (Sigma), hypoxanthine, sodium bicarbonate (NaHCO₃), and 10% human O⁺ plasma. Chloroquine diphosphate was used as a positive control. A total of 1 mg of sample was dissolved in 100µl of Dimethyl sulfoxide (DMSO, stock solution, concentration 10,000 mg/ml). Furthermore, from the stock solution, serial dilutions were made. The parasites used in this test was synchronous (ring stage) with ±1% parasitemia (5% hematocrit). A total of 2µl of test solutions with various concentrations were taken and put into each well (96 wells), then 198µl of the parasite was added (the final concentration of the test material was 100 µg/ml, 10 µg/ml, 1 µg/ml, 0.1µg/ml, 0.01 µg /ml). The test well was then put into the chamber and given mixed gas (O₂ 5%, CO₂ 5%, and N₂ 90%). The chamber containing the test wells was incubated for 48 hours at 37°C. The cultures were then harvested and a thin blood film was prepared with 20% Giemsa staining. The blood smear that has been made was calculated by counting the number of infected erythrocytes per 1000 normal erythrocytes under a microscope (1000X). The data was used to determine the percent growth and percent inhibition.

Percentage of growth was obtained by the following formula:

$$\% \text{ Growth} = \% \text{ Parasitemia} - \% \text{ growth at 0 hour}$$

The formula for calculating the % Inhibition is as follows:

$$\text{Percent inhibition} = 100\% - ((X_u/X_k) \times 100\%)$$

Information:

X_u = % growth in the test solution

X_k = % growth in negative control

Based on the percent inhibition data, statistical analysis was carried out with probit analysis of the SPSS version 20 program to determine the IC_{50} value or the concentration of the test material that could inhibit the growth of the parasite by 50%.

5.1.9 *In vitro* anticancer assay

In vitro anticancer assay was carried out on hepatocyte-derived cellular carcinoma cell line (Huh7it-1cells) by the micro tetra zolium (MTT) assay method as described by Fonseca et al. (2018). Passage (P) 18 human hepatocyte cells were cultured in Dulbecco's modified Eagle's medium (DMEM) medium added with 3.7 g of sodium bicarbonate ($NaHCO_3$), with a pH adjustment of 7-7.2. Then a complete medium was made from 500 ml of DMEM media, 50 ml of fetal bovine serum (FBS), 5 ml of nonessential amino acid (NEAA), and 6 ml of phenstrep (penicillin-streptomycin).

5.1.10 Selectivity index (SI)

The selectivity index (SI) was calculated to describe the selective activity of the extract against *Plasmodium falciparum* strain 3D7 compared with the results of its toxicity test on human hepatocyte cells. Here, the SI value was calculated by comparing the IC_{50} value of the extract cytotoxicity and the IC_{50} value of *P. falciparum* strain 3D7. The selectivity index (SI) was calculated to describe the selective activity of the extract against *P. falciparum* strain 3D7 compared with the results of its *in vitro* anticancer test on hepatocyte-derived cellular carcinoma cell line (Huh7it-1cells). In here, the *in vitro* anticancer activity was perceived as in cytotoxicity activity compared to antiplasmodial activity.

5.1.11 Data analysis

Data were expressed as the mean \pm standard deviation. Probit analysis was conducted to calculate the IC_{50} values of *in vitro* antimalarial activity using IBM SPSS Statistics for Windows, version 20.0. (IBM Corporation, Armonk, NY, USA). IC_{50} values of *in vitro* antioxidant and cytotoxicity were calculated using linear regression Microsoft Excel version 20.0 (IBM Corporation, Armonk, NY, USA).

5.2 Result

5.2.1 The number of *Aspergillus niger* spores during transformation culture of homopterocarpin from *Pterocarpus macrocarpus* Kurz. heartwood

After added homopterocarpin to the culture, total number of *Aspergillus niger* spores was calculated during biotransformation. Figure 12 showed that the total number of *A. niger* slightly increase day by day.

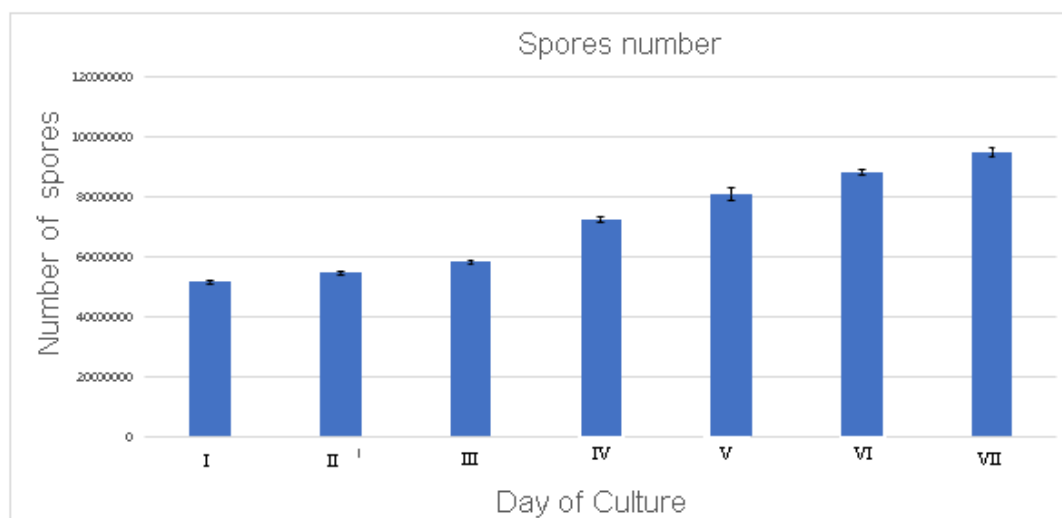


Figure 12. Spores number of *Aspergillus niger* during biotransformation culture of homopterocarpin from *Pterocarpus macrocarpus* Kurz. heartwood.

5.2.2 Metabolite profiles by GC-MS during biotransformation

Chemical analysis by GC-MS was used to determine the metabolite profile of biotransformed-culture of homopterocarpin from *Pterocarpus macrocarpus* Kurz. heartwood by *Aspergillus niger*. (Table 28 and Figure 13) (Appendix 4: Supplementary data I).

Table 28. Phytochemical components from GC/MS analysis of *Pterocarpus macrocarpus* Kurz. heartwood *n*-hexane extract in every crystallization

No.	Compound	Retention Time (min)	Relative area percentage (peak area relative to the total peak area (%))			
			I	III	V	VII
1	2,5-Furandione, 3-methyl-	3.81				36.76
2	Glycerin	3.983	41.67	100	55.15	79.86
3	2,4-Dihydroxy-2,5-dimethyl-3(2H)-furan-3-one	4.296	35.34			
4	Maltol	5.868	100	44.39		
5	5-Hydroxymethylfurfural	8.688	34.21		35.97	
6	1,2,3-Propanetriol, 1-acetate	8.965	82.22	31.87		
7	4H-Pyran-4-one, 2,3-dihydro-3,5-dihydroxy-6-methyl-	9.724	93.17	40.34	37.27	
8	2,4-Hexadienedioic acid	11.468			41.84	57.11
9	4,4-Dimethyl-3-(3-methylbut-3-enylidene)-2-methylenebicyclo[4.1.0]heptane	16.692			20.69	
10	6-Isopropenyl-4,8a-dimethyl-1,2,3,5,6,7,8,8a-octahydro-naphthalen-2-ol	17.134			21.31	
11	7-Hydroxymethylbicyclo[2.2.1]heptane-1-carboxylic acid, methyl ester	18.339		24.6		
12	3.beta.,9.beta.-Dihydroxy-3,5.alpha.,8-trimethyltricyclo[6.3.1.0(1,5)]dodecane	19.561				8.98
13	6-Isopropenyl-4,8a-dimethyl-1,2,3,5,6,7,8,8a-octahydro-naphthalen-2-ol	19.729		37.92	100	100
14	Perhydrocyclopropa[e]azulene-4,5,6-triol, 1,1,4,6-tetramethyl	21.099			12.84	14.6
15	9-Octadecenamide, (Z)-	25.998	85.32	55.85	11.54	54.58
16	Medicarpin	28.465			9.84	12.6

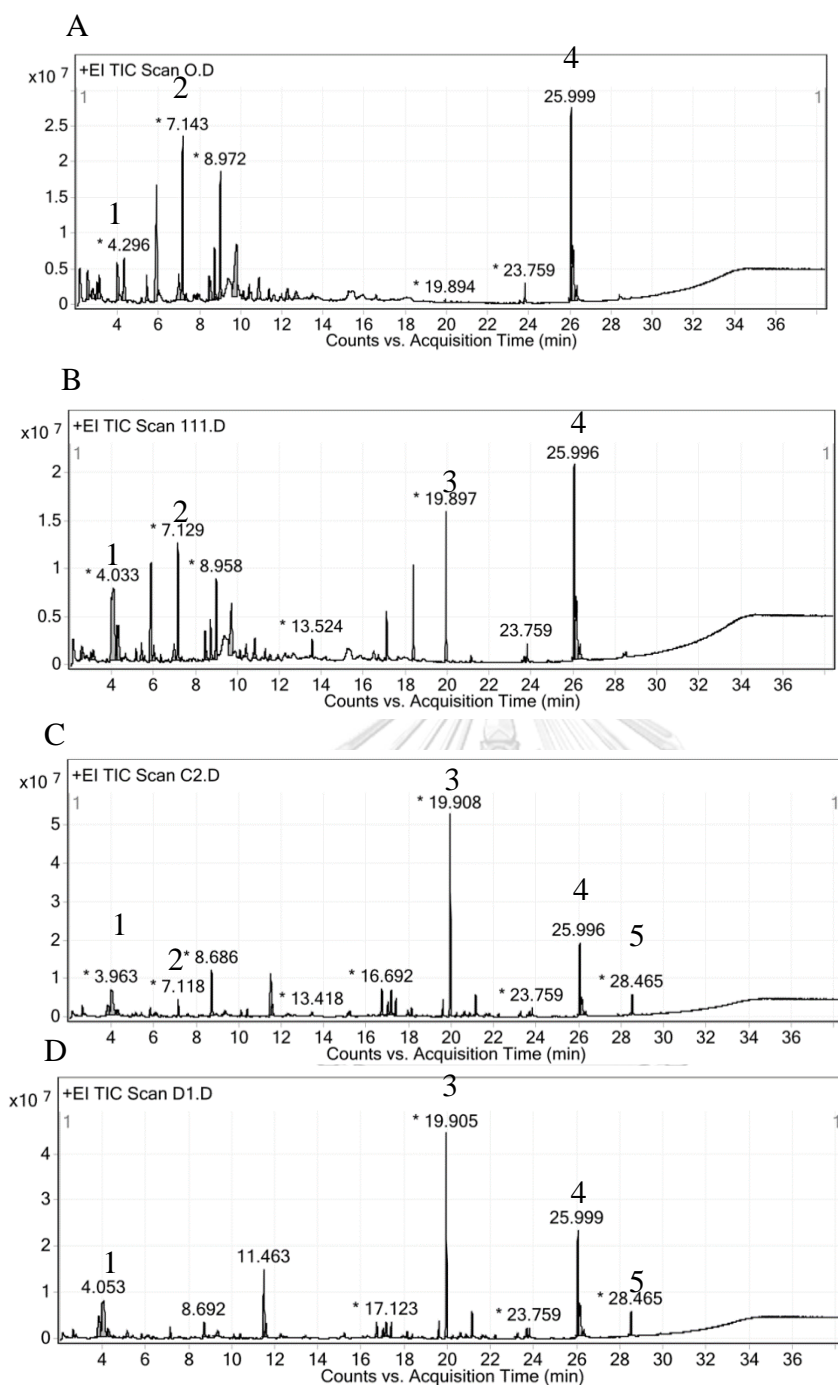


Figure 13. Chromatogram profile of biotransformation culture of homopterocarpin from *Pterocarpus macrocarpus* Kurz. heartwood by *Aspergillus niger*. A. First day of culture, B. Third day of culture, C. Fifth day of culture, D. Seventh day of culture. 1. Glycerine, 2. 4H-Pyran-4-one,2,3-dihydro-3,5-dihydroxy-6-methyl-, 3. 6-Isopropenyl-4,8a-dimethyl-1,2,3,5,6,7,8,8a-octahydro-naphthalen-2-ol, 4. 9-Octadecenamide, (Z)-, 5. medicarpin

5.2.3 Biotransformation Compound

The compound was isolated from biotransformation of homopterocarpin with *Aspergillus niger* for seven days. The structure was given in Figure 13.

Demethylhomopterocarpin/ 3-Hydroxy-9-methoxycarpan/Medicarpin

Colorless amorphous solid. Mol. formula: $C_{16}H_{14}O_4$, molecular weight 270.27 g/mol, GC-MS m/z (molecular formula): 270.3g/mol ($C_{16}H_{14}O_4$), 1H -(500MHz, $CDCl_3$): Table 29 and ^{13}C NMR (125MHz, $CDCl_3$): Table 30 (Appendix 4: Supplementary data II). Compound (2) had elemental composition $C_{16}H_{14}O_4$, deduced through GC-MS (mz 270.3 g/mol). Mass spectra indicated that the mass of this compound is 270.3 g/mol, which is 13.8 mass less than substrate (284.1) and also showed the removal of CH_2 (14 mass units). The net 13.8 mass unit were less than the substrate. Based on the spectra analysis and reference, the compound was identified as demethylhomopterocarpin / 3-hydroxy-9-methoxycarpan/medicarpin (32 mg/5L culture). Hopterocarpin was losing the methyl moiety and adding hydroxyl moiety in the medicarpin.

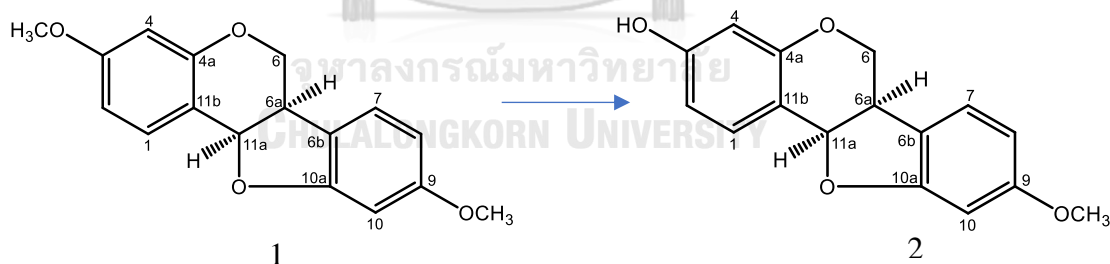


Figure 14. The structure of homopterocarpin (1) and medicarpin (2)

Table 29. ¹H-(400MHz, CDCl₃) chemical shift assignments of homopterocarpin and (500MHz, CDCl₃) medicarpin

Carbon no.	Type	Compound (1) δ _H (mult, J Hz)	Compound (2) δ _H (mult, J Hz)
1	CH	7.43 (<i>d</i> , 8.6)	7.43 (<i>d</i> , 9.2)
2	CH	6.64 (<i>dd</i> , 8.6; 2.5)	6.64 (<i>dd</i> , 8.6; 2.5)
3	C	-	-
4	CH	6.47 (<i>d</i> , 2.5)	6.47 (<i>d</i> , 2.5)
4a	C	-	-
6	CH ₂	3.64 (<i>t</i> , 11.0) 4.25 (<i>dd</i> , 11.0; 5.3)	3.64 (<i>t</i> , 11.0) 4.25 (<i>ddd</i> , 11.20; 5.3; 1.0)
6a	CH	3.53 (<i>m</i>)	3.53 (<i>m</i>)
6b	C	-	-
7	CH	7.13 (<i>d</i> , 8.5)	7.08 (<i>d</i> , 8.6)
8	CH	6.46 (<i>dd</i> , 8.5; 2.3)	6.47 (<i>dd</i> , 8.5; 2.6)
9	C	-	-
10	C	6.44 (<i>d</i> , 2.3)	6.44 (<i>d</i> , 2.3)
10a	C	-	-
11a	CH	5.51 (<i>d</i> , 6.8)	5.51 (<i>d</i> , 6.9)
11b	C	-	-
3-OCH ₃	C-OCH ₃	3.77 (<i>s</i>)	-
9-OCH ₃	C-OCH ₃	3.79 (<i>s</i>)	3.79 (<i>s</i>)

Table 30. ^{13}C -(400MHz, CDCl_3) chemical shift assignments of homopterocarpin and (125MHz, CDCl_3) medicarpin

Carbon no.	Type	Compound (1) δ_c	Compound (2) δ_c
1	CH	131.9	131.9
2	CH	109.3	109.3
3	C	161.2	161.2
4	CH	101.7	101.7
4a	C	156.7	156.7
6	CH ₂	66.7	66.7
6a	CH	39.6	39.6
6b	C	119.2	119.2
7	CH	124.8	125.2
8	CH	106.4	107.7
9	C	161.1	161.1
10	C	97.1	97.1
10a	C	160.8	160.8
11a	CH	78.7	78.7
11b	C	112.4	112.4
9-OCH ₃	C-OCH ₃	55.5	55.5

CHULALONGKORN UNIVERSITY

6-isopropenyl-4,8a-dimethyl-1,2,3,5,6,7,8,8a-octahydro-naphthalene-2-ol

White star crystal (solid) was isolated from homopterocarpin transformation culture as major compound. Mol. formula: $C_{15}H_{24}O$, molecular weight 220.35g/mol. Based on the GC-MS spectra and reference, the compound was identified as 6-isopropenyl-4,8a-dimethyl-1,2,3,5,6,7,8,8a-octahydro-naphthalene-2-ol (Retention time 15.866; 73mg / 5L culture) (Figure 15) (Appendix 4: Supplementary data III).

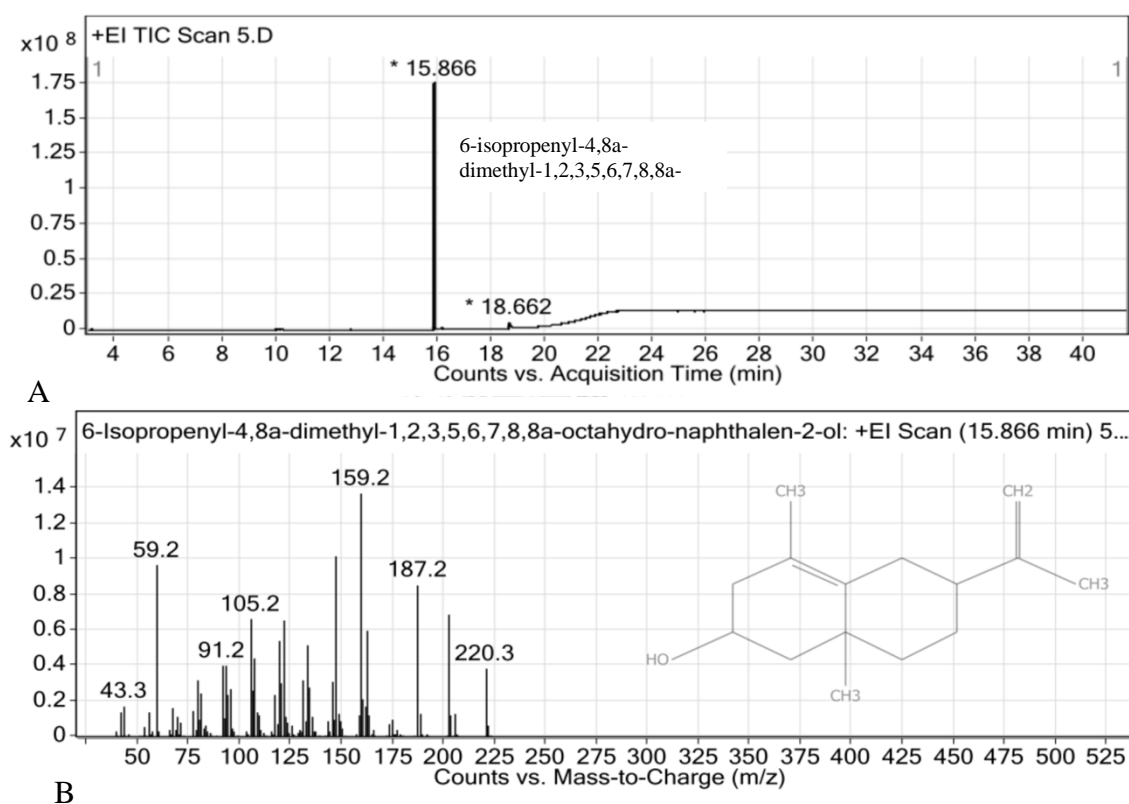


Figure 15. Chromatogram profile of 6-isopropenyl-4,8a-dimethyl-1,2,3,5,6,7,8,8a-octahydro-naphthalene-2-ol by GC-MS. A. GC-MS spectra with retention time, B. 6-isopropenyl-4,8a-dimethyl-1,2,3,5,6,7,8,8a-octahydro-naphthalene-2-ol of spectra

5.2.4 Antioxidant activities

The DPPH and ABTS assay were conducted to assess antioxidant activities. The IC_{50} value of biotransformation derived compound were shown in Table 31, (Appendix 4: Supplementary data IV).

Table 31. *In vitro* antioxidant activity of *Pterocarpus macrocarpus* Kurz. heartwood extract

No.	Extract	Antioxidant activity, IC_{50} ($\mu\text{g/ml}$)	
		DPPH	ABTS
1	Medicarpin	7.49 \pm 1.7	0.61 \pm 0.4
2	6-isopropenyl-4,8a-dimethyl-1,2,3,5,6,7,8,8a-octahydro-naphthalene-2-ol	26.17 \pm 0.91	2.12 \pm 0.97
3	Homopterocarpin	94.90 \pm 34.96	30.94 \pm 8.00
4	Ascorbic acid	5.12 \pm 2.43	2.77 \pm 1.30
5	Trolox	0.97 \pm 0.30	0.86 \pm 0.97

5.2.5 *In vitro* antimalarial activity

The IC_{50} values of biotransformation derived compound were shown in Table 32 (Appendix 4: Supplementary data V).

5.2.6 Selectivity index (SI)

The selectivity index (SI), by comparing the CC_{50} of toxicity (IC_{50} of anticancer activity) and the IC_{50} of antiplasmodial activity of the biotransformation derived compound (Table 32).

5.2.7 *In vitro* anticancer

In vitro toxicity was carried out by the MTT assay method against Huh7it-1cells. The 50% Inhibition concentration (IC_{50}) of (Table 33) (Appendix 4: Supplementary data VI).

Table 32. *In vitro* antimalarial activity of bioactive compound from homopterocarpin transformation by *Aspergillus niger* against *P. falciparum* strain 3D7

No.	Extract	% of inhibition at each concentration (µg/ml)					IC ₅₀ (µg/ml)	Selectivity Index (SI)
		10	1	0.1	0.01	0.001		
1	Medicarpin	100	84.62	57.88	34.92	12.50	0.414	84.44
2	6-isopropenyl-4,8a-dimethyl-1,2,3,5,6,7,8,8a-octahydro-naphthalene-2-ol	100	75.05	52.36	15.69	6.99	1.179	38.32
3	Homopterocarpin	97.98	78.68	52.16	30.30	15.39	0.52	495.85
4.	Chloroquine diphosphate	100	100	79.76	40.49	17.17	0.014	-

Table 33. *In vitro* anticancer activity of bioactive compound from homopterocarpin transformation by *Aspergillus niger* against hepatocyte-derived cellular carcinoma cell line (Huh7it-1cells)

No.	Extract	<i>In vitro</i> anticancer activity, IC ₅₀ (µg/ml)
1	Homopterocarpin	257.84
2	Medicarpin	34.96
3	6-isopropenyl-4,8a-dimethyl-1,2,3,5,6,7,8,8a-octahydro-naphthalene-2-ol	45.18

CHAPTER SIX

Conclusion

Infectious diseases, especially SARS-CoV-2, malaria, and microbial infection are global health concerns. The requirement for new and useful compounds are growing for treating all aspects human condition, such as infectious drug resistant. Some bioactive compounds have very bioavailability but low solubility and structural instability. Because of the phenomena, it is needed a specific effort to explore the natural material well, such as biotransformation. The aims of the study are (i) to isolate and identify bioactive compound from *S. arvensis* L. and *P. macrocarpus* Kurz., (ii) to transform selected bioactive compounds by *Aspergillus niger*, and (iii) to determine bioactivities of selected bioactive compounds before and after biotransformation. In this study, natural product (extract, fraction dan compound) has been isolated from *S. arvensis* L. leaf and *P. macrocarpus* Kurz. heartwood.

The *n*-hexane, ethyl acetate, and ethanolic extract *in vitro* antiplasmodial activity of *S. arvensis* L. leaf exhibited a good activity, with IC₅₀ values were 5.119±3.27, 2.916±2.34, and 8.026±1.23 µg/mL, respectively. Each of the extracts also exhibited high antioxidants with low cytotoxic effects. Furthermore, the ethyl acetate extract showed *in vivo* antiplasmodial activity with ED₅₀ = 46.31±9.36 mg/kg, body weight, as well as hepatoprotective, nephroprotective, and immunomodulatory activities in mice infected with *P. berghei*.

Furthermore, the *n*-hexane extract of *Sonchus arvensis* L. was fractionated by column chromatography. *n*-Hexane fraction was analysed as *In vitro* antiplasmodial and *in silico* anti-SARS-CoV-2 activity. Moreover, fractions 5–12 and 15–28 had *in vitro* antiplasmodial activities with IC₅₀ values of 2.38 and 5.03 µg/mL, respectively. The *in silico* anti-SARS-CoV-2 assay showed that β-amyrin, lupeol, α-amyrin, betulin, and taraxasterol were predicted as effective antiviral candidates by having the ability to act as inhibitors of SARS-CoV-2 protein activity.

This study also highlighted homopterocarpin isolation from a *P. macrocarpus* Kurz. *n*-hexane extract by crystallization. The ethyl acetate, ethanol, and *n*-hexane extracts, as well as homopterocarpin, exhibited antiplasmodial activity at 1.78, 2.21, 7.11, and 0.52 µg/ml, respectively, against *P. falciparum* 3D7 with low toxicity. A

compound identified by GC-MS showed *in silico* anti-SARS-CoV-2 binding affinity with stigmasterol and SARS-CoV-2 helicase of -8.2 kcal/mol. All extracts exhibited antioxidant activity against DPPH and ABTS. They also demonstrated antimicrobial activity against *B. subtilis*, the ethanol and ethyl acetate extracts against *E. coli* and *C. albicans*, and the ethanol extract against *S. aureus*.

Moreover, homopteroicarpin was bio-transformed by *Aspergillus niger* (UI X-172) in soy bean meal medium (SBM) for a week. Biotransformation derived compound was identified as medicarpin by demethylation mechanism. Medicarpin exhibited *in vitro* antioxidant activity against 1,1-diphenyl-2-picrylhydrazyl (DPPH) ($IC_{50} = 7.49 \pm 1.7$ $\mu\text{g/mL}$) and 2,2-azino-bis (3-ethylbenzothiazoline-6-sulfonic acid (ABTS) ($IC_{50} = 0.61 \pm 0.4$ $\mu\text{g/mL}$), *in vitro* antiplasmodial against *Plasmodium falciparum* strain 3D7 with $IC_{50} = 0.414$ $\mu\text{g/mL}$, and anticancer against hepatocyte-derived cellular carcinoma cell line (Huh7it-1 cells) with $IC_{50} = 34.96$ $\mu\text{g/mL}$.

This study highlighted natural product and biotransformed-derived compound from *Sonchus arvensis* L. and *Pterocarpus macrocarpus* Kurz. as antioxidant, anti SARS-Cov-2, antiplasmodial, and anticancer with low toxicity. These findings provide a foundation for further investigations of natural product for infectious diseases treatment and natural products production by biotransformation as well. These findings also lay a foundation for further investigations of natural product for future pharmaceutical applications.

APPENDIXES

APPENDIX 1

1.1 Supplementary data I: Antioxidant assay

DPPH

DPPH assay of *Sonchus arvensis* L n-hexane extract 1

Sample A

Sample B

Wavelength 517

No	Sample concentration	Abs sample A	Abs sample B	Average
	control/Blank	0,582	0,583	0,5825
1	1,075	0,368	0,399	0,3835
2	3,125	0,356	0,389	0,3725
3	6,25	0,353	0,379	0,366
4	10	0,345	0,366	0,3555
5	15	0,342	0,342	0,342
6	25	0,336	0,3395	0,33775
7	35	0,325	0,323	0,324
8	50	0,314	0,316	0,315
9	75	0,293	0,292	0,2925
10	100	0,283	0,282	0,2825
11	150	0,274	0,279	0,2765
12	200	0,277	0,275	0,276

DPPH assay of *Sonchus arvensis* L n-hexane extract 2

Sample A

Sample B

Wavelength 517

No	Sample concentration	Abs sample A	Abs sample B	Average
	control/Blank	0,637	0,632	0,6345
1	1,075	0,338	0,344	0,341
2	3,125	0,335	0,342	0,3385
3	6,25	0,327	0,336	0,3315
4	10	0,331	0,331	0,331
5	15	0,330	0,33	0,33
6	25	0,329	0,326	0,3275
7	35	0,328	0,326	0,327
8	50	0,325	0,326	0,3255
9	75	0,322	0,325	0,3235
10	100	0,318	0,319	0,3185
11	150	0,317	0,317	0,317
12	200	0,314	0,314	0,314
13	200	0,3	0,302	0,301

DPPH assay of *Sonchus arvensis* L n-hexane extract 3

Sample A

Sample B

Wavelength 517

No	Sample concentration	Abs sample A	Abs sample B	Average
	control/Blank	0,637	0,632	0,6345
1	1,075	0,338	0,344	0,341
2	3,125	0,338	0,342	0,34
3	6,25	0,337	0,336	0,3365
4	10	0,331	0,331	0,331
5	15	0,331	0,328	0,3295
6	25	0,328	0,327	0,3275
7	35	0,325	0,326	0,3255
8	50	0,322	0,325	0,3235
9	75	0,318	0,319	0,3185
10	100	0,317	0,317	0,317
11	150	0,314	0,314	0,314
12	200	0,3	0,302	0,301

DPPH assay of *Sonchus arvensis* L ethyl acetate extract 1

Sample A

Sample B

Waveleght 517

No	Sample concentration	Abs sample A	Abs sample B	Average
	control/Blank	0,516	0,519	0,5175
1	1,075	0,261	0,261	0,261
2	3,125	0,255	0,262	0,2585
3	6,25	0,266	0,262	0,264
4	10	0,262	0,257	0,2595
5	15	0,254	0,254	0,254
6	25	0,243	0,242	0,2425
7	35	0,23	0,231	0,2305
8	50	0,22	0,216	0,218
9	75	0,195	0,194	0,1945
10	100	0,181	0,179	0,18
11	150	0,208	0,168	0,188
12	200	0,137	0,137	0,137

DPPH assay of *Sonchus arvensis* L ethyl acetate extract 2

Sample A

Sample B

Waveleght 517

No	Sample concentration	Abs sample A	Abs sample B	Average
	control/Blank	0,248	0,278	0,263
1	1,075	0,139	0,137	0,138
2	3,125	0,136	0,138	0,137
3	6,25	0,129	0,133	0,131
4	10	0,13	0,125	0,1275
5	15	0,13	0,128	0,129
6	25	0,12	0,117	0,1185
7	35	0,113	0,108	0,1105
8	50	0,096	0,096	0,096
9	75	0,074	0,074	0,074
10	100	0,057	0,059	0,058
11	150	0,073	0,07	0,0715
12	200	0,075	0,078	0,0765

DPPH assay of *Sonchus arvensis* L ethyl acetate extract 3

Sample A

Sample B

Waveleght 517

No	Sample concentration	Abs sample A	Abs sample B	Average
	control/blanko	0,922		0,922
1	1,075	0,496	0,489	0,4925
2	3,125	0,495	0,475	0,485
3	6,25	0,486	0,464	0,475
4	10	0,477	0,458	0,4675
5	12,5	0,462	0,456	0,459
6	15	0,421	0,451	0,436
7	25	0,424	0,441	0,4325
8	35	0,421	0,433	0,427
9	50	0,394	0,413	0,4035
10	75	0,342	0,38	0,361
11	100	0,333	0,343	0,338
12	150	0,323	0,332	0,3275
13	200	0,321	0,322	0,3215

DPPH assay of Ethanol extract of *Sonchus arvensis* L. 1

Sample A
Sample B
Wavelength 517

No	Sample concentration	Abs sample A	Abs sample B	Average
	control/Blank	0,302	0,308	0,305
1	1,075	0,187	0,171	0,179
2	3,125	0,16	0,164	0,162
3	6,25	0,159	0,163	0,161
4	10	0,154	0,156	0,155
5	15	0,154	0,156	0,155
6	25	0,144	0,145	0,1445
7	35	0,127	0,119	0,123
8	50	0,117	0,1171	0,11705
9	75	0,107	0,1067	0,10685
10	100	0,097	0,092	0,0945
11	150	0,088	0,0898	0,0889
12	200	0,083	0,0859	0,08445

DPPH assay of Ethanol extract of *Sonchus arvensis* L. 2

Sample A
Sample B
Wavelength 517

No	sample concentration	Abs sample A	Abs sample B	Average
	control/Blank	0,516	0,519	0,5175
1	1,075	0,271	0,271	0,271
2	3,125	0,269	0,268	0,2685
3	6,25	0,266	0,262	0,264
4	10	0,262	0,257	0,2595
5	15	0,261	0,254	0,2575
6	25	0,253	0,252	0,2525
7	35	0,243	0,231	0,237
8	50	0,22	0,216	0,218
9	75	0,195	0,194	0,1945
10	100	0,181	0,179	0,18
11	150	0,178	0,168	0,173
12	200	0,137	0,137	0,137

DPPH assay of *Sonchus arvensis* L. methanolic extract 1

Sample A
Sample B
Waveleght 517

No	Sample concentration	Abs sample A	Abs sample B	Average
	control/Blank	0,591	0,606	0,5985
1	1,075	0,305	0,308	0,3065
2	3,125	0,309	0,31	0,3095
3	6,25	0,314	0,314	0,314
4	10	0,314	0,317	0,3155
5	15	0,305	0,299	0,302
6	25	0,3	0,297	0,2985
7	35	0,294	0,29	0,292
8	50	0,285	0,289	0,287
9	75	0,271	0,264	0,2675
10	100	0,302	0,296	0,299
11	150	0,277	0,27	0,2735
12	200	0,219	0,218	0,2185

DPPH assay of *Sonchus arvensis* L. methanolic extract 2

Sample A
Sample B
Wavelength 517

No	Sample concentration	Abs sample A
	control/Blank	1,043
1	1,075	0,566
2	3,125	0,549
3	6,25	0,541
4	10	0,534
5	15	0,528
6	25	0,519
7	35	0,512
8	50	0,51
9	75	0,505
10	100	0,492
11	150	0,487
12	200	0,479
13	200	0,442

DPPH assay of *Sonchus arvensis* L. methanolic extract 3

Sample A
Sample B
Waveleght 517

No	Sample concentration	Abs sample A	Abs sample B	Average
	control/Blank	0,591	0,606	0,5985
1	1,075	0,307	0,308	0,3075
2	3,125	0,312	0,31	0,311
3	6,25	0,312	0,314	0,313
4	10	0,314	0,315	0,3145
5	15	0,306	0,305	0,3055
6	25	0,28	0,297	0,2885
7	35	0,295	0,297	0,296
8	50	0,282	0,284	0,283
9	75	0,282	0,268	0,275
10	100	0,271	0,294	0,2825
11	150	0,27	0,269	0,2695
12	200	0,206	0,214	0,21

DPPH assay of ascorbic acid 1

Ascorbic acid 1
Ascorbic acid 2
wavelength 517

No	Sample concentration	Abs sample A	Abs sample B	Average
	control/Blank	0,499	0,47	0,4845
1	1,075	0,255	0,261	0,258
2	3,125	0,251	0,257	0,254
3	6,25	0,253	0,259	0,256
4	10	0,256	0,254	0,255
5	15	0,25	0,254	0,252
6	25	0,246	0,209	0,2275
7	35	0,236	0,231	0,2335
8	50	0,217	0,214	0,2155
9	75	0,196	0,193	0,1945
10	100	0,187	0,186	0,1865
11	150	0,11	0,105	0,1075
12	200	0,107	0,102	0,1045

DPPH assay of ascorbic acid 2

Ascorbic acid 1
Ascorbic acid 2
wavelength 517

No	Sample concentration	Abs sample A	Abs sample B	Average
	control/Blank	0,591	0,606	0,5985
1	1,075	0,318	0,31	0,314
2	3,125	0,309	0,325	0,317
3	6,25	0,306	0,323	0,3145
4	10	0,313	0,317	0,315
5	15	0,297	0,303	0,3
6	25	0,293	0,295	0,294
7	35	0,284	0,29	0,287
8	50	0,276	0,278	0,277
9	75	0,259	0,262	0,2605
10	100	0,247	0,26	0,2535
11	150	0,263	0,266	0,2645
12	200	0,216	0,219	0,2175

DPPH assay of ascorbic acid 3

Ascorbic acid 1
Ascorbic acid 2
wavelength 517

No	Sample concentration	Abs sample A	Abs sample B	Average
	control/Blank	0,499	0,47	0,4845
1	1,075	0,263	0,266	0,2645
2	3,125	0,259	0,265	0,262
3	6,25	0,261	0,246	0,2535
4	10	0,253	0,261	0,257
5	15	0,249	0,252	0,2505
6	25	0,238	0,242	0,24
7	35	0,227	0,224	0,2255
8	50	0,211	0,213	0,212
9	75	0,202	0,201	0,2015
10	100	0,189	0,188	0,1885
11	150	0,1	0,095	0,0975
12	200	0,097	0,103	0,1

1.2. Supplementary Data II

A. Ethyl Acetate

Concentration ($\mu\text{g/mL}$)	Replication	% Parasitemia		% Growth Average	% Inhibition Average	IC ₅₀ ($\mu\text{g/mL}$)
		0 h	48 h			
Negative Control	1	1.23	4.07	2.41	-	2.916
	2	1.03	4.80			
	3	0.76	4.38			
	Average	1.01	4.41			
100	1	1.23	0.80	0	100	
	2	1.03	0.74			
	3	0.76	0.26			
	Average	1.01	0.60			
10	1	1.23	1.07	0.71	70.54	
	2	1.03	1.08			
	3	0.76	1.07			
	Average	1.01	1.72			
1	1	1.23	1.54	1.75	27.39	
	2	1.03	1.03			
	3	0.76	1.71			
	Average	1.01	1.43			
0.1	1	1.23	2.77	2.03	15.77	
	2	1.03	2.45			
	3	0.76	2.90			
	Average	1.01	2.71			
0.01	1	1.23	3.84	2.27	0	
	2	1.03	4.65			
	3	0.76	4.04			
	Average	1.01	4.18			

Confidence Limits

	Probability	95% Confidence Limits for dosis			95% Confidence Limits for log(dosis) ^b		
		Estimate	Lower Bound	Upper Bound	Estimate	Lower Bound	Upper Bound
PROBIT ^a	.010	.003	.	.	-2.465	.	.
	.020	.008	.	.	-2.121	.	.
	.030	.012	.	.	-1.904	.	.
	.040	.018	.	.	-1.740	.	.
	.050	.025	.	.	-1.606	.	.
	.060	.032	.	.	-1.493	.	.
	.070	.040	.	.	-1.394	.	.
	.080	.050	.	.	-1.304	.	.
	.090	.060	.	.	-1.223	.	.
	.100	.071	.	.	-1.149	.	.
	.150	.144	.	.	-.840	.	.
	.200	.254	.	.	-.595	.	.
	.250	.413	.	.	-.385	.	.
	.300	.637	.	.	-.196	.	.
	.350	.954	.	.	-.020	.	.
	.400	1.399	.	.	.146	.	.
	.450	2.026	.	.	.307	.	.
	.500	2.916	.	.	.465	.	.
	.550	4.198	.	.	.623	.	.
	.600	6.079	.	.	.784	.	.
	.650	8.913	.	.	.950	.	.
	.700	13.340	.	.	1.125	.	.
	.750	20.614	.	.	1.314	.	.
	.800	33.466	.	.	1.525	.	.
	.850	58.874	.	.	1.770	.	.
	.900	119.834	.	.	2.079	.	.
	.910	142.276	.	.	2.153	.	.
	.920	171.443	.	.	2.234	.	.
	.930	210.461	.	.	2.323	.	.
	.940	264.623	.	.	2.423	.	.
	.950	343.605	.	.	2.536	.	.
	.960	467.010	.	.	2.669	.	.
	.970	681.021	.	.	2.833	.	.
	.980	1124.476	.	.	3.051	.	.
	.990	2478.642	.	.	3.394	.	.

a. A heterogeneity factor is used.

b. Logarithm base = 10.

B. N-Hexane

Concentration($\mu\text{g/mL}$)	Replication	% Parasitemia		% Growth Average	% Inhibition Average	IC ₅₀ ($\mu\text{g/mL}$)
		0 h	48 h			
Negative Control	1	1.23	4.38	2.58	-	5.119
	2	1.03	3.90			
	3	0.76	4.48			
	Average	1.01	4.25			
100	1	1.23	0.80	0	100	
	2	1.03	0.78			
	3	0.76	0.74			
	Average	1.01	0.77			
10	1	1.23	2.38	1.22	52.71	
	2	1.03	2.22			
	3	0.76	2.04			
	Average	1.01	2.21			
1	1	1.23	2.54	1.45	43.80	
	2	1.03	2.45			
	3	0.76	2.78			
	Average	1.01	2.59			
0.1	1	1.23	2.71	1.64	36.43	
	2	1.03	2.68			
	3	0.76	2.57			
	Average	1.01	2.65			
0.01	1	1.23	2.88	1.82	29.46	
	2	1.03	2.83			
	3	0.76	2.98			
	Average	1.01	2.90			

	Probability	95% Confidence Limits for dosis			95% Confidence Limits for log(dosis) ^a		
		Estimate	Lower Bound	Upper Bound	Estimate	Lower Bound	Upper Bound
PROBIT	.010	.000	.000	.000	-10.826	-24.010	-7.074
	.020	.000	.000	.000	-9.474	-20.949	-6.202
	.030	.000	.000	.000	-8.616	-19.008	-5.648
	.040	.000	.000	.000	-7.971	-17.548	-5.230
	.050	.000	.000	.000	-7.447	-16.361	-4.890
	.060	.000	.000	.000	-7.000	-15.351	-4.601
	.070	.000	.000	.000	-6.608	-14.466	-4.346
	.080	.000	.000	.000	-6.258	-13.674	-4.118
	.090	.000	.000	.000	-5.939	-12.954	-3.910
	.100	.000	.000	.000	-5.645	-12.292	-3.718
	.150	.000	.000	.001	-4.430	-9.555	-2.919
	.200	.000	.000	.005	-3.464	-7.391	-2.273
	.250	.002	.000	.020	-2.635	-5.551	-1.702
	.300	.013	.000	.070	-1.891	-3.931	-1.157
	.350	.063	.003	.265	-1.201	-2.504	-.577
	.400	.284	.046	1.460	-.547	-1.341	.164
	.450	1.219	.291	15.922	.086	-.537	1.202
	.500	5.119	1.074	280.053	.709	.031	2.447
	.550	21.493	3.232	6049.799	1.332	.509	3.782
	.600	92.342	9.107	149222.517	1.965	.959	5.174
	.650	416.646	25.527	4267363.199	2.620	1.407	6.630
	.700	2038.790	73.923	149573023.588	3.309	1.869	8.175
	.750	11312.662	229.438	7051100855.053	4.054	2.361	9.848
	.800	76253.242	801.212	520389327261.014	4.882	2.904	11.716
	.850	705020.586	3412.000	78988004874200.270	5.848	3.533	13.898
	.900	11576553.152	20953.836	44212991861498176.000	7.064	4.321	16.646
	.910	22757773.107	32452.517	204021059892008896.000	7.357	4.511	17.310
	.920	47427747.761	52179.866	1074718836645834750.000	7.676	4.718	18.031
	.930	106336693.699	87931.296	6681931496179899400.000	8.027	4.944	18.825
	.940	262002234.946	157436.142	51451479017822680000.000	8.418	5.197	19.711
	.950	732743150.782	305792.324	527997911218362700000.000	8.865	5.485	20.723
	.960	2453037790.362	666737.928	8145452807075246000000.000	9.390	5.824	21.911
	.970	10834794929.582	1737264.980	235518547016771250000000.000	10.035	6.240	23.372
	.980	78053185263.180	6199721.316	20639117471816380000000000.000	10.892	6.792	25.315
	.990	1753989502964.271	45974326.713	2383680205722373600000000000.000	12.244	7.663	28.377

a. Logarithm base = 10.

C. Ethanol

Concentration ($\mu\text{g/mL}$)	Replication	% Parasitemia		% Growth Average	% Inhibition Average	IC ₅₀ ($\mu\text{g/mL}$)
		0 h	48 h			
Negative Control	1	0.66	2.94	2.76	-	8.026
	2	0.90	2.98			
	3	1.00	4.92			
	Average	0.85	3.61			
100	1	0.66	0.78	0.10	96.38	
	2	0.90	0.80			
	3	1.00	1.27			
	Average	0.85	0.95			
10	1	0.66	2.22	2.00	27.54	
	2	0.90	2.38			
	3	1.00	3.96			
	Average	0.85	2.85			
1	1	0.66	2.45	2.17	21.38	
	2	0.90	2.54			
	3	1.00	4.08			
	Average	0.85	3.02			
0.1	1	0.66	2.68	2.40	13.04	
	2	0.90	2.71			
	3	1.00	4.36			
	Average	0.85	3.25			
0.01	1	0.66	2.83	2.57	6.88	
	2	0.90	2.88			
	3	1.00	4.54			
	Average	0.85	3.42			

Confidence Limits

	Probability	95% Confidence Limits for dosis			95% Confidence Limits for log(dosis) ^b		
		Estimate	Lower Bound	Upper Bound	Estimate	Lower Bound	Upper Bound
PROBIT ^a	.010	.003	.	.	-2.554	.	.
	.020	.007	.	.	-2.149	.	.
	.030	.013	.	.	-1.892	.	.
	.040	.020	.	.	-1.698	.	.
	.050	.029	.	.	-1.541	.	.
	.060	.039	.	.	-1.407	.	.
	.070	.051	.	.	-1.290	.	.
	.080	.065	.	.	-1.184	.	.
	.090	.081	.	.	-1.089	.	.
	.100	.100	.	.	-1.001	.	.
	.150	.231	.	.	-.636	.	.
	.200	.450	.	.	-.347	.	.
	.250	.797	.	.	-.098	.	.
	.300	1.333	.	.	.125	.	.
	.350	2.146	.	.	.332	.	.
	.400	3.372	.	.	.528	.	.
	.450	5.220	.	.	.718	.	.
	.500	8.026	.	.	.904	.	.
	.550	12.340	.	.	1.091	.	.
	.600	19.105	.	.	1.281	.	.
	.650	30.017	.	.	1.477	.	.
	.700	48.321	.	.	1.684	.	.
	.750	80.776	.	.	1.907	.	.
	.800	143.141	.	.	2.156	.	.
	.850	278.869	.	.	2.445	.	.
	.900	645.399	.	.	2.810	.	.
	.910	790.404	.	.	2.898	.	.
	.920	985.080	.	.	2.993	.	.
	.930	1254.912	.	.	3.099	.	.
	.940	1644.524	.	.	3.216	.	.
	.950	2238.548	.	.	3.350	.	.
	.960	3215.972	.	.	3.507	.	.
	.970	5020.525	.	.	3.701	.	.
	.980	9075.899	.	.	3.958	.	.
	.990	23076.770	.	.	4.363	.	.

a. A hetgeneity factor is used.

1.3. Supplementary data III

Toxicity assay of <i>Sonchus arvensis</i> L. extract_Antiplasmodial activity of <i>Sonchus arvensis</i> L. Sample: H, EA, E													
Abs 560nm													
SampeI	4000	2000	1000	500	250	100	50	25	12	6	3	1,5	DMEM
H	0,189	0,257	0,856	0,974	0,960	0,990	0,991	0,983	0,989	0,993	0,983	0,987	0,993
	0,187	0,261	0,903	0,971	0,989	0,983	0,990	0,979	0,986	0,988	0,989	0,983	0,985
	0,188	0,259	0,880	0,973	0,975	0,987	0,991	0,981	0,988	0,991	0,986	0,985	0,989
EA	0,195	0,187	0,190	0,281	0,982	0,984	0,985	0,989	0,983	0,993	0,986	0,989	0,959
	0,182	0,193	0,192	0,263	0,907	0,976	0,987	0,986	0,995	0,997	0,983	0,946	0,977
	0,189	0,190	0,191	0,272	0,945	0,980	0,986	0,988	0,989	0,995	0,985	0,968	0,968
E	0,185	0,189	0,236	0,958	0,987	0,991	0,985	0,995	0,988	0,994	0,989	0,981	0,977
	0,186	0,187	0,426	0,892	0,980	0,989	0,984	0,991	0,987	0,988	0,984	0,987	0,980
	0,186	0,188	0,331	0,925	0,984	0,990	0,985	0,993	0,987	0,991	0,987	0,984	0,979
Abs 750nm													
Conc (ug/ml)	4000	2000	1000	500	250	100	50	25	12	6	3	1,5	DMEM
H	0,190	0,192	0,194	0,199	0,202	0,211	0,213	0,211	0,210	0,216	0,205	0,203	0,203
	0,189	0,192	0,198	0,201	0,207	0,208	0,208	0,207	0,210	0,209	0,207	0,201	0,203
	0,190	0,192	0,196	0,200	0,205	0,210	0,211	0,209	0,210	0,213	0,206	0,202	0,203
EA	0,188	0,189	0,188	0,190	0,205	0,208	0,207	0,210	0,207	0,209	0,208	0,210	0,206
	0,188	0,190	0,190	0,181	0,200	0,199	0,205	0,210	0,213	0,214	0,209	0,200	0,209
	0,188	0,190	0,189	0,186	0,203	0,204	0,206	0,210	0,210	0,212	0,209	0,205	0,208
E	0,189	0,189	0,185	0,210	0,203	0,207	0,208	0,208	0,215	0,211	0,208	0,200	0,204
	0,188	0,188	0,189	0,195	0,201	0,207	0,205	0,207	0,211	0,208	0,205	0,206	0,203
	0,189	0,189	0,187	0,203	0,202	0,207	0,207	0,208	0,213	0,210	0,207	0,203	0,204

1.4. Supplementary data IV

Table of percentage results of parasitaemia treatment of positive control, negative control, and ethyl acetate extract of the leaves of *Sonchus arvensis* L.

No.	Group	Replication	D0 (%)	D1 (%)	D2 (%)	D3 (%)	D4 (%)	Percentage of Parasitemia (D4-D0) (%)	Percentage of Inhibition (%)
1	Negative control	1	1.32	2.29	3.67	5.65	7.86	6.54	
		2	1.65	2.87	4.34	5.01	7.26	5.61	
		3	1.45	2.00	3.68	5.81	7.19	5.74	
		4	1.46	2.58	4.35	5.89	7.32	5.86	
		5	1.53	2.98	4.45	5.21	7.37	5.84	
		6	1.34	2.32	3.89	5.02	7.40	6.06	
		7	1.35	2.12	3.92	5.11	7.10	5.75	
	Average								
2	Positive Control	1	1.43	0.99	0.58	0.19	0.01	-1.42	
		2	1.45	0.99	0.65	0.18	0.03	-1.42	
		3	1.53	1.23	0.54	0.23	0	-1.53	
		4	1.32	1.14	0.62	0.32	0.04	-1.28	
		5	1.54	1.34	0.61	0.44	0.02	-1.52	
		6	1.53	1.04	0.63	0.18	0	-1.53	
		7	1.54	0.98	0.54	0.34	0.02	-1.52	
	Average						-1.46		

3	P1	1	1.56	3.08	4.38	5.64	7.47	5.91	9.63
		2	1.46	3.10	4.36	5.71	7.38	5.92	0
		3	1.62	3.45	4.62	5.43	7.79	6.17	0
		4	1.53	3.67	3.90	5.34	7.56	6.03	0
		5	1.45	3.25	4.32	5.26	7.10	5.65	3.25
		6	1.43	3.45	4.43	5.49	7.43	6.00	0.99
		7	1.57	3	4.32	5.10	7.38	5.81	0
	Average							4.72	
4	P2	1	1.45	2.01	2.34	3.32	5.76	4.31	34.097
		2	1.34	2.21	2.87	3.15	5.43	4.09	27.09
		3	1.35	2.32	2.49	3.32	5.52	4.17	27.35
		4	1.54	2.19	2.67	3.32	5.45	3.91	33.28
		5	1.46	2.16	2.56	2.90	4.45	2.99	48.80
		6	1.37	2.13	2.78	3.12	5.56	4.19	30.85
		7	1.45	2.15	2.89	2.98	5.56	4.11	28.52
	Average							2.11	
5	P3	1	1.56	1.97	2.34	3.01	5.11	2.55	61.01
		2	1.54	1.90	2.45	2.79	5.06	2.50	55.43
		3	1.57	1.67	2.67	2.98	4.09	2.52	56.10
		4	1.45	2.03	2.45	2.92	4.99	2.54	56.66
		5	1.53	1.94	2.41	3.02	5.98	2.45	58.05
		6	1.52	1.98	2.54	3.09	5.32	2.8	53.80
		7	1.39	2.05	2.45	2.82	5.08	2.69	53.22
	Average							1.57	
6	P4	1	1.45	1.45	1.92	2.21	2.89	1.44	77.98
		2	1.53	1.56	1.98	2.32	3.71	1.18	78.97
		3	1.34	1.72	2.03	2.34	3.89	1.55	73.00
		4	1.56	1.45	1.99	2.24	3.69	1.13	80.72
		5	1.36	1.35	2.02	2.31	3.91	1.55	73.46
		6	1.45	1.37	1.03	2.34	4.89	1.44	76.24
		7	1.56	1.45	2.01	2.44	4.77	1.21	78.966
	Average							1.49	

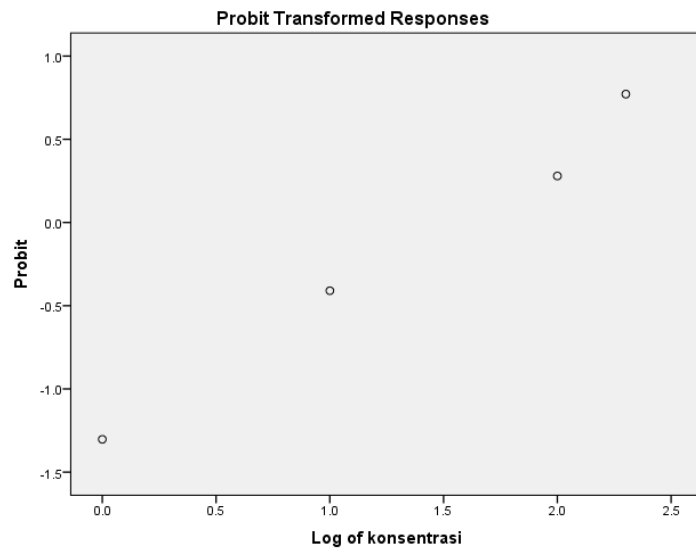
PROBIT ANALYSIS OF *IN VIVO* ANTIPLASMODIAL OF *Sonchus arvensis* L.

A. Replicaton 1 of *in vivo* antiplasmodial of *Sonchus arvensis* L

Confidence Limits

	Probability	95% Confidence Limits for concentration			95% Confidence Limits for log (concentration) ^a		
		Estimate	Lower Bound	Upper Bound	Estimate	Lower Bound	Upper Bound
	.010	.066	.000	1.116	-1.178	-4.982	.048
	.020	.138	.000	1.815	-.860	-4.328	.259
	.030	.219	.000	2.472	-.659	-3.912	.393
	.040	.311	.000	3.120	-.507	-3.600	.494
	.050	.413	.000	3.770	-.384	-3.346	.576
	.060	.526	.001	4.430	-.279	-3.130	.646
	.070	.650	.001	5.104	-.187	-2.941	.708
	.080	.786	.002	5.795	-.105	-2.771	.763
	.090	.934	.002	6.505	-.030	-2.617	.813
	.100	1.095	.003	7.235	.039	-2.476	.859
	.150	2.113	.013	11.254	.325	-1.889	1.051
	.200	3.564	.038	16.016	.552	-1.423	1.205
	.250	5.580	.094	21.716	.747	-1.025	1.337
	.300	8.347	.215	28.598	.922	-.668	1.456
	.350	12.122	.460	36.989	1.084	-.338	1.568
	.400	17.273	.943	47.346	1.237	-.026	1.675
	.450	24.330	1.882	60.331	1.386	.275	1.781
PROBIT	.500	34.084	3.699	76.961	1.533	.568	1.886
	.550	47.750	7.215	98.895	1.679	.858	1.995
	.600	67.259	14.062	129.103	1.828	1.148	2.111
	.650	95.835	27.454	173.601	1.982	1.439	2.240
	.700	139.180	53.409	246.764	2.144	1.728	2.392
	.750	208.190	101.284	389.996	2.318	2.006	2.591
	.800	325.986	180.928	741.194	2.513	2.258	2.870
	.850	549.782	305.586	1824.138	2.740	2.485	3.261
	.900	1061.201	524.607	6381.045	3.026	2.720	3.805
	.910	1243.886	591.945	8719.365	3.095	2.772	3.940
	.920	1478.159	673.180	12271.964	3.170	2.828	4.089
	.930	1786.990	773.511	17914.128	3.252	2.888	4.253
	.940	2208.774	901.159	27398.169	3.344	2.955	4.438
	.950	2812.619	1070.054	44588.814	3.449	3.029	4.649
	.960	3736.156	1306.051	79215.878	3.572	3.116	4.899
	.970	5296.928	1664.011	161012.127	3.724	3.221	5.207
	.980	8424.587	2288.295	414797.959	3.926	3.360	5.618
	.990	17505.569	3760.973	1852961.269	4.243	3.575	6.268

a. Logarithm base = 10.



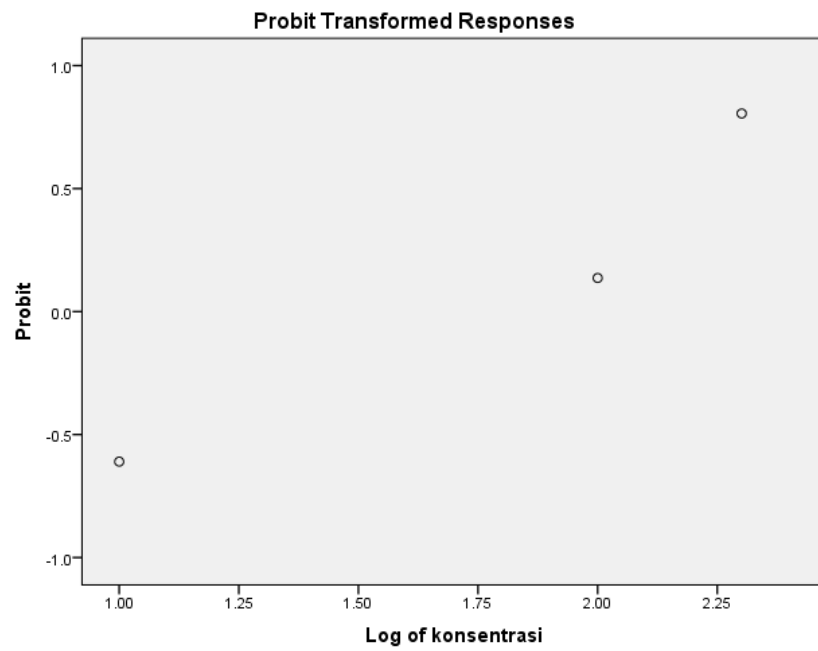
B. Replication 2 of *in vivo* antiplasmodial activity of *Sonchus arvensis* L

Confidence Limits

	Probability	95% Confidence Limits for konsentrasi			95% Confidence Limits for log(konsentrasi) ^b		
		Estimate	Lower Bound	Upper Bound	Estimate	Lower Bound	Upper Bound
	.010	.549	.	.	-.260	.	.
	.020	.935	.	.	-.029	.	.
	.030	1.311	.	.	.118	.	.
	.040	1.690	.	.	.228	.	.
	.050	2.078	.	.	.318	.	.
	.060	2.478	.	.	.394	.	.
	.070	2.891	.	.	.461	.	.
	.080	3.319	.	.	.521	.	.
	.090	3.763	.	.	.576	.	.
	.100	4.224	.	.	.626	.	.
	.150	6.817	.	.	.834	.	.
	.200	9.971	.	.	.999	.	.
	.250	13.819	.	.	1.140	.	.
	.300	18.524	.	.	1.268	.	.
	.350	24.303	.	.	1.386	.	.
	.400	31.446	.	.	1.498	.	.
	.450	40.349	.	.	1.606	.	.
PROBIT ^a	.500	51.568	.	.	1.712	.	.
	.550	65.907	.	.	1.819	.	.
	.600	84.567	.	.	1.927	.	.
	.650	109.422	.	.	2.039	.	.
	.700	143.560	.	.	2.157	.	.
	.750	192.442	.	.	2.284	.	.
	.800	266.694	.	.	2.426	.	.
	.850	390.121	.	.	2.591	.	.
	.900	629.566	.	.	2.799	.	.
	.910	706.711	.	.	2.849	.	.
	.920	801.267	.	.	2.904	.	.
	.930	919.903	.	.	2.964	.	.
	.940	1073.281	.	.	3.031	.	.
	.950	1279.659	.	.	3.107	.	.
	.960	1573.375	.	.	3.197	.	.
	.970	2028.401	.	.	3.307	.	.
	.980	2843.196	.	.	3.454	.	.
	.990	4841.169	.	.	3.685	.	.

a. A heterogeneity factor is used.

b. Logarithm base = 10.



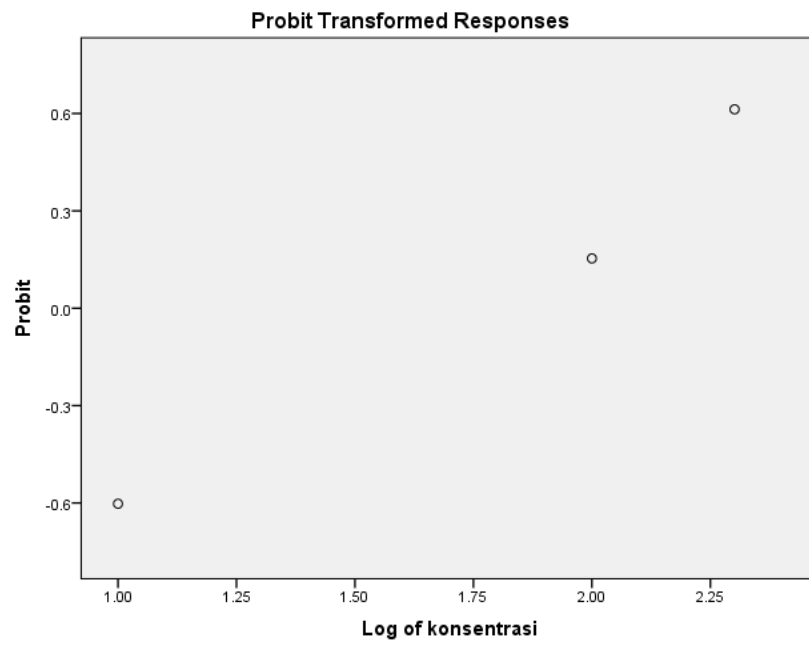
C. Replication 3 of *In vivo* antiplasmodial activity of *Sonchus arvensis* L.

Confidence Limits

	Probability	95% Confidence Limits for konsentrasi			95% Confidence Limits for log(konsentrasi) ^b		
		Estimate	Lower Bound	Upper Bound	Estimate	Lower Bound	Upper Bound
	.010	.449	.	.	-.348	.	.
	.020	.792	.	.	-.101	.	.
	.030	1.136	.	.	.056	.	.
	.040	1.490	.	.	.173	.	.
	.050	1.858	.	.	.269	.	.
	.060	2.242	.	.	.351	.	.
	.070	2.643	.	.	.422	.	.
	.080	3.063	.	.	.486	.	.
	.090	3.502	.	.	.544	.	.
	.100	3.962	.	.	.598	.	.
	.150	6.605	.	.	.820	.	.
	.200	9.913	.	.	.996	.	.
	.250	14.044	.	.	1.147	.	.
	.300	19.202	.	.	1.283	.	.
	.350	25.659	.	.	1.409	.	.
	.400	33.784	.	.	1.529	.	.
	.450	44.085	.	.	1.644	.	.
PROBIT ^a	.500	57.285	.	.	1.758	.	.
	.550	74.438	.	.	1.872	.	.
	.600	97.135	.	.	1.987	.	.
	.650	127.891	.	.	2.107	.	.
	.700	170.897	.	.	2.233	.	.
	.750	233.667	.	.	2.369	.	.
	.800	331.045	.	.	2.520	.	.
	.850	496.859	.	.	2.696	.	.
	.900	828.164	.	.	2.918	.	.
	.910	936.932	.	.	2.972	.	.
	.920	1071.342	.	.	3.030	.	.
	.930	1241.493	.	.	3.094	.	.
	.940	1463.659	.	.	3.165	.	.
	.950	1765.962	.	.	3.247	.	.
	.960	2201.822	.	.	3.343	.	.
	.970	2887.732	.	.	3.461	.	.
	.980	4141.121	.	.	3.617	.	.
	.990	7309.328	.	.	3.864	.	.

a. A heterogeneity factor is used.

b. Logarithm base = 10.



D. Replication 4 of *in vivo* antiplasmodial activity of *Sonchus arvensis* L.

Confidence Limits

	Probability	95% Confidence Limits for konsentrasi			95% Confidence Limits for log(konsentrasi) ^b		
		Estimate	Lower Bound	Upper Bound	Estimate	Lower Bound	Upper Bound
	.010	.449	.	.	-.348	.	.
	.020	.792	.	.	-.101	.	.
	.030	1.136	.	.	.056	.	.
	.040	1.490	.	.	.173	.	.
	.050	1.858	.	.	.269	.	.
	.060	2.242	.	.	.351	.	.
	.070	2.643	.	.	.422	.	.
	.080	3.063	.	.	.486	.	.
	.090	3.502	.	.	.544	.	.
	.100	3.962	.	.	.598	.	.
	.150	6.605	.	.	.820	.	.
	.200	9.913	.	.	.996	.	.
	.250	14.044	.	.	1.147	.	.
	.300	19.202	.	.	1.283	.	.
	.350	25.659	.	.	1.409	.	.
	.400	33.784	.	.	1.529	.	.
	.450	44.085	.	.	1.644	.	.
PROBIT ^a	.500	57.285	.	.	1.758	.	.
	.550	74.438	.	.	1.872	.	.
	.600	97.135	.	.	1.987	.	.
	.650	127.891	.	.	2.107	.	.
	.700	170.897	.	.	2.233	.	.
	.750	233.667	.	.	2.369	.	.
	.800	331.045	.	.	2.520	.	.
	.850	496.859	.	.	2.696	.	.
	.900	828.164	.	.	2.918	.	.
	.910	936.932	.	.	2.972	.	.
	.920	1071.342	.	.	3.030	.	.
	.930	1241.493	.	.	3.094	.	.
	.940	1463.659	.	.	3.165	.	.
	.950	1765.962	.	.	3.247	.	.
	.960	2201.822	.	.	3.343	.	.
	.970	2887.732	.	.	3.461	.	.
	.980	4141.121	.	.	3.617	.	.
	.990	7309.328	.	.	3.864	.	.

a. A heterogeneity factor is used.

b. Logarithm base = 10.

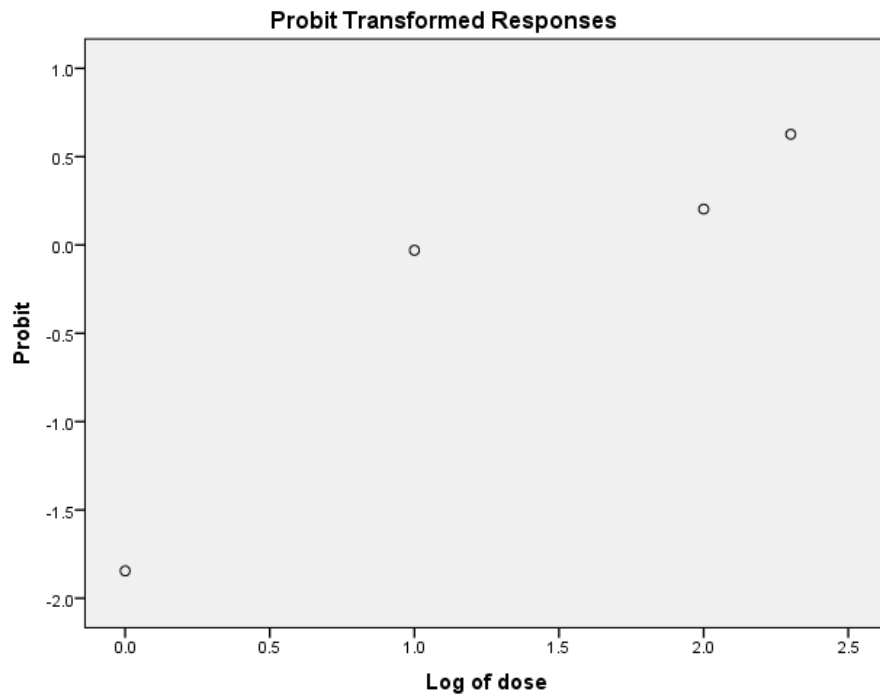
E. Replication 5 of *in vivo* antiplasmodial activity of *Sonchus arvensis* L

Confidence Limits

	Probability	95% Confidence Limits for dose			95% Confidence Limits for log(dose) ^b		
		Estimate	Lower Bound	Upper Bound	Estimate	Lower Bound	Upper Bound
	.010	.056	.	.	-1.250	.	.
	.020	.119	.	.	-.924	.	.
	.030	.192	.	.	-.717	.	.
	.040	.274	.	.	-.562	.	.
	.050	.367	.	.	-.436	.	.
	.060	.470	.	.	-.328	.	.
	.070	.584	.	.	-.234	.	.
	.080	.709	.	.	-.149	.	.
	.090	.847	.	.	-.072	.	.
	.100	.997	.	.	-.001	.	.
	.150	1.956	.	.	.291	.	.
	.200	3.342	.	.	.524	.	.
	.250	5.293	.	.	.724	.	.
	.300	7.999	.	.	.903	.	.
	.350	11.727	.	.	1.069	.	.
	.400	16.859	.	.	1.227	.	.
	.450	23.954	.	.	1.379	.	.
PROBIT ^a	.500	33.845	.	.	1.529	.	.
	.550	47.821	.	.	1.680	.	.
	.600	67.945	.	.	1.832	.	.
	.650	97.683	.	.	1.990	.	.
	.700	143.208	.	.	2.156	.	.
	.750	216.407	.	.	2.335	.	.
	.800	342.715	.	.	2.535	.	.
	.850	585.684	.	.	2.768	.	.
	.900	1149.452	.	.	3.060	.	.
	.910	1352.751	.	.	3.131	.	.
	.920	1614.555	.	.	3.208	.	.
	.930	1961.269	.	.	3.293	.	.
	.940	2437.209	.	.	3.387	.	.
	.950	3122.525	.	.	3.495	.	.
	.960	4177.703	.	.	3.621	.	.
	.970	5975.429	.	.	3.776	.	.
	.980	9615.865	.	.	3.983	.	.
	.990	20353.815	.	.	4.309	.	.

a. A heterogeneity factor is used.

b. Logarithm base = 10.



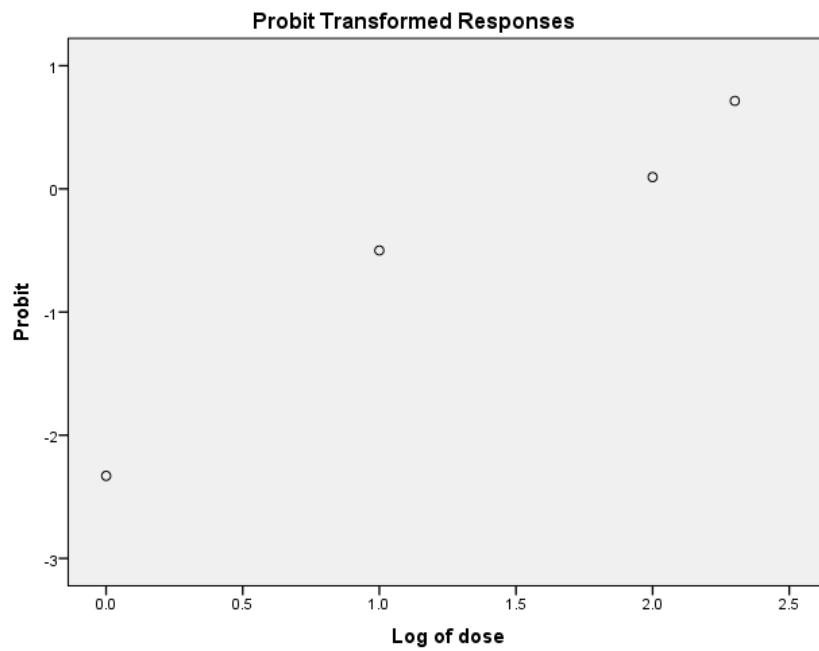
F. Replication 6 of *in vivo* antiplasmodial activity of *Sonchus arvensis* L

Confidence Limits

	Probability	95% Confidence Limits for dose			95% Confidence Limits for log(dose) ^b		
		Estimate	Lower Bound	Upper Bound	Estimate	Lower Bound	Upper Bound
	.010	.307	.	.	-.513	.	.
	.020	.560	.	.	-.252	.	.
	.030	.819	.	.	-.087	.	.
	.040	1.091	.	.	.038	.	.
	.050	1.377	.	.	.139	.	.
	.060	1.679	.	.	.225	.	.
	.070	1.998	.	.	.301	.	.
	.080	2.335	.	.	.368	.	.
	.090	2.691	.	.	.430	.	.
	.100	3.065	.	.	.486	.	.
	.150	5.259	.	.	.721	.	.
	.200	8.077	.	.	.907	.	.
	.250	11.671	.	.	1.067	.	.
	.300	16.242	.	.	1.211	.	.
	.350	22.063	.	.	1.344	.	.
	.400	29.505	.	.	1.470	.	.
	.450	39.086	.	.	1.592	.	.
PROBIT ^a	.500	51.548	.	.	1.712	.	.
	.550	67.983	.	.	1.832	.	.
	.600	90.059	.	.	1.955	.	.
	.650	120.435	.	.	2.081	.	.
	.700	163.598	.	.	2.214	.	.
	.750	227.683	.	.	2.357	.	.
	.800	328.992	.	.	2.517	.	.
	.850	505.259	.	.	2.704	.	.
	.900	866.879	.	.	2.938	.	.
	.910	987.607	.	.	2.995	.	.
	.920	1137.889	.	.	3.056	.	.
	.930	1329.658	.	.	3.124	.	.
	.940	1582.280	.	.	3.199	.	.
	.950	1929.483	.	.	3.285	.	.
	.960	2435.931	.	.	3.387	.	.
	.970	3244.195	.	.	3.511	.	.
	.980	4748.222	.	.	3.677	.	.
	.990	8654.855	.	.	3.937	.	.

a. A heterogeneity factor is used.

b. Logarithm base = 10.



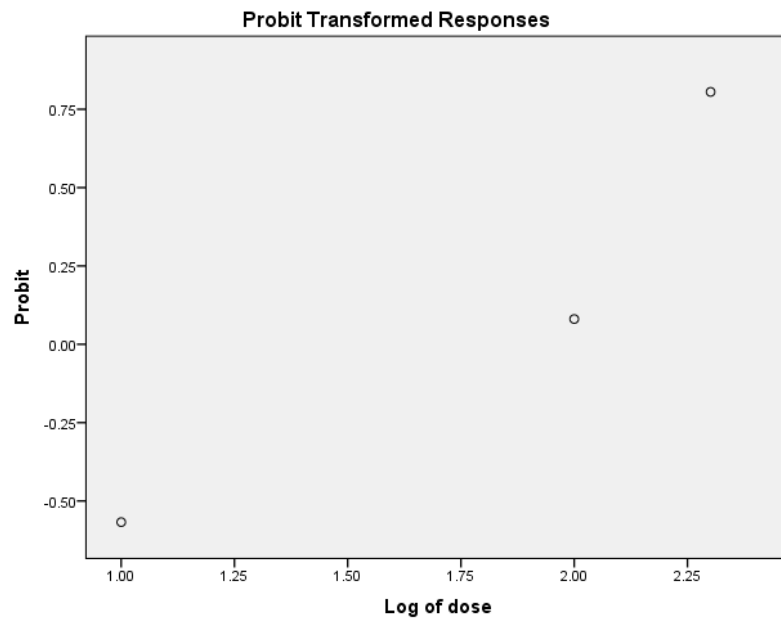
G. Replication 7 of *in vivo* antiplasmodial activity of *Sonchus arvensis* L.

Confidence Limits

	Probability	95% Confidence Limits for dose			95% Confidence Limits for log(dose) ^b		
		Estimate	Lower Bound	Upper Bound	Estimate	Lower Bound	Upper Bound
	.010	.487	.	.	-.313	.	.
	.020	.842	.	.	-.075	.	.
	.030	1.192	.	.	.076	.	.
	.040	1.549	.	.	.190	.	.
	.050	1.916	.	.	.282	.	.
	.060	2.296	.	.	.361	.	.
	.070	2.692	.	.	.430	.	.
	.080	3.103	.	.	.492	.	.
	.090	3.532	.	.	.548	.	.
	.100	3.978	.	.	.600	.	.
	.150	6.513	.	.	.814	.	.
	.200	9.637	.	.	.984	.	.
	.250	13.486	.	.	1.130	.	.
	.300	18.238	.	.	1.261	.	.
	.350	24.125	.	.	1.382	.	.
	.400	31.458	.	.	1.498	.	.
	.450	40.668	.	.	1.609	.	.
PROBIT ^a	.500	52.361	.	.	1.719	.	.
	.550	67.416	.	.	1.829	.	.
	.600	87.153	.	.	1.940	.	.
	.650	113.645	.	.	2.056	.	.
	.700	150.323	.	.	2.177	.	.
	.750	203.289	.	.	2.308	.	.
	.800	284.505	.	.	2.454	.	.
	.850	420.960	.	.	2.624	.	.
	.900	689.177	.	.	2.838	.	.
	.910	776.318	.	.	2.890	.	.
	.920	883.516	.	.	2.946	.	.
	.930	1018.549	.	.	3.008	.	.
	.940	1193.895	.	.	3.077	.	.
	.950	1431.012	.	.	3.156	.	.
	.960	1770.431	.	.	3.248	.	.
	.970	2299.940	.	.	3.362	.	.
	.980	3256.702	.	.	3.513	.	.
	.990	5634.685	.	.	3.751	.	.

a. A heterogeneity factor is used.

b. Logarithm base = 10.



1.5 Supplementary data V

A. BUN and CREATININE SERUM LEVEL

1. BUN

Standard concentration solvent= 50 mg/dL

$$\Delta A = A1 - A2$$

Standard: 0,0476

Urea level : $\Delta A \text{ Sample} / \Delta A \text{ Standard} \times \text{standard concentration (mg/dL)}$

BUN = Urea (mg/dL) x 0,467

UNINFECTED GROUP					
Replication	A1	A2	$\Delta A \text{ Smp} / \Delta A \text{ Std}$	Urea Level	BUN Level (mg/dL)
KN-1	0,0918	0,089	0,146359	7,317927	3,41
KN-2	0,001	-0,0062	0,151261	7,563025	3,53
KN-3	0,0777	0,0708	0,144958	7,247899	3,38
KN-4	0,1968	0,19	0,142857	7,142857	3,34
POSITIVE CONTROL GROUP					
Replication	A1	A2	$\Delta A \text{ Smp} / \Delta A \text{ Std}$	Urea Level	BUN Level (mg/dL)
K+1	0,0055	0,004	0,032213	1,61064	0,75
K+2	0,0061	0,0056	0,010504	0,52521	0,25
K+3	0,005	0,0028	0,046218	2,310924	1,08
K+4	0,0055	0,0036	0,039916	1,995798	0,93
NEGATIVE CONTROL GROUP					
Replication	A1	A2	$\Delta A \text{ Smp} / \Delta A \text{ Std}$	Urea Level	BUN Level (mg/dL)
K-1	0,0627	0,0575	0,299719	14,98599	6,99
K-2	0,0674	0,0526	0,310924	15,54622	7,26
K-3	-0,0592	-0,0728	0,285714	14,28571	6,67
K-4	0,0616	0,0472	0,302521	15,12605	7,06
P1					
Replication	A1	A2	$\Delta A \text{ Smp} / \Delta A \text{ Std}$	Urea Level	BUN Level (mg/dL)
P1-1	0,3551	0,3461	0,189076	9,453782	4,41
P1-2	0,056	0,062	0,12605	6,302521	2,94
P1-3	0,1627	0,162	0,112045	5,602241	2,61
P1-4	-0,0769	-0,0779	0,021008	1,05042	0,49
P2					
Replication	A1	A2	$\Delta A \text{ Smp} / \Delta A \text{ Std}$	Urea Level	BUN Level (mg/dL)
P2-1	0,3348	0,3373	0,126284	6,31419	2,95
P2-2	0,3855	0,3901	0,096639	4,831933	2,26
P2-3	0,3492	0,3452	0,084034	4,201681	1,96
P2-4	0,2698	0,2766	0,198179	9,908965	4,63
P3					
Replication	A1	A2	$\Delta A \text{ Smp} / \Delta A \text{ Std}$	Urea Level	BUN Level (mg/dL)
P3-1	0,3872	0,395	0,163866	8,193277	3,83

P3-2	0,5214	0,5332	0,247899	12,39496	5,79
P3-3	0,0312	0,0203	0,228992	11,44958	5,35
P3-4	-0,4989	-0,4907	0,172269	8,613445	4,02
P4					
Replication	A1	A2	$\Delta A \text{ Smp} / \Delta A \text{ Std}$	Urea Level	BUN Level (mg/dL)
P4-1	0,0948	0,0951	0,006303	0,315126	0,15
P4-2	0,0624	0,0568	0,117647	5,882353	2,75
P4-3	0,068	0,0641	0,086135	4,306723	2,01
P4-4	0,0468	0,0404	0,134454	6,722689	3,14

BUN LEVEL

ANOVA Test

	Sum of Squares	df	Mean Square	F	Sig.
Between Groups	97,932	6	16,322	16,464	,000
Within Groups	20,818	21	,991		
Total	118,750	27			

Post Hoc Duncan Test

Duncan^a

Kelompok	N	Subset for alpha = 0.05			
		1	2	3	4
K+	4	,7525			
P4	4	2,0125	2,0125		
P1	4		2,6125		
P2	4		2,9500		
KN	4		3,4150	3,4150	
P3	4			4,7475	
K-	4				6,9950
Sig.		,088	,080	,072	1,000

Means for groups in homogeneous subsets are displayed.

a. Uses Harmonic Mean Sample Size = 4,000.

2. CREATININE

Standard concentration solvent= 2 mg/dL

$$\Delta A = A1 - A2$$

Standard: 0,0192

Creatinine Level : $\Delta A \text{ Sample} / \Delta A \text{ Standard} \times \text{standard concentration}$ (mg/dL)

UNINFECTED GROUP				
Replication	A1	A2	$\Delta A \text{ Smp} / \Delta A \text{ Std}$	Level Kreatinin (mg/dL)
KN-1	0,0247	0,0262	0,092	0,18
KN-2	0,0237	0,0256	0,099	0,20
KN-3	0,0179	0,0175	0,021	0,23
KN-4	0,0324	0,0354	0,156	0,31
POSITIVE CONTROL GROUP				
Replication	A1	A2	$\Delta A \text{ Smp} / \Delta A \text{ Std}$	Level (mg/dL)
K+1	0,0131	0,0168	0,193	0,39
K+2	0,0233	0,0271	0,198	0,40
K+3	0,0515	0,0553	0,198	0,40
K+4	0,0095	0,0131	0,188	0,38
NEGATIVE CONTROL GROUP				
Replication	A1	A2	$\Delta A \text{ Smp} / \Delta A \text{ Std}$	Level (mg/dL)
K-1	-0,0361	-0,0208	0,797	1,59
K-2	-0,0540	-0,0349	0,995	1,99
K-3	-0,045	-0,023	1,146	2,29
K-4	-0,081	-0,061	1,042	2,08
P1				
Replication	A1	A2	$\Delta A \text{ Smp} / \Delta A \text{ Std}$	Level (mg/dL)
P1-1	0,0771	0,0784	0,068	0,14
P1-2	0,0302	0,0287	0,078	0,16
P1-3	0,0646	0,0658	0,062	0,12
P1-4	0,0573	0,0576	0,069	0,14
P2				
Replication	A1	A2	$\Delta A \text{ Smp} / \Delta A \text{ Std}$	Level (mg/dL)
P2-1	0,0106	0,014	0,177	0,35
P2-2	0,0203	0,0241	0,198	0,40
P2-3	0,0034	0,0004	0,156	0,31
P2-4	0,0039	0,0077	0,198	0,40
P3				
Replication	A1	A2	$\Delta A \text{ Smp} / \Delta A \text{ Std}$	Level (mg/dL)
P3-1	0,0095	0,0125	0,156	0,31
P3-2	0,0413	0,0436	0,120	0,24
P3-3	0,0326	0,0354	0,146	0,29
P3-4	0,0153	0,0176	0,120	0,24
P4				
Replication	A1	A2	$\Delta A \text{ Smp} / \Delta A \text{ Std}$	Level (mg/dL)
P4-1	0,0481	0,0505	0,125	0,25
P3-2	-0,0363	-0,0394	0,161	0,32
P4-3	-0,0258	-0,0257	0,114	0,23
P4-4	-0,0893	-0,0882	0,057	0,11

Sigficancy Table

	KN	K+	K-	P1	P2	P3	P4
KN		S	S	S	S	TS	TS
K+			S	S	TS	S	S
K-				S	S	S	S
P1					S	S	TS
P2						S	S
P3							TS
P4							

B. SERUM SGOT AND SGPT LEVEL

1. SGOT

SGOT Level : $\Delta A ((A1 - A2) + (A2 - A3) + (A3 - A4)) \times 2143 \times 1$

UNINFECTED GROUP					
Replication	A1	A2	A3	A4	Level (U/L)
KN-1	0,084	0,0838	0,0836	0,064	42,00
KN-2	0,5415	0,5364	0,4042	0,3792	53,71
KN-3	0,2784	0,2604	0,2475	0,2326	31,96
KN-4	0,4366	0,4317	0,4116	0,3951	35,38
POSITIVE CONTROL GROUP					
Replication	A1	A2	A3	A4	Level (U/L)
K+1	0,3461	0,3319	0,3127	0,297	33,68
K+2	0,2384	0,2021	0,2012	0,1899	24,25
K+3	0,34	0,3377	0,3373	0,3207	35,58
K+4	0,407	0,3821	0,3655	0,3477	38,19
NEGATIVE CONTROL GROUP					
Replication	A1	A2	A3	A4	Level (U/L)
K-1	0,4897	0,3548	0,2211	0,0981	263,86
K-2	0,7893	0,7552	0,7053	0,6448	129,73
K-3	0,4973	0,4009	0,2853	0,1469	296,80
K-4	0,2098	0,1806	0,1327	0,0781	117,08
P1					
Replication	A1	A2	A3	A4	Level (U/L)
P1-1	0,3545	0,302	0,2179	0,1258	102,14
P1-2	0,2837	0,2652	0,2333	0,1941	100,68
P1-3	0,0339	0,0208	-0,0418	-0,09	103,37
P1-4	0,0357	0,0003	-0,0368	-0,0923	96,52
P2					
Replication	A1	A2	A3	A4	Level U/L)
P2-1	0,1285	0,1155	0,0719	0,0417	64,77
P2-2	-0,2133	-0,3117	-0,3134	-0,3126	68,36
P2-3	-0,1002	-0,1716	-0,2633	-0,3249	73,85
P2-4	-0,3189	-0,3106	-0,3127	-0,3165	88,43
P3					
Replication	A1	A2	A3	A4	Level (U/L)
P3-1	0,0328	0,0048	-0,0619	-0,1071	76,63

P3-2	0,2443	0,2445	0,2175	0,1895	60,03
P3-3	-0,3957	-0,3905	-0,3917	-0,3929	73,79
P3-4	0,0094	-0,0123	-0,0676	-0,1177	69,82
P4					
Replication	A1	A2	A3	A4	Level (U/L)
P4-1	0,1418	0,0621	0,0781	0,0903	26,08
P4-2	0,0874	0,0851	0,0538	0,0376	34,75
P4-3	0,0875	0,1043	0,0575	0,0338	50,85
P4-4	-0,01979	-0,2582	-0,2684	-0,2586	20,75

DATA ANALYSIS OF SGOT

Significancy Table

	K+	K-	P1	P2	P3	P4
KN	TS	S	S	S	S	TS
K+		S	S	S	S	TS
K-			S	S	S	S
P1				S	S	S
P2					TS	S
P3						S
P4						

2. SGPT

SGPT LEVEL

SGPT Level: $\Delta A ((A1 - A2) + (A2 - A3) + (A3 - A4)) \times 2143 \times 1$

UNINFECTED GROUP					
Replication	A1	A2	A3	A4	Level (U/L)
KN-1	0,1088	0,1157	0,1045	0,0926	13,41
KN-2	0,119	0,127	0,1207	0,1154	11,36
KN-3	0,2057	0,2154	0,2044	0,1986	12,43
KN-4	-0,0449	-0,0466	-0,0477	-0,0503	12,4
POSITIVE CONTROL GROUP					
Replication	A1	A2	A3	A4	Level (U/L)
K+1	-0,3624	-0,3579	-0,3553	-0,3511	9,00
K+2	0,0162	0,0221	0,0234	0,0214	4,28
K+3	0,1225	0,1275	0,129	0,1278	2,56
K+4	0,0892	0,0952	0,0923	0,095	5,79
NEGATIVE CONTROL GROUP					
Replication	A1	A2	A3	A4	Level (U/L)
K-1	-0,0139	-0,0157	-0,0262	-0,0327	24,13

K-2	0,1363	0,1274	0,1099	0,099	23,38
K-3	-0,0284	-0,042	-0,0653	-0,0916	21,58
K-4	0,057	0,0624	0,0551	0,0423	27,43
P1					
Replication	A1	A2	A3	A4	Level (U/L)
P1-1	0,0234	0,0517	-0,0064	-0,027	44,17
P1-2	-0,1246	-0,0273	-0,1166	-0,1229	13,49
P1-3	-0,0221	-0,0183	-0,0277	-0,0464	40,08
P1-4	-0,0559	-0,0566	-0,0745	-0,0893	31,73
P2					
Replication	A1	A2	A3	A4	Level (U/L)
P2-1	-0,0523	-0,0723	-0,0959	-0,0898	22,74
P2-2	-0,1579	-0,2059	-0,2516	-0,2871	20,31
P2-3	-0,1335	-0,1455	-0,155	-0,1655	22,52
P2-4	-0,1766	-0,253	-0,2884	-0,3002	25,39
P3					
Replication	A1	A2	A3	A4	Level (U/L)
P3-1	-0,0715	-0,0672	-0,0803	-0,0873	15,01
P3-2	-0,0278	-0,0298	-0,0341	-0,0383	9,00
P3-3	-0,0479	-0,0497	-0,0599	-0,0659	12,87
P3-4	-0,094	-0,0927	-0,1001	-0,108	16,93
P4					
Replication	A1	A2	A3	A4	Level (U/L)
P4-1	0,01645	0,1737	0,1737	0,1751	3,16
P4-2	0,1503	0,1592	-0,1479	-0,1462	3,34
P4-3	-0,1675	-0,1621	-0,1633	-0,1622	2,36
P4-4	0,0403	0,0447	0,0403	0,0393	2,14

Significance Table

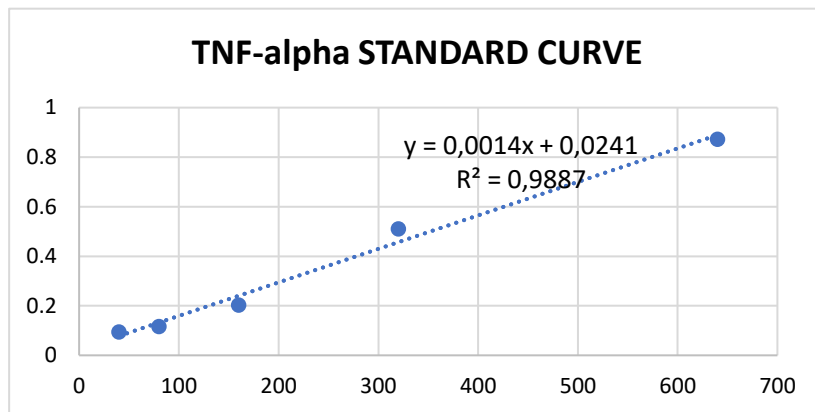
	KN	K+	K-	P1	P2	P3	P4
KN		S	S	S	S	TS	S
K+			S	S	S	S	TS
K-				TS	TS	S	S
P1					TS	S	S
P2						S	S
P3							S
P4							

C. SERUM TNF ALPHA AND IL10 LEVELS

1. TNF Alpha

Kadar (ng/mL)	OD
40	0,094
80	0,117
160	0,203
320	0,51
640	0,873

The Standard Curve



$y = 0,0014x + 0,0241, R^2=0,9887$

y = kadar TNF-alpha

x = OD TNF-alpha

Uninfected Group		
Replication	OD	Level (ng/ml)
KN-1	0,304	199,93
KN-4	0,62	425,64
KN-5	0,279	182,07
KN-6	0,348	231,36
KN-7	0,317	209,21
Positive Control Group		
Replication	OD	Level (ng/ml)
K+1	0,33	218,50
K+2	0,332	219,93
K+3	0,212	134,21
K+4	0,275	179,21
K+6	0,777	537,79
Negative Control Group		
Replication	OD	Level (ng/ml)
K-1	0,279	182,07
K-2	0,337	223,50
K-3	0,523	356,36
K-4	0,142	84,21
K-5	0,063	27,79

K-7	0,503	342,07
K-8	0,061	26,36
K-9	1,668	1174,21
P1		
Replication	OD	Level (ng/ml)
P1-2	0,759	524,93
P1-3	0,673	463,50
P1-5	0,399	267,79
P1-7	0,635	436,36
P1-8	0,37	247,07
P2		
Replikasi	OD	Level (ng/ml)
P2-1	2,172	1534,21
P2-3	0,775	536,36
P2-4	0,766	529,93
P2-5	1,144	799,93
P2-7	0,828	574,21
P3		
Replication	OD	Level (ng/ml)
P3-1	0,831	576,36
P3-2	1,127	787,79
P3-3	1,056	737,07
P3-4	1,536	1079,93
P3-5	1,507	1059,21
P3-7	0,827	573,50
P3-8	0,702	484,21
P4		
Replication	OD	Level (ng/ml)
P4-1	1,069	746,36
P4-2	0,721	497,79
P4-3	1,16	811,36
P4-4	1,208	845,64
P4-6	1,039	724,93
P4-7	0,752	519,93
P4-8	0,731	504,93

ANOVA

TFN ALPHA

	Sum of Squares	df	Mean Square	F	Sig.
Between Groups	2317688.065	6	386281.344	8.718	.000
Within Groups	1240629.624	28	44308.201		
Total	3558317.688	34			

Duncan Test (POST HOC TEST)

Duncan^a

Group	N	Subset for alpha = 0.05	
		1	2
K-	5	237.6420	
KN	5	249.6420	
K+	5	257.9280	
P1	5	387.9300	
P4	5		729.6440
P2	5		794.9280
P3	5		848.0720
Sig.		.313	.409

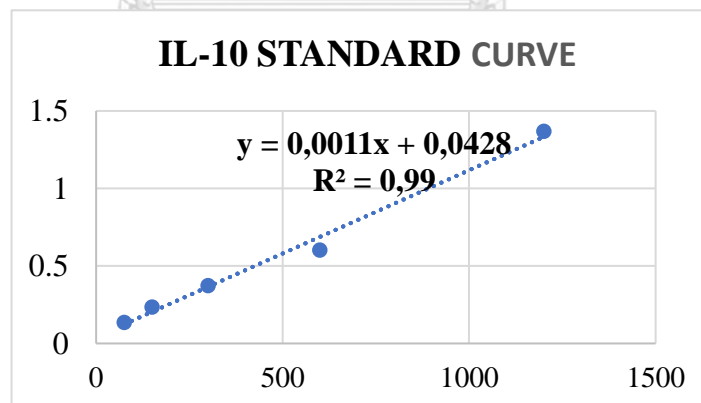
Means for groups in homogeneous subsets are displayed.

a. Uses Harmonic Mean Sample Size = 5.000.

1. IL 10 Level

Level (pg/mL)	OD
40	0,094
80	0,117
160	0,203
320	0,51
640	0,873

Standard Curve



$$y = 0,0011x + 0,0428, R^2=0,99$$

y = IL-10 level

x = OD IL-10

Uninfected Group		
Replication	OD	Level (pg/ml)
KN-1	0,157	103,82
KN-4	0,141	89,27
KN-5	0,169	114,73
KN-6	0,168	113,82
KN-7	0,158	104,73
Positive Control Group		
Replication	OD	Level (pg/ml)
K+1	0,181	125,64
K+2	0,188	132,00
K+3	0,184	128,36
K+4	0,202	144,73
K+6	0,309	242,00
K+7	0,18	124,73
Negative Control Group		
Replication	OD	Level (pg/ml)
K-1	0,133	82,00
K-2	0,104	55,64
K-3	0,172	117,45
K-4	0,136	84,73
K-5	0,153	100,18
K-7	0,173	118,36
K-9	0,225	165,64
K-10	0,196	139,27
P1		
Replication	OD	Level (pg/ml)
P1-2	0,175	120,18
P1-3	0,161	107,45
P1-5	0,188	132,00
P1-7	0,15	97,45
P1-8	0,163	109,27
P2		
Replication	OD	Level (pg/ml)
P2-1	0,161	107,45
P2-3	0,175	120,18
P2-4	0,141	89,27
P2-5	0,157	103,82
P2-7	0,165	111,09
P3		
Replication	OD	Level (pg/ml)
P3-1	0,135	83,82
P3-2	0,165	111,09
P3-3	0,167	112,91
P3-4	0,165	111,09

P3-5	0,176	121,09
P3-7	0,182	126,55
P3-8	0,135	83,82
P4		
Replication	OD	Level (pg/ml)
P4-1	0,176	121,09
P4-2	0,177	122,00
P4-3	0,163	109,27
P4-4	0,171	116,55
P4-6	0,14	88,36
P4-7	0,177	122,00
P4-8	0,171	116,55

Anova Test

ANOVA

IL10

	Sum of Squares	df	Mean Square	F	Sig.
Between Groups	5480.331	6	913.388	6.042	.000
Within Groups	4232.589	28	151.164		
Total	9712.920	34			

Duncan Test (POST HOC TEST)

IL10

Duncan^a

KELOMPOK	N	Subset for alpha = 0.05		
		1	2	3
K-	5	88.0000		
KN	5		105.2740	
P2	5		106.3620	
P1	5		113.2700	
P3	5		116.5460	116.5460
P4	5		119.6380	119.6380
K+	5			131.0920
Sig.		1.000	.108	.087

Means for groups in homogeneous subsets are displayed.

a. Uses Harmonic Mean Sample Size = 5.000.

2. APPENDIX 2

2.1 Supplementary data I

TLC chromatogram profile of n-hexane extract of *Pterocarpus macrocarpus* Kurz. crystallization

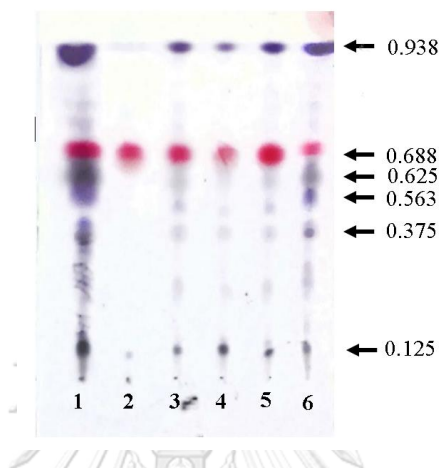


Fig. TLC analysis chromatogram profile of *Pterocarpus macrocarpus* Kurz. heartwood *n*-hexane extract purification during crystallization. Stationary phase: Silica gel GF254, mobile phase: *n*-hexane: ethyl acetate (1:1) 1. *n*-Hexane crude extract, 2. Fifth crystallization, 3. Fourth crystallization, 4. Third crystallization, 5. Second crystallization, 6. First crystallization.

2.2 Supplementary data II

GC-MS Chromatogram profile of n-hexane extract of *Pterocarpus macrocarpus* Kurz. crystallization (available in Author)

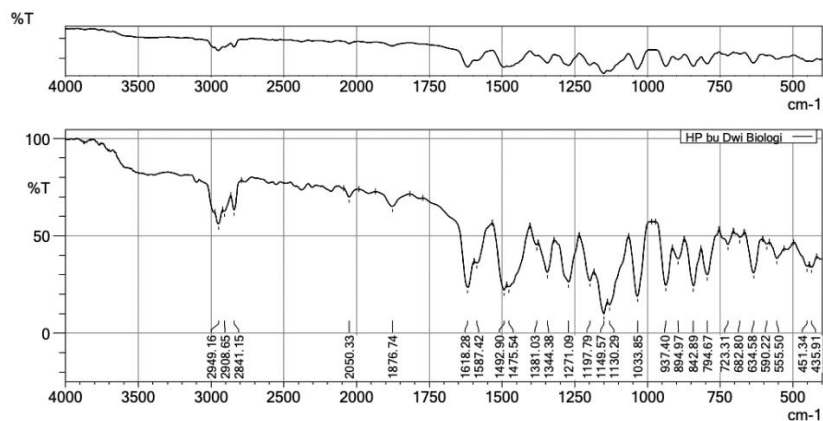
2.3 Supplementary data III

FTIR spectra of homopteroicarpin

SHIMADZU

HP bu Dwi Biologi

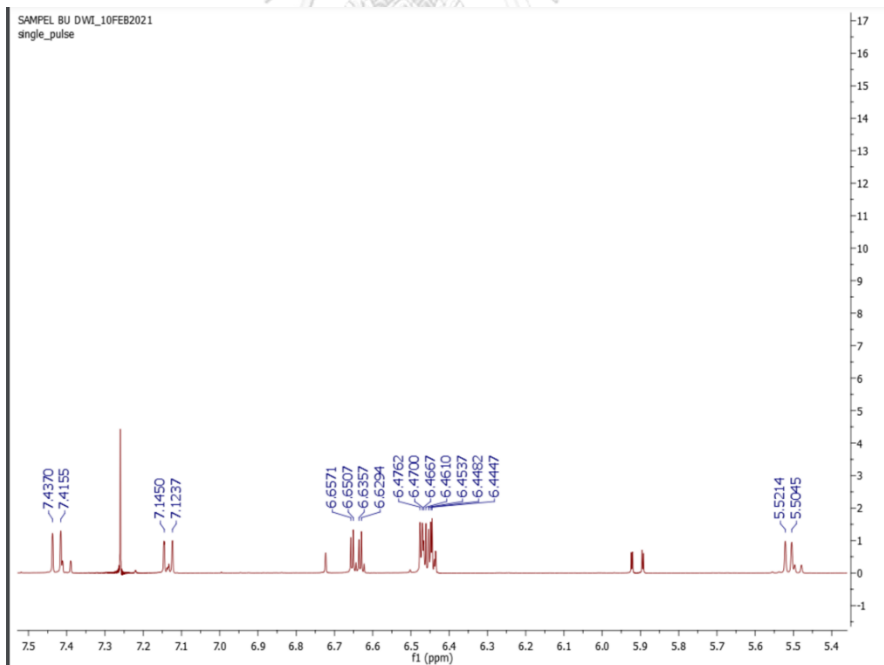
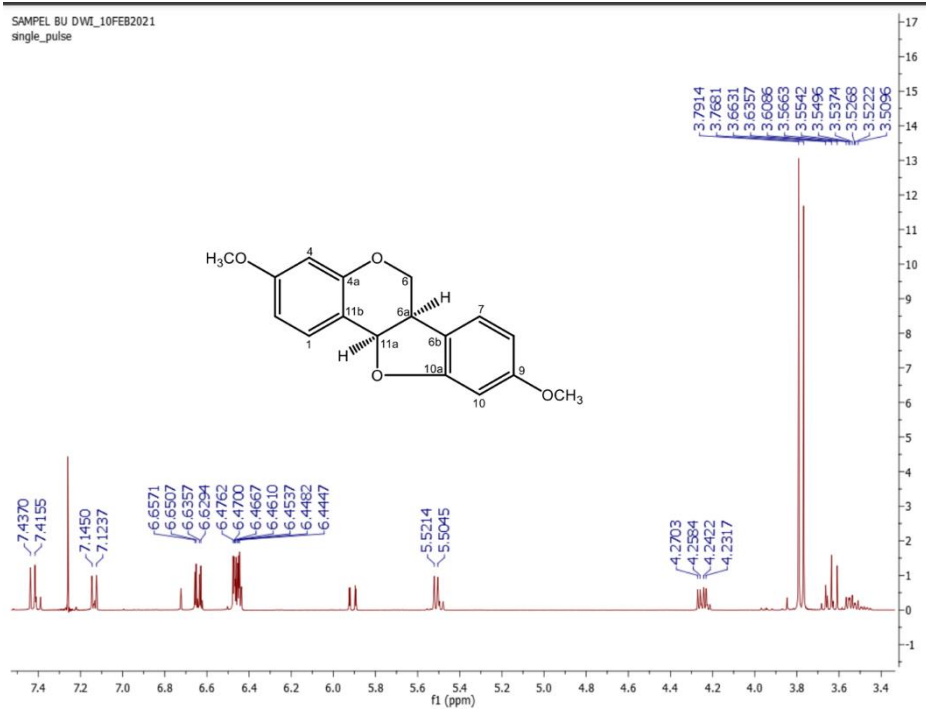
21/10/2021 9:27:28 AM



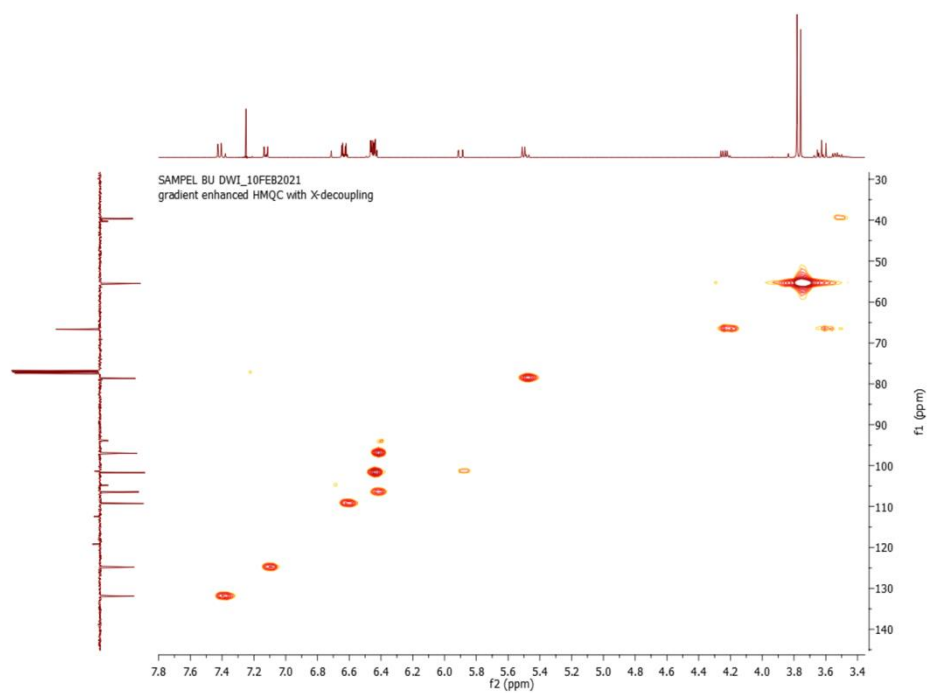
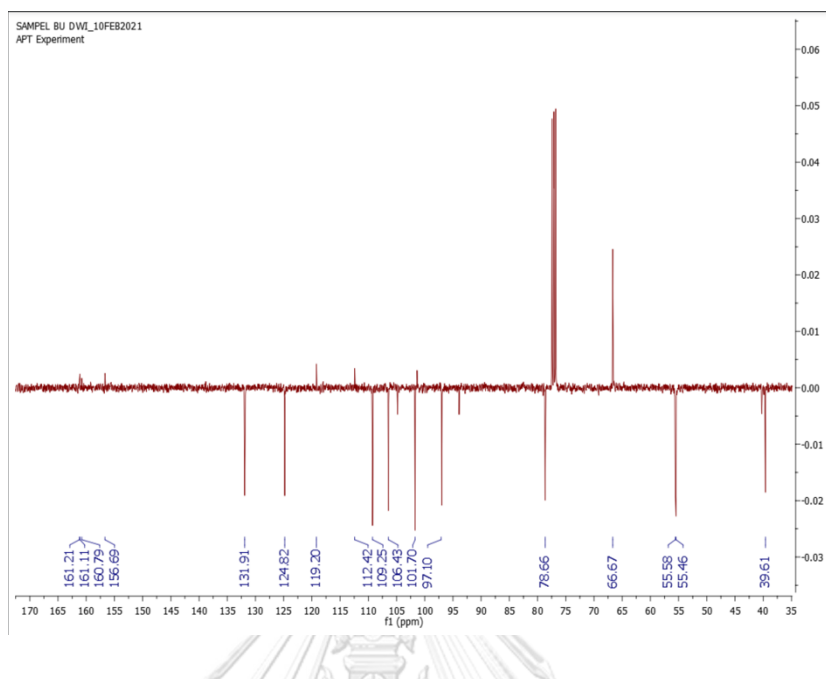
Item	Value
Acquired Date&Time	21/10/2021 9:24:23 AM
Acquired by	System Administrator
Filename	H:\DATA FTIR\20211021\HP bu Dwi Biologi1.ispd
Spectrum name	HP bu Dwi Biologi
Sample name	
Sample ID	
Option	
Comment	

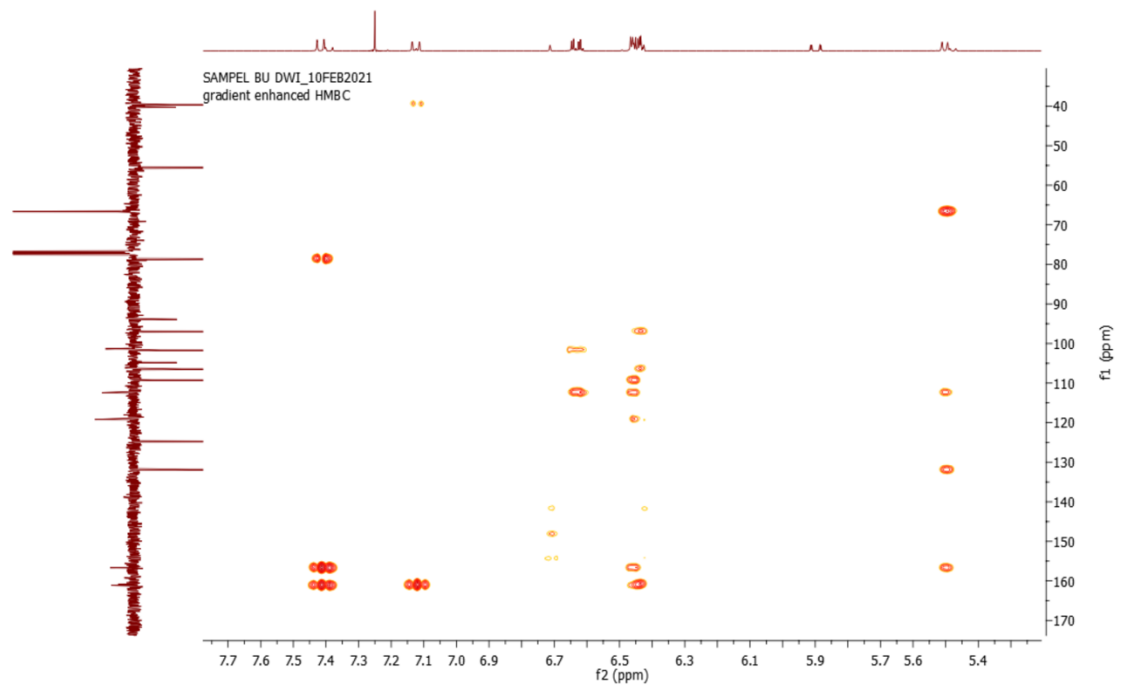
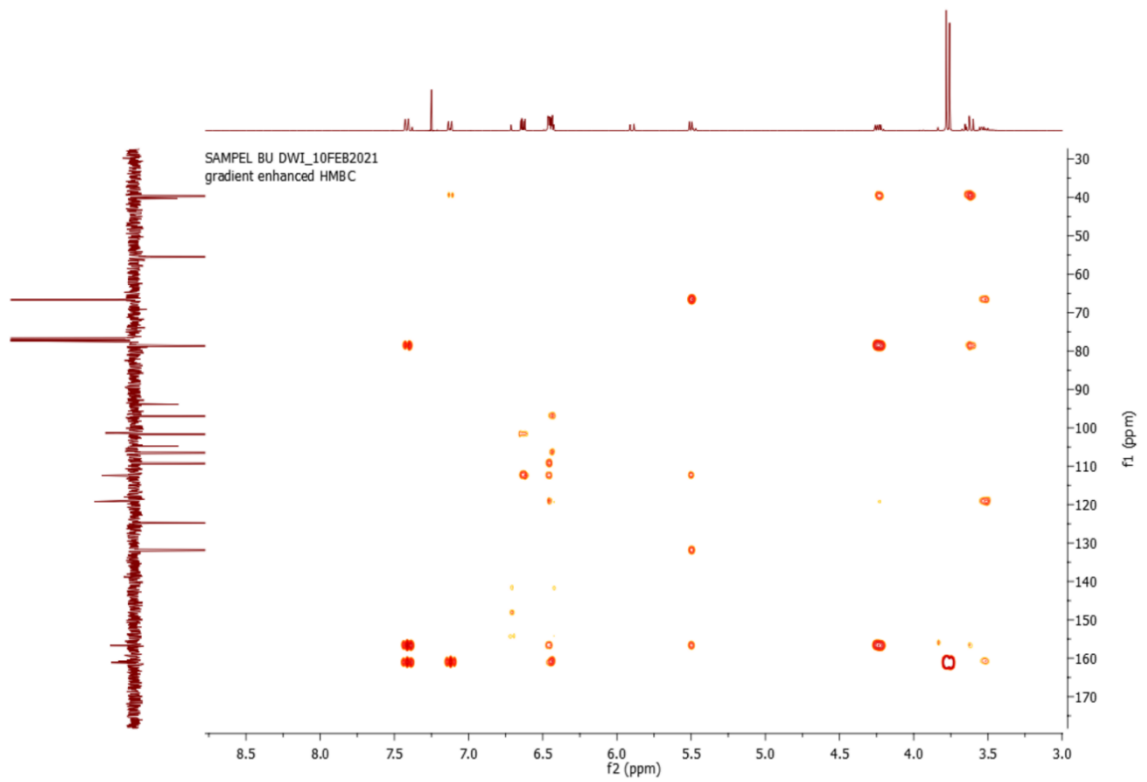
Peak	Intensity	Corr. Intensity	Base (H)	Base (L)	Area	Corr. Area	Comment
1	435.91	33.91	2.53	443.63	418.55	1612.992	39.483
2	451.34	34.45	2.35	497.63	443.63	3244.596	51.011
3	555.50	38.39	6.63	580.57	530.42	2918.640	161.544
4	590.22	45.76	1.64	603.72	580.57	1235.812	21.558
5	634.58	31.04	19.06	667.37	603.72	3719.066	545.908
6	682.80	49.28	2.87	704.02	667.37	1811.719	60.073
7	723.31	45.59	7.19	754.17	704.02	2559.138	195.640
8	794.67	29.97	16.77	815.89	754.17	3662.699	471.434
9	842.89	24.41	21.25	873.75	815.89	3712.936	578.268
10	894.97	38.24	7.75	914.26	873.75	2366.603	183.197
11	937.40	24.63	24.61	972.12	914.26	3524.570	665.583
12	1033.85	18.97	33.62	1064.71	985.62	4778.360	1096.563
13	1130.29	14.56	5.06	1138.00	1064.71	5149.724	226.860
14	1149.57	10.00	9.91	1184.29	1138.00	3726.746	196.124
15	1197.79	26.86	9.59	1234.44	1184.29	3195.615	227.858
16	1271.09	26.23	22.98	1321.24	1234.44	5380.519	955.331
17	1344.38	31.30	15.85	1375.25	1321.24	3297.011	437.011
18	1381.03	45.37	2.73	1404.18	1375.25	1482.127	57.302
19	1475.54	23.82	3.93	1483.26	1404.18	5131.468	384.617
20	1492.90	22.16	8.74	1533.41	1483.26	3219.485	244.865
21	1587.42	36.10	3.22	1595.13	1533.41	3310.715	22.380
22	1618.28	23.43	17.65	1772.58	1595.13	8043.700	-281.166
23	1876.74	65.11	7.02	1934.60	1816.94	3592.977	312.514
24	2050.33	69.99	4.12	2088.91	1992.47	2665.152	164.836
25	2841.15	63.33	9.82	2864.29	2791.00	2120.334	256.452
26	2908.65	62.63	2.24	2920.23	2864.29	1926.005	81.981
27	2949.16	56.05	6.66	2974.23	2920.23	2212.776	201.370

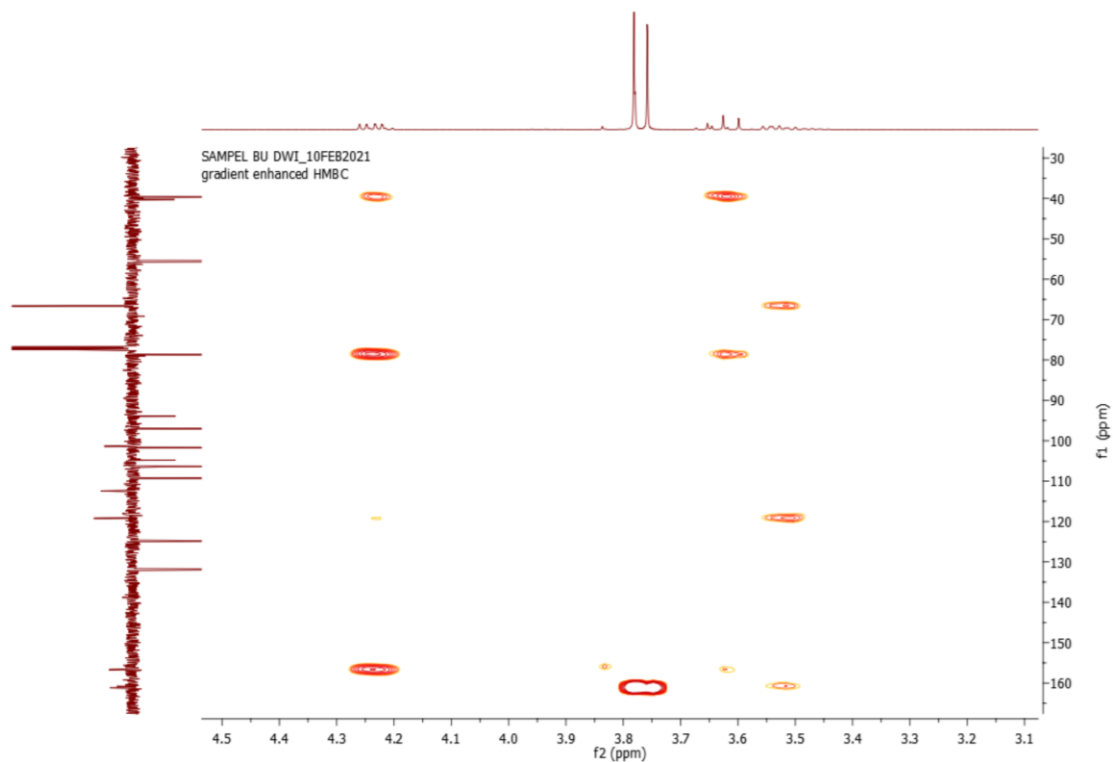
2.4 Supplementary data 4: HNMR of homopterocarpin



2.5 Supplementary data V: CNMR of homopteroicarpin

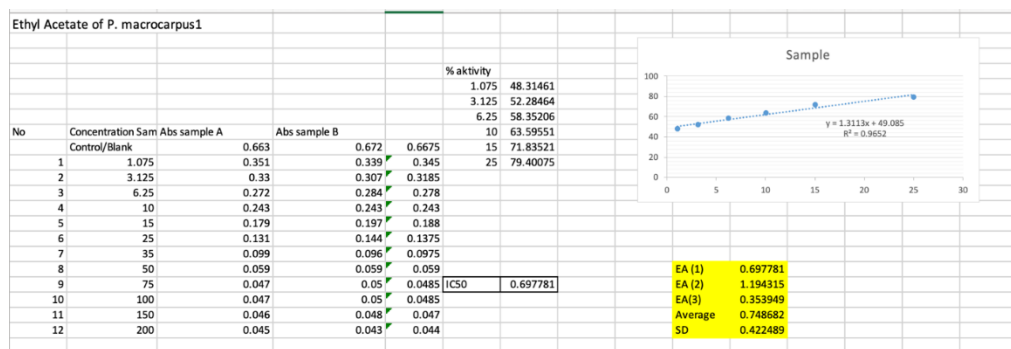
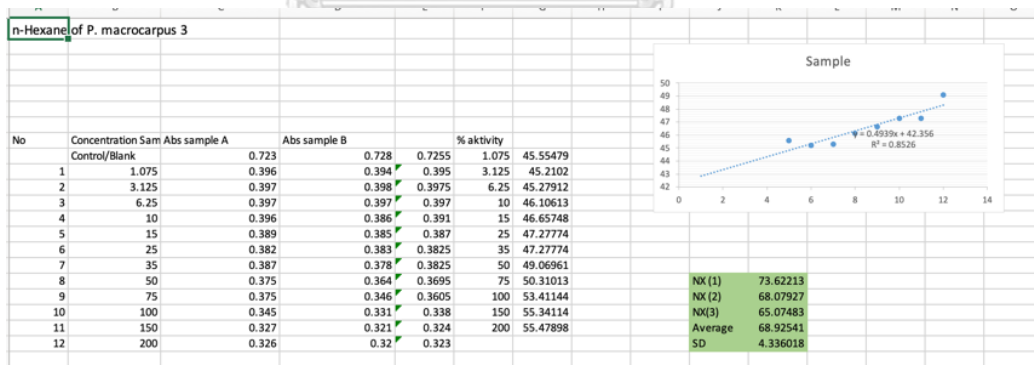
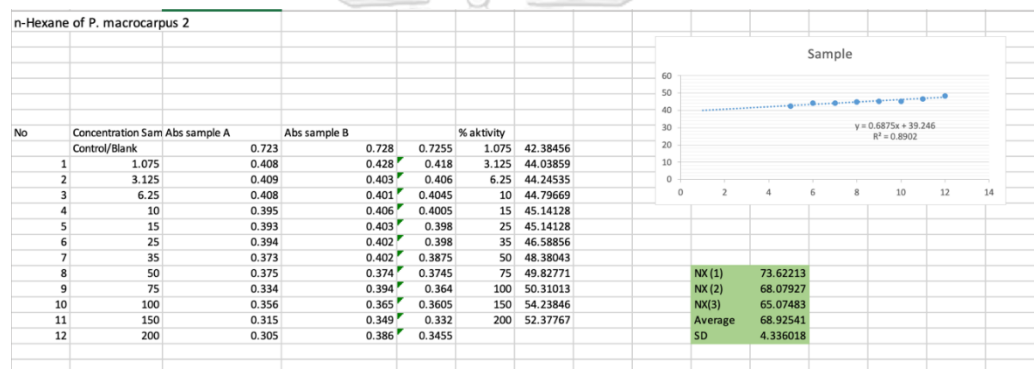
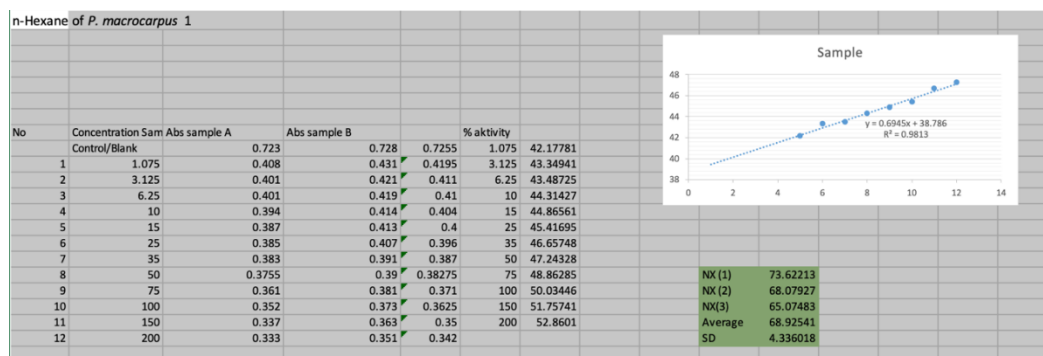


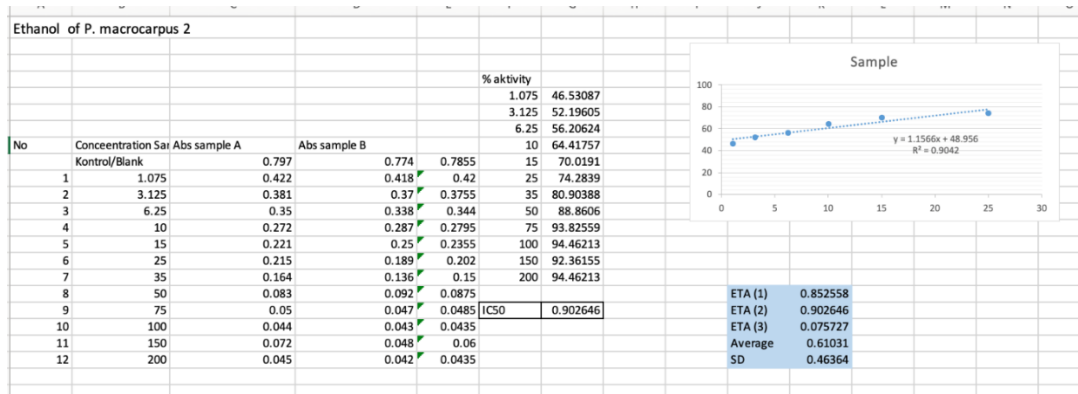
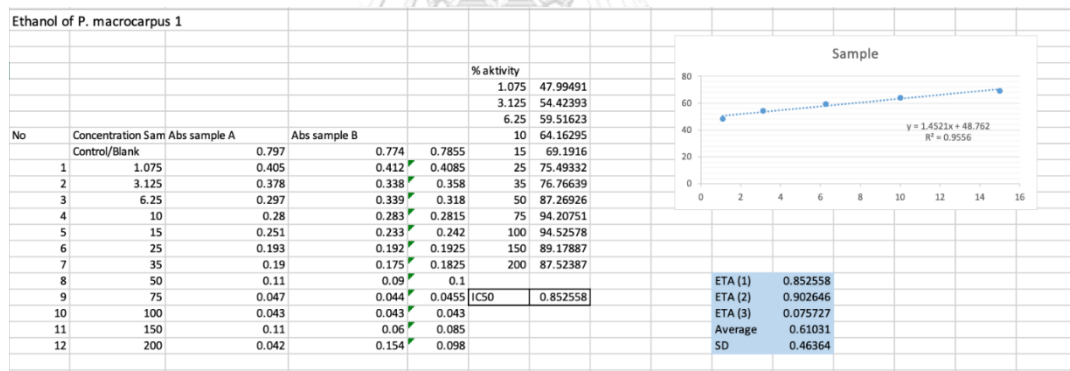
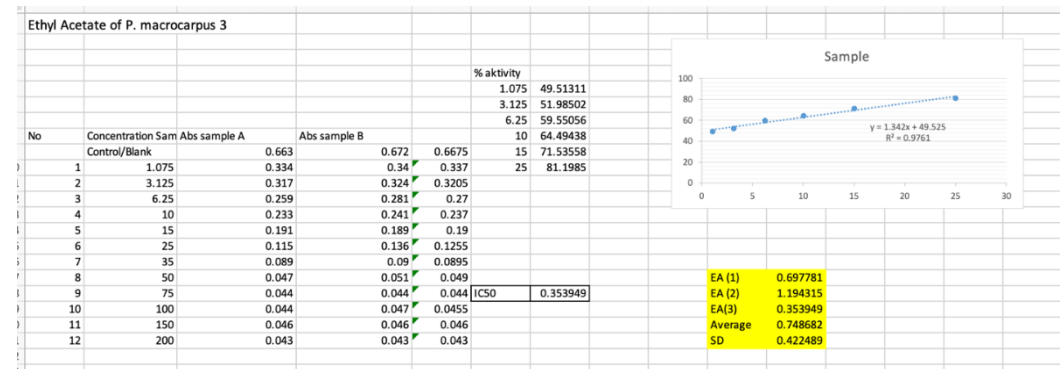
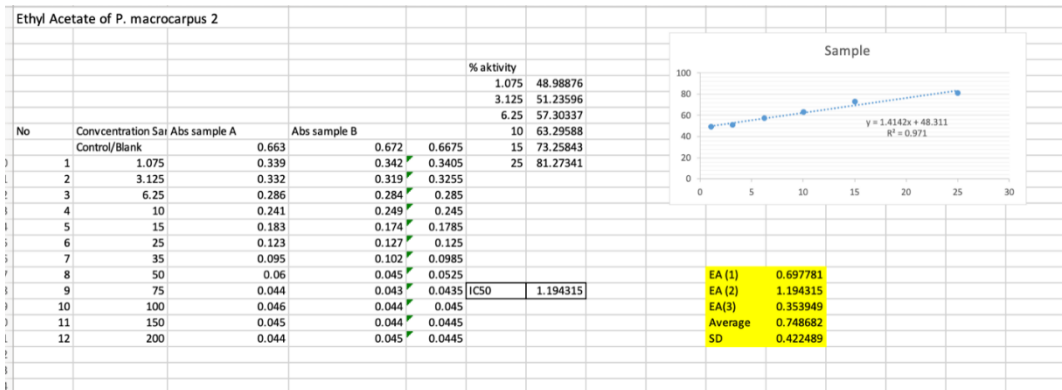




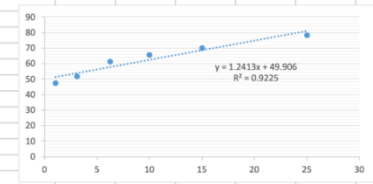
2.6 Supplementary data VI: Antioxidant activity of homopteroicarpin and Pterocarpus macrocarpus Kurz. extract

ABTS



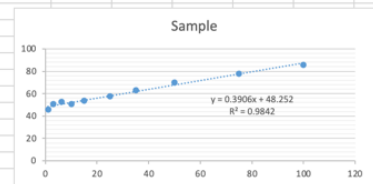


Ethanol of <i>P. macrocarpus</i> 3						
No	Concentration Sample	Abs sample A	Abs sample B	% activity	A	
	Control/Blank	0.797	0.774	0.7855	10	65.43603
1	1.075	0.416	0.409	0.4125	15	69.95544
2	3.125	0.37	0.386	0.378	25	78.29408
3	6.25	0.341	0.265	0.303	35	84.91407
4	10	0.273	0.27	0.2715	50	89.56079
5	15	0.247	0.225	0.236	75	94.39847
6	25	0.168	0.173	0.1705	100	90.32463
7	35	0.121	0.116	0.1185	200	85.48695
8	50	0.078	0.086	0.082		
9	75	0.045	0.043	0.044	IC50	0.075727
10	100	0.042	0.042	0.042		
11	150	0.1	0.052	0.076		
12	200	0.184	0.044	0.114		



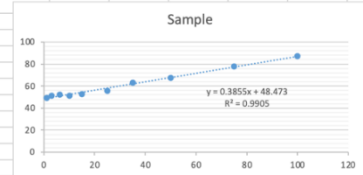
ETA (1) 0.852558
 ETA (2) 0.902646
 ETA (3) 0.075727
 Average 0.61031
 SD 0.46364

Trolox 1						
No	Concentration Sample	Abs sample A	Abs sample B	% activity	A	
	Control/Blank	0.725	0.717	0.721	10	50.83218
1	1.075	0.418	0.365	0.3915	15	53.46741
2	3.125	0.355	0.355	0.355	25	57.62829
3	6.25	0.337	0.347	0.342	50	69.76422
4	10	0.351	0.358	0.3545	75	78.01664
5	15	0.335	0.336	0.3355	100	85.71429
6	25	0.302	0.309	0.3055		
7	35	0.267	0.263	0.265		
8	50	0.21	0.226	0.218		
9	75	0.156	0.161	0.1585	IC50	4.475166
10	100	0.092	0.114	0.103		
11	150	0.187	0.207	0.197		
12	200	0.044	0.044	0.044		

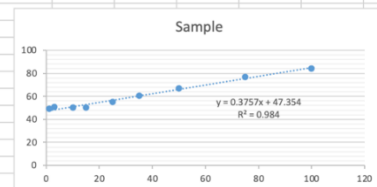


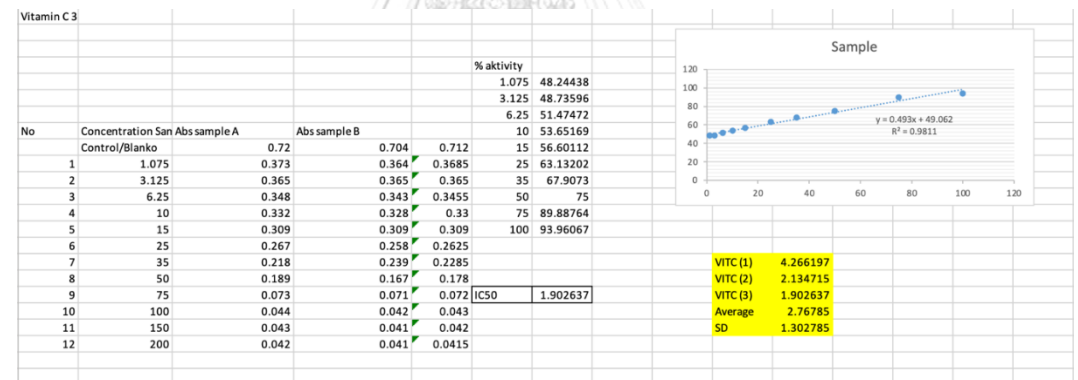
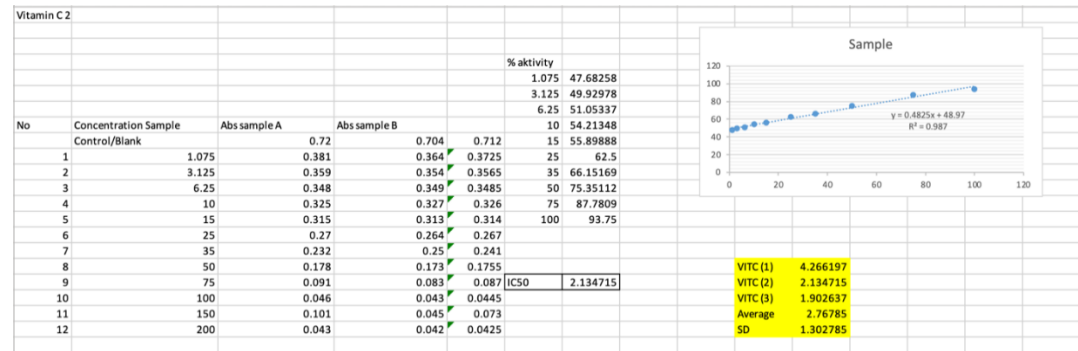
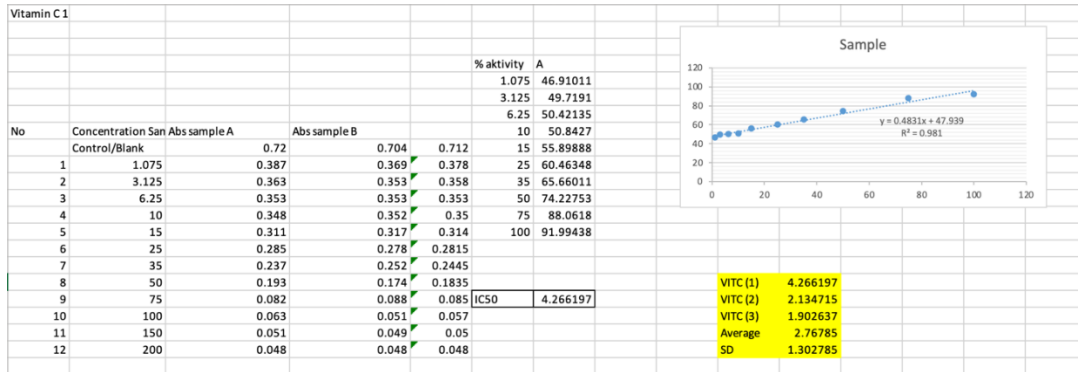
TRX(1) 4.475166
 TRX(2) 3.961089
 TRX(3) 7.042853
 Average 5.159703
 SD 1.650988

Trolox 2						
No	Concentration Sample	Abs sample A	Abs sample B	% activity	A	
	Control/Blank	0.725	0.717	0.721	10	51.17892
1	1.075	0.37	0.36	0.365	15	52.91262
2	3.125	0.357	0.347	0.352	25	55.75589
3	6.25	0.344	0.347	0.3455	35	63.17614
4	10	0.356	0.348	0.352	50	67.68377
5	15	0.337	0.342	0.3395	75	77.87795
6	25	0.332	0.306	0.319	100	87.0319
7	35	0.263	0.268	0.2655		
8	50	0.232	0.234	0.233		
9	75	0.16	0.159	0.1595	IC50	3.961089
10	100	0.095	0.092	0.0935		
11	150	0.181	0.204	0.1925		
12	200	0.042	0.041	0.0415		

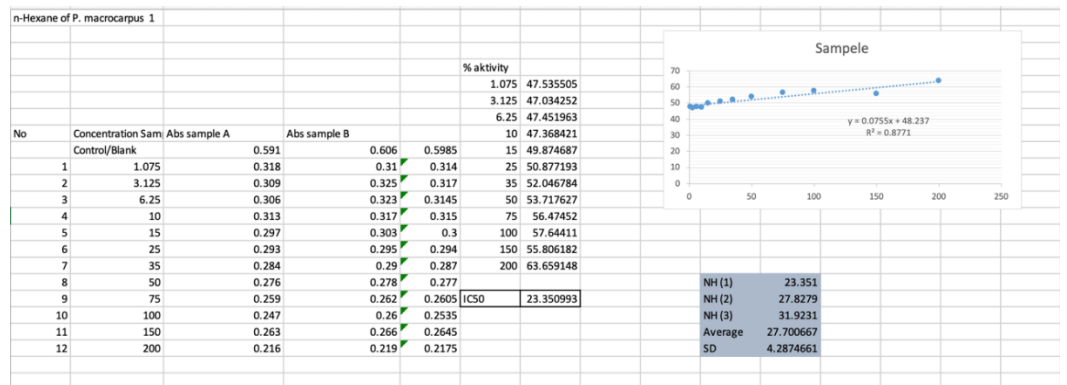


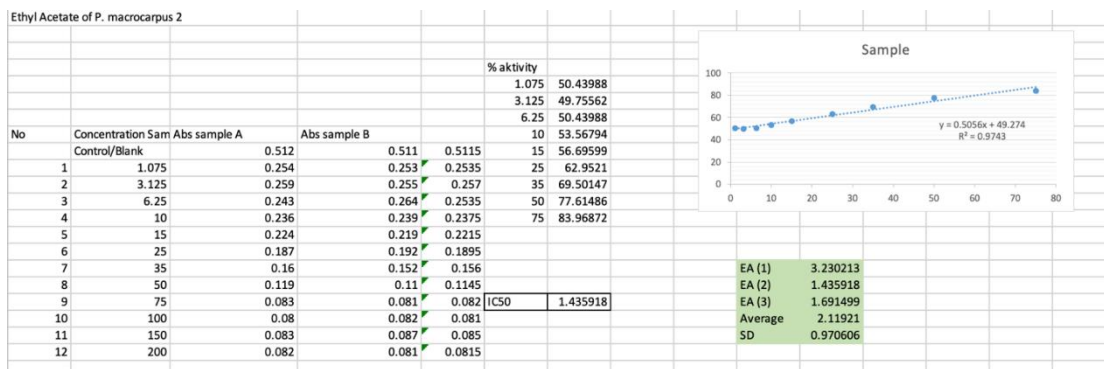
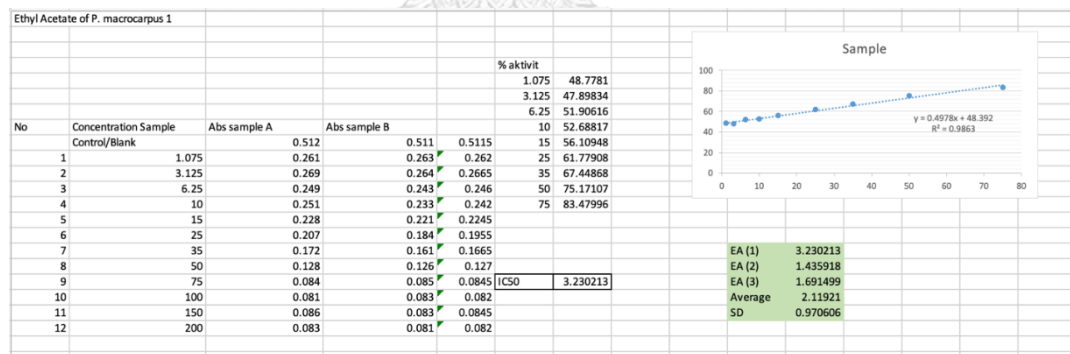
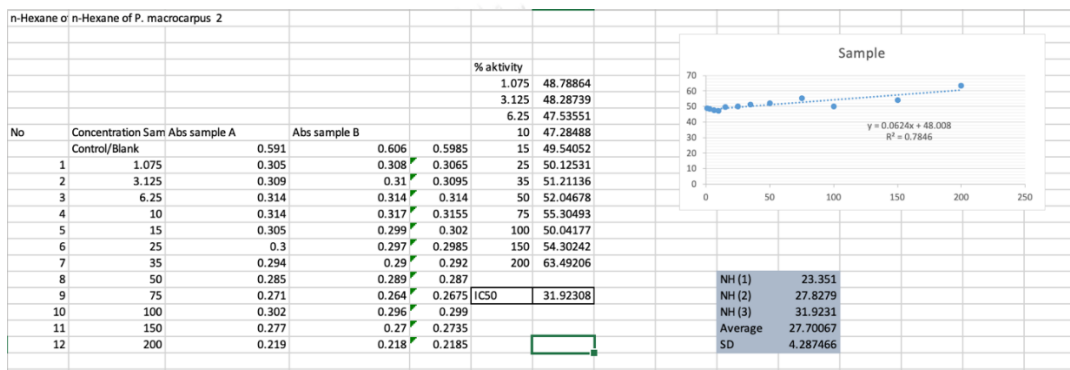
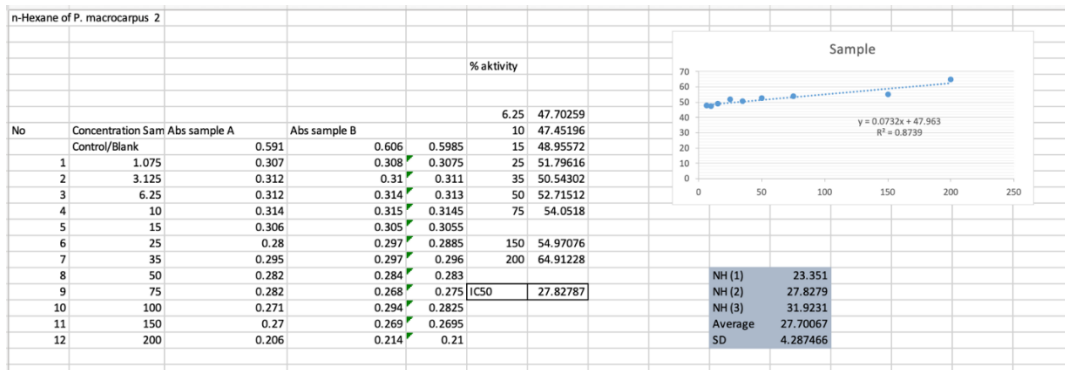
Trolox 2						
No	Concentration San	Abs sample A	Abs sample B	% activity	A	
	Control/Blank	0.725	0.717	0.721	10	50.34674
1	1.075	0.369	0.363	0.366	15	50.1387
2	3.125	0.351	0.36	0.3555	25	54.99307
3	6.25	0.346	0.469	0.4075	35	60.81831
4	10	0.361	0.355	0.358	50	66.78225
5	15	0.361	0.358	0.3595	75	76.90707
6	25	0.325	0.324	0.3245	100	84.32732
7	35	0.284	0.281	0.2825		
8	50	0.242	0.237	0.2395		
9	75	0.171	0.162	0.1665	IC50	7.042853
10	100	0.107	0.119	0.113		
11	150	0.211	0.218	0.2145		
12	200	0.043	0.044	0.0435		



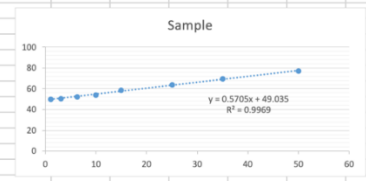


DPPH



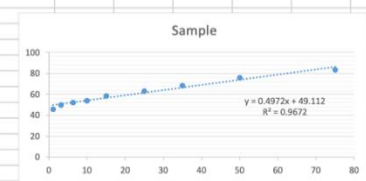


Ethyl Acetate of <i>P. macrocarpus</i> 3					
No	Concentration Sample	Abs sample A	Abs sample B	% activity	
	Control/Blank			1.075	49.65787
				3.125	50.53763
				6.25	52.29717
				10	54.15445
				15	58.45552
1	1.075	0.258	0.257	0.2575	25 63.83187
2	3.125	0.257	0.249	0.253	35 69.40371
3	6.25	0.242	0.246	0.244	50 76.9306
4	10	0.235	0.234	0.2345	
5	15	0.215	0.21	0.2125	
6	25	0.186	0.184	0.185	
7	35	0.161	0.152	0.1565	
8	50	0.122	0.114	0.118	
9	75	0.08	0.081	0.0805	IC50 1.691499
10	100	0.08	0.082	0.081	
11	150	0.081	0.082	0.0815	
12	200	0.082	0.083	0.0825	



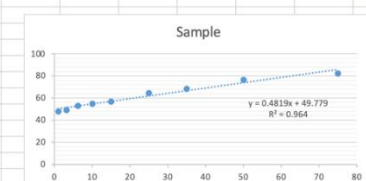
EA (1) 3.230213
 EA (2) 1.435918
 EA (3) 1.691499
 Average 2.11921
 SD 0.970606

Etahmol of <i>P. macrocarpus</i> 1					
No	Concentration Sample	Abs sample A	Abs sample B	% activity	
	Control/Blank			1.075	45.7478
				3.125	50.04888
				6.25	52.10166
				10	54.0567
				15	58.65103
1	1.075	0.286	0.269	0.2775	25 63.24536
2	3.125	0.256	0.255	0.2555	35 68.52395
3	6.25	0.245	0.245	0.245	50 76.05083
4	10	0.238	0.232	0.235	
5	15	0.217	0.206	0.2115	
6	25	0.19	0.186	0.188	
7	35	0.161	0.161	0.161	
8	50	0.124	0.121	0.1225	
9	75	0.087	0.085	0.086	IC50 1.786002
10	100	0.088	0.089	0.0885	
11	150	0.099	0.085	0.092	
12	200	0.088	0.089	0.0885	



ETA (1) 1.786002
 ETA (2) 0.458601
 ETA (3) 0.027891
 Average 0.757498
 SD 0.916375

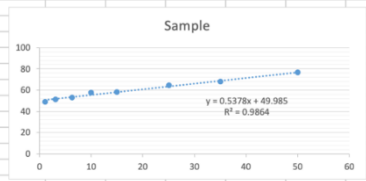
Etahmol of <i>P. macrocarpus</i> 2					
No	Concentration Sample	Abs sample A	Abs sample B	% activity	
	Control/Blank			1.075	47.99609
				3.125	49.16911
				6.25	53.079179
				10	54.83871
				15	56.989247
1	1.075	0.269	0.263	0.266	25 64.809384
2	3.125	0.261	0.259	0.26	35 68.328446
3	6.25	0.25	0.23	0.24	50 76.735093
4	10	0.232	0.23	0.231	
5	15	0.221	0.219	0.22	
6	25	0.179	0.181	0.18	
7	35	0.166	0.158	0.162	
8	50	0.125	0.113	0.119	
9	75	0.09	0.091	0.0905	IC50 0.4586014
10	100	0.086	0.091	0.0885	
11	150	0.089	0.085	0.087	
12	200	0.09	0.092	0.091	



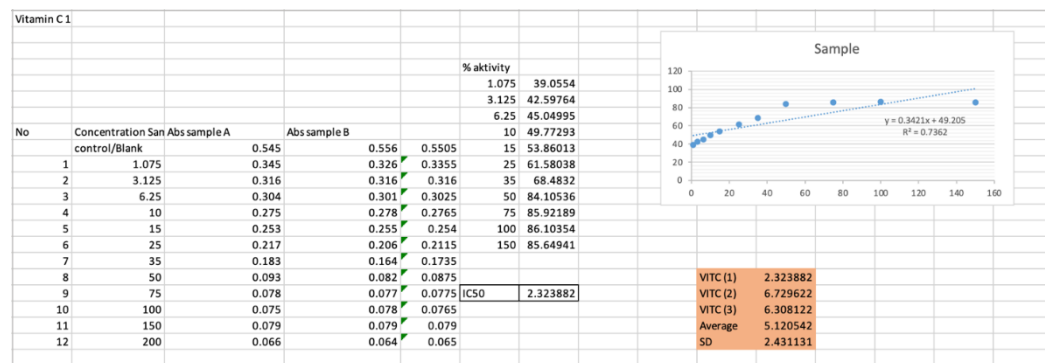
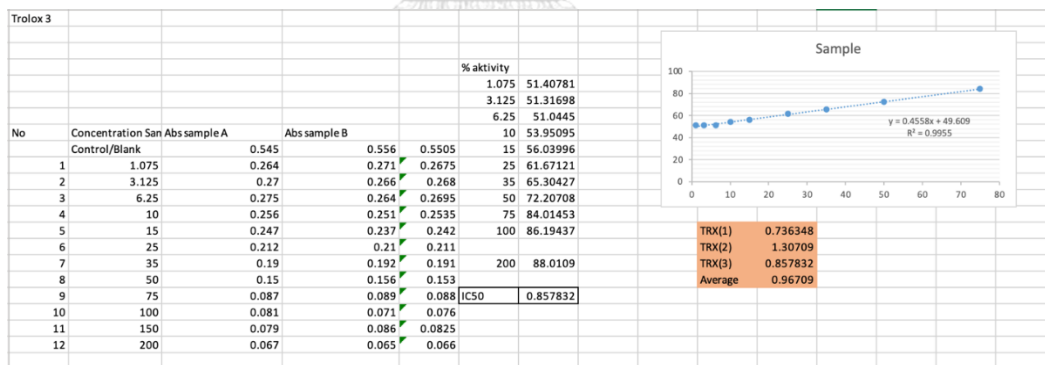
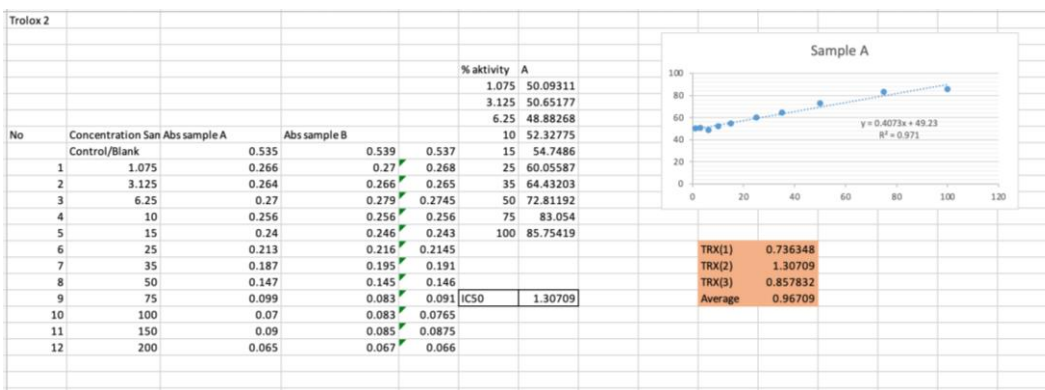
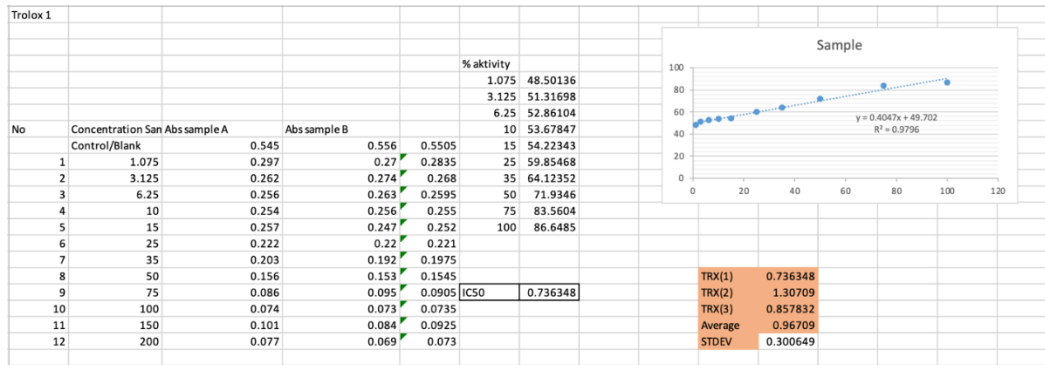
ETA (1) 1.7860016
 ETA (2) 0.4586014
 ETA (3) 0.0278914
 RATA2 0.7574981
 SD 0.9163746

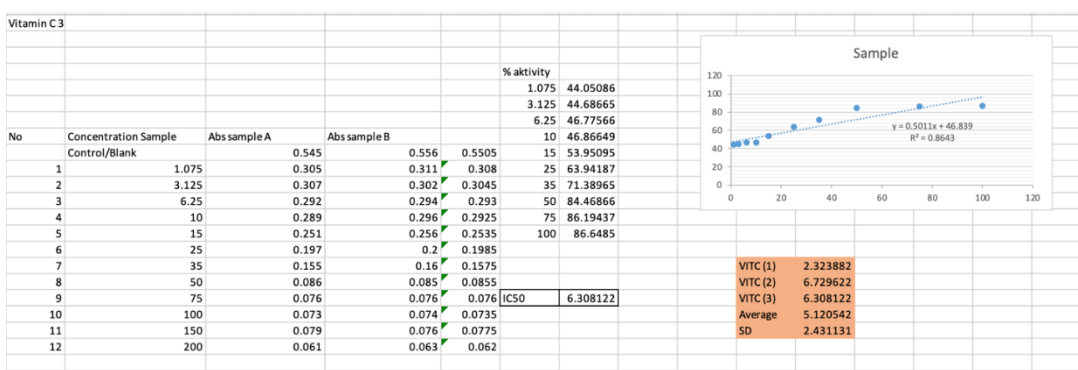
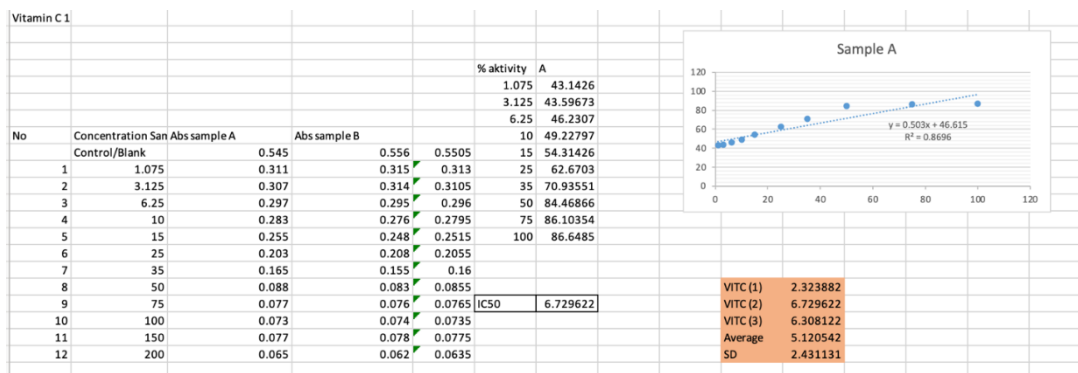
CHULALONGKORN UNIVERSITY

Etahmol of <i>P. macrocarpus</i> 3					
No	Concentration Sample	Abs sample A	Abs sample B	% activity	
	Control/Blank			1.075	49.26686
				3.125	51.2219
				6.25	52.88368
				10	57.47801
				15	58.35777
1	1.075	0.261	0.258	0.2595	25 64.32063
2	3.125	0.252	0.247	0.2495	35 67.93744
3	6.25	0.238	0.244	0.241	50 76.63734
4	10	0.229	0.206	0.2175	
5	15	0.215	0.211	0.213	
6	25	0.184	0.181	0.1825	
7	35	0.171	0.157	0.164	
8	50	0.116	0.123	0.1195	
9	75	0.095	0.086	0.0905	IC50 0.027891
10	100	0.083	0.089	0.086	
11	150	0.089	0.086	0.0875	
12	200	0.089	0.094	0.0915	



ETA (1) 1.786002
 ETA (2) 0.458601
 ETA (3) 0.027891
 RATA2 0.757498
 SD 0.916375

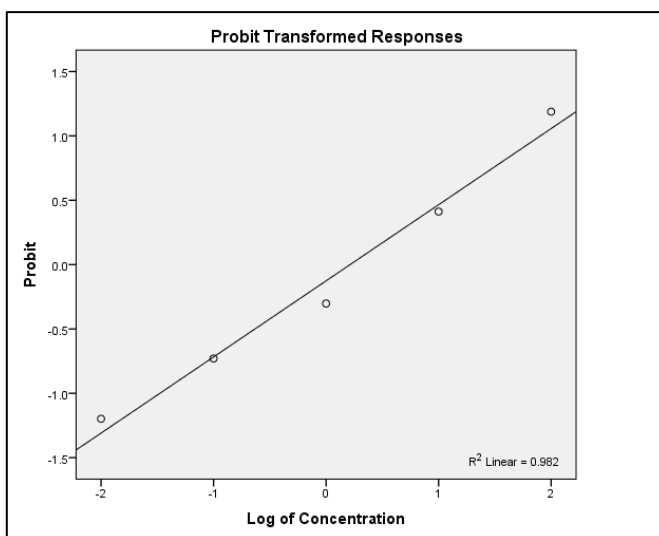




2.7. Supplementary data VII: *In vitro* antiplasmodial activity of homopterocarpin and *Pterocarpus macrocarpus* Kurz. extract

1) Ethyl acetate

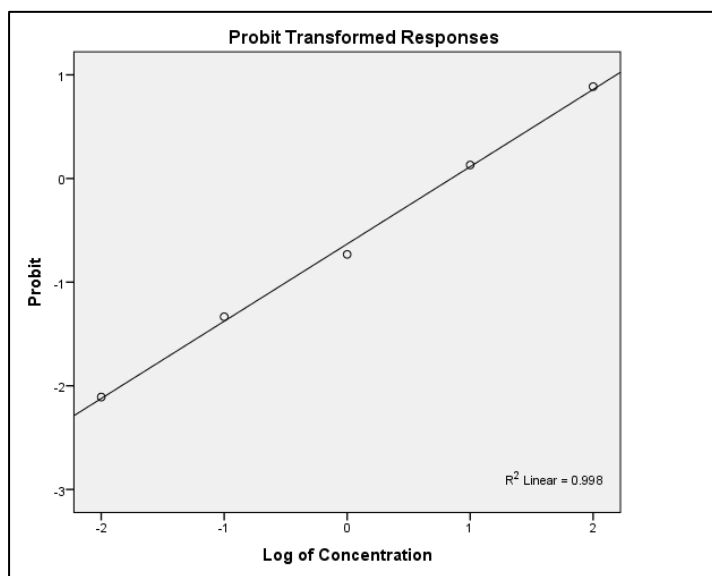
Concentration (µg/ml)	R	% Parasitemia		% Growth	% Inhibition	% Average of Inhibition
		0 h	48 h			
Negative control	1	0.78	8.18	7.40	-	-
	2	0.78	8.20	7.42	-	
100	1	0.78	1.64	0.86	88.38	88.26
	2	0.78	1.66	0.88	88.14	
10	1	0.78	3.29	2.51	66.08	65.99
	2	0.78	3.31	2.53	65.90	
1	1	0.78	5.38	4.60	37.84	38.12
	2	0.78	5.35	4.57	38.41	
0.1	1	0.78	6.43	5.65	23.65	23.28
	2	0.78	6.50	5.72	22.91	
0.01	1	0.78	7.31	6.53	11.76	11.54
	2	0.78	7.36	6.58	11.32	



$IC_{50} = 1.78 \mu\text{g/ml}$

2) N-hexane

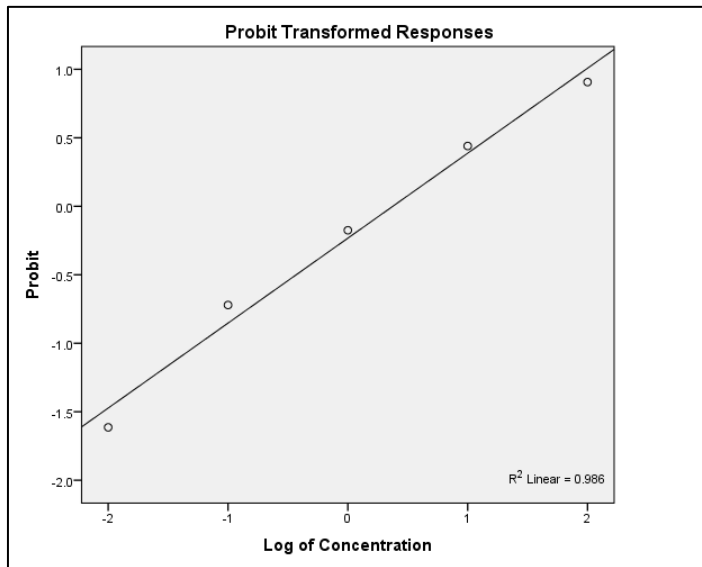
Concentration ($\mu\text{g/ml}$)	R	% Parasitemia		% Growth	% Inhibition	% Average of Inhibition
		0 h	48 h			
Negative control	1	0.78	8.18	7.40	-	-
	2	0.78	8.20	7.42	-	
100	1	0.78	2.19	1.41	80.95	81.24
	2	0.78	2.15	1.37	81.54	
10	1	0.78	4.12	3.34	54.86	55.20
	2	0.78	4.08	3.30	55.53	
1	1	0.78	6.46	5.68	23.24	23.21
	2	0.78	6.48	5.70	23.18	
0.1	1	0.78	7.53	6.75	8.78	9.11
	2	0.78	7.50	6.72	9.43	
0.01	1	0.78	8.05	7.27	1.76	1.75
	2	0.78	8.07	7.29	1.75	



$$IC_{50} = 7.11 \mu\text{g/ml}$$

3) Ethanol extract

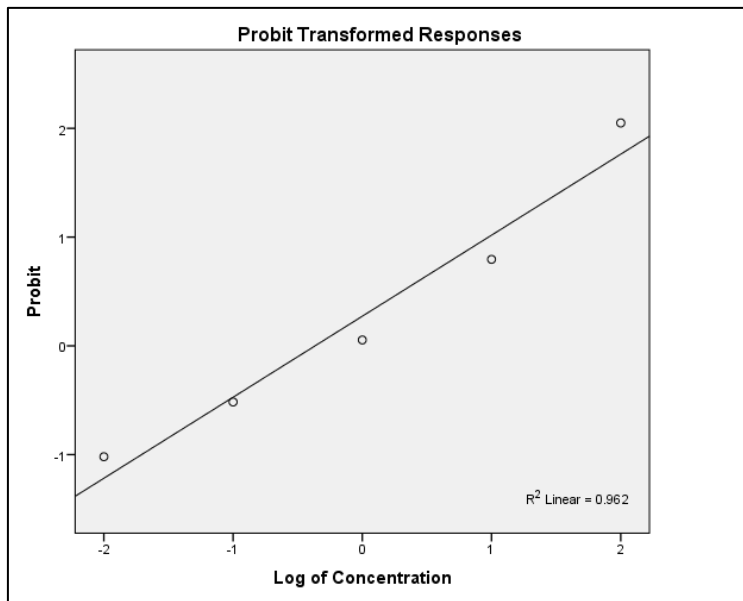
Concentration ($\mu\text{g/ml}$)	R	% Parasitemia		% Growth	% Inhibition	% Average of Inhibition
		0 h	48 h			
Negative control	1	0.78	8.18	7.40	-	-
	2	0.78	8.20	7.42	-	
100	1	0.78	2.11	1.33	82.03	81.78
	2	0.78	2.15	1.37	81.54	
10	1	0.78	3.22	2.44	67.03	67.00
	2	0.78	3.23	2.45	66.98	
1	1	0.78	4.95	4.17	43.65	43.05
	2	0.78	5.05	4.27	42.45	
0.1	1	0.78	6.43	5.65	23.65	23.55
	2	0.78	6.46	5.68	23.45	
0.01	1	0.78	7.78	7.00	5.41	5.33
	2	0.78	7.81	7.03	5.26	



$$IC_{50} = 2.21 \mu\text{g/ml}$$

4) Homopterotharpin

Concentration ($\mu\text{g/ml}$)	R	% Parasitemia		% Growth	% Inhibition	Average of Inhibition
		0 h	48 h			
Negative control	1	0.78	8.18	7.40	-	-
	2	0.78	8.20	7.42	-	
100	1	0.78	0.87	0.09	98.78	97.98
	2	0.78	0.99	0.21	97.17	
10	1	0.78	2.35	1.57	78.78	78.68
	2	0.78	2.37	1.59	78.57	
1	1	0.78	4.31	3.53	52.30	52.16
	2	0.78	4.34	3.56	52.02	
0.1	1	0.78	5.93	5.15	30.41	30.30
	2	0.78	5.96	5.18	30.19	
0.01	1	0.78	7.00	6.22	15.95	15.39
	2	0.78	7.10	6.32	14.82	



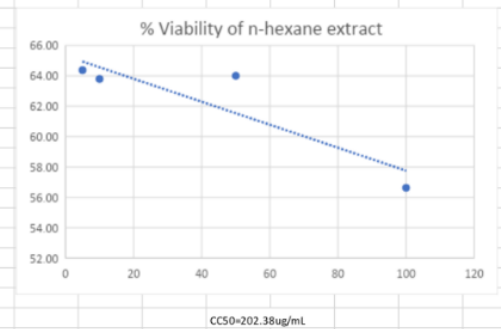
IC₅₀ = 0.52 µg/ml

2.8 Supplementary data VIII

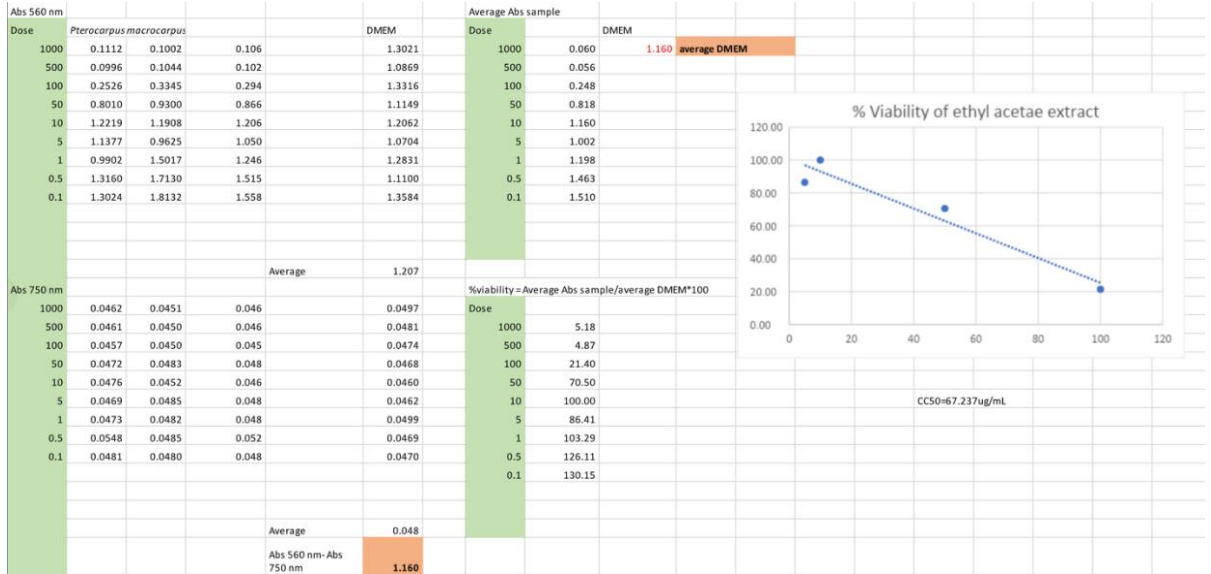
Cytotoxicity of homopteroicarpin and *Pterocarpus macrocarpus* Kurz. extract

N-hexane

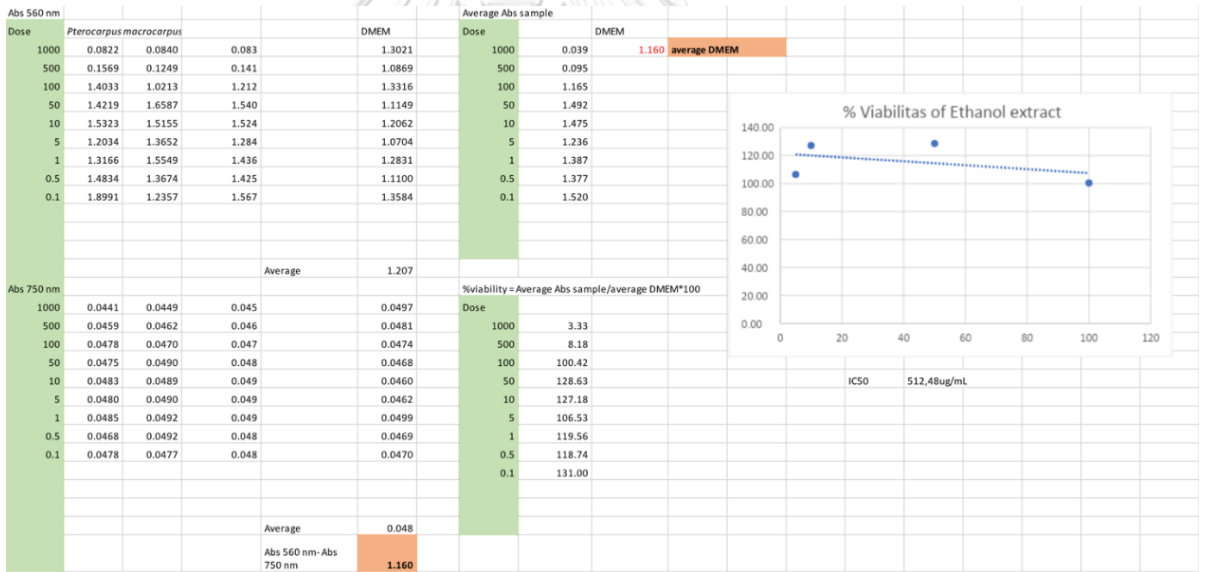
Abs 560 nm				Average Abs sample			
Dose	Pterocarpus macrocarpus			DMEM	Dose	DMEM	average DMEM
1000	0.0933	0.0870	0.090	1.3021	1000	0.045	1.207
500	0.0912	0.0889	0.090	1.0869	500	0.067	
100	0.6635	0.4748	0.569	1.3316	100	0.684	
50	0.6814	0.7630	0.722	1.1149	50	0.773	
10	1.0785	1.1842	1.131	1.2062	10	0.770	
5	1.3897	1.6483	1.519	1.0704	5	0.777	
1	1.3155	1.4077	1.362	1.2831	1	0.780	
0.5	1.2986	1.3736	1.336	1.1100	0.5	0.772	
0.1	1.4509	1.3367	1.394	1.3584	0.1	0.7775	
			Average	1.207			
Abs 750 nm				%viability = Average Abs sample/average DMEM*100			
1000	0.0451	0.0446	0.045	0.198	Dose	1000	3.75
500	0.0488	0.0462	0.048	0.203	500	5.55	
100	0.0516	0.0464	0.049	0.203	100	56.63	
50	0.0473	0.0474	0.047	0.206	50	64.00	
10	0.0469	0.0476	0.047	0.209	10	63.79	
5	0.0470	0.0479	0.047	0.204	5	64.37	
1	0.0471	0.0480	0.048	0.203	1	64.62	
0.5	0.0469	0.0488	0.048	0.209	0.5	63.96	
0.1	0.0486	0.0484	0.049	0.208	0.1	64.42	
			Average	0.205			
			Abs 560 nm- Abs 750 nm	1.002			



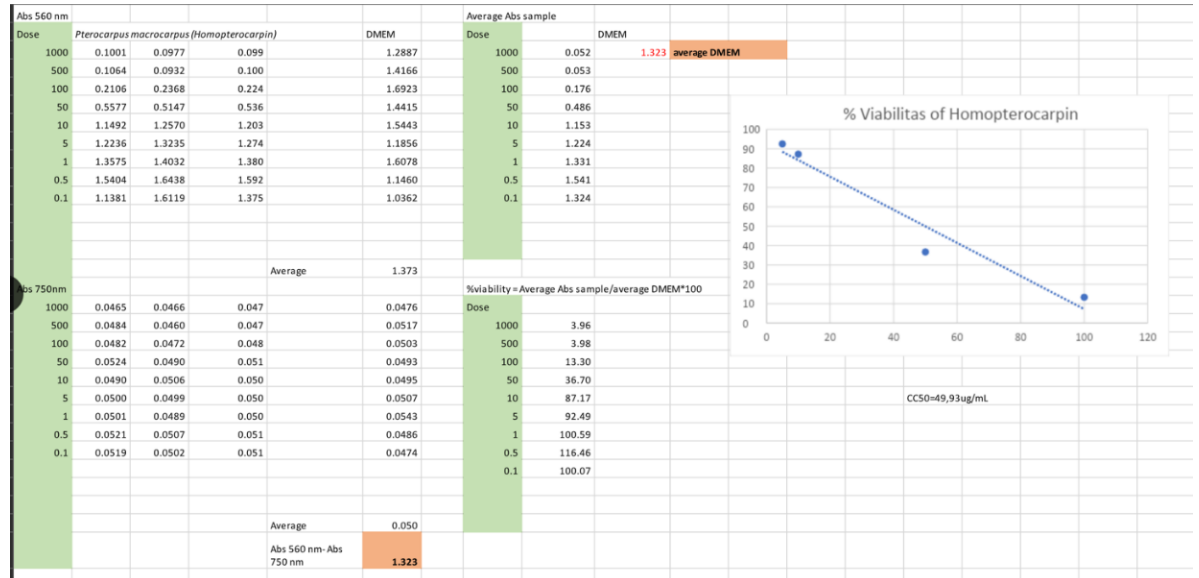
Ethyl acetate



Ethanol



Homopterotharpin



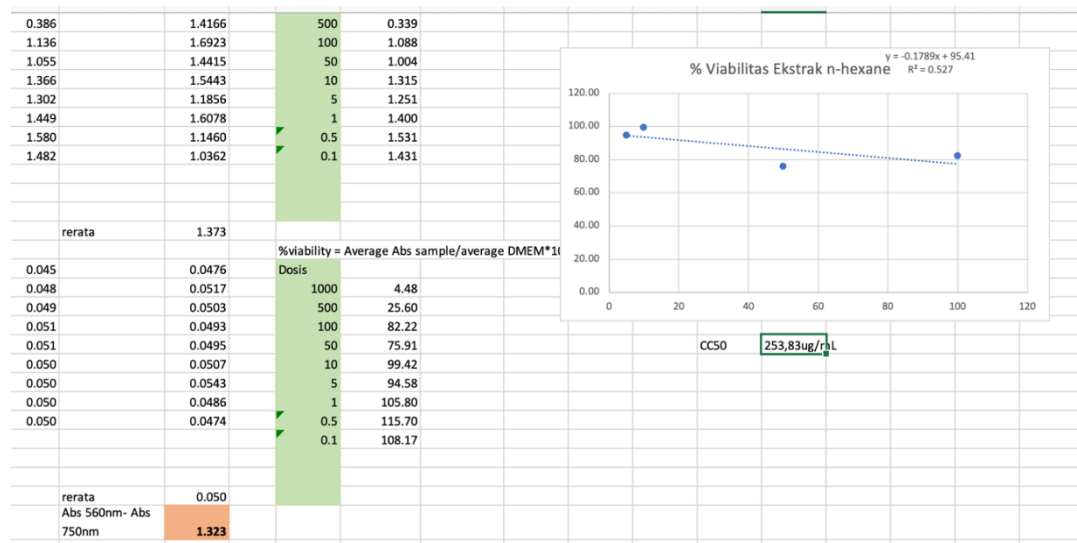
3. APPENDIX 3

3.1 Supplementary data I

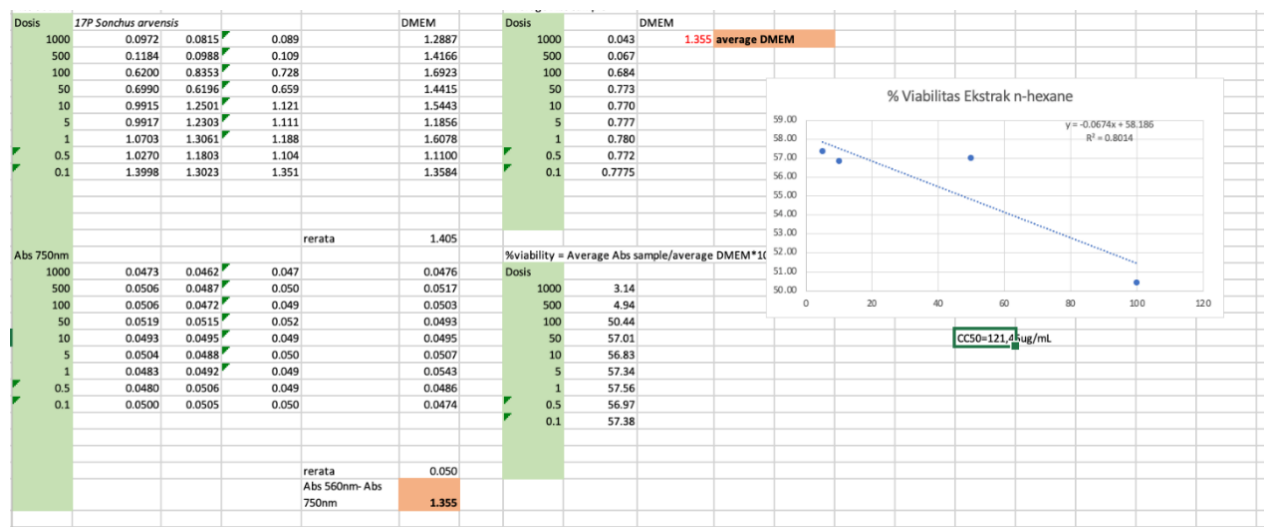
GC-MS chromatogram profil of fraction number 5-12 of *Sonchus arvensis* L. n=hexane extract (available in author)

3.2 Supplementary data III: Fraction of *Sonchus arvensis* L. n-hexane extract cytotoxicity

Fraction number 5-12



Fraction number 17-28



4 APPENDIX 4

4.1 Supplementary data I

GC-MS chromatogram profile of homopterocarpin biotransformation-culture extract (available in author)

4.2 Supplementary data III

GC-MS chromatogram profile of compound 2

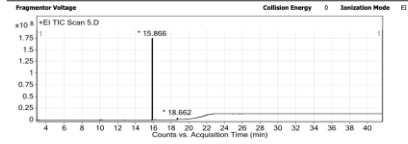
Qualitative Analysis Report

Data Filename: 5.D **Sample Name:** 5
Sample Type: 13 **Position:** STREC.CJ
Instrument Name: IGC-QQQ **User Name:** STREC.CJ
Acq Method: 20220215_Low spectra analysis_Kutuma.m **Acquired Time:** 22/2/2022 9:56:27
IHM Calibration Status: Not Applicable **DA Method:** default.m
Comment:

Expected Barcode: **Sample Amount:**
Dual Inj Vol: 0.5 **TuneName:** 205C_atunes.dlex.tune.xml
TunePath: D:\MassHunter\GCMS1\1\000 **TuneDataStamp:** 17/2/2022 13:23:38
MSFWareVersion: DSP: 7600.3200, qqqServer: G.7000.051-RLN **Acquisition Time #2:** 2022-02-22 02:56:27Z
OperatorName: STREC.CJ **RunCompletedFlag:** TRUE

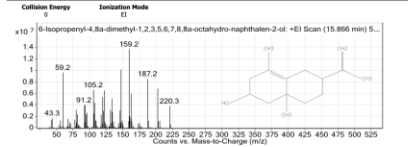
Acquisition SW Version: MassHunter GC/MS Acquisition 8.07.02.1938 08-Sep-2014 Copyright © 1989-2014 Agilent Technologies, Inc.

User Chromatograms



Peak	Start	RT	End	Height	Area	Area %
1	15.821	15.866	15.947	17509791.7	272103413.4	100
2	18.642	18.662	18.722	1246911.24	2044509.26	0.75
3	18.62	18.662	18.704	4024048.12	958724.76	3.51

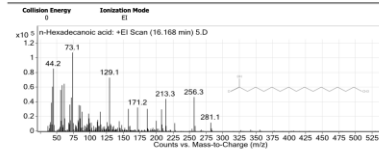
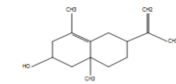
User Spectra



Qualitative Analysis Report

m/z	I	Abund
59.2	1	9652013
105.2	1	6618252.5
119.2	1	649354.5
121.2	1	6604203.5
133.2	1	3184300
147.2	1	10201548
159.2	1	11719467
162.2	1	1599336
187.2	1	8039306
200.2	1	1683717

Spectrum Structure
6-Isopropenyl-4,8a-dimethyl-1,2,3,5,6,7,8,8a-octahydro-naphthalen-2-ol

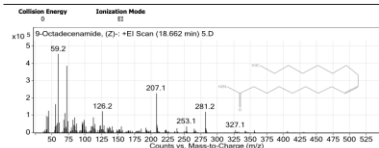


m/z	I	Abund
44.2	1	61344.08
44.2	1	85481.98
55.2	1	146345.79
57.2	1	63392.72
60.2	1	64905.19
72.2	1	46283.33
73.1	1	127590.08
129.1	1	77987.33
213.3	1	44287.61
256.3	1	65785.15

Spectrum Structure
n-Hexadecanoic acid

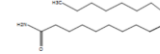
--- End of Report ---

Qualitative Analysis Report



m/z	I	Abund
41.3	1	89465.34
43.2	1	81772.52
44.2	1	127694.98
55.2	1	167589.88
59.2	1	456918.41
69.2	1	113359.72
72.2	1	387670.28
126.2	1	124681.23
207.1	1	520308.59
281.2	1	122508.08

Spectrum Structure
9-Octadecanamide, (Z)-



--- End of Report ---

4.3 Supplementary data IV

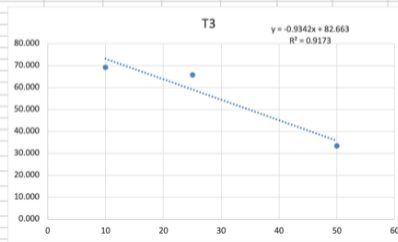
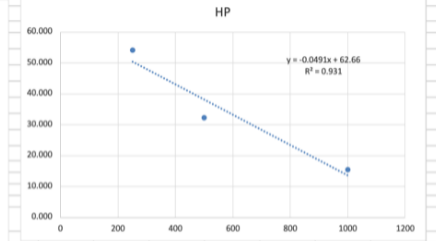
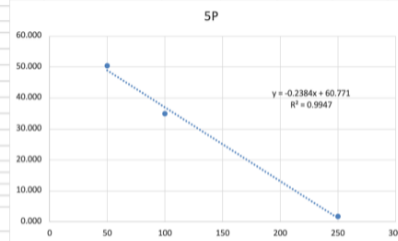
Anticancer activity of biotransformation derived compound

Sample: T3, 5P, HP									
Abs 560nm									
Sampel	1000	500	250	100	50	25	10	5	DMEM
5P	0.092	0.081	0.081	0.545	0.746	1.380	0.954	0.913	2.098
	0.087	0.079	0.080	0.753	1.576	3.154	2.070	1.189	2.347
	0.085	0.080	0.092	1.139	1.116	1.667	1.565	1.158	1.800
HP	0.395	0.453	1.478	1.813	2.062	2.848	2.277	1.628	1.646
	0.356	0.818	1.105	1.493	2.157	2.122	2.212	1.794	2.616
	0.411	0.988	1.108	1.094	1.967	2.678	1.595	1.300	2.972
T3	0.281	0.346	0.371	0.440	0.731	1.621	1.849	1.309	1.999
	0.282	0.288	0.334	0.380	0.786	1.375	1.24	0.95	2.40
	0.255	0.391	0.371	0.549	0.819	1.462	1.59	1.43	
Abs 750nm									
Conc (ug/ml)	1000	500	250	100	50	25	10	5	DMEM
5P	0.0521	0.0457	0.0471	0.0546	0.0449	0.0484	0.0455	0.0445	0.0535
	0.0501	0.0462	0.0458	0.0479	0.0492	0.0544	0.0518	0.0557	0.0576
	0.0489	0.0449	0.0513	0.0495	0.0499	0.0505	0.0498	0.0521	0.0557
HP	0.0524	0.0457	0.0484	0.0524	0.0693	0.0586	0.0521	0.0554	0.0542
	0.0479	0.0478	0.0468	0.0506	0.057	0.0636	0.0542	0.0496	0.0576
	0.0479	0.0517	0.0474	0.0484	0.0538	0.0641	0.0502	0.049	0.0668
T3	0.0491	0.0463	0.0507	0.0454	0.0464	0.0534	0.0509	0.0474	0.0531
	0.047	0.050	0.046	0.047	0.049	0.050	0.047	0.048	0.053
	0.046	0.047	0.052	0.047	0.048	0.053	0.050	0.057	
Abs sample = (Abs 560nm - background) - (Abs 750nm - background)									
Conc (ug/ml)	1000	500	250	100	50	25	10	5	DMEM
5P	0.040	0.035	0.034	0.490	0.701	1.332	0.909	0.868	2.045
	0.037	0.033	0.034	0.705	1.527	3.100	2.018	1.134	2.289
	0.036	0.035	0.041	1.089	1.066	1.617	1.515	1.106	1.745
HP	0.342	0.408	1.429	1.761	1.993	2.790	2.225	1.572	1.591
	0.308	0.770	1.058	1.442	2.100	2.058	2.158	1.744	2.558
	0.363	0.936	1.061	1.046	1.913	2.614	1.544	1.251	2.905
T3	0.232	0.300	0.320	0.395	0.685	1.568	1.798	1.261	1.946
	0.236	0.238	0.288	0.333	0.737	1.326	1.192	0.905	2.343
	0.209	0.343	0.319	0.502	0.771	1.408	1.541	1.369	0.000
%Viability = Abs sample/average abs dmem*100									
Conc (ug/ml)	1000	500	250	100	50	25	10	5	
5P	1.8	1.6	1.6	22.5	32.1	61.1	41.7	39.8	
	1.7	1.5	1.6	32.3	70.0	142.2	92.6	52.0	
	1.7	1.6	1.9	50.0	48.9	74.2	69.5	50.7	
HP	15.7	18.7	65.6	80.8	91.4	128.0	102.1	72.1	
	14.1	35.3	48.5	66.1	96.3	94.4	99.0	80.0	
	16.7	42.9	48.6	48.0	87.8	119.9	70.8	57.4	
T3	10.6	13.7	14.7	18.1	31.4	71.9	82.5	57.9	
	10.8	10.9	13.2	15.3	33.8	60.8	54.7	41.5	
	9.6	15.8	14.6	23.0	35.3	64.6	70.7	62.8	

Conc (µg/ml)	%viability	%viability	%viability	%viability	%viability	%viability	%viability	%viability	%viability
1000	1.817	1.574	1.565	15.697	14.128	16.665	20.619	10.817	9.573
500	1.619	1.500	1.592	18.697	35.335	42.040	13.748	10.913	15.752
250	1.569	1.578	1.881	65.589	48.523	48.647	14.670	13.206	14.647
100	22.477	32.335	49.954	80.761	66.147	47.968	18.096	15.294	23.023
50	32.147	70.028	48.904	91.404	96.326	87.757	31.399	23.826	35.344
25	61.101	142.179	74.156	127.972	94.413	119.899	71.927	60.821	64.006
10	41.688	92.564	69.486	102.064	99.000	70.844	82.463	54.679	70.674
5	39.821	52.000	50.711	72.128	80.005	57.381	57.862	41.514	62.775

Conc (µg/ml)	SP		HP		T3	
	%viability	SD	%viability	SD	%viability	SD
1000	1.719	0.085	15.497	1.280	10.336	0.668
500	1.570	0.062	32.324	12.399	13.471	2.432
250	1.676	0.178	54.246	9.806	14.174	0.838
100	34.922	13.920	64.959	16.429	18.804	3.913
50	50.359	18.982	91.829	4.300	33.523	1.990
25	92.479	43.534	114.095	17.517	65.784	5.646
10	67.913	25.475	90.636	17.209	69.272	13.945
5	47.511	6.691	69.838	11.485	54.050	11.132
IC50	45.18		257.84		34.96	

RESUME		
SAMPLE NAME	CC50 (µg/mL)	IC50 carcinoma (µg/mL)
SP	45.18	45.18
HP	257.84	257.84
T3	34.96	34.96



REFERENCES



จุฬาลงกรณ์มหาวิทยาลัย
CHULALONGKORN UNIVERSITY

- Abdelhamid, R., & Maa, O. (2019). Phytochemical Constituents of Plant Species of Pterocarpus (F: Leguminosae): A Review. *International Journal of Pharmacognosy and Phytochemical Research*, 11, 264-281. <https://doi.org/10.25258/phyto.11.4.5>
- Anwar, Y., Putra, A. M. J., Iftitah, E. D., Simanjuntak, P., & Kumala, S. (2019). Prediction of Geraniol Bond Mode in Aspergillus niger Linalool Dehydratase – Isomerase. *Majalah Obat Tradisional; Vol 24, No 2 (2019)*. <https://doi.org/10.22146/mot.45599>
- Asakawa, Y., Sekita, M., & Hashimoto, T. (2018). Biotransformation of Bicyclic Sesqui- and Diterpene 1,2-dials and Their Derivatives by the Fungus, Aspergillus niger. *Natural Product Communications*, 13(8), 1934578X1801300802. <https://doi.org/10.1177/1934578X1801300802>
- Chen, H., Kang, X., You, L., Wang, C., & Ye, J. (2017). Chemical Component and Antibacterial Activity of Essential Oil from Myanmar Pterocarpus macrocarpus. *Chemistry and Industry of Forest Products*, 37, 65-72. <https://doi.org/10.3969/j.issn.0253-2417.2017.06.009>
- Delyan, E. (2016). Analisis of component composition of volatile compounds of field sow thistle (Sonchus Arvensis L.) leaves using the method of gas chromatography with mass-detection. *The Pharma Innovation Journal*, 5, 118-121.
- Gao, W., Wang, Y., Basavanagoud, B., & Jamil, M. K. (2017). Characteristics studies of molecular structures in drugs. *Saudi Pharm J*, 25(4), 580-586. <https://doi.org/10.1016/j.jsps.2017.04.027>
- Hegazy, M.-E. F., Mohamed, T. A., ElShamy, A. I., Mohamed, A.-E.-H. H., Mahalel, U. A., Reda, E. H., Shaheen, A. M., Tawfik, W. A., Shahat, A. A., Shams, K. A., Abdel-Azim, N. S., & Hammouda, F. M. (2015). Microbial biotransformation as a tool for drug development based on natural products from mevalonic acid pathway: A review. *Journal of Advanced Research*, 6(1), 17-33. <https://doi.org/https://doi.org/10.1016/j.jare.2014.11.009>

- Hendriani, R., Sukandar, E., Anggadiredja, K., & Sukrasno, S. (2016). In Vitro evaluation of xanthine oxidase inhibitory activity of selected medicinal plants. *8*, 235-238.
- Jiao, L. (2018). DNA Barcode Authentication and Library Development for the Wood of Six Commercial Pterocarpus Species: The Critical Role of Xylarium Specimens. *Scientific Reports*, *8*. <https://doi.org/10.1038/s41598-018-20381-6>
- K.C.A, J., John, A., Sheikh, H., S, S., & Y.A.A, N. (2017). Study On Physicochemical Parameters And Distribution Of Phytoplankton In Kuantan Estuary, Pahang. *Environment & Ecosystem Science (EES)*, *1*, 8-12. <https://doi.org/10.26480/ees.01.2017.08.12>
- Kang, X., Csetenyi, L., & Gadd, G. M. (2019). Biotransformation of lanthanum by *Aspergillus niger*. *Appl Microbiol Biotechnol*, *103*(2), 981-993. <https://doi.org/10.1007/s00253-018-9489-0>
- Khan, M. R., & Omoloso, A. D. (2003). Antibacterial activity of *Pterocarpus indicus*. *Fitoterapia*, *74*(6), 603-605. [https://doi.org/10.1016/s0367-326x\(03\)00149-7](https://doi.org/10.1016/s0367-326x(03)00149-7)
- Kumar, A., Singh Pk Fau - Parihar, R., Parihar R Fau - Dwivedi, V., Dwivedi V Fau - Lakhota, S. C., Lakhota Sc Fau - Ganesh, S., & Ganesh, S. Decreased O-linked GlcNAcylation protects from cytotoxicity mediated by huntingtin exon1 protein fragment. (1083-351X (Electronic)).
- Mohd Ataa, N., Hazmi, I. R., & Samsudin, S. (2017). Insect's Visitation on *Melastoma malabathricum* in UKM Bangi Forest Reserve. *Environment & Ecosystem science*, *1*, 20-22. <https://doi.org/10.26480/ees.01.2017.20.22>
- Morimoto, M., Fukumoto H Fau - Hiratani, M., Hiratani M Fau - Chavasiri, W., Chavasiri W Fau - Komai, K., & Komai, K. Insect antifeedants, pterocarpan and pterocarpol, in heartwood of *Pterocarpus macrocarpus* Kruz. (0916-8451 (Print)).
- Parshikov, I. A., & Sutherland, J. B. (2014). The use of *Aspergillus niger* cultures for biotransformation of terpenoids. *Process Biochemistry*, *49*(12), 2086-2100. <https://doi.org/https://doi.org/10.1016/j.procbio.2014.09.005>
- Poudel, B., Sah, J., Subedi, S., Amatya, M., Shrestha, T., Bhupendra, C., Poudel, K., & Amatya, S. (2015). Pharmacological studies of methanolic extracts of *Sonchus*

- arvensis from Kathmandu. *Journal of Pharmacognosy and Phytochemistry*, 4, 272-276. <https://doi.org/10.5897/JPP2015.0359>
- Putra, B., Kusriani, D., & Fachriyah, E. (2013). Isolasi Senyawa Antioksidan dari Fraksi Etil Asetat Daun Tempuyung (*Sonchus arvensis* L.). *Jurnal Kimia Sains dan Aplikasi*, 16, 69. <https://doi.org/10.14710/jksa.16.3.69-72>
- Rohaeti, E., Heryanto, R., Rafi, M., Wahyuningrum, A., & Darusman, L. (2011). Prediksi kadar flavonoid total tempuyung (*Sonchus arvensis* L.) menggunakan kombinasi spektroskopi IR dengan regresi kuadrat terkecil parsial. *Jurnal Kimia*, 5, 101-108.
- Rumondang, M. (2013). Isolasi, Identifikasi Dan Uji Antibakteri Senyawa Triterpenoid Dari Ekstrak n-Heksana Daun Tempuyung (*Sonchus arvensis* L.).
- Seal, T. (2016). Quantitative HPLC analysis of phenolic acids, flavonoids and ascorbic acid in four different solvent extracts of two wild edible leaves, *Sonchus arvensis* and *Oenanthe linearis* of North-Eastern region in India. *Journal of Applied Pharmaceutical Science*, 6, 157-166. <https://doi.org/10.7324/JAPS.2016.60225>
- Singh, R. (2017). Microbial Biotransformation: A Process for Chemical Alterations. *Journal of Bacteriology & Mycology: Open Access*, 4. <https://doi.org/10.15406/jbmoa.2017.04.00085>
- Suharyanto, E., Rahayu, S., Purnama, P., Bagus Saputro, T., Wijayanti, N., Purnobasuki, H., & Wahyuni, D. (2019). Morpho-anatomical structure and DNA barcode of *Sonchus arvensis* L. *Biodiversitas Journal of Biological Diversity*, 20, 2417-2426. <https://doi.org/10.13057/biodiv/d200841>
- Sukandar, E., & Safitri, D. (2016). Evaluation of teratogenic effect of tempuyung (*Sonchus arvensis*) extract on wistar rats. 8, 761-766.
- Wu, C., Zacchetti, B., Ram, A., Wezel, G., Claessen, D., & Choi, Y. (2015). Expanding the chemical space for natural products by *Aspergillus-Streptomyces* co-cultivation and biotransformation. *Scientific Reports*, 5. <https://doi.org/10.1038/srep10868>
- Xia, Z., Qu, W., Lu, H., Fu, J., Ren, Y., & Liang, J. (2009). Sesquiterpene lactones from *Sonchus arvensis* L. and their antibacterial activity against *Streptococcus*

mutans ATCC 25175. *Fitoterapia*, 81, 424-428.
<https://doi.org/10.1016/j.fitote.2009.12.001>

Yang, S., Wu, Y., Yang, J., Yan, R., Bao, Y., Wang, K., Liu, G., & Wang, W. (2017). Isolation and identification of an extracellular enzyme from *Aspergillus Niger* with Deoxynivalenol biotransformation capability. *Emirates Journal of Food and Agriculture*, 29, 742. <https://doi.org/10.9755/ejfa.2017.v29.i10.1295>

Younis, A., Ibrahim, A. R., Ibrahim, S., Aboelsauod, K., & Kabbash, A. (2016). Microbial Transformation of Curcumin and Evaluation of the Biological Activities of the Isolated Metabolites. 8.



VITA

NAME Dwi Kusuma Wahyuni

DATE OF BIRTH 15 January 1977

PLACE OF BIRTH Jombang

INSTITUTIONS ATTENDED Faculty of Biology, Gadjah Mada University (Bachelor and Master)

HOME ADDRESS Diana Court, 9 Phetchaburi 6 Road, Thanon Phetchaburi, Ratchathewi, Bangkok 10400

PUBLICATION Ilham, M., Mukarromah, S.R., Rakashiwi, G.A., Indriati, D.T., Yoku, B.F., Purnama, P.R., Junairiah, Prasongsuk, S., Purnobasuki, H., Wahyuni, D.K. (2022) Morpho-anatomical characterization and DNA barcoding of *Achillea millefolium* L.. *Journal of Biological Diversity* 23(4).

Wahyuni, D.K., Rahayu, S., Zaidan, A.H., Ekasari, W., Prasongsuk, S. and Purnobasuki, H., 2021. Growth, secondary metabolite production, and in vitro antiplasmodial activity of *Sonchus arvensis* L. callus under dolomite [CaMg (CO₃)₂] treatment. *Plos one*, 16(8), p.e0254804.

Wahyuni, D.K., Huda, A., Faizah, S., Purnobasuki, H. and Wardojo, B.P.E., 2020. Effects of light, sucrose concentration and repetitive subculture on callus growth and medically important production in *Justicia gendarussa* Burm. f. *Biotechnology Reports*, 27, p.e00473.

Wahyuni, D.K., Rahayu, S., Purnama, P.R., Saputro, T.B., Wijayanti, N. and Purnobasuki, H., 2019. Morpho-anatomical structure and DNA barcode of *Sonchus arvensis* L. *Biodiversitas Journal of Biogical Diversity*, 20(8),

Wahyunu, D.K., Ansori, A.N.M. and Vidiyanti, F., 2017. GC-MS analysis of phytocomponents in methanolic extracts of leaf-derived callus of *Justicia gendarussa* Burm. f. *Bioscience*

Research, 14(3), pp.668-677.

Wahyuni, D.K., Purnobasuki, H., Kuncoro, E.P. and Ekasari, W., 2020. Callus induction of *Sonchus arvensis* L. and its antiplasmodial activity. *African Journal of Infectious Diseases*, 14(1), pp.1-7.

Wahyuni, D.K., Hafida, S.N., Ermayanti, T.M., Wardoyo, B.P.E., Purnobasuki, H. and Utami, E.S.W., 2017. Hairy Root Induction on *Justicia gendarussa* by Various Density of *Agrobacterium rhizogenes* strain LB 510. *Biosaintifika: Journal of Biology & Biology Education*, 9(1), pp.26-32.

Wahyuni, D.K., Vidianti, F., Purnobasuki, H., Ermayanti, T.M., Prajoga, B. and Utami, E.S.W., 2015. *Agrobacterium rhizogenes* mediated hairy root induction in *Justicia gendarussa* Burm. f. *Journal of Applied Environmental and Biological Sciences*, 5(4), pp.87-93.

MUSLIHATIN, W., WAHYUNI, D.K., NURHIDAYATI, T., WARDHANI, F.O. and ROSALIA, E., 2019. Variation induction of *Glycine max* through low dose gamma irradiation produces genetic and physiological alteration as source of tolerant variants in waterlogging conditions. *Biodiversitas Journal of Biological Diversity*, 20(11).

จุฬาลงกรณ์มหาวิทยาลัย
CHULALONGKORN UNIVERSITY

AWARD RECEIVED

1. The Best Presenter (Biodiversity Seminar (Solo). UNS,Indonesia)
2. Finalist of Quarry Life Award (PT. Indocement Indonesia)
3. Universitas Airlangga Rector Scholarship